

THE UNIVERSITY OF HULL

**ABC Terpolymers:  
Micelles, Polymersomes and Stabilisation of  
Water in Water Emulsions**

being a Thesis submitted for the Degree of Doctor of Philosophy

in the University of Hull

by

Negar Ghasdian

M.Sc. (University of Leeds)

Dec 2013

*Dedicated to the memory of my father*

*Homayoon Ghasdian*

*Who passed away during the course of this PhD*

*It broke my heart to lose you*

*But you did not go alone*

*A part of me went with you*

*In my heart you hold a place*

*That no one could ever fill*

## ACKNOWLEDGMENTS

Firstly, I would like to express my gratitude to my supervisors Dr. T. K. Georgiou, Prof. P. D. I. Fletcher and Dr. D. M. A. Buzza for their complete support, encouragement and invaluable guidance at all times and just for being great supervisors.

I would like to thank University of Hull for funding of this PhD studentship. Thanks also go to Funds for Women Graduates (FfWG) for the financial support which is gratefully acknowledged.

Thanks also go to the University of Hull Surfactant and Colloid group for their support, friendship and all the help and advice provided for my project. Extra appreciation goes to Emma Garvey and Padina Alaei for being great lab partners and supportive friends.

Thanks go to Ann Lowry and Tony Sinclair for all the TEM and SEM images which they have taken and to students Rachel Schofield, Kristian Matthews, Jonathan Pegg and Marion Parra for experimental data collected in the course of their projects with my help and guidance.

A very special “more than Thank you” goes to Ahmad for all his love, patience and support thorough these years. I could not have done this without you.

Finally, I wish to express my eternal gratitude and love to my family for all of their support, love and kindness provided to me over the years. An extra special mention goes to my parents Gisuo and Homayoon Ghasdian, my sisters Naghmeh and Natalie I could not have done this without all of your help and support so thank you very much.

## PUBLICATIONS AND PRESENTATIONS

The work contained within this PhD has given rise to the following publications and presentations:

1. N. Ghasdian; E. Church; A. P. Cottam; K. Hornsby; M. Y. Leung and T. K. Georgiou, "Novel core-first star-based quasi-model amphiphilic polymer networks", *RSC Adv.*, 2013, 3, 19070.
2. D. M. A. Buzza; P. D. I. Fletcher; N. Ghasdian and T. K. Georgiou, "Water-in-Water Emulsions based on Incompatible Polymers and Stabilised by Triblock Co-polymers – Templated Polymersomes" *Accepted Manuscript in Langmuir*, November 16, 2013.
3. N. Ghasdian; D. M. A. Buzza; P. D. I. Fletcher and T. K. Georgiou; "Worm-like Micelles based on ABC Triblock Terpolymers: Effect of Molecular Weight and Composition" *in preparation to be submitted to J. Polym. Sci. Part A: Polym. Chem.*
4. N. Ghasdian; M. A. Ward and T. K. Georgiou, "Clickable Alkyne-containing well-defined Polymers", *in preparation to be submitted to Chem. Comm.*
5. Oral presentation: "Novel Strategy to Fabricate Polymersomes via Templating water/water Emulsion, using in-house synthesised Triblock Copolymers", University of Hull, S&CG Seminar, Hull, UK, May, 2013.
6. Poster presentation: "Novel Strategy to Fabricate Polymersomes via Templating water/water Emulsion, using in-house synthesised Triblock Copolymers", University of Hull Colloquia poster presentation, Hull, UK, July, 2012 (Authors: N. Ghasdian; T. K. Georgiou; P. D. I. Fletcher and D. M. A. Buzza)

## ABSTRACT

Polymersomes are vesicles formed from block copolymers. Their large internal volumes and thick walls make them very attractive for the encapsulation of different species. However, a major issue which prevents the use of polymersomes in most of the applications is that the encapsulation efficiency of payload molecules using current encapsulation methods is too low. This problem is thought to be related to the formation mechanism of polymersomes through self-assembly of the constituent block copolymer molecules.

This project is concerned with employing a fundamentally different strategy for polymersomes formation and encapsulation based on coupling the separation properties of aqueous two phase systems (ATPSs), which are able to provide w/w emulsions, with templated self-assembly of polymersomes. This novel method provides high encapsulation efficiencies of payload species which is effective, scalable and biocompatible.

This work started by design and synthesis of a series of amphiphilic ABC terpolymers consisting of hydrophilic poly[poly(ethylene glycol) methyl ether methacrylate] (PEGMA), hydrophobic poly(*n*-butyl methacrylate) (BuMA) and hydrophilic poly[2-(dimethylamino) ethyl methacrylate] (DMAEMA) blocks of general structure  $P_x-B_y-D_z$  and varied compositional parameters using group transfer polymerisation. The synthesised terpolymers were well-characterised and their ability to self-assemble into polymer structures in aqueous solution was assessed.

In addition, we show how these terpolymers can be used as effective stabilisers to stabilise ATPS consisting of dextran and poly(ethylene glycol) in order to form stable water-in-water emulsion or templated polymersomes-like structures, based on the affinity of each block towards the ATPS. The influence of terpolymers compositional parameters on the stability of w/w emulsions or templated polymersome-like structures was investigated. In favourable cases, the emulsion drop (or templated polymersome) sizes were a few  $\mu\text{m}$  and were stable for periods in excess of 8 months. The emulsions can be inverted from dextran-in-PEG to PEG-in-dextran by increasing the volume fraction of dextran-rich aqueous phase. We demonstrate that both high and low molecular weight fluorescent solutes “self-load”

into either the dextran- or PEG-rich regions and that solute can mass transfer across the water-water interface based on its affinity towards each phase.

This work was further extended using modified silica nanoparticles (hydrophobised or PEGylated) for stabilisation of dextran-PEG ATPS. We show how the hydrophobicity and PEGphilicity of such particles can lead to relative stabilisation of dextran-PEG ATPS and formation of particle-stabilised w/w emulsions.

## LIST OF ABBREVIATIONS AND SYMBOLS

AS	Ammonium sulphate
ATPS	Aqueous two phase system
BuMA	<i>n</i> -Butyl methacrylate
BzMA	Benzyl methacrylate
CMC	Critical micelle concentration
DCDMS	Dichlorodimethylsilane
DLS	Dynamic light scattering
DMAEMA	2-(Dimethylamino) ethyl methacrylate
DMF	Dimethylformamide
DNA	Deoxy ribonucleic acid
DPPH	2, 2-Diphenyl-1-picrylhydrazyl
DSCG	Disodium cromoglycate
EO	Ethylene oxide
FITC	Fluorescein isothiocyanate
FT-IR	Fourier transform infrared spectroscopy
GPC	Gel permeation chromatography
GTP	Group transfer polymerisation
HEGMA	Hexa(ethylene glycol) methacrylate
HLB	Hydrophilic-lipophilic balance
IR	Infrared
IUPAC	International union of pure and applied chemistry
LCST	Lower critical solubility temperature
MAA	Methacrylic acid
MMA	Methyl methacrylate
MTS	1- Methoxy-1-trimethylsiloxy-2-methyl-1-propane
MW	Molecular weight
NMR	Nuclear magnetic resonance
PAA	Poly(acrylic acid)
PBA	Poly( <i>n</i> -butyl acrylate)
PDEAEMA	Poly(2-diethylaminoethyl methacrylate)
PDI	Polydispersity index
PDMAI	Poly[5-( <i>N,N</i> -dimethylamino)isoprene]

PDMS	Poly(dimethyl siloxane)
PDPA	Poly[2-(diisopropylamino)ethyl methacrylate]
PEG	Poly(ethylene glycol)
PEGDA	Poly(ethylene Glycol diacrylate)
PEGMA	Poly(ethylene glycol) methyl ether methacrylate
PEO	Poly(ethylene oxide)
PEPOX	Poly(2-(1-ethylheptyl)-2-oxazoline)
PEtOX	Poly(2-ethyl-2-oxazoline)
PMAA	Poly(methacrylic acid)
PMMA	Poly(methyl methacrylate)
PMOXA	Poly(methyl oxazoline)
PMPC	Poly[2-(methacryloyloxy)ethyl phosphorylcholine]
PNIPAM	Poly(N-isopropylacrylamide)
PO	Propylene oxide
PODFOX	Poly(2-(2,6-difluorophenyl)-2-oxazoline)
PS	Polystyrene
PVPC	Poly(vinylpyridinium chloride)
P2VP	Poly(2-vinyle pyridine)
P4VP	Poly(4-vinyle pyridine)
RALS	Right angle laser light scattering
RI	Refractive index
ROP	Ring opening polymerisation
SEM	Scanning electron microscopy
TBAB	Tetrabutylammonium bromide
TBABB	Tetrabutylammonium bibenzoate
TEM	Transmission electron microscopy
THF	Tetrahydrofuran
TMOS	Tetramethylorthosilicate
UV	Ultra violet



$a$	Optimal surface area
$c(r)$	Aqueous phase solubility of solute
$c(\infty)$	Solubility in a system with planar interface
$d$	Diameter
$\bar{d}_{agg}$	Mean diameter of aggregate
$d_h$	Hydrodynamic diameter
$d/p$	Dextran in PEG emulsion
$g$	Gravity acceleration
$h_d$	Height of dextran phase
$h_e$	Height of emulsion phase
$h_p$	Height of PEG phase
$I$	Intensity of fluorescent dye
$l$	Length of the hydrophobic block
$M_n$	Number average molecular weight
$M_w$	Weight average molecular weight
$M_r$	Relative molecular mass
$o/w$	Oil-in-water emulsion
$o/w/o$	Oil-in-water-in-oil emulsion
$p$	Packing parameter
$p/d$	PEG in dextran emulsion
$pK_a$	Logarithm of acid dissociation constant
$r$	Radius
$R$	Universal gas constant
$k_B$	Boltzmann constant
$T$	Absolute temperature
$t_{1/2}$	Half life
$t_{1/2\ coal.}$	Half-life of coalescence
$t_{1/2\ cream.}$	Half-life of creaming
$t_{1/2\ emul.}$	Half-life of emulsion
$t_{1/2\ sed.}$	Half-life of sedimentation
$t_s$	Time taken for the full emulsion separation
$v$	Velocity
$v$	Volume of the hydrophobic block
$V_m$	Molar volume of dispersed phase

$w/o$	Water-in-oil emulsion
$w/w$	Water-in-water emulsion
$W_f$	Weight fraction
$\gamma$	Surface tension
$\gamma_{ow}$	Oil-water interfacial tension
$\Delta G_d$	Gibbs free energy for particle desorption
$\Delta G_{micel.}$	Gibbs free energy for micellisation
$\Delta T$	Temperature change
$\eta$	Viscosity
$[\eta]$	Intrinsic viscosity
$\theta_{dp}$	Contact angle at dextran-PEG interface
$\theta_{ow}$	Contact angle at oil-water interface
$\lambda$	Wavelength
$\rho_{cont.}$	Density of continues phase
$\rho_{drop}$	Density of dispersed phase
$\phi_d$	Volume fractions of dextran phase
$\phi_p$	Volume fractions of PEG phase
$\phi_e$	Volume fraction of emulsion

## CONTENTS

<b>CHAPTER 1-INTRODUCTION AND LITERATURE REVIEW</b> .....	<b>16</b>
<b>1.1 Introduction</b> .....	<b>17</b>
<b>1.2 Block copolymers</b> .....	<b>19</b>
<i>1.2.1 Synthesis of block copolymers</i> .....	<b>21</b>
<i>1.2.2 Group transfer polymerisation technique</i> .....	<b>22</b>
<b>1.3 Self-assembly of amphiphilic copolymers</b> .....	<b>24</b>
<b>1.4 Aggregation of ABC terpolymers into micelles</b> .....	<b>26</b>
<i>1.4.1 Mechanism of micellisation</i> .....	<b>30</b>
<i>1.4.2 CMC measurements</i> .....	<b>31</b>
<b>1.5 Polymersomes-vesicular self-assemblies of copolymers</b> .....	<b>33</b>
<i>1.5.1 Polymersomes fabrication methods</i> .....	<b>37</b>
<i>1.5.2 Mechanism of polymersomes formation</i> .....	<b>39</b>
<b>1.6 Emulsions</b> .....	<b>41</b>
<i>1.6.1 Definition</i> .....	<b>41</b>
<i>1.6.2 Emulsion formation</i> .....	<b>41</b>
<i>1.6.3 Emulsion stability</i> .....	<b>42</b>
<i>1.6.3.1 Creaming or sedimentation</i> .....	<b>43</b>
<i>1.6.3.2 Flocculation</i> .....	<b>44</b>
<i>1.6.3.3 Coalescence</i> .....	<b>45</b>
<i>1.6.3.4 Ostwald ripening</i> .....	<b>46</b>
<i>1.6.4 Thermodynamic and kinetic stability of emulsions</i> .....	<b>46</b>
<i>1.6.5 Stabilisation of emulsions using different types of stabilisers</i> .....	<b>47</b>
<b>1.7 Aqueous two phase systems</b> .....	<b>49</b>

1.7.1 <i>Dextran-PEG ATPS</i> -----	51
<b>1.8 Water in water emulsions based on ATPS</b> -----	<b>53</b>
1.8.1 <i>Challenges in stabilisation and characterisation of w/w emulsion</i> ---	54
1.8.2 <i>Stabilisation of ATPS towards w/w emulsions</i> -----	55
<b>1.9 Research aims and strategy</b> -----	<b>56</b>
<b>1.10 Outline of thesis</b> -----	<b>57</b>
<b>1.11 References</b> -----	<b>59</b>
<b>CHAPTER 2-EXPERIMENTAL</b> -----	<b>68</b>
<b>2.1 Materials</b> -----	<b>69</b>
2.1.1 <i>Water</i> -----	69
2.1.2 <i>Pluronic<sup>®</sup> grades</i> -----	69
2.1.3 <i>Chemicals used for synthesis of hydrophobised silica nanoparticles</i> ---	69
2.1.4 <i>Chemicals used for synthesis of PEGylated silica nanoparticles</i> -----	69
2.1.5 <i>Chemicals used for synthesis of terpolymers</i> -----	69
2.1.6 <i>Chemicals used for preparation of ATPS</i> -----	71
2.1.7 <i>Fluorescence probes used for encapsulation</i> -----	71
<b>2.2 Synthesis methods</b> -----	<b>71</b>
2.2.1 <i>Synthesis of PEGylated silica nanoparticles</i> -----	71
2.2.2 <i>Synthesis of ABC terpolymers</i> -----	72
<b>2.3 Preparation procedures</b> -----	<b>75</b>
2.3.1 <i>Preparation of polymer self-assembly</i> -----	75
2.3.1.1 <i>Bulk rehydration method</i> -----	75
2.3.1.2 <i>Film rehydration method</i> -----	75
2.3.2 <i>Preparation of ATPS</i> -----	76

2.3.3 <i>Preparation of w/w emulsion</i> -----	77
2.3.4 <i>Encapsulation of fluorescent probes</i> -----	78
<b>2.4 Characterisation methods</b> -----	<b>79</b>
2.4.1 <i>Gel permeation chromatography</i> -----	79
2.4.2 <i>NMR spectroscopy</i> -----	82
2.4.3 <i>Dynamic light scattering</i> -----	83
2.4.4 <i>FT-IR spectroscopy</i> -----	84
2.4.5 <i>Fluorescence spectroscopy</i> -----	84
2.4.6 <i>Microscopy</i> -----	86
2.4.6.1 <i>Optical transmission microscopy</i> -----	86
2.4.6.2 <i>Fluorescence microscopy</i> -----	86
2.4.6.3 <i>Scanning electron microscopy</i> -----	87
2.4.6.4 <i>Transmission electron microscopy</i> -----	88
2.4.7 <i>Aqueous solution characterisation</i> -----	88
2.4.7.1 <i>Determination of pK<sub>a</sub></i> -----	88
2.4.7.2 <i>Cloud point</i> -----	89
2.4.8 <i>Stability measurement of w/w emulsion</i> -----	89
<b>2.5 References</b> -----	<b>91</b>
<b>CHAPTER 3-DESIGN, SYNTHESIS AND CHARACTERISATION OF TERPOLYMERS</b> -----	<b>92</b>
<b>3.1 Introduction</b> -----	<b>93</b>
<b>3.2 Terpolymers design and synthesis</b> -----	<b>93</b>
<b>3.3 Determination of terpolymers composition and molecular weight</b> -----	<b>97</b>
<b>3.4 Aqueous solution characterisation of terpolymers</b> -----	<b>102</b>
<b>3.4.1 Hydrodynamic diameter</b> -----	<b>102</b>

3.4.2 <i>Micelle diameter</i> .....	105
3.4.3 <i>CMC of terpolymers</i> .....	106
3.4.4 <i>Effective pK<sub>a</sub> of terpolymers</i> .....	109
3.4.5 <i>Cloud points of terpolymers</i> .....	111
3.5 <b>Conclusion</b> .....	112
3.6 <b>References</b> .....	114
<b>CHAPTER 4-PRELIMINARY OBSERVATIONS OF TERPOLYMERS SELF-ASSEMBLY IN AQUEOUS SOLUTION</b> .....	116
4.1 <b>Introduction</b> .....	117
4.2 <b>Study of self-assembly of terpolymers in aqueous solution by DLS</b> .....	118
4.3 <b>Study of self-assembly of ABC terpolymers in aqueous solution by high resolution techniques</b> .....	121
4.4 <b>Conclusion</b> .....	124
4.5 <b>References</b> .....	125
<b>CHAPTER 5-WATER-IN-WATER EMULSIONS BASED ON ATPS AND STABILISED BY TERPOLYMERS–TEMPLATED POLYMERSOMES</b> .....	126
5.1 <b>Introduction</b> .....	127
5.2 <b>Stabilisation of dextran-PEG ATPS using ABA terpolymers, Pluronics<sup>®</sup></b> .....	129
5.2.1 <i>Effect of Pluronics<sup>®</sup> concentration, composition and MW on stability of w/w emulsion</i> .....	131
5.2.2 <i>Micrographs of w/w emulsions stabilised using Pluronics<sup>®</sup></i> .....	135
5.3 <b>Stabilisation of dextran-PEG ATPS using ABC terpolymers</b> .....	138
5.3.1 <i>Effect of ABC terpolymer composition on emulsion type</i> .....	140
5.3.2 <i>Effect of relative volume fractions of the dextran-PEG phases on emulsion type</i> .....	142

5.3.3 <i>Effect of relative volume fractions of the dextran-PEG phases on emulsions mean drop size</i> -----	145
5.3.4 <i>Effect of relative volume fractions of the dextran-PEG phases on emulsion stability</i> -----	146
5.3.5 <i>Effect of shifting to a higher tie-line in dextran-PEG ATPS phase diagram on emulsion stability and type</i> -----	149
5.3.6 <i>Effect of terpolymer composition on emulsion stability</i> -----	151
5.3.7 <i>Effect of terpolymer molecular weight on emulsion stability</i> -----	158
5.3.8 <i>Effect of emulsion stability on emulsion drop size</i> -----	159
5.3.9 <i>Variation of emulsion drop size over time</i> -----	161
5.3.10 <i>Effect of increasing terpolymer concentration on emulsions</i> -----	163
5.3.11 <i>Effect of varying pH on emulsions stability</i> -----	164
5.3.12 <i>Effect of emulsification duration and method on the stability of emulsion</i> -----	164
5.3.13 <i>Effect of polymer architecture on emulsions stability</i> -----	166
5.3.14 <i>Drying the templated polymersomes</i> -----	167
5.3.15 <i>Dilution of the templated polymersomes</i> -----	168
<b>5.4 Encapsulation/segregation of solutes within templated polymersomes</b> ---	<b>170</b>
<b>5.5 Applications of templated polymersomes based on w/w emulsion</b> -----	<b>174</b>
<b>5.6 Conclusion</b> -----	<b>175</b>
<b>5.7 References</b> -----	<b>179</b>
<b>CHAPTER 6-STABILISATION OF W/W EMULSIONS BY MODIFIED SILICA NANOPARTICLES</b> -----	<b>180</b>
<b>6.1 Introduction</b> -----	<b>181</b>
<b>6.2 Stabilisation of w/w emulsion by hydrophobised silica nanoparticles</b> ----	<b>183</b>
<b>6.2.1 Silica nanoparticles characteristics</b> -----	<b>183</b>

6.2.2 <i>Effect of hydrophobicity extent of silica nanoparticle on emulsion stability</i> -----	183
6.2.3 <i>Effect of silica nanoparticles concentration on emulsion stability</i> ---	185
6.3 <b>Stabilisation of w/w emulsion by PEGylated silica nanoparticles</b> .....	189
6.3.1 <i>PEGylated silica nanoparticles synthesis and characteristics</i> .....	189
6.3.2 <i>Effect of PEGylated nanoparticle size on emulsion stability</i> -----	194
6.3.3 <i>Effect of varying dextran-PEG volume fractions on emulsion stability</i> -----	196
6.4 <b>Conclusion</b> .....	198
6.5 <b>References</b> -----	199
<b>CHAPTER 7-CONCLUSION AND FUTURE WORK</b> .....	201
7.1 <b>Summary of main findings</b> .....	202
7.2 <b>Future work</b> .....	206
7.3 <b>References</b> .....	209
<b>APPENDIX</b> .....	210



# **CHAPTER 1**

## **INTRODUCTION AND LITERATURE REVIEW**

## 1.1 Introduction

The delivery of active therapeutic molecular species depends on their effective encapsulation since these species should be protected from several undesired environmental conditions. Lipid based vesicles, so called liposomes, have been used widely for encapsulation and delivery of active pharmaceutical species. However, there are certain limitations associated with using liposomes, as their lipid-based precursors are generally obtained from natural sources which might have inconsistent composition, quality and limited structural variety.<sup>1</sup> In addition, the lipid based vesicles are generally leaky specially when undergo undirected hydrolysis or oxidation of their building blocks in solution which causes their short shelf-life. Hence, there have been extensive investigations on similar analogues to fulfil these limitations.

Polymer-based vascular structures, so called polymersomes, are promising alternatives which have great potential for encapsulation, targeting and delivery of a variety of active species and have attracted enormous attentions during the last two decades with the first publication in 1995.<sup>2-4</sup> Polymersomes are spherical vesicles formed from self-assembly of amphiphilic block copolymers and compare to their lipid-based analogous they benefit from a robust type of membrane with decreased permeability.<sup>5-7</sup> In addition, unlike the lipid-based vesicles, an unlimited range of synthetic polymers can be used as precursors for formation of these polymer-based vesicles with well-defined structural and physiochemical properties. Therefore, polymersomes with desired properties can be prepared with specific potential for encapsulation of different species.

However, the formation of polymersomes using conventional techniques is not a straightforward route and it is associated with a number of challenges. Moreover, a major issue which prevents the use of polymersomes in most of their potential applications is that the encapsulation efficiency of payload molecules using current encapsulation methods is too low. This problem is thought to be related to the formation mechanism of polymersomes through self-assembly of the constituent block copolymer molecules.

Hence, an investigation for employing novel alternative approaches for formation of polymer-based vesicles is desired. The exciting and challenging aim of this project is to develop a fundamentally different strategy for polymersomes formation and encapsulation based on coupling the separation properties of aqueous polymer mixtures with templated self-assembly of polymersomes. Aqueous two phase systems (ATPSs) are entirely aqueous systems consisting of two polymers which phase separate into two phases. Such systems have been widely used for partitioning and separation of macromolecules. Emulsification of ATPS results in the formation of w/w emulsions which are thermodynamically unstable. However, it is presumed that amphiphilic terpolymers containing hydrophilic terminal blocks and a hydrophobic middle block would adsorb at the formed water-water interface, which results in kinetically stabilisation of such system or in other words, possible formation of templated polymersomes. Using this strategy, the encapsulant would be self-loaded into the interior cavity of polymersomes prior to their formation. Consequently, selective encapsulation of species would be achieved while using an efficient, scalable and biocompatible strategy.

The main focus of this thesis is to investigate whether in-house synthesised amphiphilic terpolymers containing particular blocks with specific affinity towards ATPS enable the formation of a stable w/w emulsion or in other words templated polymersomes. Initially, a couple of commercially available ABA terpolymers are attempted to fulfil the proposed research strategy. This work is followed by synthesis and characterisation of a series of ABC terpolymers with varied compositional design, which are used for formation of templated polymersomes. Finally, this work is extended by investigating whether modified silica nanoparticles can stabilise emulsified ATPSs and result in the formation of particle stabilised w/w emulsion.

This chapter introduces the basic concepts and knowledge underlying the work presented in this thesis. Firstly, a brief introduction on amphiphilic block copolymers is given followed by reviewing their behaviour and self-assembly in aqueous solutions with specific interest on terpolymers. In addition, the conventional methods employed for fabrication of polymersomes are reviewed. Furthermore, the main concepts of emulsions and ATPSs are discussed and the previous reported studies on the stabilisation of w/w emulsions are reviewed. Finally, the main aims and research

strategy are discussed in details and a brief overview of the following chapters is given in order to introduce the general outlines of the thesis.

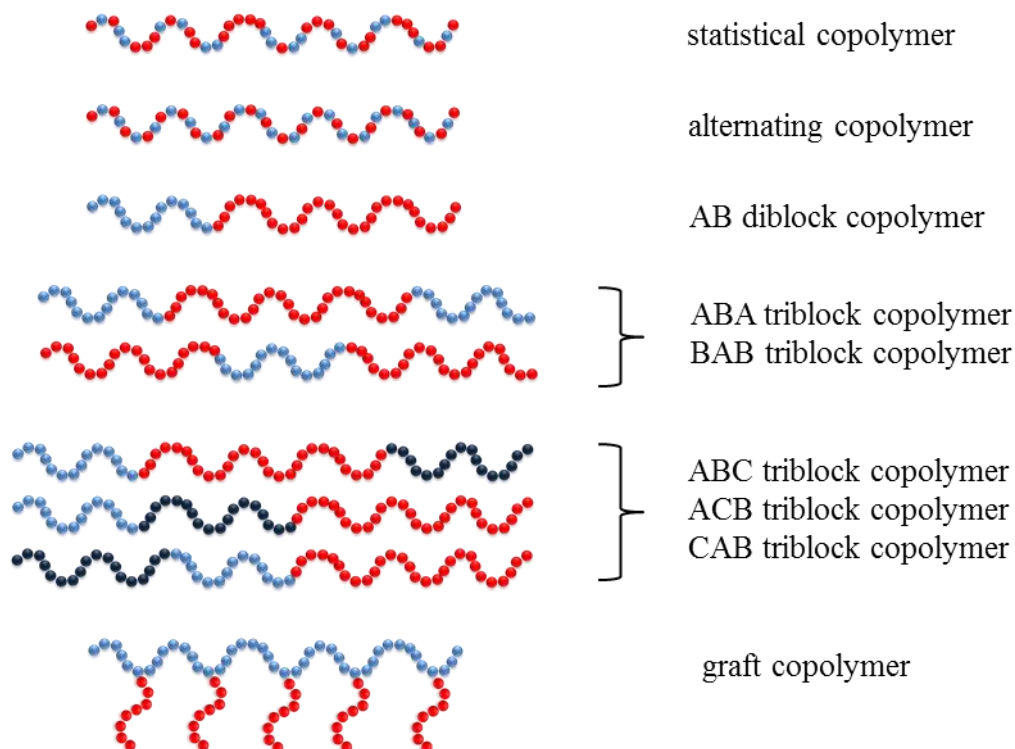
## 1.2 Block copolymers

Over the past decades the self-assembly of small amphiphilic molecules has been studied extensively due to their wide range of applications. Small amphiphilic molecules, so called *surfactants* (surface active agents), consist of a hydrophilic head and one or more hydrophobic tails. The specific structure of surfactants has provided the possibility of formation of various types of aggregates either in bulk or solution with different morphologies such as spheres, cylinders, lamellae and vesicles.<sup>6, 8</sup>

However, an alternative class of amphiphilic molecules has enabled the fabrication of similar aggregates with analogous morphologies based on similar principles to that of the surfactants.<sup>2, 9, 10</sup> This class of molecules known as synthetic *block copolymers* exhibit promising properties compared to surfactants. For instance, due to their mechanical and physical properties, block copolymer aggregates benefit from higher stability and robustness.<sup>11</sup> Also, recent developments in controlled polymerisation techniques have given rise to huge interest in synthesis of block copolymers of various architectures with well-defined structures. Therefore, the self-assembly of amphiphilic copolymers has attracted considerable attention over the last decades due to the endless combinations of their physical properties, architecture and potential applications in several different materials and research areas, such as biomaterials, microelectronics, photoelectric materials and catalysts.<sup>12, 13</sup>

Before going through the literature related to self-assembly of block copolymers, it will be helpful to define some terminology at the outset. *Copolymer* is a macromolecule consisting of two or more constituent units (monomers). Based on how these units are arranged along the chain, different types of copolymers can be introduced, such as statistical, alternating, block and graft copolymers.<sup>14</sup> Figure 1.1 illustrates different types of copolymers schematically.

**Figure 1.1.** Typical structures of copolymers.



As seen in Figure 1.1, *block copolymers* are a class of copolymers consisting of two or more covalently bonded blocks in a linear sequence, which are chemically distinct and immiscible.<sup>14</sup> Based on the number of constituent blocks and their sequences, different types of block copolymers can be formed. For example, block copolymers consisting of two distinct monomers A and B can make various structures, such as linear AB diblock or ABA and BAB triblock, while if a third C block is introduced based on a different monomer then ABC, ACB and BAC triblocks can be formed.<sup>15</sup> Based on the number of blocks in a block copolymer, polymer nomenclature can be varied. As IUPAC (International Union of Pure and Applied Chemistry) suggested copolymers consisting of two monomers are termed diblock or bipolymers, those containing three monomers are called triblock or terpolymers, those obtained from four monomers are tetrablocks or quaterpolymers, etc.<sup>16</sup> In this work, block copolymers are referred to by the later terminology.

The huge interest in block copolymers arises mainly from their surface activity which makes them attractive potentials to be used as dispersants, emulsifiers, wetting agents, foam stabilisers, flocculants, viscosity modifiers, etc.<sup>13, 17, 18</sup>

In particular, because of block copolymer segmental incompatibility, they show fascinating behaviour in solution leading to formation of various types of aggregations. The main application of block copolymer aggregations is to incorporate in solubilisation of bio-active components either by being covalently linked to active components or encapsulating process where they form soluble vascular aggregation.<sup>13</sup> Also, the self-assembly of amphiphilic block copolymers on the interface is of interest for stabilisation of emulsions,<sup>19</sup> supporting the nanoparticles colloidal solutions<sup>20</sup> and modification of surfaces.<sup>21</sup>

In literature, a large number of studies on self-assembly of block copolymers are focused on diblock copolymers. However, in the following sections an overview on the self-assembly of terpolymers with the emphasis on ABC terpolymers is given, since ABC terpolymers were the main focus of this thesis. Firstly though, a brief overview of typical synthetic strategies of block copolymers will be described.

### ***1.2.1 Synthesis of block copolymers***

Block copolymers are mainly synthesised by employing *living* or *controlled* polymerisation techniques. Living or controlled polymerisation methods enable the synthesis of structurally well-defined polymers with pre-determined molecular weights and compositions as well as narrow molecular weight distributions.<sup>22</sup>

In particular, living polymerisation is a kind of addition polymerisation in which the growing polymer chains are neither able to terminate or undergo any chain transfer during the polymerisation. In the other words, chain termination and chain transfer reactions are absent, while the initiation rate is much larger than the rate of the chain propagation. Therefore, the initiation of monomers occurs in relatively same time and the polymer chains grow in a constant rate which results in similar chain lengths (low polydispersity).<sup>23</sup> In living polymerisation methods, each molecule of initiator starts the formation of one polymer chain, thereby, the degree of polymerisation of final polymer can be predefined and tailored by manipulating the ratio of monomer concentration to initiator concentration. In fact, the degree of polymerisation is equal to  $[\text{monomer}]/[\text{initiator}]$ . This enables to fabricate polymers with specific pre-defined molecular weights.

Living polymerisation was first reported in 1956 by Michael Szwarc when he invented the living anionic polymerisation of styrene.<sup>24, 25</sup> After that, a number of living polymerisation techniques were reported, namely, living anionic polymerisation, living cationic polymerisation, ring opening metathesis polymerisation (ROP), atom transfer radical polymerisation (ATRP), reversible addition fragmentation chain transfer (RAFT) and group transfer polymerisation (GTP). In this work GTP technique was used to synthesis ABC terpolymers and it will be discussed in details in the next section.

### ***1.2.2 Group transfer polymerisation technique***

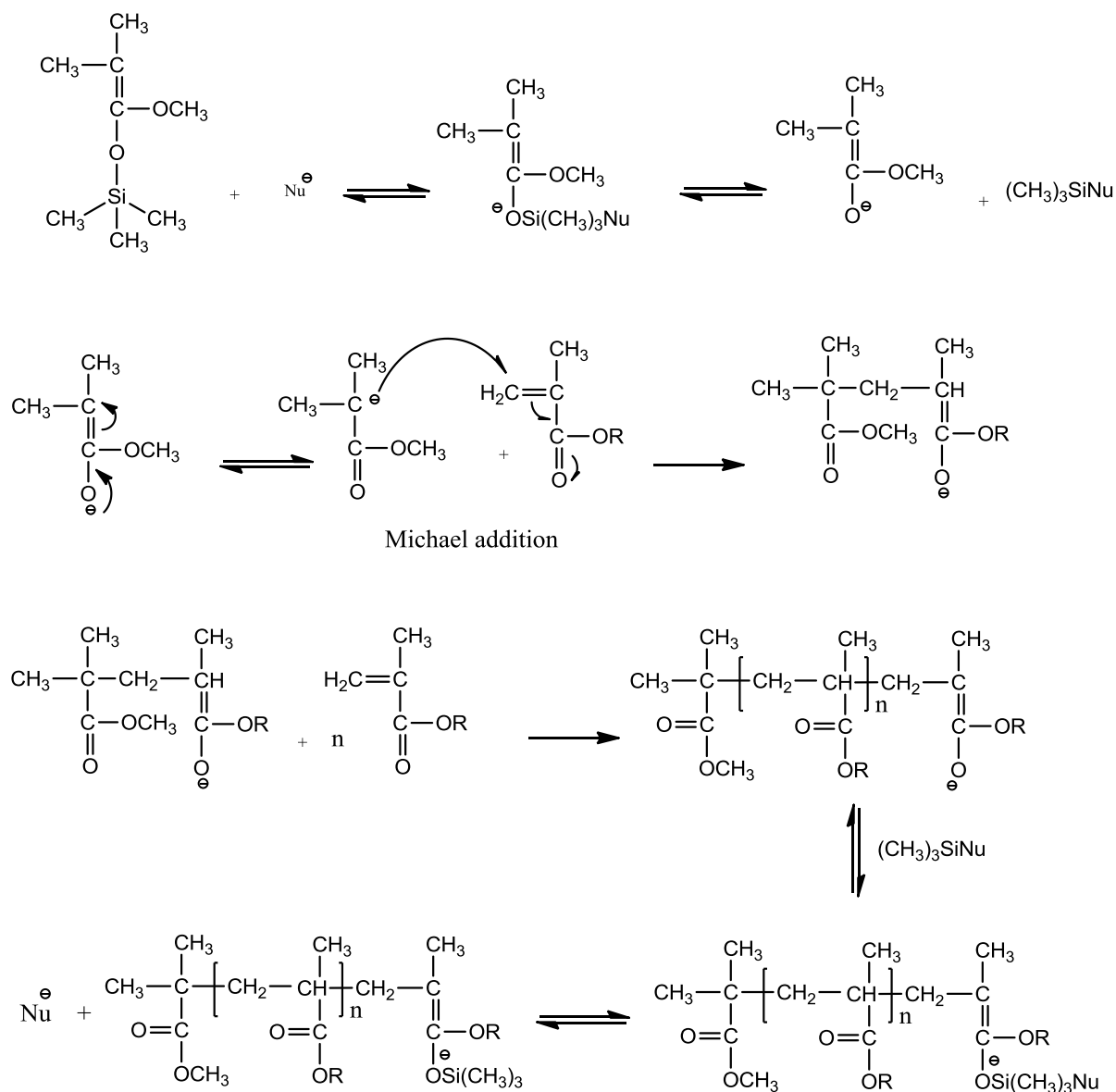
Webster and co-workers reported GTP for the first time in early 1980s.<sup>26</sup> Compare to other living polymerisation techniques such as ATRP and RAFT, GTP is a fast and cost effective method which can be easily scaled-up for the industrial production because it can be performed at room temperature and at high concentrations so there is no need for cooling systems and the excessive use of solvents.<sup>27</sup> GTP is mainly used to polymerise acrylates and methacrylate based monomers. For this study, three methacrylate monomers were used: poly(ethylene glycol) methyl methacrylate (PEGMA), *n*-butyl methacrylate (BuMA) and 2-(dimethylamino) ethyl methacrylate (DMAEMA).

GTP provides excellent architectural control and polymers with very low polydispersity indices can be produced. In addition, unlike other living polymerisation techniques such as ATRP and ROP no metallic or halide impurities remain in the synthesised polymers after polymerisation, which can be advantageous for production of polymers with biomedical applications.<sup>27</sup>

The initiator which is commonly used in GTP is a silyl ketene acetal, 1-methoxy-1-trimethylsiloxy-2-methyl-1-propane (MTS), which initiates the propagation by reacting to a monomer via a Michael addition reaction, in which the silyl group is transferred to the new added monomer and therefore, creates a new terminal silyl ketene acetal group. The polymerisation is catalysed by nucleophilic anions such as tetrabutylammonium bibenzoate (TBABB),  $\text{HF}_2^-$ ,  $\text{CN}^-$  and  $\text{N}_3^-$  or Lewis acids like  $\text{ZnBr}_2$  and  $\text{AlBu}_2\text{Cl}$ . During the propagation step, the catalyst associated with silicon atom and subsequently activates transfer of the trimethylsilyl

group to the new monomer. <sup>28</sup> Figure 1.2 illustrates the mechanism of GTP for a methacrylate monomer.

**Figure 1.2.** Group transfer polymerisation of a methacrylate monomer (with R as a side group), initiated by MTS and catalysed by TBABB).



Any compound containing hydrogen donor (like water or molecules that contain carboxyl acid and hydroxyl groups) causes the rapid termination of GTP, thus, very dry conditions must be provided during the polymerisation and all the reagents and solvent must be purified and dried carefully. Consequently, by the addition of a proton donor, such as water, alcohol or acids, GTP can be terminated. In addition, it is possible to terminate the reaction by coupling the living chain with



active species. This enables the synthesis of polymers with a functional terminated group.<sup>28</sup> In spite of all the advantages of GTP, the maximum molecular weight that can be achieved with narrow polydispersity index ( $PDI < 1.3$ ) is about 20000 (g/mol) which can be considered as one of the main GTP limitations.<sup>29</sup>

### 1.3 Self-assembly of amphiphilic copolymers

Self-assembly can be defined as the spontaneous formation of well-defined structures from components of a system by non-covalent forces, which results in a more ordered system.<sup>30, 31</sup> As mentioned above, amphiphilic block copolymers self-assemble in the presence of a selective solvent, a solvent that is not compatible with all the blocks of the block copolymer. Competing interactions between long-range repulsive hydrophilic/hydrophobic interactions and short-range attractive interactions result in self-assembly of amphiphilic block copolymers. Similar to low molecular surfactants, block copolymers can self-assemble into various morphologies in solution, such as spherical micelles,<sup>32, 33</sup> rods,<sup>34</sup> discs,<sup>35</sup> vesicles,<sup>36</sup> etc. However, the dynamic of the aggregate formation and equilibration in solution is much slower for block copolymers due to much lower diffusion coefficients.<sup>37</sup>

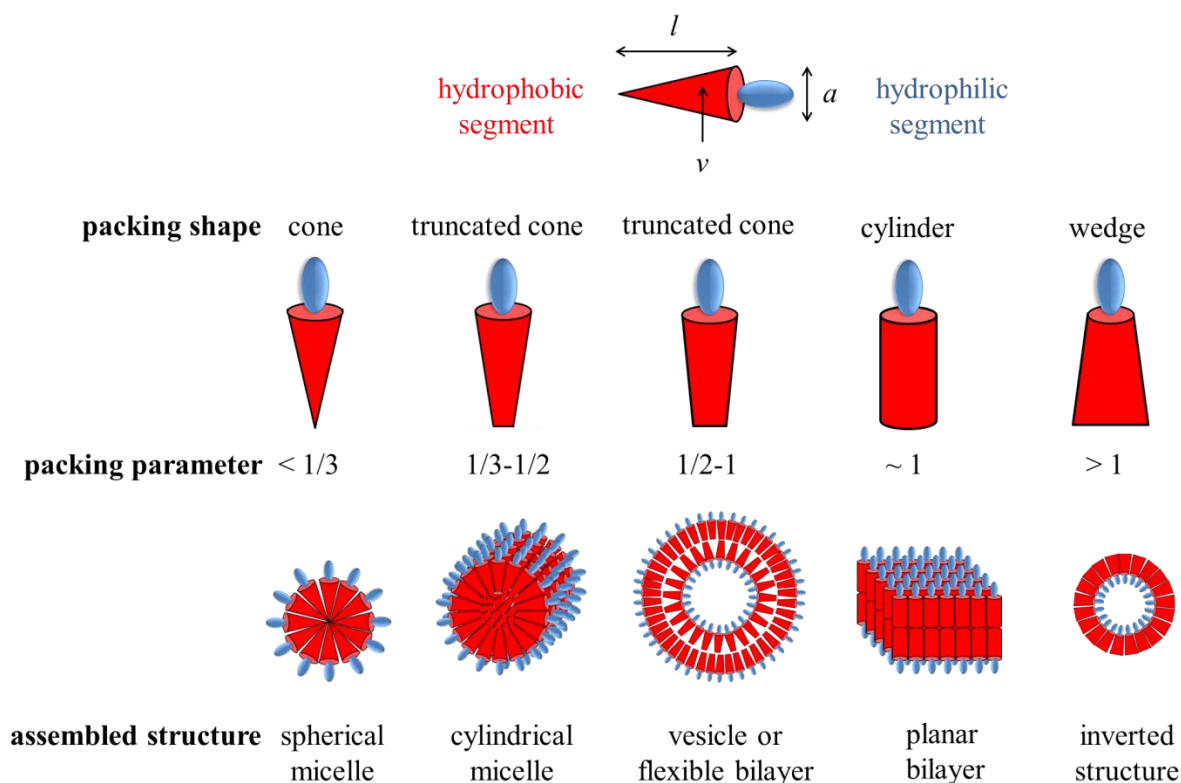
The morphology of the final self-assembly structure depends strongly on the shape of the individual block copolymers constituting the aggregate and it can be predicted considering their packing parameter (also called shape factor). Dimensionless packing parameter  $p$  is defined as following:<sup>6</sup>

$$p = \frac{v}{al} \quad \text{Eq. 1.1}$$

Where  $v$  and  $l$  are the volume and length of the hydrophobic block while  $a$  is the optimal surface area per molecule at the interface<sup>6</sup>. The relationship between the packing parameter magnitude and morphology of the resultant self-assembly can be summarised in Figure 1.3. As can be seen, amphiphilic block copolymers with packing parameters of  $p < 1/3$  give rise to formation of spheres,  $1/3 < p < 1/2$  cylinders,  $1/2 < p < 1$  vesicles or flexible bilayer,  $p = 1$  planar bilayers and  $p > 1$  inverted structures.

However, there are other factors which control the morphology of the resultant self-assembly, such as chemical structure of the copolymer, the hydrophilic/hydrophobic balance, copolymer concentration in solution, type of organic solvent, the ratio of organic solvent/aqueous solvent, presence of salt and its concentration, pH of the solution and temperature.<sup>38</sup> Among the mentioned factors, it has been proposed that the volume ratio of hydrophilic/hydrophobic blocks of the copolymer plays a more important role in the morphology of the resultant self-assembly but it is not a determinant factor. Generally, block copolymers with hydrophilic/hydrophobic length ratios greater than 1:1 form spherical micelle, ratios less than 1:2 favour formations of vascular structures and ratios less than 1:3 might lead to formation of vesicles, inverted microstructure or other complex structures. However, under different conditions, a range of morphologies can be formed from a same amphiphilic block copolymer. Therefore, it is the overall balance between free energy contributions of different constituents in self-assembly as well as other kinetic factors which determine the final morphology of the self-assemblies.<sup>39</sup> In the following sections, studies related to self-assembly of amphiphilic ABC terpolymers into micelles and polymersomes are reviewed.

**Figure 1.3.** The effect of the packing parameter on the structures of formed assemblies.



#### 1.4 Aggregation of ABC terpolymers into micelles

During the past decades, self-assembly of AB diblock copolymers in selective solvents have been extensively studied and well understood.<sup>11, 12, 40-42</sup> It is well-established that the copolymer composition and the interaction parameters influence the final structure of the formed self-assembly and diverse nano-sized aggregations such as micelles, vesicles, lamellar aggregations, etc. can be formed. Comparing to the extent of the work which have been done on self-assembly of diblock copolymers, a limited number of publications are available related to ABC terpolymers. Introduction of a third block makes the self-assembly behaviour of ABC terpolymers significantly more diverse and complex compared to diblock copolymers and therefore, their behaviour in selective solvents is not fully understood. ABC terpolymers can self-assemble into variety of micelle types with mixed or compartmentalised cores or coronas depending on the incompatibilities of blocks, compatibility of each block towards solvent, rigidity of the blocks and volume fraction of each block.<sup>43-45</sup>

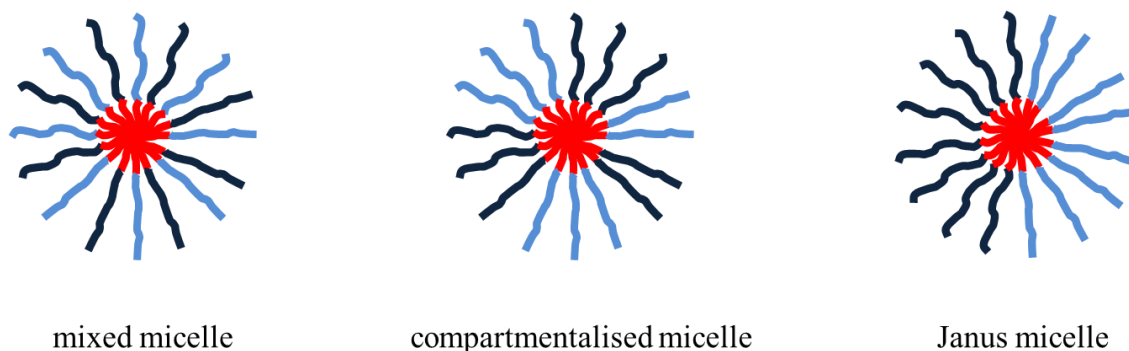
One of the early works on formation of ABC terpolymers micelles was reported by Patrickios et al.<sup>46</sup> who demonstrated the formation of small sized micelle with small aggregation number in aqueous solution as a function of pH for terpolymers consisting of PDMAEMA, poly(methyl methacrylate) (PMMA) and poly(methacrylic acid) (PMAA) blocks, which were synthesised via the GTP technique. The authors varied the block sequence of the terpolymers and compared them with a random terpolymer regarding the micelle formation. Similar work was done using terpolymers consisting of methylvinyl ether, ethylvinyl ether and methyl tri(ethylene glycol) vinyl ether.<sup>47</sup> Micelles formed in the presence of high salt concentration and it was found that the micelle size, aggregation number, micelle-unimer equilibrium and cloud point can be affected by the block sequence and salt concentration. Afterwards, micelles of terpolymers consisting of MMA, DMAEMA and hexa(ethylene glycol) methacrylate (HEGMA) were prepared in aqueous solution.<sup>48</sup> The dependence of micelle size and cloud points to the block sequence and the position of thermoresponsive DMAEMA block were investigated. Later on, terpolymers based on benzyl methacrylate (BzMA), DMAEMA and HEGMA were found to form micelles<sup>49</sup> and the dependency of micelle size to block sequence was studied. High molecular weight terpolymers consisting of styrene, 2-vinylpyridine and methacrylic acid were studied in terms of forming micelles by Giebeler and Stadler.<sup>50</sup> The formation of three different core-shell micelles from a single terpolymer consisting of PEG, 2-(diethylamino)ethyl methacrylate (DEAEMA) and 2-(succinyloxyethylmethacrylate) as a function of pH was reported by Cai and Armes.<sup>51</sup> The driving forces for forming these three types of micelles were found to be hydrogen-bonding, inter-polyelectrolyte complexation and hydrophobic interactions. Formation of monodispersed core-shell-corona micelles from terpolymers based on styrene, 2-vinyl pyridine and ethylene oxide monomers in water was also reported.<sup>52</sup> It was found that the size of micelles changes as a function of pH. At pH < 5 micelles size increases due to the protonation of pyridine units while at basic pH deprotonation of pyridine units cause collapse of the inner poly (2-vinyl pyridine) block and decrease in micelle size. Gadgzinowski and Sosnowski<sup>53</sup> demonstrated the formation of biodegradable and biocompatible micelles based on poly(ethylene oxide-*b*-glycidol-*b*-L,L-lactide) terpolymers with potential in biomedical application for transformation of hydroxyl groups. The

structural properties of this type of micelles can be tuned by the molecular characteristics of the terpolymers. Tuning the micellar properties by chemical modification of terpolymer blocks was further investigated by Zhou et al.<sup>54</sup> They illustrated by selective fluorination of the poly(1, 2-butadiene) block to fluorinated poly (1,2-butadiene) in poly(ethylene oxide-*b*-styrene-*b*-1,2-butadiene) terpolymer, it is possible to transform core-corona spherical micelles to core-shell-corona oblate elliptical micelles due to the high hydrophobicity of the fluorinated poly (1,2-butadiene). Recently, Ward and Georgiou systematically investigated how the molecular weight, architecture and composition of triblock terpolymers influences their self-assembly and thermoresponsive behaviour.<sup>55</sup>

As reviewed, depending on the selectivity of the prevailing solvent towards each block of terpolymers, a wide range of micellar self-assemblies can be formed in solution which can be classified in three types. Firstly, ABC terpolymers with one solvophilic (like solvent) terminal block (A or C) and two solvophobic (hate solvent) blocks (B and C or A and B) which yield core-shell-corona or core-corona structures. Secondly, ABC terpolymers with both terminal block solvophilic (A and C) and the middle block solvophobic (B) tend to self-assemble into micelles with mixed or compartmentalised coronas. The last group are ABC terpolymers with a solvophilic middle block (B) and solvophobic terminals (A and C) lead to formation of flower-like micelles.

This work focuses on the second type of ABC terpolymers with A and C solvophilic and middle block (B) solvophobic in aqueous solutions. In this class of ABC terpolymers, depending on the compatibility of A and C blocks, three types of micelles can be formed namely, micelles with mixed coronas, micelles with compartmentalised coronas (patchy surface micelles) and Janus micelles (see Figure 1.4).

**Figure 1.4.** Schematic presentation of three types of micelles formed from ABC terpolymer with solvophilic A and C blocks (dark and light blue chains) and solvophobic middle block (red chains).



Micelles with mixed coronas, also known as *heteroarm starlike micelles* due to their similar appearance to heteroarm star copolymers,<sup>56</sup> form particularly when the solvophilic A and C blocks are compatible or interacting with each other. Tsitsilianis and Sfika<sup>56</sup> reported the formation of micelles with mixed coronas based on polystyrene-*b*-poly(2-vinyl pyridine)-*b*-poly(methyl methacrylate), PS-*b*-P2VP-*b*-PMMA terpolymer. Micelles were prepared in toluene where hydrophilic P2VP block formed the micelles core while hydrophobic PS and PMMA constituted the mixed corona. Later on they demonstrated formation of micelles with mixed coronas in aqueous solution as a function of pH, using poly(2-vinylpyridine)-*b*-poly(methyl methacrylate)-*b*-(poly(acrylic acid)) terpolymer, P2VP-*b*-PMMA-*b*-PAA.<sup>57</sup> Micelles with mixed coronas were formed at low pH (1-2), since terminal P2VP and PAA blocks exhibit attractive interactions.

Micelles with segregated or compartmentalised coronas form when two terminal blocks are partially incompatible in solution. Muller and coworkers showed the formation of micelles with segregated coronas (patchy corona) as a function of temperature, using a series of poly(ethylene oxide)-*b*-poly(*n*-butyl acrylate)-*b*-poly(N-isopropylacrylamide), (PEO-*b*-PBA-*b*-PNIPAM) terpolymers in aqueous solution.<sup>58</sup> At ambient temperature, both terminal blocks were soluble in the solution and formed the mixed coronas while PBA middle block formed the core. Once temperature raised to 45°C the solubility of PNIPAM diminished and segregation between PEO and PNIPAM occurred, which was resulted in formation of micelles with segregated coronas. Recently, a theoretical simulation modelled a

series of ABC terpolymer with solvophobic B block linked to solvophilic A block and thermoresponsive C block.<sup>59</sup> In the simulation, the solubility of thermoresponsive C block was designed to reduce with decreasing the temperature. Also the length of the C block was varied while A and B kept constant. It was revealed that by decreasing the temperature and increasing the length of thermoresponsive C block, micelles with B core and mixed A and C corona first transform to worm-like micelles with segmented A and C coronas and further to spherical micelles with compartmentalised B core, C patches (raspberry-like) and A corona.

Janus micelles are form due to the extreme segregation of corona where each solvophilic block occupies a hemisphere. They have been prepared using different approaches, such as dispersing the core cross-linked self-assembled triblock copolymer in bulk into selective solvent,<sup>60</sup> encapsulation of PS sphere by Janus sheets<sup>61</sup> and exchanging the solvent with a selective solvent for C block.<sup>62</sup>

#### ***1.4.1 Mechanism of micellisation***

The spontaneous self-assembly of amphiphilic copolymers in selective solvent (water) is due to the *hydrophobic effect* which forces the hydrophobic blocks to associate with each other in order to minimise their exposure to water, while the hydrophilic blocks tend to face outer aqueous solution. The hydrophobic effect is an entropically driven process in which highly ordered water molecules with highly dynamic hydrogen bonding network are disrupted by addition of nonpolar salute (hydrophobic block). This disruption is unfavourable in terms of free energy of the system because of the significant loss in transitional and rotational entropy of water molecules. Once the hydrophobic blocks aggregate together, the exposed surface area of nonpolar molecules to water molecules reduces, therefore, the disruptive effect is minimised which results in higher entropy of the system.<sup>63, 64</sup> The Gibbs free energy for micellisation is defined as bellow:<sup>63</sup>

$$\Delta G_{micel} = RT \ln(CMC) \qquad \text{Eq. 1.2}$$

Where, R is the universal gas constant, T is the absolute temperature and CMC is the critical micelle concentration. The CMC is defined as the concentration at which surfactant molecules or amphiphilic copolymers self-assemble in solution to

create a micro-phase separation in a way that the surfactant has a minimal energy effect on the bulk solution.<sup>65</sup> In the next section, methods used for CMC measurement are described.

#### ***1.4.2 CMC measurements***

There are many methods to measure the CMC of amphiphilic copolymers such as tensiometry,<sup>66, 67</sup> spectrofluorometry,<sup>67-71</sup> conductometry,<sup>67-71</sup> sound velocity,<sup>72</sup> static and dynamic light scattering,<sup>73</sup> which are all based on an abrupt change in the related physical properties upon micelle formation.

In this work the CMC of amphiphilic terpolymers was measured by pyrene fluorescence spectroscopy to verify the effect of terpolymers composition on the CMC point. Kalyanasundaram and Thomas<sup>74</sup> first reported the pyrene fluorescence spectroscopy measurements in 1977 and since then it has been widely used to measure the CMC of various amphiphilic molecules because of its high sensitivity. Pyrene fluorescence spectrum illustrates two relatively strong intensity peaks at  $\lambda_{\text{max}} = 373$  and 383 nm, known as  $I_1$  and  $I_3$  respectively (see Figure 1.5).

The intensity of  $I_1$  or  $I_3$  is dependent on solvent polarity and the hydrophobicity of the surrounding environment, making them useful for studying the aggregation properties of amphiphilic molecules. At very low concentration of amphiphile ( $< \text{CMC}$ ) pyrene freely interacts with polar solvent. Upon increasing the concentration of amphiphile in the solution, the intensity of either  $I_1$  or  $I_3$  increases as the microenvironment of pyrene changes from polar to non-polar and pyrene preferentially interacts with the hydrophobic portion of amphiphile. At CMC, the high hydrophobicity of the micellar core minimizes the hydrophobic interactions of pyrene with the solvent and therefore the intensity of either  $I_1$  or  $I_3$  stops or slows changing.<sup>74</sup> Figure 1.6 illustrates a typical graph of intensity of  $I_3$  peak versus concentration of amphiphilic copolymer. The concentration at which intensity of either  $I_1$  or  $I_3$  stops changing is reported as CMC.



**Figure 1.5.** Fluorescence spectra of pyrene ( $5 \times 10^{-7}$  M) in aqueous solutions of polystyrene<sub>23</sub>-*b*-poly(tertbutylacrylate)<sub>30</sub> at different concentrations. <sup>69</sup>

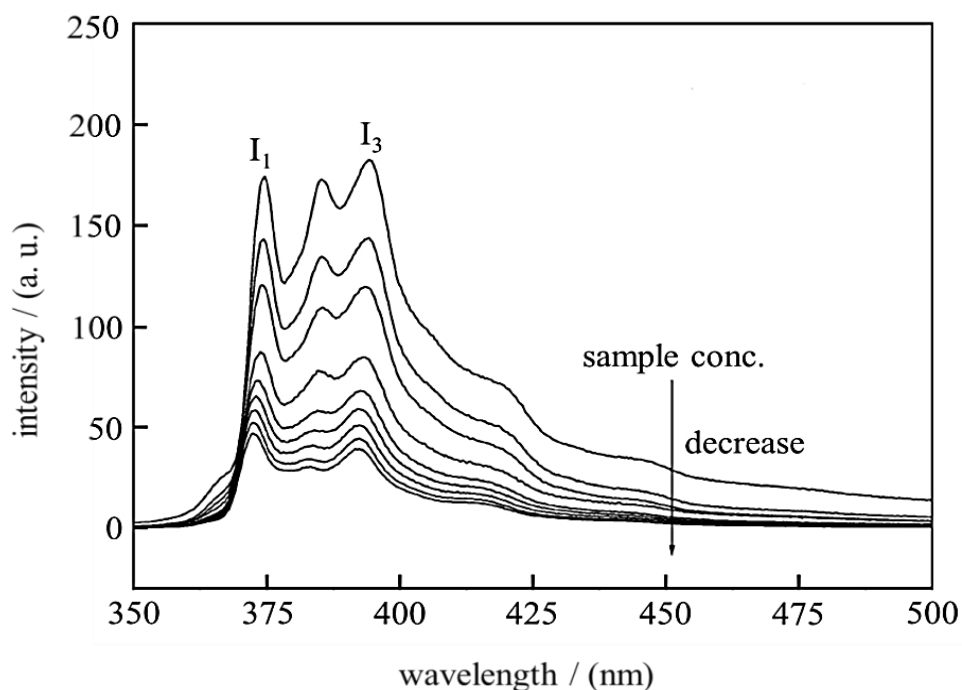
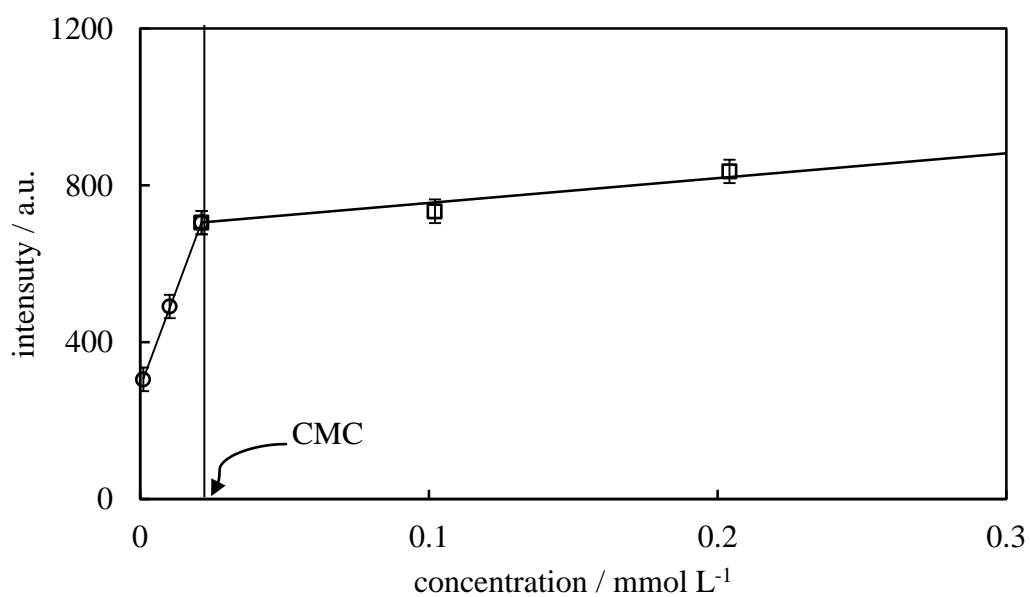


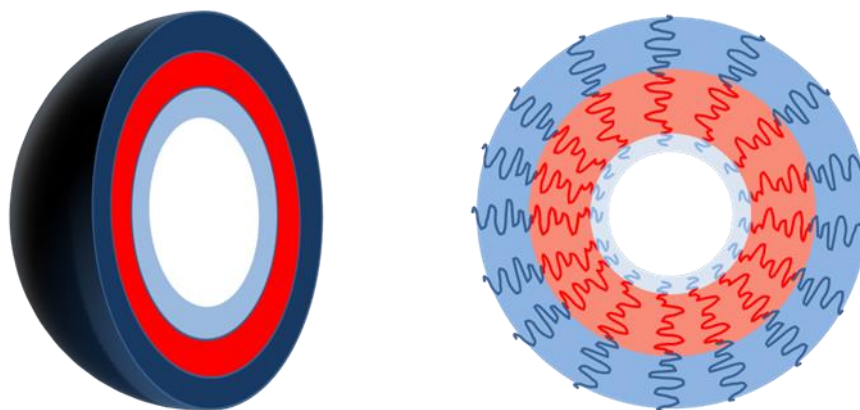
**Figure 1.6.** Determination of CMC by plotting the fluorescent intensity of pyrene at 383 nm ( $I_3$ ) versus different concentrations of PEGMA<sub>8</sub>-*b*-BuMA<sub>38</sub>-*b*-DMAEMA<sub>19</sub> terpolymer solution. Error bars are corresponding to standard deviations.



## 1.5 Polymersomes-vesicular self-assemblies of copolymers

Polymersomes are a class of artificial vesicles formed by the self-assembly of amphiphilic block copolymers. These polymeric vesicles are hollow spheres with a hydrophobic bilayer or monolayer membrane and hydrophilic internal and external coronas with size ranging from 50 nm to 5  $\mu\text{m}$  or more (see Figure 1.7).<sup>75, 76</sup> The term polymersome, polymer-based liposome, was first invented by Discher and his co-workers in 1999 when they reported this class of vesicles for the first time.<sup>77</sup> The reason behind this naming comes from the similarity of polymersome structure to liposomes, which are vesicles formed naturally from lipids. Polymersomes are also called polymer vesicles in some literatures.

**Figure 1.7.** 2D and 3D schematic presentation of a polymersome formed from ABC terpolymers with hydrophilic A and C blocks (dark blue and light blue chains respectively) and hydrophobic B block (red chains).



Both polymersomes and liposomes can encapsulate molecules due to their structure, which provides a physical membrane that can isolate the encapsulated molecule from external surroundings. However, compared to lipid-based vesicles, polymersomes benefit from certain advantages. Firstly, they are more robust due to greater wall thickness and are easier to be tailored. Synthetic copolymers can be easily and systematically altered to form vesicles with the desirable size and properties. Furthermore, synthetic polymers can easier be modified to attach specific functional groups that could for example enhance the uptake from a specific type of cells like cancer cells, thus enhance targeted drug delivery. Consequently, in the last

decade there has been a considerable interest in the synthesis, design, formulation and encapsulating properties of these novel vesicles.<sup>78</sup>

The large internal cavity and thick walls of polymersomes make them promising carriers for many molecules; including drugs, medical imaging contrast agents, health-supplements and vital nutrients.<sup>3, 79, 80</sup> It is important to notice that polymersomes unlike the conventional micelles, which are also formed by amphiphilic block copolymers and are used to encapsulate hydrophobic molecules, can carry *both* hydrophilic and hydrophobic molecules. Therefore, not only polymersomes can deliver hydrophobic molecules which without encapsulation are unpalatable or fail to be absorbed, but also can deliver hydrophilic molecules like DNA that need to be protected from degradation (environmental or enzymatic).<sup>39</sup>

Additionally, as it was mentioned above, biologically active molecules can be attached onto the hydrophilic exterior corona of polymersome to alter the interaction of that with the surroundings<sup>81</sup> and consequently be used for targeted drug delivery. Finally, the feasibility of manipulation of the polymersomes structures enables the control over their permeability, release rates and stability.

Similar to liposomes, the macromolecules used for polymersomes formation are amphiphilic. Polymers with amphiphilic nature consist of both hydrophilic and hydrophobic blocks. Depending on hydrophilic/hydrophobic ratio and self-assembly conditions, when hydrated the polymers can self-assemble into polymer vesicles. The spontaneous self-assembly of amphiphilic copolymers is due to the hydrophobic effect and the tendency of hydrophobic blocks to associate with each other to minimise their exposure to water, while the hydrophilic blocks tend to face inner and outer hydrated solution (water), thereby, confine the two interfaces of the membrane.<sup>82</sup>

The polymersomes features can be tailored by varying the copolymer's characteristics, for example by varying the chemical structure of the block copolymer, the membrane fluidity, permeability and the corona functionalisation can be altered. In addition, by altering the polymer block length or by changing the solvent ratios, the size of polymer vesicles can be controlled.<sup>38</sup> Finally, the thickness

of the membrane can also be altered from several nanometres to tens of nanometres (5-30 nm) by changing the length of the hydrophobic block.<sup>83</sup>

In recent years, significant studies have been done in the field of polymer vesicles by many research groups. A number of outstanding vascular structures have been prepared from terpolymers which are reviewed in this section. ABC terpolymers with hydrophilic A and C terminal blocks and hydrophobic B middle block can form vesicles with A and C external and internal coronas while the insoluble B block forms the membrane. The first work on formation of vascular structures from ABC terpolymer was reported by Yu and Eisenberg<sup>84</sup> in 1998 when they reported a preliminary study of a variation of morphologies formed from (PS<sub>180</sub>-*b*-PMMA<sub>67</sub>-*b*-PAA<sub>37</sub>) by gradual replacing the good solvent of the polymer solution (dioxane or THF or DMF) with water which is a poor solvent for PS and PMMA blocks. They suggested upon addition of adequate amount of water to polymer solution, polymer aggregation morphology turns from micelles into polymersomes consisting of PS which is sandwiched between two PMMA layers and finally hydrophilic inner and outer PAA coronas. Later on, Bieringer and co-workers<sup>85</sup> reported the formation of polymersomes from poly[5-(N,N-dimethylamino)isoprene]-*b*-polystyrene-*b*-poly(*tert*-butyl methacrylate) terpolymer (PDMAI-*b*-PS-*b*-PBuMA) in solution as a function of pH. Polymersomes made from AB and BC diblock copolymers, with A and C hydrophilic coronas and B block as membrane have been reported before by Luo and Eisenberg.<sup>86</sup> It was found that according to the length, the longer A block preferred the more spacious external coronas while shorter C block favoured the more crowded internal coronas to better accommodate the geometric demands. The same phenomenon was observed for ABC terpolymers by Stoenescu and Meier<sup>87</sup> when they used (poly(ethylene oxide)-*b*-poly(dimethyl siloxane)-*b*-poly(methyl oxazoline)) terpolymer (PEG-*b*-PDMS-*b*-PMOXA) to form vascular structures by direct dissolution of terpolymer in aqueous solution. They observed terpolymers with long PMOXA block (PEG<sub>45</sub>-*b*-PDMS<sub>67</sub>-*b*-PMOXA<sub>346</sub>) provide polymersomes with PMOXA external coronas while PEG<sub>45</sub>-*b*-PDMS<sub>40</sub>-*b*-PMOXA<sub>97</sub> with shorter PMOXA block length forms polymersomes with PMOXA internal coronas. They selectively labelled one end of terpolymer with a fluorescent dye (7-methoxycoumarin) and used quenching experiments to determine whether the labelled hydrophilic PMOXA block was oriented toward the interior or

the exterior of the vesicles. In addition, Liu and Eisenberg<sup>88</sup> demonstrated that it is possible to control the occupying tendency of terpolymer terminal blocks as a function of pH once one of the terminal block ionised at acidic pHs and the other one ionised at basic pHs. They prepared polymersomes using poly(acrylic acid)-*b*-polystyrene-*b*-poly(4-vinyl pyridine) terpolymer (PAA<sub>26</sub>-*b*-PS<sub>890</sub>-*b*-P4VP<sub>40</sub>) which possess both acidic PAA and basic P4VP blocks. The polymersomes were prepared via gradual solvent displacement of polymer solution from a good solvent (DMF) for all blocks to a bad solvent (water). The chains of the ionised block at a given pH start to repel each other and therefore, require more space and preferentially occupy the more spacious external corona. Using this strategy, it is possible to simply invert the vascular structure as a function of pH. Recently, Eisenberg et al.<sup>89</sup> prepared breathing vascular structure based on PEO<sub>45</sub>-*b*-PS<sub>130</sub>-*b*-PDEAEMA<sub>120</sub> by gradual solvent replacement of basic dioxane polymer solution with water. By incorporating a stimuli responsive PDEAEMA block into the vesicular wall, it turns to be thicker or thinner as a function of pH. At basic solution the PDEAEMA block incorporate with the PS block to form the membrane while PEO block forms the inner and outer coronas. At acidic pH, the vesicle wall is consisting of a PS-PDEAEMA-PS type of structure in which the hydrophilic PDEAEMA block in acidic pH is now sandwiched between two hydrophobic PS blocks, while the hydrophilic PEO blocks form the inner and outer coronas. More recently, Kempe et al.<sup>90</sup> reported formation of vascular structures of poly(2-(2,6-difluorophenyl)-2-oxazoline)-*b*-poly(2-(1-ethylheptyl)-2-oxazoline)-*b*-poly(2-ethyl-2-oxazoline) terpolymer (PODFOX<sub>23</sub>-*b*-PEPOX<sub>28</sub>-*b*-PEtOX<sub>49</sub>) which were formed by direct dissolution of polymer in water. They found that firstly cylindrical micelles with PODFOX core, PEPOX shell and PEtOX corona were formed which later on due to the low solubility of PEtOX block converted to rolled cylindrical micelles to reduce their exposure to water. They suggested the formed rolled cylindrical micelles were a meta-stable intermediate structure between cylindrical micelles and vesicles. The structure of formed polymersomes was based on hydrophilic PEtOX inner and outer coronas, while PODFOX block were sandwiched between two PEPOX layers in the formed membrane. Very recently, Du and coworkers<sup>91</sup> reported the preparation of pH-responsive vesicles from terpolymers containing hydrophilic poly[2-(methacryloyloxy)ethyl phosphorylcholine] (PMPC), pH-sensitive (hydrophobic at

6.2-6.8) poly[2-(diisopropylamino)ethyl methacrylate] (PDPA) and cross-linkable hydrophilic PDMAEMA blocks (PMPC<sub>25</sub>-*b*-PDMAEMA<sub>23</sub>-*b*-PDPA<sub>136</sub>), while they varied the PDPA block degree of polymerisation from 136 to 71 to 37. Also, they used PMPC<sub>25</sub>-*b*-PDPA<sub>107</sub>-*b*-PDMAEMA<sub>14</sub> in which the PDMAEMA block was in the middle while PMPC and PDMAEMA were the terminal blocks. Vesicles were formed from terpolymers with relatively long PDPA block by changing the pH from acidic (pH: 2) to neutral in pure water. At pHs above 6.2, the PDPA block becomes hydrophobic and therefore can form the vesicle membrane which is sandwiched between two hydrophilic PDMAEMA shells while PMPC blocks formed the inner and outer coronas in all cases. In the case of PMPC-*b*-PDMAEMA-*b*-PDPA, the PDMAEMA chains formed the middle shell between the PDPA membrane and PMPC coronas. Terpolymers with shortest PDPA block length just formed micelles. When PMPC<sub>25</sub>-*b*-PDPA<sub>107</sub>-*b*-PDMAEMA<sub>14</sub> terpolymer was used, the PDMAEMA incorporated with PMPC to form mixed coronas while PDPA formed the membrane.

### ***1.5.1 Polymersomes fabrication methods***

A number of methods have been employed in order to prepare polymersome either from bi- or terpolymers during the last couple of decades which are reviewed in this section. The first approach for fabrication of polymersomes is solvent free approach which includes film rehydration method, polymer hydration method and electro formation method. Generally, in all solvent free methods, the amphiphilic polymer is brought in contact with the aqueous medium in its dry state and is subsequently hydrated to yield vesicles.<sup>92</sup>

For example in film rehydration method, firstly the amphiphilic polymer is dissolved in an organic solvent followed by evaporation of the solvent to form a polymeric film on the glass surface. Subsequently, by addition of aqueous buffer, the polymeric film is rehydrated to form the polymersomes.<sup>77, 93</sup> Normally polymersomes prepared using this method, have small multi-lamellar structures with a broad size distribution.

In polymer rehydration method, amphiphilic polymer is not hydrated as a thin film but is directly hydrated as bulk powder in aqueous buffer solution. In this

method, similar size, size distribution and structures to film rehydration method is generally observed.<sup>92</sup>

In electro formation method, similar to film rehydration method, firstly a thin film of polymers is prepared but not on a glass surface. Instead, the polymer film is spread on a pair of electrodes and electric current is applied after addition of aqueous buffer to facilitate the hydration process. Employing this method, mono-dispersed polymersomes with micrometre size range were obtained although low yield was achieved.<sup>77, 93, 94</sup> Except the polymer rehydration method, all mentioned solvent free methods are not absolute solvent-free method, because of the involvement of organic solvent during the film preparation prior to the vesicle formation.

The second approach for the preparation of polymersomes is solvent displacement approach, in which initially the amphiphilic copolymers are dissolved in an organic solvent which can dissolve both blocks. Then by gradual addition of water to the copolymer solution under vigorous stirring, the hydrophobic blocks tend to associate together to have the lowest contact with the water and therefore form the polymersome membrane, whereas, the hydrophilic blocks are solvated to form the corona which can stabilise the polymersomes. In this method, the final ratio of organic solvent/water can strongly affect the morphology of resultant self-assembly. The organic co-solvent can be removed by dialysis which is time consuming and economically unfavourable. In addition, removal of organic solvent can sometimes lead to a change in the morphology in the resultant self-assembly or even break down of the self-assembly. The resultant polymersomes are relatively small and their size distribution is broad.<sup>92</sup>

The third method used for the polymersomes preparation is w/o/w double emulsion method. In this method a uniform double emulsion is formed employing microfluidic technique as a template for assembly of amphiphilic polymer into vesicle structure.<sup>95, 96</sup> The organic solvent in w/o/w double emulsion is normally volatile and contains the amphiphilic polymer. By evaporation of organic solvent ultimately, the w/o/w emulsion converts to vascular structure. Using this technique, micron size polymersomes with very narrow polydispersity were formed.

### ***1.5.2 Mechanism of polymersomes formation***

Based on the theoretical calculations and simulations which studied and modelled the polymersomes formation in aqueous solution, two different mechanisms have been proposed.<sup>39</sup> For simplification, these two mechanisms are illustrated in Figure 1.8 for a diblock copolymer.

In Mechanism I, primarily, the amphiphilic block copolymers (blue-red chains in Figure 1.8) start to self-assemble into small spherical micelles in a relatively rapid process. The spherical micelles then grow up to large spherical micelles by the evaporation-condensation-like process. The large spherical micelles are energetically unfavourable and thus the large micelles take the solvents into them to lower the energy. This mechanism is believed to occur in the systems at which an organic co-solvent with partial solubility in water is used (solvent displacement method), therefore water can diffuse slowly into the interior of the formed self-assembly.<sup>39</sup>

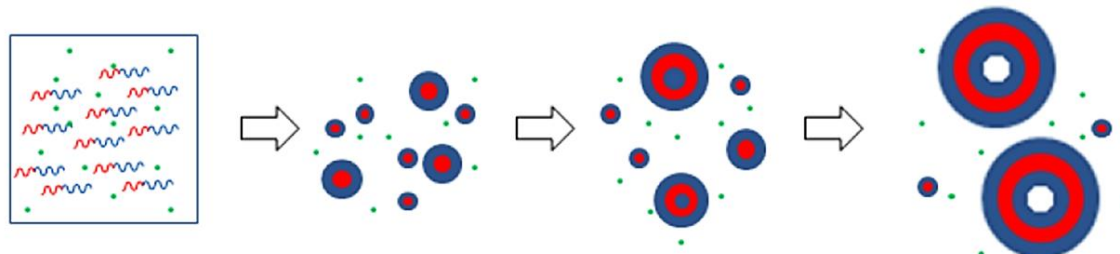
In Mechanism II, similar to mechanism I, at first, small spherical micelles are formed rapidly through self-assembly of amphiphilic block copolymers, which later on through collision process evolve into larger micelles with a cylindrical and/or open disk-like micellar structures. The formed disk-like micelles slowly approach to form polymersomes. The micelle growth process and the closure process are slower than the first spherical micelle formation process. This mechanism normally occurs when film rehydration method is used for the preparation of polymersomes, at which system undergoes vigorous agitation or shear providing enough energy for the initially formed micelles and disk-like micelles to collide and form polymersomes.<sup>39</sup>

Adams et al. proposed that the formation mechanism of polymersomes may affect the loading efficiency of hydrophilic molecules.<sup>97</sup> As it can be seen in Figure 1.8, Mechanism II involves the wrap up of disk-like micelles, which allows a relatively high efficiency encapsulation of hydrophilic molecules, by trapping them during this process. Conversely, in mechanism I, the small micelles growth leads to formation of polymersomes without having the chance to trap the hydrophilic molecules. This mechanism produces vesicles in which encapsulation of payload species is either absent or very low.

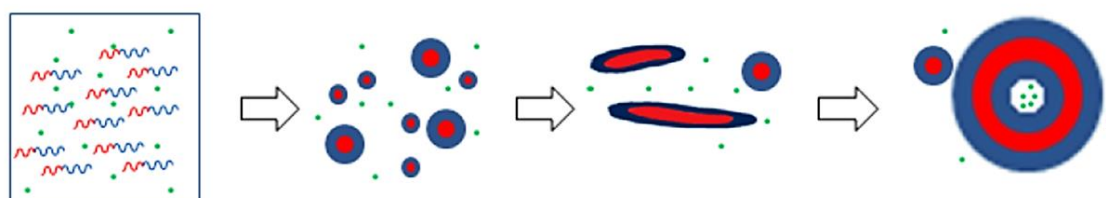



**Figure 1.8.** Schematic representation of two polymersomes formation mechanisms, mechanism I and mechanism II. Blue and red colours are corresponding to the hydrophilic and hydrophobic chains, respectively. Small green dots are corresponding to the payload molecules during the encapsulation process.


Mechanism I



Mechanism II



 amphiphile polymer

 payload molecule

The derived evidence from encapsulation studies<sup>97,98</sup> show that polymersomes formation mostly occurs through mechanism I, since very low payload efficiency during the encapsulation process has been reported. Therefore, as it mentioned before the major barrier that needs to overcome in order for polymersomes to be applicable as delivery carriers, is their low encapsulation efficiency using the current encapsulation methods.

## **1.6 Emulsions**

### ***1.6.1 Definition***

Emulsions are part of two-phase systems and they are defined as thermodynamically unstable heterogeneous systems of two or more immiscible liquids, where one of the phases is dispersed in the other as drops with size in micrometre range.<sup>99</sup> Emulsions can be made kinetically stable by addition of surfactants, polymers or particles which could be adsorbed at the two phase interface. Generally, there are two types of simple emulsions, one where oil drops are dispersed in water, which are called oil-in-water (o/w) emulsions and one where water drops are dispersed in oil phase, named water-in-oil (w/o) emulsion. However, more complex systems such as water-in-oil-in-water (w/o/w) or oil-in-water-in-oil (o/w/o), called multiple emulsions are also exist.<sup>100</sup> Nevertheless, in this work none of such o/w or w/o systems are considered and instead a new class of emulsions called water-in-water (w/w) emulsions which can be formed from ATPSs are studied.

### ***1.6.2 Emulsion formation***

When two immiscible liquids are placed together in a container, a layer of the less dense liquid forms on the top of the more dense liquid. This separation represents their thermodynamically most stable state. In the fully separated state both liquids have the minimum contact area with each other and therefore, the free energy of system is at its lowest. By applying energy to the system, it is possible to disperse one phase in the other one and produce large interface between two phases. However, due to high free energy of the system, the dispersed phase is moving and drops collide and merge (coalesce) to form larger drops and finally form the separated two phases in the absence of agitation. In order to stabilise the dispersed phase in the continuous phase it is necessary to use emulsifiers (stabilisers) to avoid the drops merging. Before describing the role of emulsifiers in stabilisation of emulsions, it is worthy to explain some basics for a better understanding.

As described before, by applying energy to two immiscible liquids, a large interface in compare to separated two phases is formed. Interface by definition is a boundary between two phases where they come into contact. When two liquids are

brought into contact, the surface where they make contact is called interfacial area. The work required to produce more interface (bring more molecules from the interior to the interface) between two liquids is known as interfacial tension. As interfacial tension is in fact the applied force per unit length or applied work per unit area, its unit can be expressed as mN/m or J/m<sup>2</sup>.<sup>99</sup>

From the thermodynamic point of view, in the bulk liquid molecules attract each other and each molecule is pulled equally in all directions by its neighbouring molecules, resulting in cancellation of forces and a net force of zero. However, on the surface molecules experience an imbalance of forces, therefore the net forces applied on the surface molecules is not zero and they are pulled inward. Therefore, some internal pressure is created and forces the liquid surface to contract to the minimal area. When two immiscible liquids are brought into contact with each other, the molecules experience an imbalance of forces at the interface. This leads to an accumulation of free energy at the interface. The excess energy is called surface free energy and causes the two liquids to have the minimum interfacial area. Therefore, formation of larger interfacial area for two immiscible liquids when being mixed is thermodynamically unfavourable as associated with higher interfacial energy.<sup>101</sup>

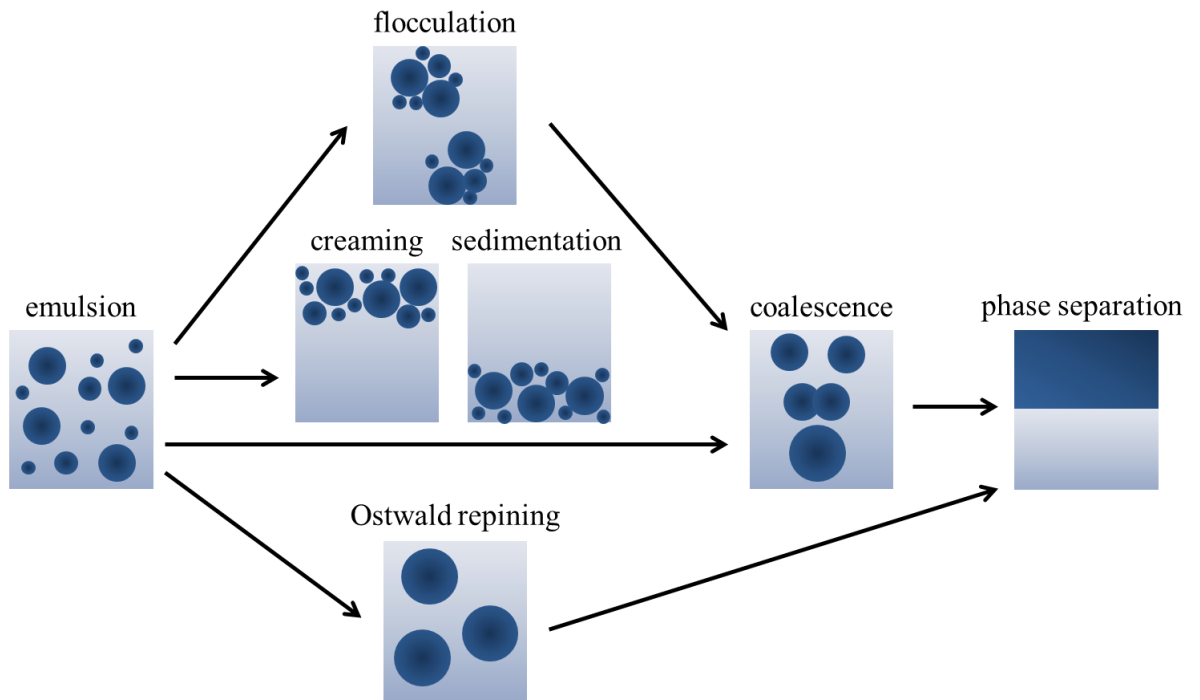
The role of emulsifier then is to decrease the interfacial tension. When emulsifier is added to the system while it is emulsifying, it adsorbs at the interface and stabilises the emulsion by reducing the interfacial tension and forming a protective layer around the dispersed phase to prevent droplets coalescence.<sup>101</sup>

### ***1.6.3 Emulsion stability***

Emulsion stability is the ability of an emulsion to resist changes in its properties and retain them unchanged over time. However, due to the thermodynamically unstable nature of emulsions, they undergo changes over time. As mentioned before, this is due to the large free energy of the system which cannot be compensated by entropy contributions. The slower emulsion changes over time, the more stable is the emulsion. Commonly, the stability of emulsions is assessed by monitoring their basis parameters, including number of dispersed drops, size distribution of drops and their spatial arrangement. A number of processes may cause the instability of emulsions over time depending on conditions. The four main

instability mechanisms commonly observed in emulsions are creaming or sedimentation, flocculation, coalescence and Ostwald ripening<sup>99</sup> which are shown in Figure 1.9.

**Figure 1.9.** Main instability mechanisms involved in breakdown of emulsions.



### 1.6.3.1 Creaming or sedimentation

Creaming or sedimentation occurs due to the difference in density of two phases (continuous and dispersed phases), consequently, emulsion drops tend to move up or down through the continuous phase under gravity. Creaming is the upward movement of dispersed phase under gravity to top of the system without any change in drop size distribution, which is due to the lower density of dispersed phase in compare to continuous phase. Oppositely, sedimentation is the downward movement of the dispersed phase due to the fact that they are denser than the continuous phase.<sup>99</sup> Stokes law illustrates a qualitative indication of factors affecting the creaming or sedimentation velocity ( $v$ ) of droplets in an emulsion:

$$v = \frac{2 g r^2 (\rho_{cont.} - \rho_{drop})}{9 \eta_{cont.}} \quad \text{Eq. 1.3}$$

Here,  $v$  is creaming or sedimentation velocity,  $g$  is the gravity acceleration,  $r$  is the radius of the droplet,  $\eta$  is the viscosity of continuous phase,  $\rho_{\text{cont.}}$  and  $\rho_{\text{drop}}$  are the densities of continuous and dispersed phases, respectively. As it can be seen in Stokes equation, the density difference between two liquids, the viscosity of the continuous phase and the drop size affect the creaming or sedimentation velocity. There are several ways to minimise creaming or sedimentation process.<sup>102-104</sup> One way is to minimise the density difference between two phases by either adding a weighting agent to the less dense phase or using a highly dense emulsifier. Secondly, by using efficient homogenisers smaller size droplets can be formed which reduces the creaming or sedimentation rate. In addition, by increasing the viscosity of continuous phase through addition of thickeners or gelling agents, the velocity of droplets decreases which lead to slower creaming or sedimentation process. Finally, by increasing the number of droplets in continuous phase, droplets will be closely packed which results in less movement of them.

Creaming or sedimentation process can be assessed by simply visualising a whitish layer on top or bottom of the emulsion. By measuring the volume fraction of this layer over time the creaming or sedimentation rate can be determined. However, visual observation might be not accurate enough in the cases where creaming or sedimentation is quick or the distinction between the continuous phase and the creamed or sediment layer is difficult to be visualised. In this case, some other techniques such as light scattering<sup>104</sup> or ultrasonic imaging<sup>105</sup> can be useful.

#### *1.6.3.2 Flocculation*

Emulsion droplets are constantly moving because of the Brownian motion, gravity or mechanical agitation which causes their collision. This collision might result in flocculation process in which dispersed drops aggregate and create large clusters of drops in the continuous phase. In this process, the thin film of continuous phase between droplets do not rupture, therefore, droplets do not merge together and keep their identity. The rate and extent of flocculation is related to the frequency and probability of emulsion droplets to collide. The frequency of collision is corresponding to the Brownian motion or shear flow, while the probability of collision is associated with the interaction energy. Three components contribute in the droplets interaction energy, namely, van der Waals attraction, electrostatic

repulsion and steric repulsion. Depending on strength of the inter-drop forces, this process can be reversible by gentle agitation. The weaker the inter-drop forces, the easier the breakup of flocculation. Emulsions with large drop size distribution give rise to flocculation since the differential creaming (or sedimentation) rate of small and large drops cause them to come into close proximity more than an emulsion with mono-dispersed drop size.<sup>99</sup> By regulating the interactions between the droplets, it is possible to control the rate and extent of flocculation within an emulsion. There are several ways to reduce the flocculation rate, such as increasing the concentration of emulsifier in ionic emulsions, addition of ionic surfactants to non-ionic emulsions and using long chain polymer emulsifiers.<sup>99</sup>

Flocculation process can be assessed by microscopic observation of emulsion but special care should be taken to not break the flocs while the microscope sample is prepared. The size of flocs can be determined by particle sizing instruments<sup>106</sup> or image analysis techniques<sup>107</sup> which also help to determine the flocculation rate over time.

#### *1.6.3.3. Coalescence*

Coalescence is the process in which emulsion drops combine together and merge to form larger drops. This process is irreversible and the thin film of continuous phase between drops interface is ruptured.<sup>99</sup> Coalescence results in destabilisation of emulsions by formation of large droplets which leads to phase separation of emulsions. Emulsion droplets are constantly moving and when they move very close to each other, their surface might deform and flattened. This causes an increase in surface area of droplets in contact with each and rupture of the thin film, subsequently coalescence occurs. Coalescence of emulsion droplets is significantly dependent on the continuous phase and emulsifier properties as well as colloidal and hydrodynamic interactions between droplets. There are a few methods to control and reduce the coalescence rate in emulsions, based on decreasing droplets contact and thin film rupture,<sup>108</sup> such as using charged emulsifiers to induce electrostatic repulsion between droplets and using proteins or fine solid particles to be adsorbed at the interface and form a physical barrier preventing coalescence.

Coalescence process can be studied using optical microscopy technique by monitoring changes in droplets size and shape over time. Also, by using particle sizing techniques the droplet size and size distribution can be measured over time.

#### 1.6.3.4 Ostwald ripening

Ostwald ripening is a process in which the small drops of dispersed phase gradually dissolve in the continuous phase and redeposit onto the bigger size drops over time as the bigger drops are energetically more favourable.<sup>99</sup> According to the Kelvin equation, the solubility of dispersed phase in continuous phase increases as the drop size decreases.

$$c(r) = c(\infty) \exp\left(\frac{2\gamma V_m}{rRT}\right) \quad \text{Eq. 1.4}$$

Here,  $c(r)$  is the aqueous phase solubility ( $\text{m}^3 \text{m}^{-3}$ ) of solute (dispersed phase) with radius  $r$ ,  $c(\infty)$  is the solubility in a system with only planar interface,  $\gamma$  is the interfacial tension between two phases,  $V_m$  is the molar volume of dispersed phase,  $R$  is universal gas constant and  $T$  is the absolute temperature.

Therefore, Ostwald ripening process can be minimised by increasing the size of droplets. In practice as the average drop size increases, Ostwald ripening slows down. However, at this condition it is more likely that flocculation and coalescence occur. Another way to reduce Ostwald ripening process is to use emulsifiers that do not increase the solubility of the dispersed phase in the continuous phase. Also by using appropriate additives which reduce the solubility of dispersed phase, Ostwald ripening process can be minimised.<sup>99</sup> Similar methods used for assessing the coalescence process can be used for characterisation of emulsions in terms of Ostwald ripening process.

#### 1.6.4 Thermodynamic and kinetic stability of emulsions

Studying emulsions from thermodynamic point of view provides information regarding processes taking place during emulsification or afterwards, while kinetics study gives information about the rate at which these processes occur. For instance, the phase separation of an emulsion is due to the thermodynamic instability while the time taken for the dispersed drops to merge is corresponding to kinetics point of

view. As it stated before, emulsions are thermodynamically unstable but they could be kinetically stable over period of time using the appropriate stabilisers by reducing the rate of instability processes over time. Next section describes the stabilisation of emulsions using different types of stabilisers.

### ***1.6.5 Stabilisation of emulsions using different types of stabilisers***

Emulsions can be stabilised by the mean of surfactants, polymers and particles or a mixture of them. In this work stabilisation of emulsions by amphiphilic block copolymers and particles is of particular interest.

Emulsions can be stabilised by polymers in a way that a protective film of polymers is formed at the liquid-liquid interface which can provide a steric hindrance and effectively prevent the coalescence of the dispersed phase.<sup>5-7</sup> In addition, polymers can also increase the stability of emulsions by thickening the continuous phase where the rate of creaming or sedimentation of dispersed phase decreases in the system.<sup>109</sup> There are certain criteria for a polymer to act as an effective stabiliser against destabilisation processes introduced earlier. Firstly, polymer should provide a complete coverage of the emulsions droplets. Incomplete coverage may result in flocculation or coalescence as a result of van der Waals attractive forces. Secondly, there should be strong adsorption or anchoring of the polymer molecule to the surface of emulsion droplets in order to protect the interface. Finally, existence of a fragment which can be strongly solvated to provide effective steric stabilisation is necessary. These essential criteria can be best served using amphiphilic block copolymers.<sup>110</sup> Similar to surfactants, the hydrophilic/hydrophobic block ratio of copolymers can determine the type of formed emulsion. At equal volume fractions of oil and water phases, polymers with long hydrophilic and short hydrophobic chains results in the formation of oil-in-water emulsions, whereas polymers containing larger hydrophobic block form water-in-oil emulsions.<sup>111</sup>

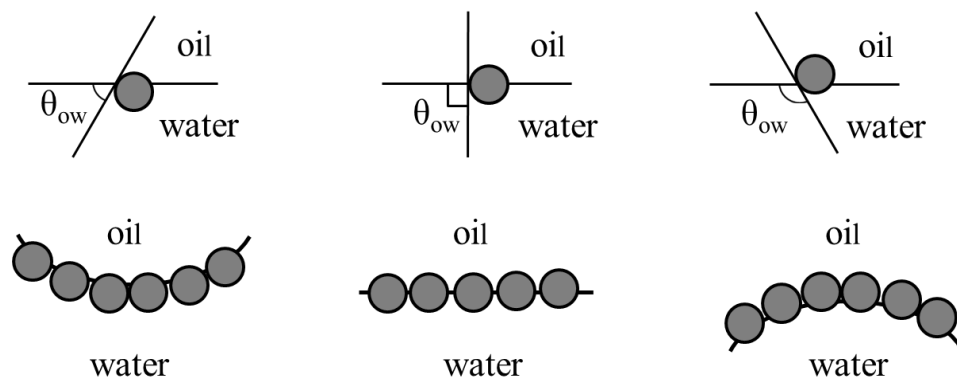
Particles also have been widely used for stabilisation of emulsions, known as Pickering emulsions.<sup>112</sup> Unlike surfactant and amphiphilic polymers that are in a state of rapid dynamic equilibrium with their unimers attaching and detaching from the interface on a micro-second time scale,<sup>113</sup> particles are almost irreversibly trapped at the liquid-liquid interface.<sup>114</sup> In particle stabilised emulsion systems,



colloidal particles can accumulate at the liquid-liquid interface to form a steric barrier against coalescence. Similar to surfactant or polymer stabilised emulsions, particles should provide almost a coherent monolayer on the interface as a mechanical barrier in order to prevent coalescence.<sup>115</sup>

For particles to adsorb at a liquid-liquid interface they do not need to be amphiphilic, rather it is the degree to which a particle is wetted by one or other of the liquids that adsorbs and anchors a particle to the interface. Wettability of a solid particle is a property that is intrinsically linked to whether a particle will adsorb at a liquid-liquid interface to stabilise the emulsion and determine the type of resulting emulsion (i.e. oil-in-water or water-in-oil). Wettability of particles at the interface can be quantified by the contact angle  $\theta_{ow}$  that the particle makes with oil-water interface. It is well-established that particles with  $\theta_{ow} < 90^\circ$  results in formation of oil-in-water emulsion, whereas water-in-oil emulsion forms when the  $\theta_{ow} > 90^\circ$ <sup>114</sup> (see Figure 1.10). This is similar to what is seen in surfactant or polymer stabilised emulsions, where it is the hydrophilic-hydrophobic balance that is responsible for the emulsion type. It should be noted that particle with too hydrophobic or hydrophilic characteristics would tend to remain dispersed in either the oil or aqueous phase respectively and would not adsorb at the fluid interface, resulting in highly unstable emulsions.

**Figure 1.10.** Location of solid particles at oil-water interface, with  $\theta_{ow}$  (measured through the aqueous phase) and the corresponding monolayer curvature when  $\theta_{ow}$  is less than  $90^\circ$ , equal to  $90^\circ$  and greater than  $90^\circ$  from left to right.



Considering a small, (typically less than a micron in diameter) spherical particle of radius  $r$ , the energy  $\Delta G_d$  needed for particle desorption from a water/oil interface of tension  $\gamma_{ow}$ , with contact angle of  $\theta_{ow}$  to either the oil or water phase is given by following equation:

$$\Delta G_d = \pi r^2 \gamma_{ow} (1 \pm \cos \theta_{ow})^2 \quad \text{Eq. 1.5}$$

The sign inside of the bracket is negative for removal of a particle into the bulk water phase, whereas for its removal into the bulk oil phase, the sign is positive. The maximum value of  $\Delta G_d$  is when the particle make  $90^\circ$  contact angle with the interface, where particles is held most strongly at the interface. In contrast, for particles with a contact angle between  $0-20^\circ$  or  $160-180^\circ$ , the energy needed for desorption  $\Delta G_d$  of particles from the interface drops down rapidly. When the  $\Delta G_d$  is close to thermal energy of the system, particles are not held at the interface irreversibly and are in a dynamic state of perpetual adsorption and desorption, consequently emulsion is very unstable. Therefore, the contact angle which particles make with the interface and particle radius has a key influence on the adsorption of the particles to the interface and stabilisation of emulsions.

### 1.7 Aqueous two phase system

ATPSs are aqueous mixtures of particular polymer-polymer or polymer-salt pairs at specific concentrations which can form two immiscible homogeneous phases in equilibrium. The ATPSs have been extensively used for the separation and partitioning of cell particles and biomolecules.<sup>116</sup> In this thesis polymer-polymer pair ATPSs are investigated.

The difference in the properties of ATPSs is small compared with the ordinary two-phase systems such as oil/water. For instance, the density difference is small, as well as the difference in refractive indices of the two phases. The small refractive index difference sometimes even makes it difficult to detect the interface. In addition, the interfacial tension in such systems is small (0.1-0.001 mN/m) and the formed boundary almost has a right angle with the wall of the test tubes. The most characteristic feature of ATPSs is that both phases are aqueous and the water content is between 85-99 wt.%.<sup>116</sup>

Such liquid phase separation in mixtures containing polymers was first reported by Beijerinck in 1896.<sup>117</sup> He observed that if aqueous solutions of gelatine and agar or gelatine and soluble starch were mixed, a turbid mixture which separated into two liquid layers is obtained. These systems were then further studied in detail by Ostwald and Hertel<sup>118, 119</sup> who found certain concentrations were necessary for the phase separation. Later studies on these systems gave evidence that incompatibility of the used polymers is required for the phase separation of ATPS. When two polymer solutions are mixed, there are three potential outcomes:

1. Incompatibility: the two polymer solutions phase separate and are collected in two different phases. This is the most common outcome for pairs of uncharged polymers.
2. Miscibility: the two polymer solutions are completely miscible. A homogenous solution forms.
3. Complex Coacervation: the two polymer solutions phase separate, but are collected in one phase, with a second phase made up mostly of solvent. This is a special case which occurs for solutions of two oppositely charged polymers.

To determine the result of the mixing of two polymers, two main factors must be taken into consideration, the first being the entropy gain due to mixing of the polymers and the second being the intermolecular interactions between the two different polymers. The gain in entropy is a direct consequence of the number of molecules involved in the mixing process, so it can be approximated that the entropy of mixing is the same for both small and large molecules. Conversely, the interaction energy between molecules tends to increase with the size of molecules, as it is a sum of the interactions of each segment of the molecule. Polymers are large molecular weight molecules, so it follows that in most cases the interaction energy (per mole) between molecules that dominates the phase behaviour of the system.

Consider that the interaction between two polymers is repulsive; each molecule is in its more thermodynamically stable situation when surrounded by like molecules (in the bulk). When mixed, the molecules are no longer in this energetically favoured condition, consequently, incompatibility arises and the system phase separates to give two phases each enriched with one or the other polymers.

Repulsive interactions between polymers are mainly due to different chain lengths and/or structural differences in the two polymers (this being the situation that would normally be expected in non-charged unlike polymers). However, if the interaction between two polymers is attractive, meaning unlike polymers attract one another and polymers are collected in a common phase, with a second phase being made up of mostly solvent. For this to occur, polymers must be strongly electrostatically attracted to one another i.e. complex coacervation. Finally, if interactions are neither repulsive nor attractive, polymers may be miscible and a homogenous solution is resulted.<sup>116</sup> Several pairs of polymers have been used forming aqueous two-phase systems, such as:

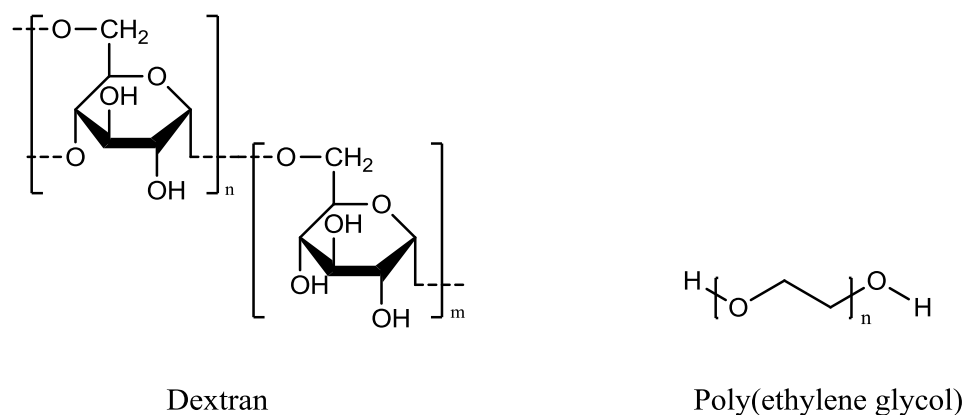
- Dextran - PEG
- Dextran - Ficoll
- Dextran – polyvinylalcohol
- Ficoll – PEG
- Polyvinylalcohol – PEG
- Dextran – hydroxypropyl starch<sup>120</sup>

Among the mentioned polymer pairs, the dextran-PEG pair was chosen for the preparation of ATPS in this work which is described in the next section.

### ***1.7.1 Dextran-PEG ATPS***

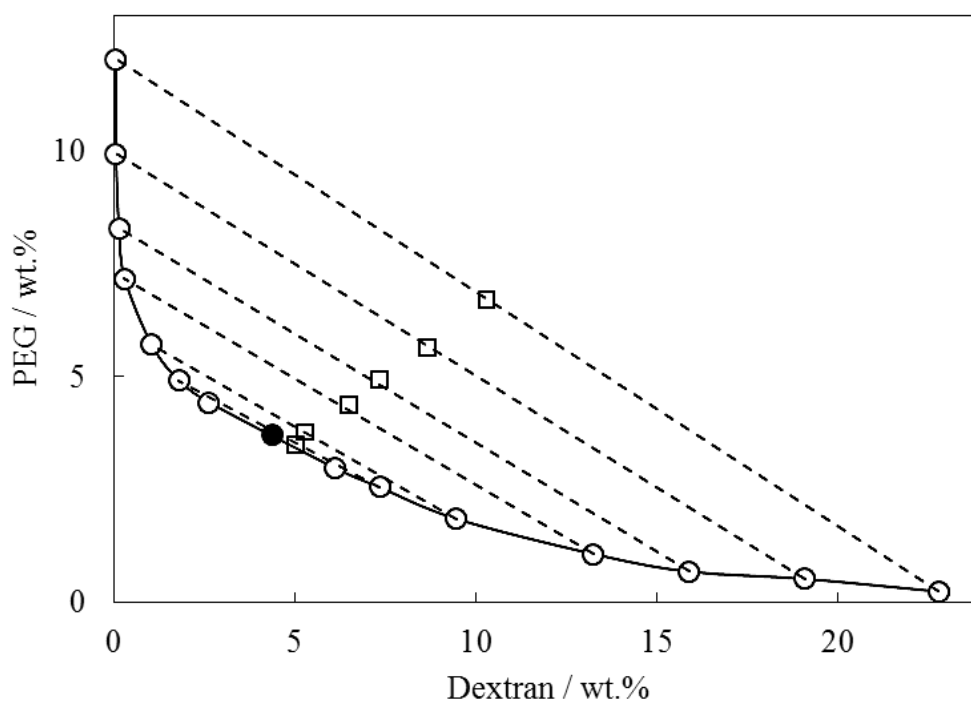
Dextran-PEG ATPS is one of the most studied ATPSs which was chosen for this study, since the phase diagrams, equilibrium phase behaviour and partitioning ability of this system are available in the literature.<sup>116</sup> More importantly, dextran and PEG are both biocompatible and have been widely used in biomedical applications. Dextran is a type of branched polysaccharide consisting of glucose molecules which have  $\alpha$ -1,6 glycosidic linkage between glucose molecules within the straight chain and  $\alpha$ -1,3 linkage within the branched chains. Dextran is available commercially and generally is synthesised from sucrose by some bacterium such as *Leuconostoc mesenteroides* and *Streptococcus mutans*. PEG is a linear polyether polymer consisting of ethylene glycol repeating units. The chemical structure of dextran and PEG is shown in Figure 1.11.

**Figure 1.11.** Chemical structures of dextran and PEG.



A better understanding of behaviour of dextran-PEG system in aqueous solution is given by their phase diagram. Figure 1.12 shows the phase diagram of ATPS containing the two hydrophilic polymers dextran and PEG at 20 °C <sup>116</sup>. In a mixture consisting of dextran, PEG and water, a two phase system will only arise when the constituents are present in a certain range of properties. The constituent at which phase separation occurs may be represented in a phase diagram.

**Figure 1.12.** Phase diagram of the dextran-PEG ATPS, dextran 500 ( $M_r$ : 500,000) and PEG 6000 ( $M_n$ : 6000 g/mol) at 20 °C. <sup>116</sup>



As it can be seen in this Figure, concentration of PEG is plotted versus concentration of dextran (the concentrations are expressed in weight per cent, wt. %). The curved line separating two areas is called a binodal. All mixtures which have compositions represented by points above the line give rise to phase separation, while mixtures represented by points below the line give a homogenous solution. The more the composition of the phase systems approaches to the binodal the less is the difference between the two phases. All compositions at the binodal are critical in the sense that a small change in composition gives rise to a drastic change in the system, namely from a one-phase system to a two-phase system. The lines across the binodal are called tie lines. Any total composition represented by points on the same tie line will give rise to phase systems with the same phase compositions, but with different volume fractions of the two phases. The square symbol on each tie line is where the volume fractions of the two phases are equal. In this work, concentrations corresponding to a tie line far away from the binodal were chosen to do the experiments with, in order to prevent any dramatic (phase) change in the system. Too high concentrations were also avoided, because, as the concentration of the polymer increases in the system, it becomes more viscous and it takes longer time to achieve phase separation.

### **1.8 Water in water emulsions based on ATPS**

Theoretically, a water-in-water (w/w) emulsion is a kind of system which consists of droplets of water-solvated molecules in another continuous aqueous solution. Both the droplet and continuous phases contain different molecules that are entirely water-soluble. As such, when two entirely aqueous solutions containing different water-soluble molecules are mixed together, water droplets containing predominantly one component are dispersed in water solution containing another component. In the case of using dextran-PEG ATPS, upon mixing the ATPS one phase will be dispersed into the other one depending on the volume fraction of each phase. Therefore, water-in-water (w/w) emulsion can be prepared based on ATPS if an appropriate emulsifier could stabilise the system.

### ***1.8.1 Challenges in stabilisation and characterisation of w/w emulsion***

The main challenge in preparing w/w emulsion based on ATPS system is the low interfacial tension of these systems. As mentioned before, the interfacial tension is very low in these systems (0.1-0.001 mN/m) comparing to oil/water interface (30-50 mN/m), which makes it difficult for the emulsifier to be adsorbed at the interface. Consequently, finding an appropriate emulsifier which can penetrate in both phases as well as having tendency to be adsorbed at the interface is quite challenging. It is less obvious what types of species might adsorb at aqueous PEG-dextran interface and thereby stabilise w/w emulsions based on an ATPS. In addition, the interactions of two polymers in aqueous solution is quite complex on its own and introducing a third component as an emulsifier, makes the study of these systems even more tricky.

Characterisation of w/w emulsions is also challenging due to the sensitivity of these systems to dilution. Upon diluting the w/w emulsion even though it is stabilised, the equilibrium phase separation between two polymer phases, which causes their immiscibility vanishes. Consequently, the dispersed phase dissolves in the continuous phase. For example it is not possible to determine the type of emulsion by drop test, since upon introducing one drop of the w/w emulsion into either of the constituent polymer solution (dextran or PEG solution), it will be dissolved instead of being re-dispersed. Moreover, it is not possible to determine the drop size and drop size distribution of w/w emulsion using light scattering techniques, as these systems cannot be diluted up and the refractive indices of two polymer phases are quite similar. Employing microscopic techniques is more suitable way for characterisation of w/w emulsion. However, due to higher viscosity of w/w emulsion compared to ordinary o/w emulsion, special care must be taken into account for the sample preparation in microscopic techniques. Also, any trace of impurity can strongly influence the phase behaviour and equilibrium of ATPSs, therefore all used glassware should be extremely clean and all ingredients should be purified prior to usage.

Although stabilisation of water-in-water emulsions based on ATPSs is a challenge, they are associated with a number of advantages. Their first advantage is their ability to selectively separate and partition a wide range of biomolecules or

active species which can be encapsulated within the formed polymeric film after stabilisation of w/w emulsion. Secondly, because of their low interfacial tension, the required energy input for the formation of emulsion is very low compare to conventional emulsions. In addition, unlike to conventional o/w emulsions, these systems are entirely aqueous systems and there is no use of any organic solvent. Therefore, w/w emulsions are an environmentally friendly alternative to o/w emulsions and subsequently can be promising replacement for o/w emulsions where the biocompatibility of the system matters.

### ***1.8.2 Stabilisation of ATPS towards w/w emulsions***

Recently water-in-water emulsion (w/w) has attracted many attentions among colloids scientists. However, there are just a few papers describing the formation and stabilisation of these systems which are reviewed in this section. Ossenbach-Sauter and Riess described stabilisation of water-in-water emulsions containing mixtures of poly(vinylpyridinium chloride) (PVPC) and PEG polymers with diblock PVPC-*b*-PEG copolymers.<sup>121</sup> Jin et al. illustrated the stabilisation of w/w emulsions based on dextran-PEG ATPS by using sodium alginate as stabiliser. They discussed that sodium alginate forms a charged thin layer around the dispersed dextran rich phase which stabilises the droplets in PEG rich continuous phase.<sup>122</sup> Guorong and Zhihai described the use of a water-in-water emulsion consisting of PEG and poly(acrylamide) (PAA) ATPS for aqueous polymerisation of acrylamide.<sup>123</sup> Sagis discussed some theoretical aspects relating to the thermodynamics<sup>124</sup> and dynamics<sup>125</sup> of controlled release in water-in-water emulsions.

Simon et al.<sup>126</sup> reported the formation of w/w emulsion consisting of water solvated dispersed liquid crystal disodium cromoglycate (DSCG) in continuous phase containing a range of water soluble non-ionic, anionic and cationic polymers which have potential to exclude DSCG to form water solvated drops. They found that the non-ionic polymers form quite stable w/w emulsion (30 days) via providing steric hindrance which prevent from coalescence of the droplets.

It is well established that particles of suitable wettability will adsorb at a fluid interface with an adsorption energy which is typically large relative to alternative stabilisers such as surfactants or polymers.<sup>127</sup> Primarily, Poortinga reported the



formation of microcapsules consisting of a shell of aggregated colloids based on w/w emulsion as a template consisting of either two polysaccharides or one polysaccharide and one protein stabilised for a short time (a few days) with fat particles.<sup>128</sup> Afterwards, Firoozmand and co-workers<sup>129</sup> described the formation of w/w emulsion based on gelatine-starch ATPS which could be stabilised for a short time using amphoteric polystyrene latex particles. He reported that the gelatine-dextran ATPS phase separates quickly, but upon addition of latex particles the phase separation slowed down, although still phase separation occurred. Very recently, Nicolai et al. reported formation of w/w emulsion based on dextran-PEG ATPS stabilised using Fluorescent spherical latex particles<sup>130</sup> and globular whey protein  $\beta$ -lactoglobulin ( $\beta$ -lg) particles<sup>131</sup> which can be adsorbed at the dextran-PEG interface. In some cases the stability of the prepared emulsions was in a period of weeks.

Finally, microfluidic devices and ATPS have been combined for fabrication of w/w emulsions. Song et al.<sup>132</sup> reported microextraction and electrohydrodynamic generation of micro-droplets based on tetrabutylammonium bromide (TBAB) and ammonium sulfate (AS) ATPS. Shum et al. described the formation of w/w jets and emulsion based on several ATPSs, namely, PEG/dextran, PEGDA/dextran, PEG/K<sub>3</sub>PO<sub>4</sub> and PEGDA/K<sub>3</sub>PO<sub>4</sub> using microfluidic device.<sup>133</sup>

To the best of our knowledge terpolymers have not been used for preparation and stabilisation of w/w emulsion. In this work, one of the main aims was to investigate whether amphiphilic terpolymers with hydrophilic terminal blocks and hydrophobic middle blocks can act as effective stabilisers for w/w emulsions. The research strategy is described in the next section.

## **1.9 Research aims and strategy**

In this work, a series of amphiphilic ABC terpolymers with well-defined structures, compositions and molecular weights is synthesised and fully characterised. In addition, their ability to form different types of polymer aggregates using conventional methods is assessed. Moreover, the ability of this type of terpolymers to act as effective stabilisers to form water-in-water emulsions based on ATPS is investigated. Along with stabilisation of w/w emulsion, the formed dispersed phase can be also considered as a template for the formation of

polymersomes through adsorption of ABC terpolymers at the dispersed ATPS interface.

As it was stated before, dextran-PEG ATPS is chosen for the preparation of w/w emulsion. It is assumed that an ABC terpolymer consisting of hydrophilic terminal A and C blocks, which have different affinities for the PEG and dextran rich phases of the ATPS and hydrophobic middle B block (to form polymersomes membrane) can form polymersomes by being templated around w/w emulsion drops. Selective partitioning of encapsulant molecules (species that can be encapsulated within polymersomes) between ATPS two phases prior to emulsification would lead to their efficient encapsulation. This novel method would avoid the use of organic solvents unlike the conventional methods used for the encapsulation of different species within the polymersomes.

Therefore, the specific aims of this work are (i) to synthesis a series of ABC terpolymers with well-defined structures and compositions, (ii) to determine whether these in-house synthesised ABC terpolymers self-assemble to form micelles and polymersomes based on the conventional methods, (iii) how the formed self-assembly properties depends on the block sizes and molecular weights of the terpolymers (iv) whether ABC terpolymers can stabilise water-in-water emulsion based on the PEG-dextran system; (v) how the emulsion properties such as type, drop size and stability depend on the block sizes of the terpolymer and (vi) how solute molecules distribute within the water-in-water emulsion (or templated polymersome) systems. In addition to ABC terpolymers, a couple of ABA terpolymers with simpler structure are used for stabilisation of dextran-PEG ATPS in this work. Moreover, modified silica nanoparticles in terms of their hydrophobicity and PEG content are used for the stabilisation of such systems.

### **1.10 Outline of thesis**

The outline of this thesis can be described as following:

Chapter 2 summarises the chemicals and procedures which have been used throughout this work. This chapter also briefly describes the basic principles of the employed techniques for the characterisation of in-house synthesised terpolymers and modified silica nanoparticles.

Chapter 3 is concerned with the design, synthesis and characterisation of amphiphilic ABC terpolymers with pre-determined compositions and molecular weights. The synthesised terpolymers are characterised in terms of their actual compositions and molecular weights as well as their hydrodynamic diameter, CMC,  $pK_a$  and cloud point when hydrated in aqueous solution. In addition, the effect of varying terpolymers composition and molecular weights on their hydrodynamic diameter, CMC and  $pK_a$  values is explained.

Some preliminary observations of terpolymers solutions when hydrated in bulk or as thin film have been described in chapter 4. The main aim of this chapter is to investigate whether a selection of synthesised ABC terpolymers with constant composition but varied molecular weight are able to form polymersomes using a couple of reviewed conventional methods.

Chapter 5 details whether ABA and ABC terpolymers can be used as effective stabilisers for formation of w/w emulsions based on ATPSs and possible formation of templated polymersomes. In addition, it describes how the emulsion properties such as type, drop size and stability depend on the block sizes and average molecular weight of the ABC terpolymers. Finally, this chapter illustrates how solute molecules distribute and self-load within the water-in-water emulsion (or templated polymersome) system.

The work on stabilisation of w/w emulsions is further extended in chapter 6 by using modified silica nanoparticles. Two types of silica nanoparticles with specific characteristics will be used in this chapter in order to stabilise ATPSs and possible formation of templated colloidosomes. This chapter explains how the characteristics of these nanoparticles affect emulsion properties.

Chapter 7 summarises the obtained conclusions throughout this thesis and presents the possible future work in this area. The references used throughout this work are listed at the end of the each chapter.

## 1.11 References

1. R. Lipowsky and E. Sackmann, *Structure and Dynamics of Membranes- From Cells to Vesicles*, 1st. edn., Elsevier B. V., Amsterdam, 1995.
2. L. Zhang and A. Eisenberg, *Science*, 1995, **268**, 1728.
3. O. Onaca, R. Enea, D. W. Hughes and W. Meier, *Macromol. Biosci.*, 2009, **9**, 129.
4. C. LoPresti, H. Lomas, M. Massignani, T. Smart and G. Battaglia, *J. Mater. Chem.*, 2009, **19**, 3576.
5. V. D. H. Napper, *Polymeric Stabilization of Colloidal Dispersions*, Academic Press, London, 1983.
6. J. N. Israelachvili, *Intermolecular and Surface Forces*, 3rd. edn., Elsevier, Amsterdam, 2011.
7. G. J. Fleer, M. A. C. Stuart, J. M. H. M. Scheutjens, T. Cosgrove and B. Vincent, *Polymers at Interfaces*, Chapman and Hall, London, 1993.
8. C. Fong, T. Le and C. J. Drummond, *Chem. Soc. Rev.*, 2012, **41**, 1297.
9. J. C. M. V. Hest, D. A. P. Delnoye, M. W. P. L. Baars, M. H. P. V. Genderen and E. W. Meijer, *Science*, 1995, **268**, 1592.
10. L. Zhang, K. Yu and A. Eisenberg, *Science*, 1996, **272**, 1777.
11. Y. Mai and A. Eisenberg, *Chem. Soc. Rev.*, 2012, **41**, 5969.
12. G. Riess, *Prog. Polym. Sci.*, 2003, **28**, 1107.
13. P. Alexandridis and B. Lindman, *Amphiphilic Block Copolymers: Self-Assembly and Applications*, 1st. edn., Elsevier, Amsterdam, 2000.
14. A. D. Jenkins, P. Kratochvíl, R. F. T. Stepto and U. W. Suter, *Pure Appl. Chem.*, 1996, **68**, 2287.
15. T. P. Lodge, *Macromol. Chem. Phys.*, 2003, **204**, 265.
16. A. D. McNaught and A. Wilkinson, *Pure Appl. Chem.*, 1996, **68**, 2287.

17. G. Riess, G. Hurtrez and P. Bahadur, *Encyclopedia of polymer science and engineering*, 2nd. edn., Wiley, New York, 1985.
18. V. M. Nace, *Nonionic surfactants: polyoxyalkylene block copolymers*, Marcel Dekker, New York, 1996.
19. R. Pons, *Polymeric surfactants as emulsion stabilizers*, Elsevier, Amsterdam, 2000.
20. T. Sakai and P. Alexandridis, *Langmuir*, 2004, **20** 8426.
21. M. Tirrell, *Solvents and Self-Organization of Polymers*, Kluwer Academic Publishers, Dordrecht, 1996.
22. J. Jagur-Grodzinski, *Living and controlled polymerization: synthesis, characterization and properties of the respective polymers and copolymers*, Nova Science Publishers New York, 2005.
23. A. Ravve, *Principles of polymer chemistry*, Plenum Publisher, New York, 2000.
24. M. Szwarc, M. Levy and R. Milkovich, *J. Am. Chem. Soc.*, 1956, **78**, 2656.
25. M. Szwarc, *Nature*, 1956, **176**, 1168.
26. O. W. Webster, W. R. Hertler, D. Y. Sogah, W. B. Farnham and T. V. RajanBabu, *J. Am. Chem. Soc.*, 1983, **105**, 5706.
27. O. W. Webster, *Adv. Polym. Sci.*, 2004, **167**, 1.
28. R. J. Young and P. A. Lovell, *Introduction to Polymers*, 2nd. edn., Nelson Thornes Ltd, Cheltenham, 2000.
29. G. G. Odian, *Principles of Polymerization*, 4th. edn., John Wiley & Sons Inc., Hoboken, 2004.
30. S. Forster and T. Plantenberg, *Angew. Chem. Int. Ed.*, 2002, **41**, 688.
31. M. Muthukumar, C. K. Ober and E. I. Thomas, *Science*, 1997, **277**, 1225.
32. E. S. Read and S. P. Armes, *Chem. Commun.*, 2007, 3021.

33. R. K. O'Reilly, C. J. Hawker and K. L. Wooley, *Chem. Soc. Rev.*, 2006, **35**, 1068.
34. X. Wang, G. Guerin, H. Wang, Y. Wang, I. Manners and M. A. Winnik, *Science*, 2007, **317**, 644.
35. I. K. Voets, A. d. Keizer, P. d. Waard, P. M. Frederik, P. H. H. Bomans, H. Schmalz, A. Walther, S. M. King, F. A. M. Leermakers and M. A. Cohen-Stuart, *Angew. Chem., Int. Ed.*, 2006, **45**, 6673.
36. L. Zhang and A. Eisenberg, *J. Am. Chem. Soc.*, 1996, **118**, 3168.
37. Z. Erlangung, University of Potsdam 2005.
38. P. L. Soo and A. Eisenberg, *J. Polym. Sci., Part B: Polym. Phys.*, 2004, **42**, 923.
39. J. Du and R. K. O'Reilly, *Soft Matter*, 2009, **5**, 3544.
40. E. B. Zhulina and O. V. Borisov, *Macromolecules*, 2012, **45**, 4429.
41. O. V. Borisov, E. B. Zhulina, F. A. M. Leermakers and A. H. E. Muller, *Adv. Polym. Sci.*, 2011, **241**, 57.
42. I. W. Hamley, *The physics of block copolymers*, Oxford University Press, New York, 1998.
43. L. Leibler, *Macromolecules*, 1980, **13**, 1602.
44. F. S. Bates and G. H. Fredrickson, *Annu. Rev. Phys. Chem.*, 1990, **41**, 525.
45. B. D. Olsen and R. A. Segalman, *Mater. Sci. Eng. R.*, 2008, **62**, 37.
46. C. S. Patrickios, W. R. Hertler, N. L. Abbott and T. A. Hatton, *Macromolecules*, 1994, **27**.
47. C. S. Patrickios, C. Forder, S. Armes and N. Billingham, *J. Polym. Sci., Part A: Polym. Chem.*, 1997, **35**, 1181.
48. A. I. Triftaridou, M. Vamvakaki and C. S. Patrickios, *Polymer*, 2002, **43**, 2921.

49. M. S. Kyriakou, S. C. Hadjiyannakou, M. Vamvakaki and C. S. Patrickios, *Macromolecules*, 2004, **37**, 7181.
50. E. Giebler and R. Stadler, *Macromol. Chem. Phys.*, 1997, **198**, 3815.
51. Y. Cai and S. P. Armes, *Macromolecules*, 2004, **37**, 7116.
52. J. Gohy, N. Willet, S. Varshney, J. Zhang and R. Jerome, *Angew. Chem.*, 2001, **113**, 3314.
53. M. Gadgzinowski and S. Sosnowski, *J. Polym. Sci., Part A: Polym. Chem.*, 2003, **41**, 3750.
54. Z. Zhou, Z. Li, Y. Ren, M. Hillmyer and T. Lodge, *J. Am. Chem. Soc.*, 2003, **125**, 10182.
55. M. A. Ward and T. K. Georgiou, *Soft Matter*, 2012, **8**, 2737.
56. C. Tsitsilianis and V. Sfika, *Macromol. Rapid. Commun.*, 2001, **22**, 647.
57. V. Sfika, C. Tsitsilianis, A. Kiriy, G. Gorodyska and M. Stamm, *Macromolecules*, 2004, **37**, 9551.
58. A. Walther, C. Barner-Kowollik and A. H. E. Muller, *Langmuir*, 2010, **26**, 12237.
59. O. Moulτος, L. N. Gergidis and C. Vlahos, *Macromolecules*, 2012, **45**, 2570.
60. Y. Liu, V. Abetz and A. H. E. Muller, *Macromolecules*, 2003, **36**, 7894.
61. L. Gao, K. Zhang and Y. C. 2012, *ACS Macro. Lett.*, 2012, **1**, 1143.
62. B. Fang, A. Walther, A. Wolf, Y. Xu, J. Yuan and A. H. E. Muller, *Angew. Chem., Int. Ed.*, 2009, **48**, 2877.
63. J. Chapman, *Micelles, Monolayers, and Biomembranes*, Wiley-Liss, New York, 1995.
64. C. Tanford, *The Hydrophobic Effect*, 2nd. edn., John Wiley & Sons, New York, 1980.

65. D. F. Evans and H. Wennerstrom, *In The Colloidal Domain: Where Physics, Chemistry, and Biology Meet*, 2nd. edn., Wiley-VCH, New York, 1999.
66. P. Goon, C. Manohar and V. V. Kumar, *J. Colloid Interface Sci.*, 1987, **119**, 177.
67. K. S. Birdi, *Handbook of Surface and Colloid Chemistry*, CRC Press, New York, 1997.
68. Y. Nakahara, T. Kida, Y. Nakatsuji and M. Akashi, *Langmuir*, 2005, **21**, 6688.
69. I. Astafieva, X. F. Zhong and A. Eisenberg, *Macromolecules*, 1993, **26**, 7339.
70. C. Goncalves, J. A. Martins and F. M. Gama, *Biomacromolecules*, 2007, **8**, 392.
71. A. Dominguez, A. Fernandez, N. Gonzalez, E. Iglesias and L. J. Montenegro, *J. Chem. Educ.*, 1997, **74**, 1227.
72. R. Zielinski, S. Ikeda, H. Nomura and S. Kato, *J. Colloid Interface Sci.*, 1987, **119**, 398.
73. H. I. Unal, C. Price, P. M. Budd and R. H. Mobbs, *Eur. Polym. J.*, 1994, **30**, 1037.
74. K. Kalyanasundaram and J. K. Thomas, *J. Am. Chem. Soc.*, 1977, **99**, 2039.
75. B. M. Discher, H. Bermudez, D. A. Hammer, D. E. Discher, Y. Won and F. S. Bates, *J. Phys. Chem. A*, 2002, **106**, 2848.
76. M. Antonietti and S. Förster, *Adv. Mater.*, 2003, **15**, 1323.
77. M. B. Discher, Y. Won, D. S. Ege, J. Lee, F. S. Bates, D. E. Discher and D. A. Hammer, *Science*, 1999, **284**, 1143.
78. E. G. Bellomo, M. D. Wyrsta, L. Pakstis, D. J. Pochan and T. J. Deming, *Nat. Mater.*, 2004, **3**, 244.
79. F. Meng, Z. Zhong and J. Feijen, *Biomacromolecules*, 2009, **10**, 197.



80. S. Litvinchuk, Z. Lu, P. Rigler, T. D. Hirt and W. Meier, *Pharm. Res.*, 2009, **26**, 1711.
81. P. Broz, S. M. Benito, C. Saw, P. Burger, H. Heider, M. Pfisterer, S. Marsch, W. Meier and P. Hunziker, *J. Controlled Release*, 2005, **102**, 475.
82. D. E. Discher and F. Ahmed, *Annu. Rev. Biomed. Eng.*, 2006, **8**, 323.
83. Y. Yu, L. Zhang and A. Eisenberg, *Macromolecules*, 1998, **31**, 1144.
84. G. Yu and A. Eisenberg, *Macromolecules*, 1998, **31**, 5546.
85. R. Bieringer, V. Abetzl and A. H. E. Muller, *Eur. Phys. J. E: Soft Matter Biol. Phys.*, 2001, **5**, 5.
86. L. Luo and A. Eisenberg, *Angew. Chem., Int. Ed.*, 2002, **41**, 1001.
87. R. Stoenescu and W. Meier, *Chem. Commun.*, 2002, **24**, 3016.
88. F. Liu and A. Eisenberg, *J. Am. Chem. Soc.*, 2003, **125**, 15059.
89. S. Yu, T. Azzam, I. Roullier and A. Eisenberg, *J. Am. Chem. Soc.*, 2009, **131**, 10557.
90. K. Kempe, R. Hoogenboon, C. A. Fustin, J. F. Gohy and U. S. Schubert, *Chem. Commun.*, 2010, **46**, 6455.
91. J. Du, L. Fan and Q. Liu, *Macromolecules*, 2012, **45**, 8275.
92. K. K. Tokarczyk, J. Grumelard, T. Haeefele and W. Meier, *Polymer*, 2005, **46**, 3540.
93. J. C. M. Lee, H. Bermudez, B. M. Discher, M. A. Sheehan, Y. Y. Won, F. S. Bates and D. E. Discher, *Biotechnol. Bioeng.*, 2001, **73**, 135.
94. R. Dimova, U. Seifert, B. Pouligny, S. Forster and H. G. Dobereiner, *Eur. Phys. J. E: Soft Matter Biol. Phys.*, 2002, **7**, 241.
95. E. Lorenceau, A. S. Utada, R. Darren, G. Cristobal, M. Joanicot and D. A. Weitz, *Langmuir*, 2005, **21**, 9183-9186.

96. H. C. Shum, J. W. Kim and D. A. Weitz, *J. Am. Chem. Soc.*, 2008, **130**, 9543.
97. D. J. Adams, S. Adams, D. Atkins, M. F. Butler and S. Fuzeland, *J. Control Release*, 2008, **128**, 165.
98. A. J. Parnell, N. Tzokova, P. D. Topham, D. J. Adams, S. Adams, C. M. Fernyhough, A. J. Ryan and R. A. L. Jones, *Faraday Discuss.*, 2009, **143**, 29.
99. B. P. Binks, *Modern Aspects of Emulsion Science*, Royal Society of Chemistry, Cambridge, 1998.
100. N. Garti, *Colloid Surf. A-Physicochem. Eng. Asp.*, 1997, **123**, 233.
101. J. Sjoblom, *Emulsions and Emulsions Stability*, 2nd. edn., Taylor & Francis Group LLC, New York, 2006.
102. G. O. Phillips and P. A. Williams, *Handbook of Hydrocolloids*, CRC Press, Cambridge, 2000.
103. E. Dickinson and M. Golding, *Colloid Surf. A-Physicochem. Eng. Asp.*, 1998, **144**, 167.
104. R. Chanamai and D. J. McClements, *Colloid Surf. A-Physicochem. Eng. Asp.*, 2000, **172**, 79.
105. T. K. Basaran, K. Demetriades and D. J. McClements, *Colloid Surf. A-Physicochem. Eng. Asp.*, 1998, **136**, 169.
106. R. Pichot, The University of Birmingham, 2010.
107. P. Jokela, P. D. I. Fletcher, R. Aveyard and J. R. Lu, *J. Colloid Interface Sci.*, 1990, **134**, 417.
108. A. Kabalnov, *Curr. Opin. Colloid Interface Sci.*, 1998, **3**, 270.
109. E. Dickinson, *An Introduction to Food Colloids*, Oxford University Press, Oxford, 1992.
110. T. Tadros, *Adv. Colloid Interface Sci.*, 2009, **147**, 281.

111. J. L. Salager, L. Marquez, A. A. Pena, M. Rondon, F. Silva and E. Tyrode, *Ind. Eng. Chem. Res.*, 2000, **39**, 2665.
112. S. U. Pickering, *J. Chem. Soc.*, 1907, **91**, 2001.
113. D. E. Tanbe and M. M. Sharma, *Adv. Colloid Interface Sci.*, 1994, **52**, 1.
114. R. Aveyard, B. P. Binks and J. H. Clint, *Adv. Colloid Interfac. Sci.*, 2003, **100**, 503.
115. A. Dobry and F. Boyer-Kawenoki, *J. Polymer Sci.*, 1947, **2**, 90.
116. P. Albertsson, *Partition of cell particles and macromolecules*, Wiley-Interscience, New York, 1971.
117. M. W. Beijerinck, *Zbl. Bakt.*, 1896, **2**, 698.
118. W. Ostwald and R. Kohler, *Kolloid-Z.*, 1927, **43**, 131.
119. W. Ostwald and R. H. Hertel, *Kolloid-Z.*, 1929, **47**, 258.
120. E. D. Fisher and I. A. Sutherland, *Separation Using Aqueous Phase Systems*, Plenum Press, New York, 1989.
121. M. Ossenbach-Sauter and G. Riess, *C. R. Academie. Sci. Paris Ser. C*, 1976, **283**, 269.
122. T. Jin; L. Chen; H. Zhu, *Stable polymer aqueous/aqueous emulsion system and uses thereof*. US Patent 6,805,879 B2, 19 Oct. **2004**.
123. S. Guorong and C. A. Zihai, *J. Appl. Polymer Sci.*, 2009, **111**, 1409.
124. L. M. C. Sagis, *J. Phys. Chem. A*, 2007, **111**, 3139.
125. L. M. C. Sagis, *J. Controlled Release*, 2008, **131**, 5.
126. K. A. Simon, P. Sejwal, R. B. Gerech and Y. Y. Luk, *Langmuir*, 2007, **23**, 1453.
127. B. P. Binks, *Curr. Opin. Colloid Interface Sci.*, 2002, **7**, 21.
128. A. T. Poortinga, *Langmuir*, 2008, **24**, 1644.

129. H. Firoozmand, B. S. Murray and E. Dickinson, *Langmuir*, 2009, **25**, 1300.
130. G. Balakrishnan, T. Nicolai, L. Benyahia and D. Durand, *Langmuir*, 2012, **28**, 5921.
131. B. T. Nguyen, T. Nicolai and L. Benyahia, *Langmuir*, 2013, **29**, 10658.
132. Y. S. Song, Y. H. Choi and D. H. Kim, *J. Chromatogr., A*, 2007, **1162**, 180.
133. H. C. Shum, J. Varnell and D. A. Weitz, *Biomicrofluidics*, 2012, **6**, 012808.

## **CHAPTER 2**

### **EXPERIMENTAL**

## 2.1 Materials

### 2.1.1 Water

Water was purified by passing through an Elgastat Prima reverse osmosis unit followed by a Millipore Milli-Q reagent water system. Its surface tension was  $71.9 \text{ mN m}^{-1}$  at  $25^\circ\text{C}$ , in good agreement with literature. <sup>1</sup>

### 2.1.2 Pluronic<sup>®</sup> grades

Pluronic<sup>®</sup> grades F108 (MW: 14600 g/mol), F127 (MW: 12600 g/mol) and F68 (MW: 8400 g/mol) were purchased from Sigma, UK. The characteristics of these Pluronics<sup>®</sup> are listed in Table 2.1. All Pluronics<sup>®</sup> were used as supplied without further purification unless specified otherwise.

**Table 2.1.** Characteristics of Pluronic<sup>®</sup> grades.

Pluronic <sup>®</sup> Name	MW g/mol	HLB	Formula	EO%	PO%
F68	8400	29	EO <sub>76</sub> PO <sub>29</sub> EO <sub>76</sub>	80%	20%
F127	12600	22	EO <sub>100</sub> PO <sub>65</sub> EO <sub>100</sub>	70%	30%
F108	14600	27	EO <sub>132</sub> PO <sub>50</sub> EP <sub>132</sub>	80%	20%

### 2.1.3 Chemicals used for synthesis of hydrophobised silica nanoparticles

Silica nanoparticles with different hydrophobicities (0%, 20%, 33%, 50% and 58%) with smooth surface and size ranging from 100-500 nm were used. <sup>2</sup>

### 2.1.4 Chemicals used for synthesis of PEGylated silica nanoparticles

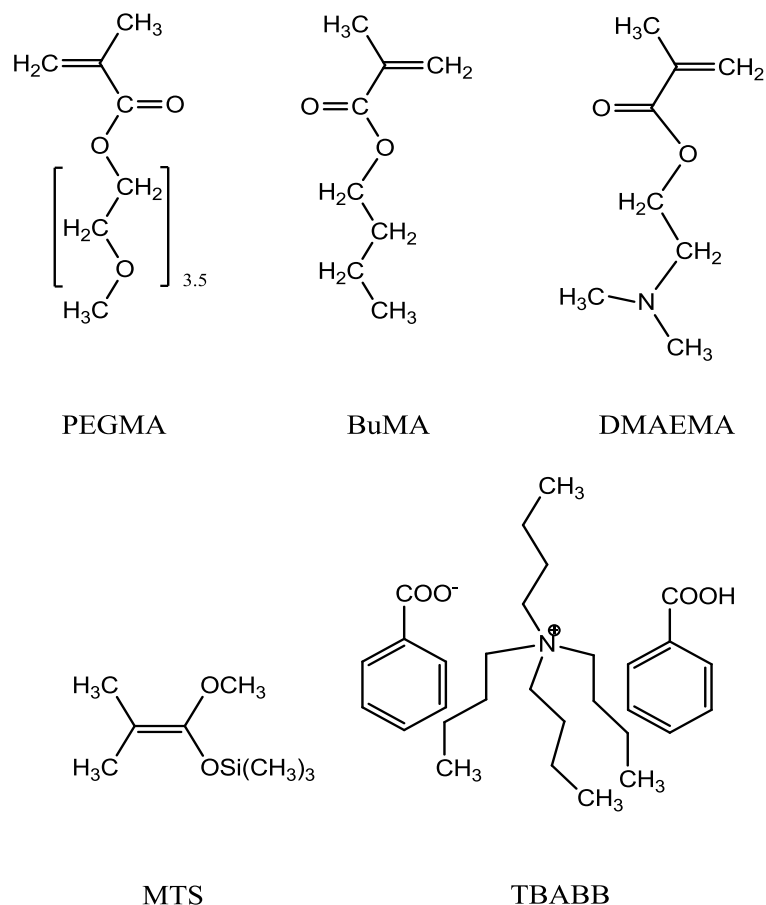
Poly(ethylene glycol) methyl ether (MW: 6000 g/mol) and tetramethyl orthosilicate ( $\geq 99\%$ ) were purchased from Aldrich, UK. Ammonium hydroxide (1 molar, 30 wt.%) was purchased from Prime Chemicals, UK. Solvents ethanol and methanol were purchased from Fisher Scientific, UK.

### 2.1.5 Chemicals used for synthesis of terpolymers

1-Methoxy-1(trimethylsiloxy)-2-methyl propene initiator (MTS, 99%), sodium metal, 2,2-diphenyl-1-picrylhydrazyl hydrate free radical inhibitor (DPPH,

99%) and poly(ethylene glycol) methyl ether methacrylate monomer (PEGMA, 99%, MW = 300 g/mol with number of ethoxy units  $n = 4.5$ ), were purchased from Aldrich, UK. Tetrabutylammonium hydroxide (40% in water), benzoic acid (99%), basic alumina ( $\text{Al}_2\text{O}_3$ , 95%), potassium metal, 2-(dimethylamino)ethyl methacrylate monomer (DMAEMA, 99%) and *n*-butyl methacrylate monomer (BuMA, 99%) were purchased from Acros Organics, UK. The polymerisation catalyst was tetrabutylammonium bibenzoate (TBABB) and was in-house synthesised by the reaction of tetrabutylammonium hydroxide and benzoic acid as described by Dicker et al.<sup>3</sup> The dried catalyst powder was stored in a round-bottom flask under vacuum until use. Tetrahydrofuran (THF, 95%) used as polymerisation solvent, *n*-hexane (95%) used as precipitation solvent were purchased from Fisher Scientific. Dichlorodimethylsilane (DCDMS, 99.5%) hydrophobising agent for glassware surface was purchased from Fluka, UK. Figure 2.1 illustrates the chemical structure of polymerisation initiator, catalyst and monomers.

**Figure 2.1.** Chemical structures of monomers, GTP initiator and catalyst used for synthesis of terpolymers using GTP technique.



### ***2.1.6 Chemicals used for preparation of ATPS***

Dextran 500 from *Leuconostoc* spp was purchased from Aldrich, UK. PEG (MW: 6,000 g/mol) was purchased from Acros Organics UK. They were both used as supplied without further purification unless specified otherwise. Hydrochloric acid (37 vol./vol.%) were purchased from Fisher Scientific, UK.

### ***2.1.7 Fluorescence probes used for encapsulation***

Fluorescein-isothiocyanate-dextran (99%) conjugate with dextran 500 kDa (0.003-0.020 mol fluorescein per mol of glucose repeat unit) fluorescein sodium salt (Sigma, 99%) and pyrene (Sigma, 98%) were purchased from Aldrich, UK. Rhodamine 6G 99% was purchased from Acros Organics, UK.

## **2.2 Synthesis methods**

### ***2.2.1 Synthesis of PEGylated silica nanoparticles***

The synthetic procedure for preparation of PEG-coated (PEGylated) silica particles was the same for all prepared particles and involved a sol-gel method, so called Stöber procedure.<sup>4</sup> Reaction was based on hydrolysis of tetramethyl orthosilicate (TMOS) in methanol media in the presence of methyl ether terminated PEG, catalysed by ammonia.<sup>5</sup>

By varying initial concentrations of reagents, the size of the obtained nanoparticles can be manipulated. Table 2.2 summarises the amount of chemicals used for preparation of PEGylated silica nanoparticles with different sizes used in this study. The synthesis of PEGylated silica nanoparticles with size  $289.6 \pm 18.6$  nm is described in detail as an example. Firstly, PEG (10 g, 1.7 mmol) was dissolved in a mixture of ammonium hydroxide (25 mL, 30 wt.%) and methanol (60 mL). Then, TMOS (1 mL, 1.03 g, 6.76 mmol) was added dropwise to initiate the hydrolysis reaction. Upon mixing, the solution became slightly cloudy and it was left to stir overnight at room temperature for a full reaction to occur. To purify the prepared particles, approximately 100 mL of ethanol was added to the reaction mixture and the mixture was centrifuged for 10 minutes at 6000 rpm using a Thermo Scientific, Sorvall Biofuge Primo centrifuge. Silica particles were then washed three times first with Milli-Q water and then ethanol via re-dispersing them in the solvent followed



by centrifugation as described above to ensure all unreacted PEG and TMOS were removed. Finally, the resultant particles were dried under vacuum for three days at room temperature. Pure silica was also prepared by the same method in the absence of PEG methyl ether for means of comparison with PEGylated samples in characterisation.

**Table 2.2.** Amount of chemicals used for synthesis of PEGylated and pure silica nanoparticles.

Sample	Reaction Composition			
	Ammonium hydroxide (mL)	Methanol (mL)	TMOS (mL)	PEG (g)
1	15	60	0.5	10
2	25	60	1.0	10
3	38	60	1.0	10
Pure Silica	25	60	1.0	10

### 2.2.2 Synthesis of ABC terpolymers

The DMAEMA and BuMA monomers were passed twice through basic alumina columns to remove inhibitors and protic impurities. They were subsequently stirred over CaH<sub>2</sub> for few hours in the presence of added free radical inhibitor, DPPH (a few mg) and were kept under argon atmosphere refrigerated until distillation before use. PEGMA was passed twice through basic alumina columns as a 50 v/v% solution in THF and stirred overnight over calcium hydride before being filtered directly into the reaction flask using a 0.45 µm syringe filter. Because of the non-volatile nature of PEGMA and its inability to distil, no DPPH was added to it. The initiator was distilled once prior the polymerisation. The polymerisation solvent (THF) was dried by refluxing it for three days over a potassium/sodium amalgam prior to polymerisation. All glassware was hydrophobised via reaction of dichlorodimethylsilane (DCDMS) vapour to the SiOH groups of the glass surface to ensure their dryness over polymerisation procedure. After washing them with ethanol, water and acetone respectively, they were dried overnight at 120 °C and assembled hot under dynamic vacuum before use.

The synthetic procedure was the same for all polymers and involved a sequential group transfer polymerisation (GTP), similar to other studies where the PEGMA macromonomer was used.<sup>6-10</sup> The synthesis of PEGMA<sub>6</sub>-*b*-BuMA<sub>35</sub>-*b*-DMAEMA<sub>37</sub> (theoretical structure, abbreviated to P<sub>6</sub>-B<sub>35</sub>-D<sub>37</sub>) is described in detail as an example. Freshly distilled THF (117 mL) and MTS (0.50 mL, 0.43 g, 2.46 mmol) were syringed into a 250 mL round bottom flask containing TBABB (~10 mg) previously sealed with a septum and purged with argon. Then PEGMA was added (8.1 mL of a 50 %v/v solution in THF, 4.3 g, 14.2 mmol) using a syringe fitted with an in-line filter; this caused a temperature rise of 2.8°C. After 15 minutes the exothermic reaction had abated and two 0.1 mL aliquots of the reaction solution were extracted for GPC and <sup>1</sup>H NMR analysis. Then, the BuMA (13.6 mL, 12.2 g, 8.6 mmol) was added using a syringe which led to a temperature increase of 8.1°C. Subsequently, two more 0.1 mL aliquots were collected for GPC and <sup>1</sup>H NMR analysis. DMAEMA (15.2 mL, 14.2 g, 90.2 mmol) was added which gave a final temperature increase of 8.8°C and final GPC and <sup>1</sup>H NMR samples were obtained. All the synthesised copolymers were recovered by precipitation by addition of *n*-hexane and dried at room temperature in a vacuum oven for two weeks. For the reactant quantities noted above, this exemplar synthesis is expected to yield the product P<sub>6</sub>-B<sub>35</sub>-D<sub>37</sub>; in fact, the final measured polymer structure was P<sub>11</sub>-B<sub>60</sub>-D<sub>64</sub>. This difference is due to deactivation of the initiator, normally caused by ingress of trace amounts of water and acidic impurities.<sup>3</sup> In total, 38 ABC terpolymers of general structure P<sub>x</sub>-B<sub>y</sub>-D<sub>z</sub> with different block lengths *x*, *y* and *z* were synthesised and characterised. Table 2.3 summarises the amount of chemicals used for terpolymer synthesis and the corresponding released exothermic temperatures for addition of each block (the first, second and third ΔTs are corresponding to PEGMA, BuMA and DMAEMA block respectively).

**Table 2.3.** Amounts of chemicals used for synthesis of PEGMA-*b*-BuMA-*b*-DMAEMA terpolymers and the released exothermic temperature during the polymerisation of each block (the first, second and third  $\Delta T$ s are corresponding to PEGMA, BuMA and DMAEMA block respectively).

No.	Theoretical Structure	THF (mL)	MTS (mL)	PEGMA (mL)	BuMA (mL)	DMAEMA (mL)	$\Delta T_{1-3}$ (°C)
1	P <sub>9</sub> -B <sub>20</sub> -D <sub>24</sub>	85	0.5	12.7	7.8	10.0	5.7, 5.4, 8.2
2	P <sub>9</sub> -B <sub>27</sub> -D <sub>24</sub>	93	0.5	12.7	10.5	10.0	7.1, 8.0, 8.2
3	P <sub>9</sub> -B <sub>34</sub> -D <sub>24</sub>	102	0.5	12.7	13.2	10.0	3.8, 7.8, 7.5
4	P <sub>15</sub> -B <sub>27</sub> -D <sub>20</sub>	98	0.5	21.1	10.5	8.3	5.8, 6.4, 4.4
5	P <sub>20</sub> -B <sub>27</sub> -D <sub>15</sub>	99	0.5	28.1	10.5	6.2	6.6, 1.8, 2.3
6	P <sub>5</sub> -B <sub>27</sub> -D <sub>30</sub>	96	0.5	7.03	10.5	12.4	3.9, 8.6, 10.4
7	P <sub>13</sub> -B <sub>27</sub> -D <sub>36</sub>	123	0.5	19.0	10.5	14.9	3.2, 4.2, 8.2
8	P <sub>5</sub> -B <sub>27</sub> -D <sub>12</sub>	64	0.5	7.0	10.5	5.0	4.2, 11.3, 6.5
9	P <sub>18</sub> -B <sub>35</sub> -D <sub>14</sub>	110	0.5	25.0	13.6	5.6	6.4, 5.4, 2.1
10	P <sub>17</sub> -B <sub>35</sub> -D <sub>16</sub>	111	0.5	23.3	13.6	6.6	5.1, 3.7, 1.9
11	P <sub>15</sub> -B <sub>35</sub> -D <sub>19</sub>	112	0.5	21.0	13.6	7.9	5.2, 5.1, 3.0
12	P <sub>12</sub> -B <sub>35</sub> -D <sub>24</sub>	113	0.5	17.5	13.6	9.8	3.9, 6.8, 5.3
13	P <sub>10</sub> -B <sub>35</sub> -D <sub>28</sub>	115	0.5	14.4	13.6	11.6	4.1, 8.2, 6.5
14	P <sub>9</sub> -B <sub>35</sub> -D <sub>30</sub>	115	0.5	13.1	13.6	12.3	3.1, 8.1, 7.2
15	P <sub>7</sub> -B <sub>35</sub> -D <sub>34</sub>	117	0.5	10.0	13.6	14.1	3.5, 10.4, 11.0
16	P <sub>6</sub> -B <sub>35</sub> -D <sub>36</sub>	117	0.5	8.1	13.6	15.1	2.8, 8.1, 8.8
17	P <sub>4</sub> -B <sub>35</sub> -D <sub>40</sub>	118	0.5	5.8	13.6	16.4	2.4, 10.5, 11.2
18	P <sub>2</sub> -B <sub>35</sub> -D <sub>43</sub>	120	0.5	3.2	13.6	17.9	1.1, 8.7, 10.3
19	P <sub>1</sub> -B <sub>35</sub> -D <sub>45</sub>	120	0.5	1.7	13.6	18.8	0.6, 8.5, 10.8
20	P <sub>2</sub> -B <sub>9</sub> -D <sub>6</sub>	31	0.5	1.7	3.5	2.6	2.0, 10.0, 9.0
21	P <sub>4</sub> -B <sub>15</sub> -D <sub>11</sub>	50	0.5	2.8	5.9	4.4	1.5, 11.2, 8.6
22	P <sub>6</sub> -B <sub>21</sub> -D <sub>15</sub>	70	0.5	3.9	8.3	6.1	2.0, 9.3, 6.5
23	P <sub>7</sub> -B <sub>27</sub> -D <sub>19</sub>	90	0.5	5.0	10.6	7.9	2.1, 9.0, 6.0
24	P <sub>9</sub> -B <sub>33</sub> -D <sub>23</sub>	109	0.5	6.2	13.0	9.7	0.9, 8.9, 6.3
25	P <sub>10</sub> -B <sub>39</sub> -D <sub>28</sub>	130	0.5	7.3	15.4	11.4	2.1, 10.4, 7.8
26	P <sub>12</sub> -B <sub>45</sub> -D <sub>32</sub>	148	0.5	8.4	17.7	13.2	1.6, 9.0, 6.3
27	P <sub>2</sub> -B <sub>14</sub> -D <sub>15</sub>	39	0.4	2.6	4.4	4.9	2.0, 9.6, 9.9
28	P <sub>5</sub> -B <sub>28</sub> -D <sub>29</sub>	76	0.4	5.1	8.8	9.7	3.4, 11.4, 12.4
29	P <sub>7</sub> -B <sub>42</sub> -D <sub>44</sub>	113	0.4	7.7	13.4	14.6	3.6, 8.3, 9.6
30	P <sub>8</sub> -B <sub>49</sub> -D <sub>51</sub>	132	0.4	9.0	15.3	17.0	5.1, 11.9, 9.5
31	P <sub>9</sub> -B <sub>56</sub> -D <sub>59</sub>	150	0.4	10.3	17.5	19.5	2.6, 9.6, 9.4
32	P <sub>11</sub> -B <sub>70</sub> -D <sub>73</sub>	188	0.4	12.9	22.0	24.3	1.1, 4.8, 6.7
33	P <sub>12</sub> -B <sub>56</sub> -D <sub>35</sub>	126	0.4	13.2	17.4	11.6	3.8, 10.5, 6.8
34	P <sub>11</sub> -B <sub>59</sub> -D <sub>34</sub>	127	0.4	12.7	18.3	11.3	3.9, 11.4, 7.6

No.	Theoretical Structure	THF (mL)	MTS (mL)	PEGMA (mL)	BuMA (mL)	DMAEMA (mL)	$\Delta T_{1-3}$ (°C)
35	P <sub>11</sub> -B <sub>61</sub> -D <sub>33</sub>	127	0.4	12.2	18.9	10.8	4.1, 11.9, 5.9
36	P <sub>10</sub> -B <sub>63</sub> -D <sub>32</sub>	127	0.4	11.8	19.6	10.4	3.9, 11.3, 6.3
37	P <sub>9</sub> -B <sub>55</sub> -D <sub>28</sub>	112	0.4	10.4	17.3	9.2	3.5, 13.5, 7.1
38	P <sub>12</sub> -B <sub>74</sub> -D <sub>37</sub>	150	0.4	13.8	23.1	12.3	3.2, 9.6, 4.4

## 2.3 Preparation procedures

In this section, the procedures employed for the preparation of polymer self-assembly in aqueous solution, ATPS, w/w emulsions and encapsulation of fluorescent probes within the prepared polymsomes are described.

### 2.3.1 Preparation of polymer self-assembly

#### 2.3.1.1 Bulk rehydration method

Polymer self-assemblies were prepared for a selection of synthesised terpolymers using bulk rehydration method. Terpolymer solution was prepared by dissolving 50 mg of terpolymer in 5 g of deionised water to give 1 wt.% polymer solution. The pH of this solution was first adjusted at 2 via addition of HCl (2 M) followed by gradual increasing of pH via addition of dilute NaOH solution (0.02 M), while the size of formed aggregation were checked frequently using DLS technique.

#### 2.3.1.2 Film rehydration method

Polymer self-assemblies were prepared using film rehydration method for a selection of synthesised terpolymers. First a thin film of terpolymer was prepared on glass surface of 50 mL round bottom flask by dissolving 50 mg of terpolymer in 2 mL of THF followed by evaporation of the solvent using a rotary evaporator at room temperature at 300 rpm for duration of 5 minutes. Afterwards, deionised water (5 mL) was gradually added to the flask containing the polymer thin film and subsequently the flask was hand-shaked for 30 minutes. The samples were left for 1 hour to rest and then were characterised in terms other their size using DLS at 25, 37 and 50 °C.

### 2.3.2 Preparation of ATPS

ATPSs consisting of dextran and PEG with a range of volume fractions of dextran rich and PEG rich phases were prepared based on the phase diagram Albertsson<sup>11</sup> provided in his book (see Figure 2.2). Tie line 'F' and 'G' which are far from the critical point were chosen for the preparation of dextran-PEG ATPSs with different volume fractions. ATPS were prepared by dissolving the required amount of PEG and dextran in adequate deionised water to give 5 g of ATPS in total. Table 2.4 and 2.5 illustrates the used amounts of dextran, PEG and water in wt.% for the preparation of ATPS and their corresponding obtained volume fractions on tie line 'F' and 'G'. The volume fractions of dextran rich and PEG rich phases were calculated after a complete phase separation by dividing the height of each phase to the total height of the ATPS in sample vial.

**Figure 2.2.** Phase diagram of the Dextran ( $M_w = 500$  kDa) and PEG ( $M_w = 6$  kDa) system at 20°C. The solid line shows the binodal and the dashed lines in the two-phase region show tie-lines terminating in the unfilled circles. The filled circle indicates the plait point. The unfilled triangle and square symbols indicate different ATPS compositions used for emulsion preparation on tie line F and G respectively.

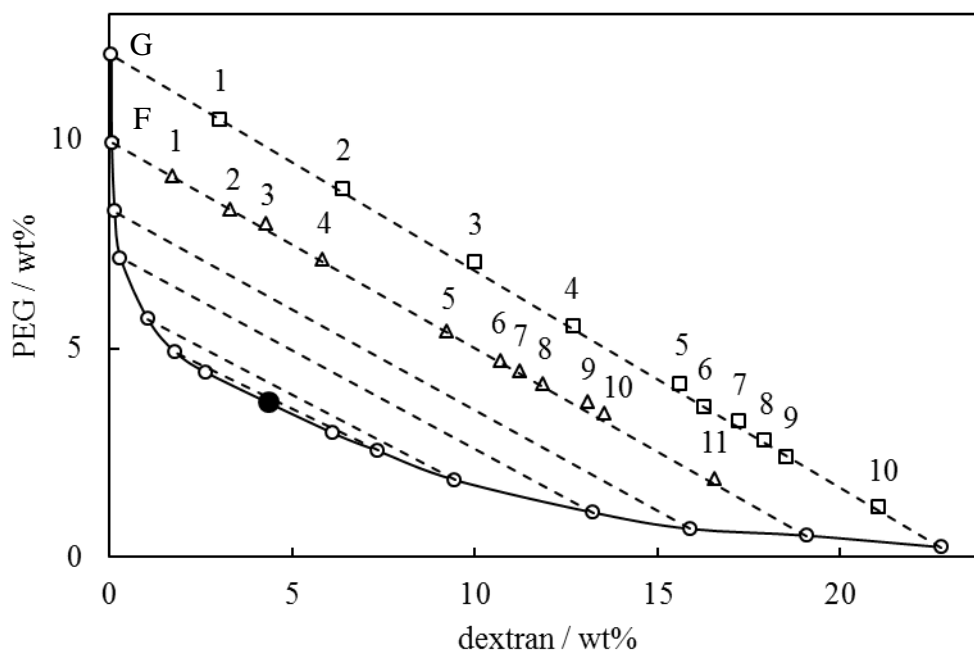


**Table 2.4.** Composition of prepared dextran-PEG ATPSs and their corresponding volume fractions after a full phase separation over tie line ‘F’.

Tie line F					
Point	Dextran wt. %	PEG wt. %	Water wt. %	$\phi_{\text{dextran}}$	$\phi_{\text{PEG}}$
1	1.72	9.12	89.16	0.16	0.84
2	3.30	8.33	88.37	0.21	0.79
3	4.28	8.00	87.72	0.23	0.77
4	5.84	7.13	87.03	0.30	0.70
5	9.24	4.96	85.80	0.50	0.50
6	10.71	4.71	84.58	0.55	0.45
7	11.25	4.46	84.29	0.56	0.44
8	11.86	4.13	84.01	0.62	0.38
9	13.09	4.00	82.91	0.63	0.37
10	13.54	3.26	83.20	0.74	0.26
11	16.55	1.86	81.59	0.86	0.14

**Table 2.5.** Composition of prepared dextran-PEG ATPSs and their corresponding volume fractions after a full phase separation over tie line ‘G’.

Tie line G					
Point	Dextran wt. %	PEG wt. %	Water wt. %	$\phi_{\text{dextran}}$	$\phi_{\text{PEG}}$
1	3.03	10.46	86.51	0.15	0.85
2	6.38	8.80	84.82	0.31	0.69
3	10.02	7.06	82.92	0.45	0.55
4	12.70	5.53	81.77	0.55	0.45
5	15.61	4.13	80.26	0.68	0.32
6	16.30	3.60	80.10	0.70	0.30
7	17.23	3.26	79.51	0.75	0.25
8	17.92	2.80	79.28	0.77	0.23
9	18.54	2.40	79.06	0.79	0.21
10	21.05	1.20	76.75	0.84	0.06

### 2.3.3 Preparation of w/w emulsion

In this study hydrophobised silica nanoparticles, PEGylated silica nanoparticles, ABA Pluronics<sup>®</sup> and ABC terpolymers were used as stabiliser for stabilisation of ATPS based w/w emulsions. The procedure of emulsion preparation was quite similar in terms of used stabiliser with slight differences in preparation procedures which are described here.

In the case of using either hydrophobised or PEGylated silica nanoparticles 1, 2, 3 and 4 wt.% of nanoparticles, 9.24 wt.% dextran and 4.96 wt.% PEG was added to adequate amount of deionised water to give 5 g of emulsion in total (The amount of used deionised water was decreased according to increase in concentration of stabiliser in the system). The prepared mixture was then stirred using a magnetic stirrer bar for a few hours to ensure full dissolution of dextran and PEG in water. Afterwards, the prepared mixture was homogenised using an Ultra-Turrax T25 basic IKA Labortechnik homogeniser with an 8 mm dispersing head at 11000 rpm for duration of two minutes. Emulsions were prepared in screw-capped (caps fitted with foil liners) glass sample tubes of inner diameter 19 mm and length 71 mm and were kept at room temperature.

In the case of using Pluronic<sup>®</sup> 1-10 wt.% of stabiliser was added to the system and the same procedure was repeated for the emulsion preparation while the amount of added milliQ water was deducted accordingly.

In the case of using ABC terpolymers, 1 wt.% of stabiliser was used in all cases, unless stated otherwise. Also, the pH of the mixture was adjusted to the desired pH (4, 5, 6 or 7) prior to emulsification using 2 M HCl in order to ensure full dissolution of ABC terpolymers in the system. Using a magnetic stirrer bar (dimensions 11 x 4 mm), the mixtures were then emulsified by stirring at 500 rpm for either 2 hours or 30 minutes using an IKA stirrer hotplate.

#### ***2.3.4 Encapsulation of fluorescent probes***

Fluorescent probes namely, fluorescein, FITC-dextran and rhodamine 6G were used as encapsulant for study of permeation rate of the adsorbed ABC terpolymers film around the emulsion dispersed phase. Fluorescent probes (0.04 mg/mL of fluorescein and rhodamine 6G, 0.2 mg/mL FITC-dextran with different partitioning ability between dextran and PEG rich phases were added to the w/w emulsion either prior or after addition of stabiliser.

## 2.4 Characterisation methods

### 2.4.1 Gel permeation chromatography

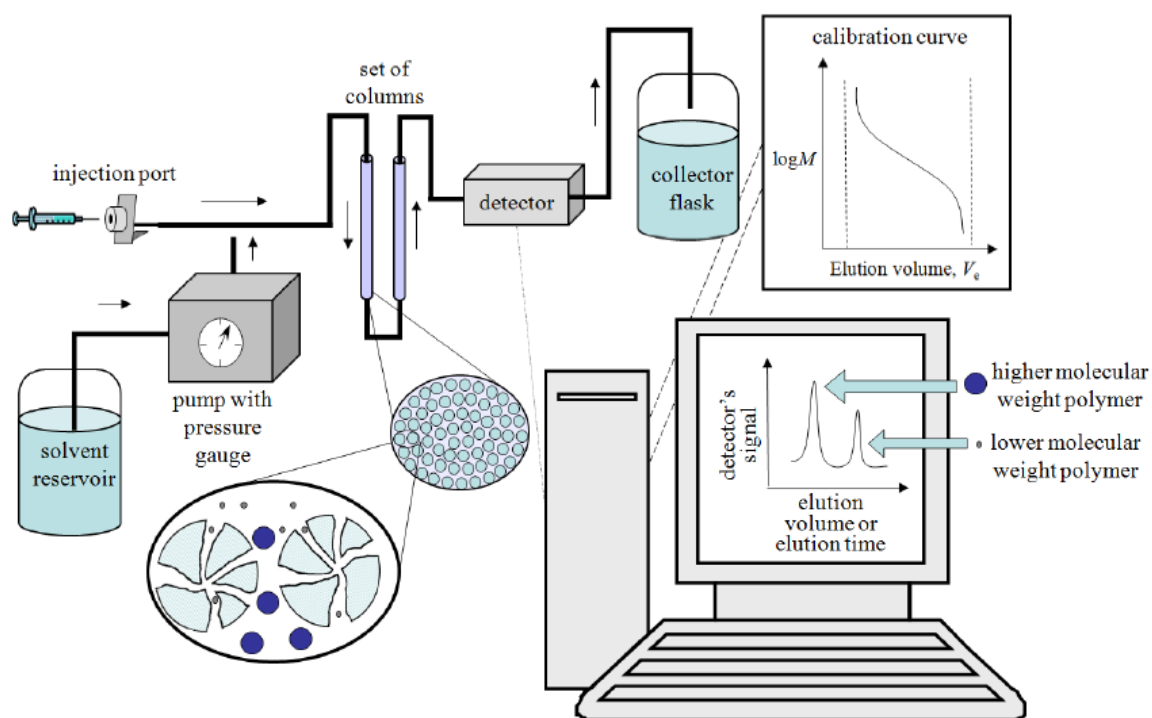
Gel permeation chromatography (GPC), also called size exclusion chromatography (SEC), is a technique to analyse polymers in terms of their molecular weight and molecular size distributions (polydispersity). In fact, GPC is an effective method used for separation of macromolecules based on their hydrodynamic volumes (volume of molecule when it is hydrated). In this technique at first a small fraction (100  $\mu\text{L}$ ) of diluted polymer solution (100 mg/mL) is injected into the sample inlet and subsequently it flows through a column by a solvent stream. The column is packed with beads of a porous gel, normally cross-linked polystyrene or silica based gels, in which the porosity of gels is a determinant factor for the separation of molecules. The stream of solvent carries the polymer with them through the porous gels. Partitioning of polymer chains between the mobile phase (eluent) and stationary phase (gel beads), results in retention of polymer inside the column. The smaller the size of polymers, the more they diffuse between and within the pores of the gel beads and therefore, they go through a longer pathway through the column. Conversely, the larger molecules are not able to go within the pores due to their large hydrodynamic volume and so they pass through the column without entering into the pores. Therefore, they have a short pathway and they elute from column earlier compared to smaller molecules. In other words, polymer molecules elute from the chromatography column in order of decreasing their hydrodynamic volumes (or molecular size in solution). The time that it takes for a molecule to elute from the column is called retention or elution time. The bigger the size of the molecule, the shorter is the retention time and vice versa. Using a detector which is normally sensitive to change in refractive index (RI) and/or viscosity, ultraviolet (UV) absorption and/or infrared (IR) absorption, the concentration of polymers is monitored in the eluted eluent, which is a qualitative indication of the molecular weight distribution of polymers (see Figure 2.3).<sup>12</sup>

GPC itself does not give an absolute molecular weight. However, retention volume or retention time of the unknown polymer can be converted to the quantitative values of molecular weight using two main approaches, namely, peak-position approach and universal calibration approach. In peak-position approach,



polymer samples with narrow PDI and known molecular weight are used to calibrate the column and their retention volumes or times are determined. Then a plot of  $\log(MW)$  versus retention time is used to determine the molecular weight and molecular weight distribution of unknown polymer. However, this method is subjected to error as the used polymer samples for the calibration are usually PS or/and PMM, which usually differ from the unknown polymers in structure and conformation. The second approach, universal calibration, is based on using polymer hydrodynamic volume which is independent of the polymer structure and proportional to  $([\eta]*M)$ , where  $[\eta]$  and  $M$  are intrinsic viscosity and molecular weight respectively. In this technique a viscometer detector is utilised to measure the intrinsic viscosity directly. Afterwards, a calibration curve of  $\log([\eta]*M)$  is plotted versus retention time or volume, using polymer samples with narrow PDI and known molecular weight. Then, the retention time or retention volume of unknown sample is compared with the prepared universal calibration plot to give the precise molecular weight, as the intrinsic viscosity is known from the viscometer detector. This method can be used for evaluation of any other polymer regardless of their structure and conformation in solution.<sup>13</sup>

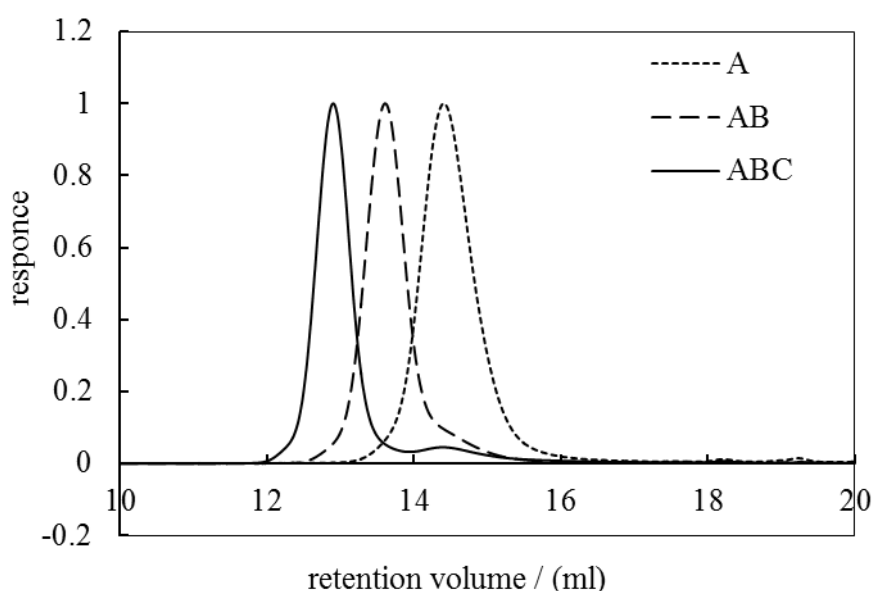
**Figure 2.3.** Schematic representation of GPC instrumentation.<sup>14</sup>



Chromatograms corresponding to block copolymers and their precursor are an indication of their successful synthesis. As each block of copolymer is added the total molecular weight of copolymer increases, therefore, it is eluted and detected earlier than its precursor. For example, for an ABC terpolymer three peaks are distinguishable on GPC chromatograms which are corresponding to A, AB and ABC respectively. Figure 2.4 shows typical GPC chromatograms for a terpolymer and its bi- and homopolymer precursors.

The number average molecular weight ( $M_n$ ) and polydispersity indices of all the PEGMA homopolymers, the intermediate PEGMA-*b*-BuMA biopolymers and the final PEGMA-*b*-BuMA-*b*-DMAEMA terpolymers were determined by GPC using a single PL Mixed 'E' Polymer Laboratories column. THF containing 5 vol.% triethylamine was the mobile phase and was pumped with a flow rate of 1 mL/min using a Viscotek vt7510 pump. A Viscotek 3580 differential refractometer was used to measure the refractive index signal. The calibration curve was based on nine narrow MW linear poly(methyl methacrylate)s (PMMA)s with MWs of 690, 5720, 1020, 1200, 1960, 4000, 8000, 13300 and 20010 g/mol.

**Figure 2.4.** Typical GPC chromatogram corresponding to an ABC terpolymer and its precursor AB bipolymer and A homopolymer.



### 2.4.2 NMR spectroscopy

Polymer characterisation by NMR (Nuclear Magnetic Resonance spectroscopy) provides detailed information of polymers. This information includes monomer type, polymer type (block or statistical), polymer structure, polymer block ratios, polymer molecular weight, degree of polymerisation of each block, polymer tacticity, polymer chain branching and polymer end groups.

Basic principle of NMR is based on the absorption and re-emission of electromagnetic radiation when magnetic nuclei with a spin are placed in a magnetic field. Generally, nuclei with a non-zero spin quantum number ( $I > 0$ ) have an intrinsic magnetic moment. The most studied nuclei are  $^1\text{H}$  and  $^{13}\text{C}$ ; in addition, other nuclei such as  $^{15}\text{N}$ ,  $^{31}\text{P}$ , etc. can be studied by NMR spectroscopy. When a sample is placed in a magnetic field, the nuclei of the atoms possessing magnetic momentum align with the magnetic field. Then by applying pulses of energy in the radio frequency range perpendicular to the magnetic field, nuclei begin to spin around the axis of the magnetic field (perpendicular to magnetic field). Those frequencies that match the energy level difference in the nuclei are absorbed and the other frequencies are not. This spinning is for a short time and the nuclei start moving towards being parallel to the magnetic field again. As the nuclei relax they emit a characteristic frequency which provides a signal and it is detectable. This signal is dependent on the nuclei type, the electron environment and magnetic field strength. Therefore, not only the identification of elements in a sample is possible, but also the type of molecule and molecule structure can be determined. Also, it is possible to quantitatively determine how much of an element or molecule is present in the sample by strength of the NMR signals in a NMR spectrum.

$^1\text{H}$  NMR characterisation of synthesised terpolymers and their precursors was carried out on a JEOL (400 MHz) spectrometer in  $\text{CDCl}_3$  at room temperature at concentration of about 200 mg/mL. The relative areas of the peaks were determined by electronic integration of the relative peak areas on the NMR spectrum.

### 2.4.3 Dynamic light scattering

Dynamic light scattering (DLS) technique also known as Photon Correlation Spectroscopy (PCS) has been widely used for characterisation of polymer solutions. In this technique, particles in a solution are illuminated by a laser beam and the intensity fluctuations in scattered light are measured. The size of the particles can be determined by analysing the measured scattering intensity fluctuation.

In this study DLS was mainly used to determine the size of PEGylated silica nanoparticles, hydrodynamic diameter of terpolymers and the size of their aggregation in solution. A Malvern ZetaSizer Nano ZS equipped with a 4mW He-Ne laser, operating at wavelength of 673 nm was used for the DLS measurements at angle of 175°. Samples were run for two minutes in disposable polystyrene cuvettes and each measurement repeated for at least three times, then the obtained data was averaged.

For size measurements of PEGylated silica nanoparticles, a dispersion of particles in deionised water (1 wt.%) was prepared via homogenisation for 2 minutes using an Ultra Turrax T25 basic IKA Labortechnik homogeniser with 8 mm dispersing head at 11000 rpm. To determine the hydrodynamic diameter of terpolymers and the size of their micelles in aqueous solution, a series of terpolymer solutions with a range of concentrations (bellow and above CMC) and the pH adjusted to 7 were prepared by diluting up the prepared 1 wt.% terpolymers stock solutions. Prior to DLS measurement, polymer solution samples were filtered through 0.45 µL PTFE syringe filters and were left at rest for 30 minutes.

The ABC terpolymers hydrodynamic diameters and their micelle size in aqueous solution were also calculated theoretically using random coil configuration model <sup>15</sup> and spherical micelle based on ABC terpolymers model <sup>10</sup> which are summarised in equation 2.1 and 2.2 respectively as bellow:

$$d_{\text{dimer}} = 2 \times \left( 2 \times 2.20 \times \frac{DP}{3} \right)^{\frac{1}{2}} \times 0.154 \quad \text{Eq. 2.1}^{15}$$

$$d_{\text{micelle}} = (DP_{\text{hydrophobe}} \times 0.254) + 2 \times (DP_{\text{longer hydrophile}} \times 0.254) \quad \text{Eq. 2.2}^{10}$$

Where, DP is the degree of polymerisation, 0.154 value is the length of carbon-carbon bond along the polymer backbone and 0.254 value is the projected length of each monomer along the polymer chain. Degree of polymerisation of each block was determined based on the GPC and  $^1\text{H}$  NMR experimental data.

#### **2.4.4 FT-IR spectroscopy**

Fourier transform infrared spectroscopy (FT-IR) is a technique which is used to identify molecules based on their constituent bonds. Molecules absorb specific frequencies that are characteristic of their structure. In this technique an infrared radiation ( $4000$  to  $400\text{ cm}^{-1}$ ) is emitted to the sample and some specific wavelengths of the radiation which have the same frequency as the vibrational frequency of the bonds are selectively absorbed by the sample. This causes a change in dipole moment of sample molecules. Consequently, the vibrational energy levels of sample molecules transfer from ground state to excited state. Analysis of the transmitted radiation using a Fourier Transform instrument reveals the extent of absorbed energy at each frequency or wavelength. The frequency, number of absorption peaks and intensity of absorption is corresponding to vibrational energy gap, number of vibrational freedom of the molecule and the change of the dipole moment of the molecule respectively. Therefore, useful structural information can be obtained by analysing the infrared spectrum.

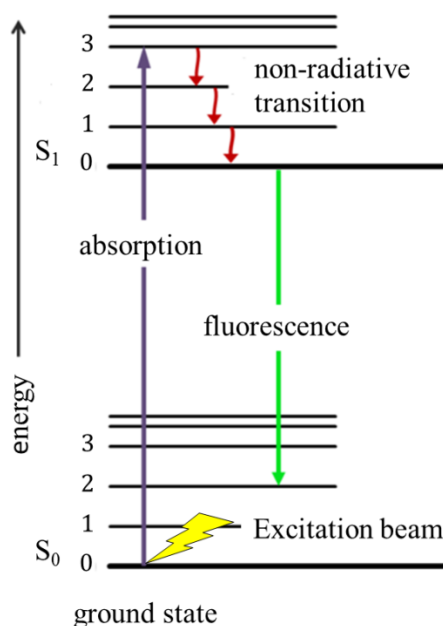
The PEG content of PEGylated silica nanoparticles was determined using a Perkin Elmer spectrum RX1 FT-IR spectrometer. A calibration curve was obtained by plotting the absorption peak area characteristic to PEG at  $2888\text{ cm}^{-1}$  versus concentration of PEGylated silica nanoparticles present in prepared KBr disks. For preparation of KBr disks, the amount of KBr was kept constant whilst the amount of PEG polymer was systematically varied. In each case 120 mg of KBr was thoroughly ground with 1, 2, 4 and 6 mg of the PEGylated silica sample.

#### **2.4.5 Fluorescence spectroscopy**

Fluorescence spectroscopy is a technique which is used to analyse fluorescence emission of a fluorescent sample. Generally, molecules are in their lowest vibrational level of the ground electronic state at room temperature. When a beam of light is emitted to fluorescent molecules, they absorb light at a particular

wavelength and elevate to excited states. After a brief interval of time, they lose their excess energy by returning to any of the vibrational levels of the ground state and subsequently emit light of longer wavelength in the form of fluorescence emission (see Figure 2.5).

**Figure 2.5.** Transitions giving rise to absorption and fluorescence emission spectra.



Fluorescence emission spectrum can be obtained by plotting the fluorescence emission intensity at any given excitation wavelength, while the intensity of excitation light is constant.

In this work a Perkin ElmerLS55 fluorescence spectrometer equipped with a thermostated cell holder was used to measure the emission intensity of the pyrene (a fluorescent probe) dissolved in amphiphilic terpolymer solution as a function of polymer concentration, in order to find the CMC of terpolymers. The fluorescence emission spectra of the pyrene were recorded from 350 to 470 nm after excitation at 300 nm. The slit width was set at 5 nm for both excitation and emission. Pyrene fluorescence spectrum illustrates two relatively strong intensity peaks at  $\lambda_{\text{max}}=373$  and 383 nm, known as  $I_1$  and  $I_3$  respectively. The intensity of  $I_1$  or  $I_3$  is strongly dependent on the polarity of the environment and hence can be used to determine the CMC of the amphiphilic species in aqueous solution as explained in section 1.4.2. A series of solutions with a range of terpolymer concentration (0.001- 1 wt.%) and a

fixed concentration of pyrene (1  $\mu\text{M}$ ) were prepared. The fluorescent emission of pyrene was measured in a quartz cell while the reference solution was terpolymer solution at the same concentration. The emission intensity of peak  $I_3$  was plotted as a function of terpolymer concentration and the CMC value was taken from the intersection of the best fit lines.

#### **2.4.6 Microscopy**

In this work optical transmission microscopy, fluorescence microscopy, transmission electron microscopy and scanning electron microscopy were employed as characterisation tools to study the samples. The characteristics of these different techniques are described individually in the following sections.

##### *2.4.6.1 Optical transmission microscopy*

In optical transmission microscopy, visible light is transmitted through the sample (illuminated from below and observed from above) and subsequently it passes through several lenses in order to provide a magnified view of the sample. In this work an Olympus BX51 optical microscope equipped with a 12-bit Olympus camera (model DP70) was used with a series of objectives of 4x, 10x, 20x, 50x and 100x magnification. Microscopy samples were prepared by placing one drop of sample on a microscope slide, covered by a coverslip. In some cases, the sample was held within an aluminium foil gasket of 11  $\mu\text{m}$  thickness which separated the microscope slide and cover slip. Image Pro Plus software was used to measure the size distribution of the dispersed particles or droplets from each micrograph. More than 100 particles or droplets were manually selected and data were exported to Microsoft Excel for data analysis. Scale bars for the micrographs were determined using a Pyser-SGI S78 graticule and added to the digital micrographs using the image editing functions in Microsoft PowerPoint.

##### *2.4.6.2 Fluorescence microscopy*

In fluorescence microscopy, sample containing fluorescing species is illuminated with specific wavelength light which is absorbed and results in excitation of fluorescent species. Subsequently, the excited species emit lower energy light of longer wavelength which is then separated and filtered through a dichromic mirror

and spectral emission filter. Desired wavelength transmits through the filter towards the detector which is then collected by the eyepiece for observation.

In this work the same microscope set, used for transmission microscopy, was fitted with a series of fluorescent filter sets corresponding to the adsorption and emission wavelength of some specific fluorescent dyes, where required. The characteristics of the used filter sets in this study are summarised in Table 2.6. Sample preparation was similar to that of the transmission microscopy.

**Table 2.6.** Characteristics of the used fluorescent filter sets.

Commercial name	Description	$\lambda_{\text{excit.}}(\text{nm})$	$\lambda_{\text{emit.}}(\text{nm})$	Used dye
U-MWIBA2	Wide-band with band-pass barrier filter	460-490	510 IF	FITC Fluorescein
U-MWIG2	Wide-band with interface barrier filter	520-550	580 IF	Rhodamine

Using the Line Profile command in Image Pro Plus software, the colour intensity corresponding to FITC or Fluorescein (green regions) and rhodamine (red regions) were converted to numerical values for determination of permeation rate of fluorescent probes in the encapsulation studies.

#### 2.4.6.3 Scanning electron microscopy

Scanning electron microscopy (SEM) utilises an electron beam emitted from an electron gun instead of a light beam. The electron beam follows a vertical path through electromagnetic fields and lenses which finally focus the electron beam on the sample. Once the electron beam hit the sample, due to the interaction of electron beam with atoms at the surface of the sample, a variety of signals is produced, namely, X-ray, backscattered electrons and secondary electrons which are collected by two detectors and converted to the final image. SEM benefits from a large depth of field due to the narrow nature of the electron beam which yields a characteristic 3D high resolution image of the surface structure.

In this study a Zeiss EVO60 SEM fitted with a LaB6 emitter, with an accelerating voltage of 20 kV and a probe current of 70 pA was used. Wet samples were placed on circle microscope cover slip and dried at room temperature. The



dried samples on glass surface were attached to an aluminium sample mount using carbon impregnated sticky disk. Any excess or loose material was removed by compressed air. The prepared mounts were then coated with either carbon or Au-Pd film of approximately a few nanometres (2-10 nm) thickness using a Polaron SC7640 sputter coater.

#### *2.4.6.4 Transmission electron microscopy*

Transmission electron microscopy (TEM) uses high energy electrons with an accelerating voltage up to 300 kV. The electron beam is accelerated to near the speed of light with wavelength about a million times shorter than light waves. Passing an electron beam through a thin-section specimen, results in scattered electrons. Using a sophisticated system consisting of electromagnetic lenses, the scattered electrons are focused into an image which provides a highly magnified view of the sample.

In this work, the TEM Images were obtained using a Gatan Ultrascan 4000 digital camera attached to a Jeol 2010 TEM running at 120kV. The sample was prepared as following; a glow-discharged carbon-coated copper grid was floated onto a drop of sample on parafilm for two minutes. Excess sample was wicked from the grid using filter paper and the grid was rinsed by transferring it to a drop of pure water for a few seconds. The grid was wicked again with filter paper and then transferred to a drop of 1 wt.% aqueous uranyl acetate for 1 minute as a negative stain. Excess stain was removed with filter paper and the grid allowed to air dry.

#### *2.4.7 Aqueous solution characterisation*

Aqueous solutions of the synthesised terpolymers were characterised in terms of their effective  $pK_a$  and cloud points, which are described in the next sections.

##### *2.4.7.1 Determination of $pK_a$*

Polymers containing ionisable pendant groups in their monomer units can be ionised in acidic, neutral or basic environment depending on their  $pK_a$  value. In definition,  $pK_a$  is the negative logarithm value of the acid dissociation constant ( $K_a$ ) of an acid. Acid dissociation constant and  $pK_a$  value for an acid HA can be defined in equations as bellow:

$$pK_a = -\log_{10} K_a$$

**Eq. 2.3**

The  $pK_a$  value is in fact a numeric value for the strength of an acid. The stronger the acid the lower is the value of  $pK_a$ . When the pH of a solution is equal to the  $pK_a$  value, the acid is half dissociated. Once the pH of the solution is either less or more than the  $pK_a$  value, the acid is in its protonated and deprotonated state respectively.

In order to find the  $pK_a$  value of the synthesised terpolymers, 1 wt.% aqueous solutions of them were titrated between pH= 2 and 12 using a standard NaOH 0.2 M solution under continuous stirring. The pH was measured using a Fisher brand Hydrus 400 pH meter. The  $pK_a$ s were calculated as the pH at 50% ionization by plotting the pH values versus the volume of added NaOH solution.

#### *2.4.7.2 Cloud point*

Cloud point is a temperature at which a polymer is no longer soluble and begins to phase separate due to the reverse solubility versus temperature in aqueous solutions.

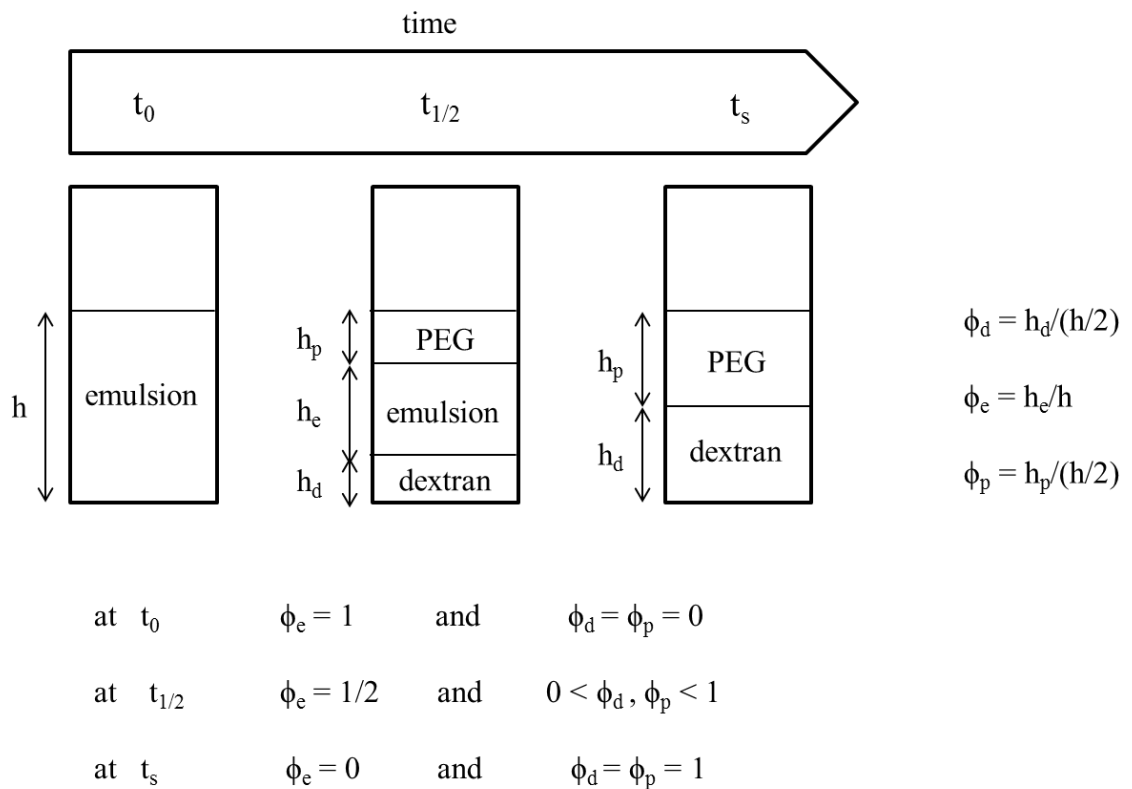
An IKA stirrer hotplate, VWR VT-5 temperature controller and oil bath were used for the cloud point measurements. Polymer solutions (1 wt.%) were made in glass vials, suspended in a temperature controlled oil bath and stirred with small magnetic bars. The solutions were heated at a rate of 1°C/min over a range of 20–90 °C and observed for a visual indication of cloud point.

#### *2.4.8 Stability measurement of w/w emulsion*

The stabilities of the emulsions, incubated within the screw capped glass vessels used for their preparation, were assessed by recording the volume fractions of resolved PEG ( $\phi_p$ , upper less dense region) and dextran ( $\phi_d$ , lower denser region) phases and unresolved emulsion ( $\phi_e$ , middle region) as a function of time. The volume fraction of PEG and dextran regions was determined by dividing the height of that region ( $h_p$ , or  $h_d$ ) to half of the total height ( $h$ ) of the mixture in the glass vessels where the 0.5:0.5 volume fractions of dextran and PEG was used for the preparation of the emulsion. When initial volume fractions of dextran and PEG were varied in the system for preparation of emulsion, the volume fraction of each phase

after phase separation was calculated accordingly. The volume fraction of emulsion region was obtained by dividing the height of the emulsion region ( $h_e$ ) to the total height ( $h$ ) of the mixture. Time was recorded in hour unit and  $t_0$ ,  $t_{1/2}$  and  $t_s$  can be defined as the start time (upon stopping emulsification), half-life time and full separation time (when complete phase separation occurred) respectively (see Figure 2.6).

**Figure 2.6.** Determination of volume fraction of dextran, emulsion and PEG region resolved or remained from the emulsion over time.



## 2.5 Reference

1. N. B. Vargaftik, B. N. Volkov and L. D. Voljak, *J. Phys. Chem. Ref. Data*, 1983, **12**, 817.
2. B. P. Binks and S. O. Lumsdon, *Langmuir*, 2000, **16**, 8622.
3. I. B. Dicker, G. M. Cohen, W. B. Farnham, W. R. Hertler, E. D. Laganis and D. Y. Sogah, *Macromolecules*, 1990, **23**, 4034.
4. W. Stöber, A. Fink and E. Bohn, *J. Colloid Interface Sci.*, 1968, **26**, 62.
5. H. Xu, F. Yan, E. E. Monson and R. Kopelman, *J. Biomed. Mater. Res., Part A*, 2003, **66**, 870.
6. N. H. Raduan, T. S. Horozov and T. K. Georgiou, *Soft Matter*, 2010, **6**, 2321.
7. M. A. Ward and T. K. Georgiou, *J. Polym. Sci., Part A: Polym. Chem.*, 2010, **48**, 775.
8. M. A. Ward and T. K. Georgiou, *Soft Matter*, 2012, **8**, 2737.
9. M. A. Ward and T. K. Georgiou, *J. Polym. Sci., Part A: Polym. Chem.*, 2013, **51**, 2850.
10. M. A. Ward and T. K. Georgiou, *Polym. Chem.*, 2013, **4**, 1893.
11. P. Albertsson, *Partition of cell particles and macromolecules*, Wiley-Interscience, New York, 1971.
12. R. J. Young and P. A. Lovell, *Introduction to Polymers*, 2nd. edn., Nelson Thornes Ltd, Cheltenham, 2000.
13. C. E. Carraher, *Introduction to Polymer Chemistry*, 2nd. edn., CRC Press, New York, 2010.
14. B. Sitharaman, *Nanobiomaterials Handbook*, CRC Press New York, 2011.
15. P. C. Hiemenz, *Polymer Chemistry: The Basic Concepts*, Marcel Dekker, New York, 1984.

## **CHAPTER 3**

### **DESIGN, SYNTHESIS AND CHARACTERISATION OF TERPOLYMERS**

### **3.1 Introduction**

Developments in synthesis techniques of block copolymers as well as the endless combinations of polymers physical and chemical properties have made them valuable material with potential applications in different areas. In particular, because of block copolymer segmental incompatibility, they show fascinating behaviour in both bulk and solution. In this work a series of amphiphilic terpolymers with potential application in formation of polymersomes and stabilisation of w/w emulsions were designed, synthesised and characterised. In this chapter the design and characterisation of these amphiphilic terpolymers are described and discussed in details.

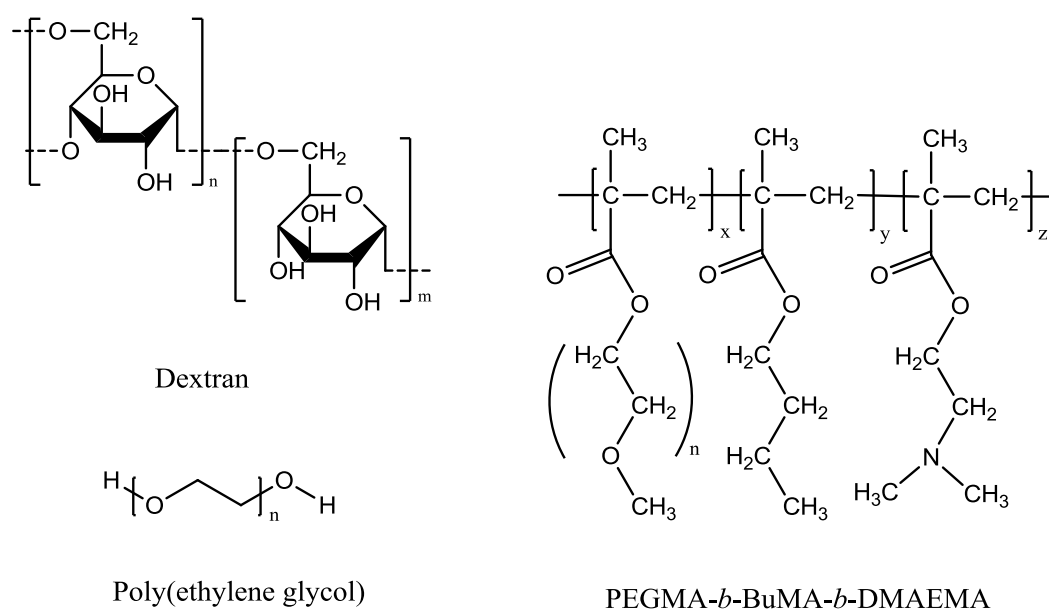
### **3.2 Terpolymers design and synthesis**

A series of amphiphilic ABC terpolymers consisting of 38 terpolymers with varied compositions, block ratios and molecular weights were designed in order to form polymersomes either in aqueous solutions or by templating w/w emulsions based on dextran-PEG ATPS. As it was mentioned before, the main aim of this project was to prepare polymersomes based on w/w emulsions, therefore, in first place the emphasis on the design of terpolymers was on their ability to stabilise w/w emulsions at which the stability arises from polymersomes formation around the dispersed phase. The second aim was to also examine some of the synthesised terpolymers in terms of their ability to form polymersomes in aqueous solution.

The ABC terpolymers consisted of a hydrophilic non-ionic monomer PEGMA, a non-ionic hydrophobic monomer BuMA and a hydrophilic ionisable and thermo-responsive monomer DMAEMA. The hydrophobic monomer, BuMA consists the B block, which is in the middle of the terpolymer where the two hydrophilic monomers PEGMA and DMAEMA form the A and C blocks, respectively. The reason behind choosing these monomers and ABC type terpolymer was firstly the possibility of contribution of the amine functional groups of DMAEMA block in formation of hydrogen bond with the dextran hydroxyl groups. Consequently, it was assumed that the DMAEMA block has tendency to remain in dextran rich phase. Secondly, it was presumed the PEGMA block with a comb like structure consisting of a polymethacrylate back bone and PEG brushes has an affinity with the PEG rich phase, since they both have same chemical structure. As a

result this type of amphiphilic terpolymers is expected to have the ability to stabilise a w/w emulsion consisting of dextran and PEG rich phases. In addition, the presence of BuMA block in the structure of this terpolymer enhances the possibility of polymersomes formation in such system. For a better understanding, the chemical structures of PEGMA<sub>x</sub>-*b*-BuMA<sub>y</sub>-*b*-DMAEMA<sub>z</sub> terpolymer, dextran and PEG are shown in Figure 3.1.

**Figure 3.1.** The chemical structures of the PEGMA-*b*-BuMA-*b*-DMAEMA terpolymer, dextran and PEG.



At the beginning of this project, because of unfamiliar behaviour of terpolymers in emulsified dextran-PEG ATPS and also the unknown requirements of terpolymers in terms of their molecular weight, composition, A/C block ratio, hydrophobic content, etc. for being adsorbed at the dextran-PEG interface, the design of terpolymers was quite challenging. Therefore, initially, it was decided to systematically vary three main factors in the composition of ABC terpolymers. The first three factors varied are as following:

1. Length of B was varied at a constant A/C block ratio.
2. The A/C blocks ratio was varied at a constant B block length.
3. The lengths of A and C block was varied at a constant A/C ratios and constant B block.

Then based on the obtained results, the compositional requirements of ABC terpolymers which are necessary for stabilisation of w/w emulsions, or in the other words, for formation of polymersomes based on w/w emulsions, were recognised and further optimised by varying other factors. When the best composition was recognised, the molecular weight of terpolymers was varied at a constant composition in order to improve the stability of the system. In total for this work 38 ABC terpolymers all having the general structure PEGMA<sub>x</sub>-*b*-BuMA<sub>y</sub>-*b*-DMAEMA<sub>z</sub> were synthesised and studied in terms of their ability to stabilise w/w emulsions based on dextran-PEG ATPS and to form templated polymersomes. For convenience from this point onwards these terpolymers will be referred to as P<sub>x</sub>-B<sub>y</sub>-D<sub>z</sub> throughout this thesis, where P, B and D stand for PEGMA, BuMA and DMAEMA blocks respectively with their corresponding degree of polymerisations assigned with x, y and z.

All the terpolymers were synthesised using the GTP technique. Specifically, a mono-functional initiator was used for initiation of polymerisation followed by the sequential addition and polymerisation of the three monomers: PEGMA, BuMA and DMAEMA. The composition of terpolymers was varied by changing the amount of the monomer additions. Table 3.1 illustrates the design and schematic structure of terpolymers synthesised in this study. The PEGMA, BuMA and DMAEMA units are shown in light blue, red and dark blue, respectively.

**Table 3.1.** Classification of synthesised terpolymers based on the varied factors in their composition.

Polymer Schematic Structure	Polymer Structure P <sub>x</sub> -B <sub>y</sub> -D <sub>z</sub>	Varied Factors
	P <sub>7</sub> -B <sub>48</sub> -D <sub>33</sub> P <sub>13</sub> -B <sub>52</sub> -D <sub>35</sub> P <sub>41</sub> -B <sub>56</sub> -D <sub>32</sub>	varying A at constant B and C
	P <sub>13</sub> -B <sub>52</sub> -D <sub>35</sub> P <sub>13</sub> -B <sub>65</sub> -D <sub>38</sub> P <sub>13</sub> -B <sub>67</sub> -D <sub>36</sub> P <sub>13</sub> -B <sub>76</sub> -D <sub>40</sub> P <sub>14</sub> -B <sub>81</sub> -D <sub>43</sub>	varying B at constant A and C



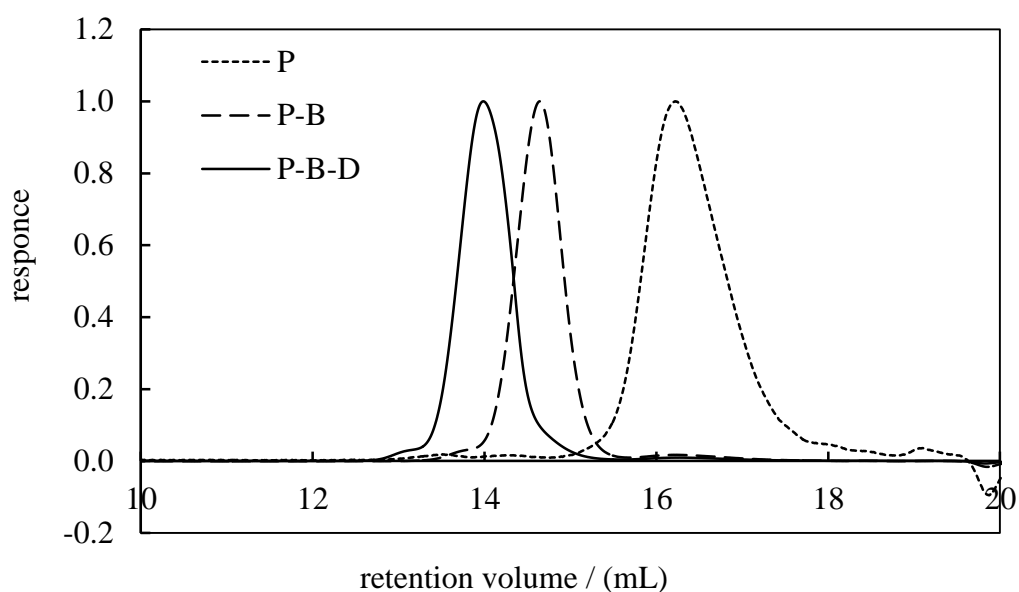
Polymer Schematic Structure	Polymer Structure $P_x-B_y-D_z$	Varied Factors
	$P_{13}-B_{67}-D_{36}$ $P_{13}-B_{76}-D_{40}$ $P_{14}-B_{70}-D_{73}$	varying C at constant A and B
	$P_{13}-B_{76}-D_{40}$ $P_{41}-B_{56}-D_{32}$	varying A/B at constant C and similar DP
	$P_{27}-B_{54}-D_{14}$ $P_7-B_{51}-D_{39}$	varying A/C at constant B and similar DP
	$P_{12}-B_{60}-D_{62}$ $P_{14}-B_{81}-D_{43}$	varying B/C at constant A and similar DP
	$P_{16}-B_{32}-D_{39}$ $P_7-B_{51}-D_{39}$	varying A/B at constant C and similar MW
	$P_{23}-B_{40}-D_{33}$ $P_8-B_{45}-D_{53}$	varying A/C at constant B and similar MW
	$P_8-B_{45}-D_{53}$ $P_7-B_{51}-D_{39}$	varying B/C at constant A and similar MW
	$P_5-B_{34}-D_{22}$ $P_{10}-B_{33}-D_{27}$ $P_{16}-B_{32}-D_{39}$ $P_{22}-B_{44}-D_{60}$	varying A and C at constant A/C ratio and constant B
	$P_2-B_{13}-D_{10}$ $P_3-B_{21}-D_{15}$ $P_4-B_{26}-D_{19}$ $P_5-B_{34}-D_{22}$ $P_6-B_{41}-D_{28}$ $P_7-B_{48}-D_{33}$ $P_7-B_{51}-D_{39}$	varying MW at constant composition
	$P_4-B_{18}-D_{17}$ $P_6-B_{36}-D_{32}$ $P_9-B_{47}-D_{47}$ $P_{11}-B_{60}-D_{64}$ $P_{12}-B_{60}-D_{62}$ $P_{14}-B_{70}-D_{73}$ $P_{15}-B_{80}-D_{85}$	varying MW at constant composition

Polymer Schematic Structure	Polymer Structure $P_x-B_y-D_z$	Varied Factors
	$P_{14}-B_{29}-D_{17}$ $P_8-B_{38}-D_{19}$ $P_8-B_{32}-D_{28}$ $P_4-B_{30}-D_{34}$ $P_{13}-B_{34}-D_{24}$ $P_7-B_{33}-D_{33}$	random compositions at constant MWs
	$P_{28}-B_{49}-D_{25}$ $P_{11}-B_{58}-D_{36}$ $P_{19}-B_{49}-D_{55}$ $P_{18}-B_{66}-D_{48}$ $P_4-B_{65}-D_{84}$	random compositions at random MWs

### 3.3 Determination of terpolymers composition and molecular weight

The number average and weight average molecular weight ( $M_n$  and  $M_w$ ) of all synthesised terpolymers as well as their molecular weight distributions were determined using GPC. The GPC chromatograms confirmed a successful sequential polymerisation. In particular, with the addition of the second and third monomer the peak shifts to the left, at higher  $M_n$ s and without the presence of any other peaks that could indicate partial deactivation of polymer chains, unsuccessful addition of the second or the third monomer and/or unreacted monomer. Figure 3.2 shows a typical GPC chromatogram of synthesised terpolymers corresponding to P3:  $P_{18}-B_{66}-D_{48}$  and its diblock and homopolymer precursors. If there were any other peaks from partial deactivation, they were less than 5%. The actual  $M_n$ s obtained from GPC was quite close to that of the theoretical ones, although in some cases due to the partial deactivation of initiator, the obtained  $M_n$ s were higher which is quite common in GTP as it is a highly sensitive polymerisation technique. Also, the initial deactivation of initiator has been reported to be due the slight impurity of big monomers, like PEGMA, which are not distillable due to their high molecular weights.<sup>1-4</sup> Polydispersity indices lower than 1.2 were obtained in all cases indicating narrow molecular weight distributions as reported for typical linear copolymers synthesised by GTP.<sup>5-9</sup>

**Figure 3.2.** GPC chromatographs of P29: P<sub>9</sub>-B<sub>47</sub>-D<sub>47</sub> terpolymer and its precursors P<sub>9</sub>-B<sub>47</sub> diblock and P<sub>9</sub> homopolymer.



The synthesised terpolymers were characterised in terms of their compositions by <sup>1</sup>H NMR spectroscopy. Figure 3.3 shows a typical <sup>1</sup>H NMR spectrum of P3: P<sub>18</sub>-B<sub>66</sub>-D<sub>48</sub>.

The composition of terpolymers were determined from their <sup>1</sup>H-NMR spectra by the integral ratio of the signals from the six methyl protons next to the amine of DMAEMA (peak 'o', 2.22 ppm) to the three methyl protons at the end of the PEG chain (peak 'e', 3.31 ppm) to two methyl protons next to carboxyl group of BuMA (peak 'h', 3.88 ppm) as following:

$$\text{wt. fraction of PEGMA} = \frac{\frac{e}{3} MW_P}{\frac{e}{3} \times MW_P + \frac{h}{2} \times MW_B + \frac{o}{6} \times MW_D} \quad \text{Eq. 3.1}$$

$$\text{wt. fraction of BuMA} = \frac{\frac{h}{2} MW_B}{\frac{e}{3} \times MW_P + \frac{h}{2} \times MW_B + \frac{o}{6} \times MW_D} \quad \text{Eq. 3.2}$$

$$\text{wt. fraction of DMAEMA} = \frac{\frac{o}{6} MW_D}{\frac{e}{3} \times MW_P + \frac{h}{2} \times MW_B + \frac{o}{6} \times MW_D} \quad \text{Eq. 3.3}$$

Where,  $MW_P$ ,  $MW_B$  and  $MW_D$  are molecular weights of PEGMA, BuMA and DMAEMA monomers respectively. The actual weight fractions of each block in all synthesised terpolymers were found in good agreement with the theoretical values. Thus overall the synthesis was successful. The actual degrees of polymerisation of the P, B and D blocks in the final terpolymers ( $x$ ,  $y$ ,  $z$ ) were determined using a combination of the GPC and  $^1H$  NMR data in a way that the calculated weight fractions obtained from  $^1H$  NMR were combined with the weight average molecular weight ( $M_w = PDI * M_n$ ) of the terpolymer as measured using GPC. Table 3.2 shows the molecular weights, compositions and degrees of polymerisation of the synthesised terpolymers.

**Figure 3.3.**  $^1H$  NMR spectrum ( $CDCl_3$ , 400 MHz) corresponding to P3: P<sub>18</sub>-B<sub>66</sub>-D<sub>48</sub>.

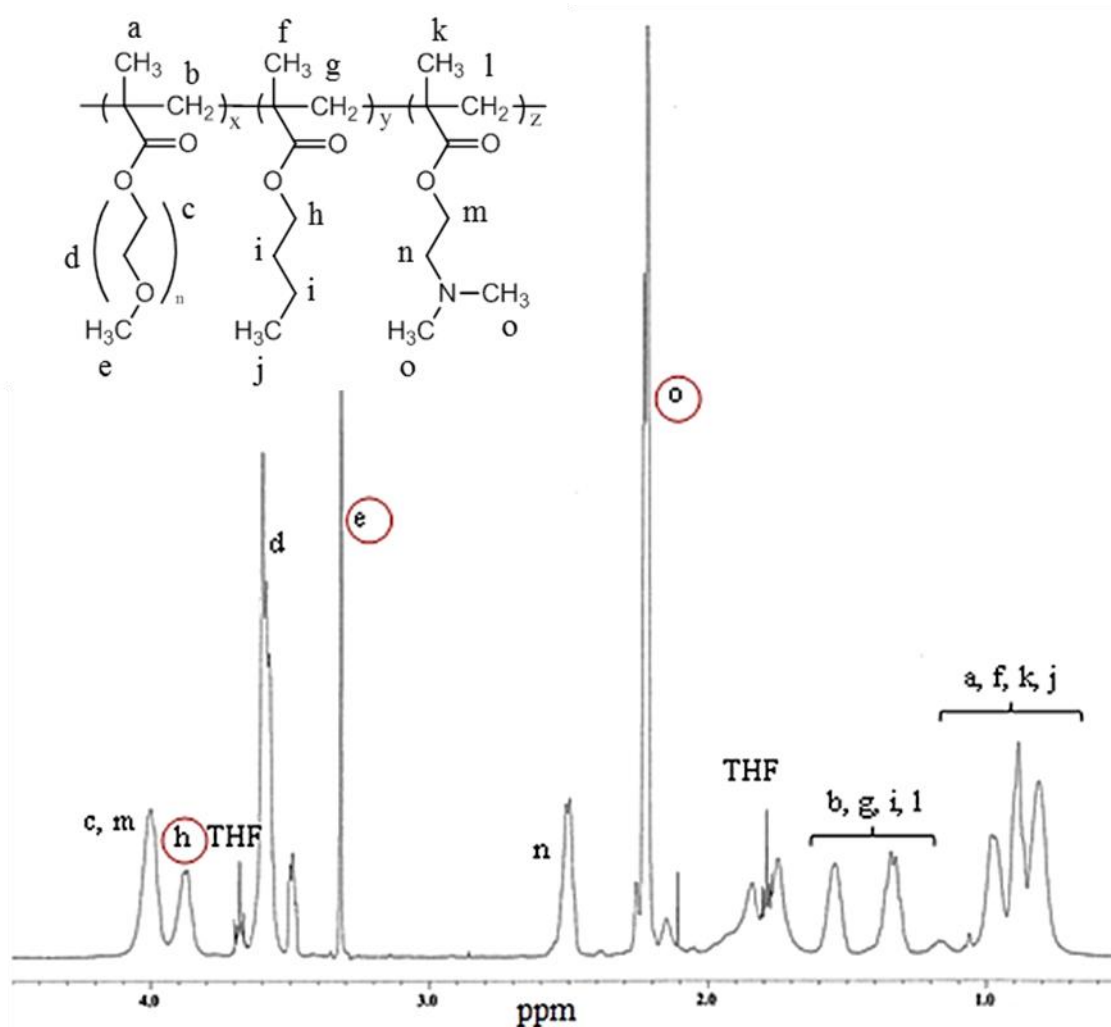


**Table 3.2.** Terpolymers characteristics obtained based on GPC and <sup>1</sup>H NMR spectroscopy.

Polymer No.	Theoretical Structure	Actual Structure	Theoretical Composition P-B-D W <sub>f</sub>	Actual Composition P-B-D W <sub>f</sub>	Theoretical MW g/mol	M <sub>w</sub> g/mol	M <sub>n</sub> g/mol	PDI
1	P <sub>9</sub> -B <sub>20</sub> -D <sub>24</sub>	P <sub>16</sub> -B <sub>32</sub> -D <sub>39</sub>	0.29-0.31-0.40	0.31-0.29-0.39	9300	15500	14000	1.13
2	P <sub>9</sub> -B <sub>27</sub> -D <sub>24</sub>	P <sub>19</sub> -B <sub>49</sub> -D <sub>55</sub>	0.26-0.37-0.37	0.27-0.32-0.40	10300	21300	18800	1.15
3	P <sub>9</sub> -B <sub>34</sub> -D <sub>24</sub>	P <sub>18</sub> -B <sub>66</sub> -D <sub>48</sub>	0.24-0.43-0.33	0.24-0.41-0.33	11300	22300	19800	1.15
4	P <sub>15</sub> -B <sub>27</sub> -D <sub>20</sub>	P <sub>23</sub> -B <sub>40</sub> -D <sub>33</sub>	0.39-0.33-0.27	0.38-0.32-0.29	11500	17800	16000	1.12
5	P <sub>20</sub> -B <sub>27</sub> -D <sub>15</sub>	P <sub>41</sub> -B <sub>56</sub> -D <sub>32</sub>	0.49-0.31-0.19	0.48-0.31-0.20	12200	25300	22000	1.16
6	P <sub>5</sub> -B <sub>27</sub> -D <sub>30</sub>	P <sub>8</sub> -B <sub>45</sub> -D <sub>53</sub>	0.15-0.38-0.47	0.14-0.37-0.48	10000	17100	15300	1.13
7	P <sub>13</sub> -B <sub>27</sub> -D <sub>36</sub>	P <sub>22</sub> -B <sub>44</sub> -D <sub>60</sub>	0.29-0.29-0.42	0.30-0.28-0.42	13400	22300	19300	1.16
8	P <sub>5</sub> -B <sub>27</sub> -D <sub>12</sub>	P <sub>8</sub> -B <sub>38</sub> -D <sub>19</sub>	0.21-0.53-0.26	0.23-0.50-0.28	7200	10800	9800	1.09
9	P <sub>18</sub> -B <sub>35</sub> -D <sub>14</sub>	P <sub>28</sub> -B <sub>49</sub> -D <sub>25</sub>	0.43-0.40-0.17	0.43-0.36-0.20	12600	19300	17900	1.09
10	P <sub>17</sub> -B <sub>35</sub> -D <sub>16</sub>	P <sub>27</sub> -B <sub>54</sub> -D <sub>14</sub>	0.41-0.40-0.20	0.45-0.42-0.12	12600	18000	16800	1.08
11	P <sub>15</sub> -B <sub>35</sub> -D <sub>19</sub>	P <sub>14</sub> -B <sub>29</sub> -D <sub>17</sub>	0.36-0.40-0.24	0.38-0.38-0.24	12400	11000	9100	1.19
12	P <sub>12</sub> -B <sub>35</sub> -D <sub>24</sub>	P <sub>13</sub> -B <sub>34</sub> -D <sub>24</sub>	0.29-0.40-0.31	0.31-0.39-0.30	12300	12500	11300	1.11
13	P <sub>10</sub> -B <sub>35</sub> -D <sub>28</sub>	P <sub>10</sub> -B <sub>33</sub> -D <sub>27</sub>	0.24-0.40-0.36	0.26-0.39-0.35	12400	11900	10700	1.12
14	P <sub>9</sub> -B <sub>35</sub> -D <sub>30</sub>	P <sub>8</sub> -B <sub>32</sub> -D <sub>28</sub>	0.22-0.40-0.36	0.22-0.40-0.38	12400	11300	10000	1.14
15	P <sub>7</sub> -B <sub>35</sub> -D <sub>34</sub>	P <sub>7</sub> -B <sub>33</sub> -D <sub>33</sub>	0.17-0.40-0.43	0.17-0.39-0.44	12400	12000	10600	1.12
16	P <sub>6</sub> -B <sub>35</sub> -D <sub>36</sub>	P <sub>11</sub> -B <sub>60</sub> -D <sub>64</sub>	0.14-0.40-0.45	0.15-0.39-0.46	12400	21900	17800	1.22
17	P <sub>4</sub> -B <sub>35</sub> -D <sub>40</sub>	P <sub>4</sub> -B <sub>30</sub> -D <sub>34</sub>	0.10-0.40-0.50	0.11-0.39-0.50	12400	10800	9400	1.15
18	P <sub>2</sub> -B <sub>35</sub> -D <sub>43</sub>	P <sub>8</sub> -B <sub>91</sub> -D <sub>114</sub>	0.05-0.40-0.55	0.07-0.39-0.54	12300	33200	28500	1.16
19	P <sub>1</sub> -B <sub>35</sub> -D <sub>45</sub>	P <sub>4</sub> -B <sub>65</sub> -D <sub>84</sub>	0.02-0.40-0.57	0.05-0.39-0.56	12300	23600	20600	1.15
20	P <sub>2</sub> -B <sub>9</sub> -D <sub>6</sub>	P <sub>2</sub> -B <sub>13</sub> -D <sub>10</sub>	0.21-0.45-0.33	0.13-0.47-0.40	2800	4000	3400	1.14

<b>Polymer No.</b>	<b>Theoretical Structure</b>	<b>Actual Structure</b>	<b>Theoretical Composition P-B-D W<sub>f</sub></b>	<b>Actual Composition P-B-D W<sub>f</sub></b>	<b>Theoretical MW g/mol</b>	<b>M<sub>w</sub> g/mol</b>	<b>M<sub>n</sub> g/mol</b>	<b>PDI</b>
21	P <sub>4</sub> -B <sub>15</sub> -D <sub>11</sub>	P <sub>3</sub> -B <sub>21</sub> -D <sub>15</sub>	0.24-0.42-0.34	0.14-0.48-0.38	5100	6200	5700	1.09
22	P <sub>6</sub> -B <sub>21</sub> -D <sub>15</sub>	P <sub>4</sub> -B <sub>26</sub> -D <sub>19</sub>	0.25-0.42-0.33	0.14-0.48-0.38	7100	7900	7200	1.07
23	P <sub>7</sub> -B <sub>27</sub> -D <sub>19</sub>	P <sub>5</sub> -B <sub>34</sub> -D <sub>22</sub>	0.24-0.43-0.33	0.15-0.49-0.36	8900	9800	9100	1.07
24	P <sub>9</sub> -B <sub>33</sub> -D <sub>23</sub>	P <sub>6</sub> -B <sub>41</sub> -D <sub>28</sub>	0.25-0.43-0.33	0.15-0.48-0.37	11000	12000	11300	1.07
25	P <sub>10</sub> -B <sub>39</sub> -D <sub>28</sub>	P <sub>7</sub> -B <sub>48</sub> -D <sub>33</sub>	0.23-0.43-0.34	0.15-0.49-0.37	12900	14100	13000	1.07
26	P <sub>12</sub> -B <sub>45</sub> -D <sub>32</sub>	P <sub>7</sub> -B <sub>51</sub> -D <sub>39</sub>	0.24-0.43-0.33	0.13-0.47-0.40	15000	15500	14300	1.07
27	P <sub>2</sub> -B <sub>14</sub> -D <sub>15</sub>	P <sub>4</sub> -B <sub>18</sub> -D <sub>17</sub>	0.12-0.40-0.48	0.17-0.40-0.43	4900	6400	5900	1.07
28	P <sub>5</sub> -B <sub>28</sub> -D <sub>29</sub>	P <sub>6</sub> -B <sub>36</sub> -D <sub>32</sub>	0.15-0.40-0.45	0.15-0.43-0.42	10000	11900	11300	1.06
29	P <sub>7</sub> -B <sub>42</sub> -D <sub>44</sub>	P <sub>9</sub> -B <sub>47</sub> -D <sub>47</sub>	0.14-0.40-0.46	0.16-0.40-0.44	15000	16700	15700	1.06
30	P <sub>8</sub> -B <sub>49</sub> -D <sub>51</sub>	P <sub>12</sub> -B <sub>60</sub> -D <sub>62</sub>	0.14-0.40-0.46	0.16-0.39-0.45	17400	21900	20400	1.07
31	P <sub>9</sub> -B <sub>56</sub> -D <sub>59</sub>	P <sub>14</sub> -B <sub>70</sub> -D <sub>73</sub>	0.14-0.40-0.47	0.16-0.39-0.45	19900	25600	23500	1.09
32	P <sub>11</sub> -B <sub>70</sub> -D <sub>73</sub>	P <sub>15</sub> -B <sub>80</sub> -D <sub>85</sub>	0.13-0.40-0.46	0.15-0.39-0.46	24700	29200	26300	1.11
33	P <sub>12</sub> -B <sub>56</sub> -D <sub>35</sub>	P <sub>13</sub> -B <sub>52</sub> -D <sub>35</sub>	0.21-0.47-0.32	0.23-0.44-0.32	17000	16800	14600	1.15
34	P <sub>11</sub> -B <sub>59</sub> -D <sub>34</sub>	P <sub>13</sub> -B <sub>65</sub> -D <sub>38</sub>	0.19-0.49-0.31	0.21-0.48-0.31	17000	19200	17300	1.11
35	P <sub>11</sub> -B <sub>61</sub> -D <sub>33</sub>	P <sub>13</sub> -B <sub>67</sub> -D <sub>36</sub>	0.19-0.51-0.30	0.21-0.50-0.29	17100	19100	17200	1.11
36	P <sub>10</sub> -B <sub>63</sub> -D <sub>32</sub>	P <sub>13</sub> -B <sub>76</sub> -D <sub>40</sub>	0.18-0.53-0.30	0.19-0.51-0.30	17000	21000	19300	1.09
37	P <sub>9</sub> -B <sub>55</sub> -D <sub>28</sub>	P <sub>11</sub> -B <sub>58</sub> -D <sub>36</sub>	0.18-0.52-0.29	0.19-0.48-0.33	14900	17000	15300	1.11
38	P <sub>12</sub> -B <sub>74</sub> -D <sub>37</sub>	P <sub>14</sub> -B <sub>81</sub> -D <sub>43</sub>	0.18-0.53-0.29	0.18-0.51-0.30	19900	22400	20400	1.10

### 3.4 Aqueous solution characterisation of terpolymers

#### 3.4.1 Hydrodynamic diameter

The theoretical and experimental (actual) hydrodynamic diameter of terpolymers in aqueous solution were calculated and determined, respectively. Specifically, the theoretical value of hydrodynamic diameters of terpolymers unimers were calculated based on their random coil configuration in solution,  $d_{\text{unimer}} = 2 \times (2 \times 2.20 \times (\text{DP}/3))^{1/2} \times 0.154$ .<sup>10</sup> The actual diameters of terpolymers unimers obtained by DLS at concentrations lower than CMC were in good agreement with the theoretical ones as it can be seen in Table 3.3. The values of actual hydrodynamic diameters of terpolymers were slightly less than that of the theoretical ones, as the terpolymers might have coiled more than the random configuration in aqueous solution. In addition, as it can be seen in Figure 3.4 the hydrodynamic diameter of terpolymers unimers depends on the molecular weight of terpolymers.<sup>11</sup> In particular, by increasing the polymer  $M_n$  the hydrodynamic diameter increases, as expected and observed before in similar studies.<sup>12</sup>

Moreover, it was found that the hydrodynamic diameter of unimers was affected by the terpolymers composition. For instance comparing P5: P<sub>41</sub>-B<sub>56</sub>-D<sub>32</sub> and P36: P<sub>13</sub>-B<sub>76</sub>-D<sub>40</sub> which both has similar total degree of polymerisation and DMAEMA content with increasing content of BuMA and decreasing content of PEGMA, the hydrodynamic diameter of unimer decreases from 4.1 nm for P5 to 3.5 nm for P36 as the longer BuMA chain coils more and results in smaller diameter of unimers in water. Another example is P30: P<sub>12</sub>-B<sub>60</sub>-D<sub>62</sub> and P38: P<sub>14</sub>-B<sub>81</sub>-D<sub>43</sub> which both has same total degree of polymerisation and PEGMA content with an increasing BuMA content and decreasing DMAEMA content. The same trend was observed as the unimer hydrodynamic diameter decreased from 4.3 nm for P30 to 3.5 nm for P38. Therefore, the longer hydrophobic chain in terpolymer composition causes the polymer chains to be more curled up in solution and thus show a smaller hydrodynamic diameter.

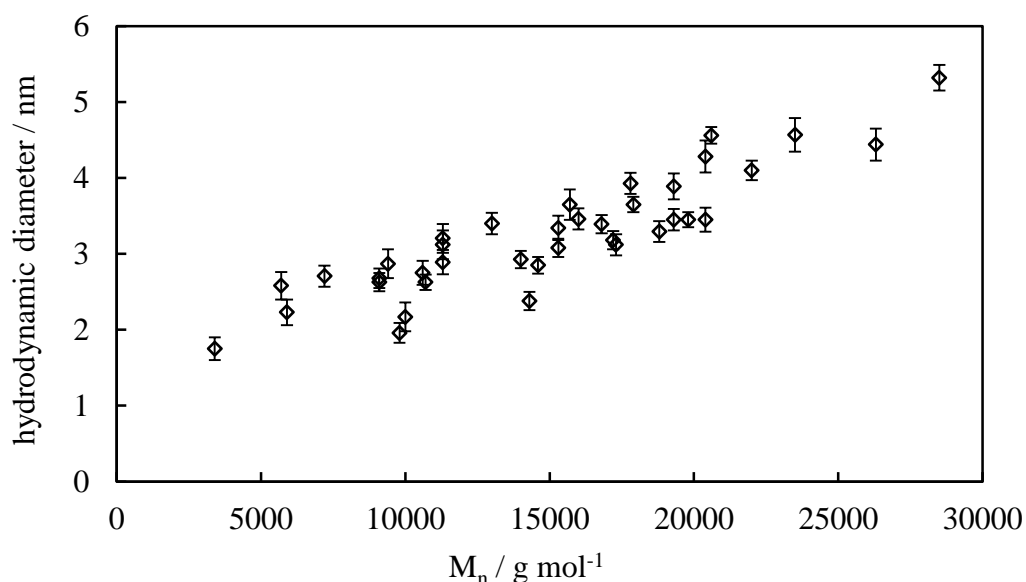
**Table 3.3.** Summary of terpolymers characteristics in aqueous solution.

Polymer Number	Polymer Structure	Theoretical Unimer $d_h$ (nm)	Actual Unimer $d_h$ (nm)	Theoretical $D_{micelle}$ (nm)	Actual $D_{micelle}$ (nm)	CMC mmol/L	pK <sub>a</sub>	Cloud Point °C
1	P <sub>16</sub> -B <sub>32</sub> -D <sub>39</sub>	3.5	2.9	27.9	24.3	9.90 x10 <sup>-2</sup>	6.4	52
2	P <sub>19</sub> -B <sub>49</sub> -D <sub>55</sub>	4.1	3.3	40.4	38.3	7.26 x10 <sup>-2</sup>	6.7	50
3	P <sub>18</sub> -B <sub>66</sub> -D <sub>48</sub>	4.3	3.4	41.1	39.3	5.01 x10 <sup>-2</sup>	6.2	-
4	P <sub>23</sub> -B <sub>40</sub> -D <sub>33</sub>	3.6	3.5	26.9	25.1	9.75 x10 <sup>-2</sup>	6.4	55
5	P <sub>41</sub> -B <sub>56</sub> -D <sub>32</sub>	4.2	4.1	35.0	35.3	7.51 x10 <sup>-2</sup>	6.0	-
6	P <sub>8</sub> -B <sub>45</sub> -D <sub>53</sub>	3.8	3.3	38.3	35.6	1.00 x10 <sup>-2</sup>	6.5	-
7	P <sub>22</sub> -B <sub>44</sub> -D <sub>60</sub>	4.2	3.9	41.7	38.6	1.43 x10 <sup>-2</sup>	6.4	58
8	P <sub>8</sub> -B <sub>38</sub> -D <sub>19</sub>	3.0	2.0	19.3	17.4	2.08 x10 <sup>-2</sup>	5.8	-
9	P <sub>28</sub> -B <sub>49</sub> -D <sub>25</sub>	3.8	3.6	26.7	24.3	1.67 x10 <sup>-2</sup>	6.2	-
10	P <sub>27</sub> -B <sub>54</sub> -D <sub>14</sub>	3.6	3.4	27.4	25.8	1.21 x10 <sup>-2</sup>	5.4	-
11	P <sub>14</sub> -B <sub>29</sub> -D <sub>17</sub>	2.9	2.6	16.0	13.2	4.72 x10 <sup>-2</sup>	5.9	59
12	P <sub>13</sub> -B <sub>34</sub> -D <sub>24</sub>	3.1	2.9	20.8	18.7	1.28 x10 <sup>-2</sup>	6.0	-
13	P <sub>10</sub> -B <sub>33</sub> -D <sub>27</sub>	3.1	2.6	22.1	17.3	2.31 x10 <sup>-2</sup>	6.6	58
14	P <sub>8</sub> -B <sub>32</sub> -D <sub>28</sub>	3.1	2.2	22.3	18.5	1.50 x10 <sup>-2</sup>	6.4	52
15	P <sub>7</sub> -B <sub>33</sub> -D <sub>33</sub>	3.2	2.7	25.1	18.2	3.24 x10 <sup>-2</sup>	6.5	-
16	P <sub>11</sub> -B <sub>60</sub> -D <sub>64</sub>	4.3	3.9	48.3	42.6	1.87 x10 <sup>-2</sup>	6.2	-
17	P <sub>4</sub> -B <sub>30</sub> -D <sub>34</sub>	3.1	2.9	24.9	23.3	9.21 x10 <sup>-2</sup>	6.5	-
18	P <sub>8</sub> -B <sub>91</sub> -D <sub>114</sub>	5.4	5.3	81.0	76.4	1.14 x10 <sup>-2</sup>	6.0	-
19	P <sub>4</sub> -B <sub>65</sub> -D <sub>84</sub>	4.6	4.6	59.9	56.4	6.11 x10 <sup>-2</sup>	6.2	-
20	P <sub>2</sub> -B <sub>13</sub> -D <sub>10</sub>	1.9	1.7	8.4	6.6	6.15 x10 <sup>-2</sup>	6.2	53
21	P <sub>3</sub> -B <sub>21</sub> -D <sub>15</sub>	2.3	2.6	12.9	12.2	5.29 x10 <sup>-2</sup>	6.3	51



Polymer Number	Polymer Structure	Theoretical Unimer $d_h$ (nm)	Actual Unimer $d_h$ (nm)	Theoretical $D_{micelle}$ (nm)	Actual $D_{micelle}$ (nm)	CMC mmol/L	pK <sub>a</sub>	Cloud Point °C
22	P <sub>4</sub> -B <sub>26</sub> -D <sub>19</sub>	2.6	2.7	16.3	16.4	1.28 x10 <sup>-2</sup>	6.4	-
23	P <sub>5</sub> -B <sub>34</sub> -D <sub>22</sub>	2.9	2.7	19.8	16.2	3.35 x10 <sup>-2</sup>	6.2	-
24	P <sub>6</sub> -B <sub>41</sub> -D <sub>28</sub>	3.2	3.1	24.6	19.5	8.13 x10 <sup>-2</sup>	6.2	-
25	P <sub>7</sub> -B <sub>48</sub> -D <sub>33</sub>	3.5	3.4	29.0	27.1	7.4 x10 <sup>-3</sup>	6.7	-
26	P <sub>7</sub> -B <sub>51</sub> -D <sub>39</sub>	3.7	2.4	32.8	31.4	5.5 x10 <sup>-3</sup>	6.4	-
27	P <sub>4</sub> -B <sub>18</sub> -D <sub>17</sub>	2.3	2.2	13.2	11.0	1.72 x10 <sup>-1</sup>	6.2	54
28	P <sub>6</sub> -B <sub>36</sub> -D <sub>32</sub>	3.2	3.2	25.4	25.5	5.54 x10 <sup>-2</sup>	6.4	49
29	P <sub>9</sub> -B <sub>47</sub> -D <sub>47</sub>	3.8	3.6	35.8	33.4	4.48 x10 <sup>-2</sup>	6.4	-
30	P <sub>12</sub> -B <sub>60</sub> -D <sub>62</sub>	4.3	4.3	46.7	44.0	3.05 x10 <sup>-2</sup>	6.4	-
31	P <sub>14</sub> -B <sub>70</sub> -D <sub>73</sub>	4.7	4.6	54.9	55.8	2.48 x10 <sup>-2</sup>	6.4	-
32	P <sub>15</sub> -B <sub>80</sub> -D <sub>85</sub>	5.0	4.8	63.5	57.1	1.22 x10 <sup>-2</sup>	6.9	-
33	P <sub>13</sub> -B <sub>52</sub> -D <sub>35</sub>	3.7	2.8	31.0	29.1	6.22 x10 <sup>-3</sup>	6.0	-
34	P <sub>13</sub> -B <sub>65</sub> -D <sub>38</sub>	4.0	3.1	35.8	32.6	4.34 x10 <sup>-3</sup>	5.8	-
35	P <sub>13</sub> -B <sub>67</sub> -D <sub>36</sub>	4.0	3.2	35.3	33.3	4.16 x10 <sup>-3</sup>	5.6	-
36	P <sub>13</sub> -B <sub>76</sub> -D <sub>40</sub>	4.2	3.4	39.6	37.0	2.02 x10 <sup>-3</sup>	5.4	-
37	P <sub>11</sub> -B <sub>58</sub> -D <sub>36</sub>	3.8	3.1	33.0	32.1	5.46 x10 <sup>-3</sup>	5.8	-
38	P <sub>14</sub> -B <sub>81</sub> -D <sub>43</sub>	4.4	3.4	42.4	39.3	1.11 x10 <sup>-3</sup>	5.4	-

**Figure 3.4.** Variation of terpolymers hydrodynamic diameter versus the overall number average molecular weight of terpolymers. Error bars represent the standard deviations in the polymer hydrodynamic diameter from three separate measurements of the same solution.

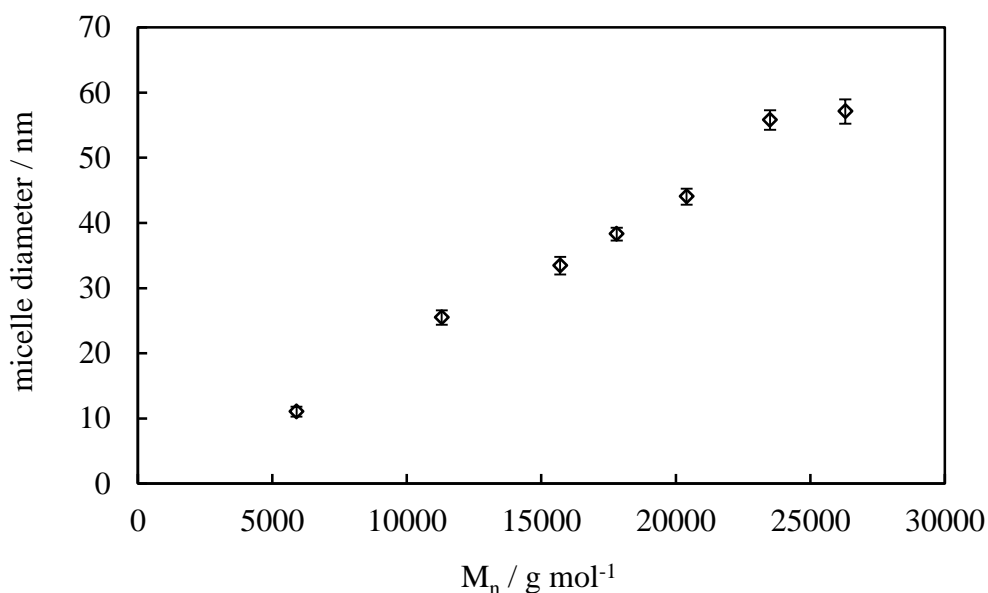


### 3.4.2 Micelle diameter

All terpolymers were found to form micelles in water at 1 wt.% as it was expected due to their amphiphilic nature. The experimental micelles diameter measured by DLS were smaller than the theoretical ones, as expected, because a fully stretched polymer chain configuration was assumed in the used theoretical model where  $d_{\text{micelle}} = (DP_{\text{hydrophobic}} \times 0.254) + 2 \times (DP_{\text{longer hydrophilic}} \times 0.254)$ . Table 3.3 illustrates the theoretically calculated and experimentally measured micelles diameters. It was found that the size of the micelles was affected by the terpolymers composition and molecular weight. For instance comparing P30: P<sub>12</sub>-B<sub>60</sub>-D<sub>62</sub> and P38: P<sub>14</sub>-B<sub>81</sub>-D<sub>43</sub> where both have a similar total degree of polymerisation and PEGMA content while the BuMA content increases in P38 and instead DMAEMA content decreases, the size of the micelles decreases from 44 nm for P30 to 39 nm for P38.<sup>13</sup> In addition, comparing P35: P<sub>13</sub>-B<sub>67</sub>-D<sub>36</sub>, P36: P<sub>14</sub>-B<sub>76</sub>-D<sub>40</sub> and P31: P<sub>14</sub>-B<sub>70</sub>-D<sub>73</sub> which all have similar block length of PEGMA and BuMA with increasing content of DMAEMA (longer hydrophilic block), the micelles size increases from 34 to 37 to 56 nm, respectively. Moreover, the micelles size increases linearly with the increase in terpolymers chain length while the composition is kept constant. This

trend can be observed when comparing the size of micelles formed by P27, P28, P29, P30, P16, P31 and P32 as it can be seen in Figure 3.5. In particular, the size of the micelles increases as the length of the longer hydrophilic block increases. This effect is due to the fact that hydrophobic BuMA core of the micelles is collapsed, whereas the hydrophilic block is extended. Therefore, the size of the micelle depends more on the hydrophilic block rather than the collapsed hydrophobic block.

**Figure 3.5.** Variation of micelle diameter over molecular weight of constituent terpolymers with PEGMA, BuMa, DMAEMA weight fraction of 0.16, 0.40 and 0.44 respectively. Error bars represent the standard deviations in the micelles diameters from three separate measurements of the same solution.

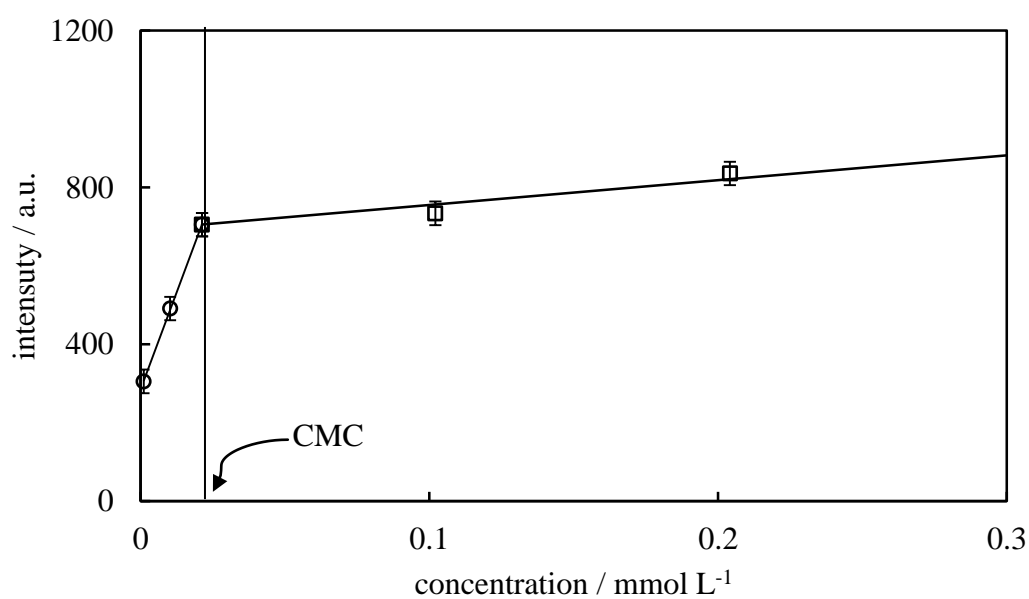


### 3.4.3 CMC of terpolymers

CMC of the terpolymers was determined by measuring the emission fluorescence intensity of pyrene at 383 nm present in terpolymer solution over a range of concentrations. At low polymer concentrations (<CMC) the intensity of pyrene fluorescence emission is close to that of the pyrene in pure water. Below the CMC, as the concentration of polymer in solution increases, the fluorescent intensity increases dramatically indicating that polymers start to aggregate and pyrene incorporate in the hydrophobic region of aggregate. With further increasing of concentration, the intensity reaches a maximum followed by a slow increase or plateau after the CMC. Plotting the intensity versus concentration of terpolymer in

solution gives a breaking point which is pointed as CMC (see Figure 3.6). Compared with low molar mass surfactants, terpolymers exhibit a remarkably lowered CMC values and the formed micelles are generally more stable.

**Figure 3.6.** Determination of CMC by plotting the fluorescent intensity of pyrene at 383 nm versus different concentrations of P5:P<sub>8</sub>-B<sub>38</sub>-D<sub>19</sub> terpolymer solution. Error bars represent the standard deviations in the fluorescence intensity obtained from three separate measurements of the same solution.



The CMC of all terpolymers was determined and is illustrated in Table 3.3. Comparing the obtained CMC values, it was found that the hydrophobic content of terpolymers has a significant effect on CMC of terpolymers. As it can be seen in Figure 3.7, plotting the CMC values of P33, P34, P35, P36, P37 and P38 versus their hydrophobic/hydrophilic ratio (obtained from DP of BuMA / (DP of PEGMA+ DP of DMAEMA)), showed that as the hydrophobicity of terpolymers increases, the CMC decreases about six times from  $6.2 \times 10^{-3}$  to  $1.1 \times 10^{-3}$  mmol/L. This result is in good agreement with the literature <sup>14</sup> and proved that terpolymers with longer hydrophobic chain start to aggregate at lower concentrations of polymer in the solution. In addition, it was observed that the CMC of terpolymers significantly decreases by increasing the average molecular weight of terpolymers when keeping the composition constant. This can be concluded by plotting the CMC values of P27, P28, P29, P30, P31, P32 which all have similar composition, 0.16: 0.40: 0.44 weight fractions for P: B: D, but different  $M_n$ s ranging from 5900 to 26300 g/mol

respectively. As it can be seen in Figure 3.8, the CMC was reduced about ten times from  $1.72 \times 10^{-1}$  mmol/L to  $1.22 \times 10^{-2}$  mmol/L for P27 to P32 terpolymer that had the lowest and highest number average molecular weight, respectively.<sup>15</sup>

**Figure 3.7.** Effect of hydrophobicity of P-B-D terpolymers on their CMC values. Error bars represent the standard deviations in the CMC values obtained from three separate measurements of the same solution.

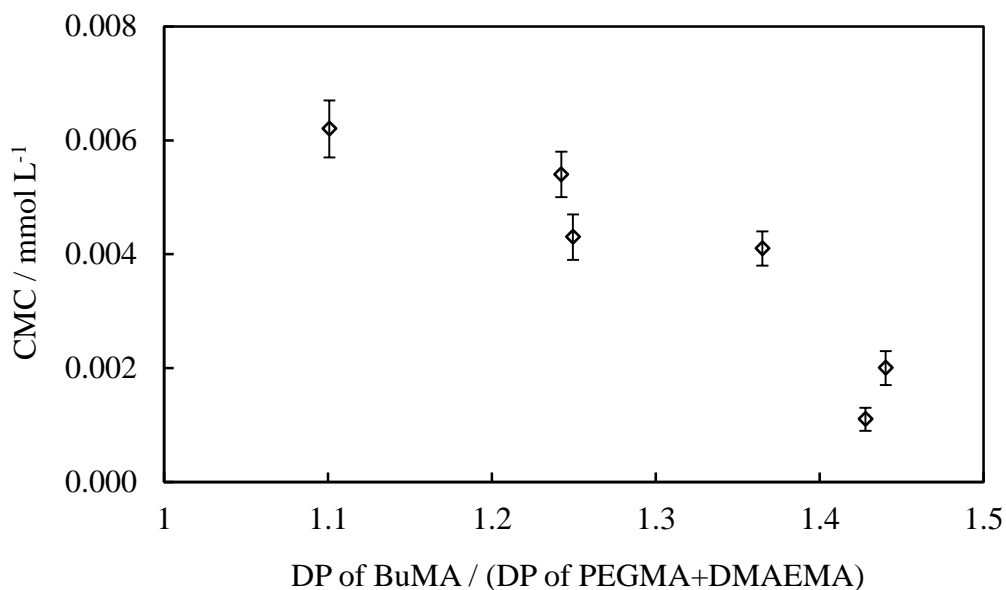
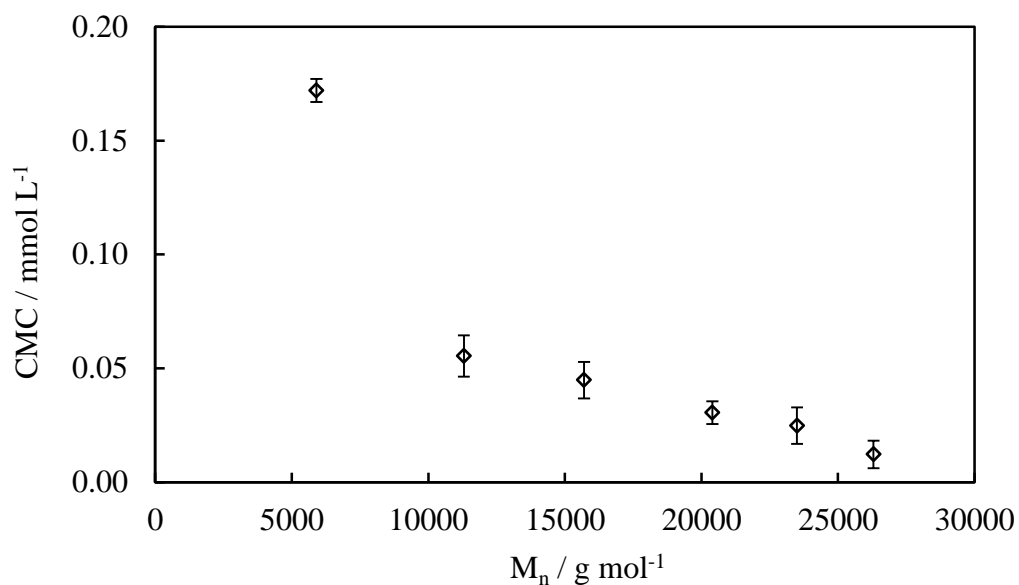


**Figure 3.8.** Effect of number average molecular weight of P-B-D terpolymers on their CMC values. Error bars represent the standard deviations in the CMC values obtained from three separate measurements of the same solution.



### 3.4.4 Effective $pK_a$ of terpolymers

Polymers containing ionisable pendant groups in their monomer units can be ionised in acidic, neutral or basic environment depending on their  $pK_a$  value. In definition,  $pK_a$  is the negative logarithm value of the acid dissociation constant ( $K_a$ ) of an acid. Acid dissociation constant and  $pK_a$  value for an acid HA can be defined in equations as bellow:



$$K_a = \frac{[A^-][H^+]}{HA} \quad \text{Eq. 3.5}$$

$$pK_a = -\log_{10}K_a \quad \text{Eq. 3.6}$$

The  $pK_a$  value is in fact a numeric value for the strength of an acid. The stronger the acid the lower is the value of  $pK_a$ . When the pH of a solution is equal to the  $pK_a$  value, the acid is half dissociated. Once the pH of the solution is either less or more than the  $pK_a$  value, the molecule is in its protonated and deprotonated state, respectively. When the polymer is ionised in solution, the electrostatic repulsion of charged pendant groups affects the physical properties of the polymer.

In this work, the DMAEMA unites of terpolymer are ionisable due to the  $-N(CH_3)_2$  group which can be protonated to  $-NH(CH_3)_2^+$  in the presence of acid. The effective  $pK_a$ s of the DMAEMA units in the terpolymers were determined by a potentiometric titration. By plotting the obtained pHs over the volume of added NaOH, the  $pK_a$  can be determined as the pH at which 50% of the DMAEMA groups are protonated, thus the point where half of the added volume of NaOH solution for complete deprotonation was consumed (see Figure 3.9). The  $pK_a$  values were in the range of 5.4 to 7 which are in good agreement with previous publications on polymers containing DMAEMA monomer.<sup>16-18</sup> The obtained  $pK_a$ s values are summarised in Table 3.3 By plotting the  $pK_a$ s values versus the hydrophobic/hydrophilic ratio of terpolymer, it was observed that the  $pK_a$  decreases as the hydrophobicity of the terpolymers increases (see Figure 3.10), as it was expected and observed before.<sup>12, 13</sup> This can be attributed to the reduction in the

polymer dielectric constant due to the incorporation of hydrophobic BuMA block into terpolymer. Reduction of the dielectric constant causes a more difficult ionisation of DMAEMA unites and therefore, reduces the  $pK_a$  values.<sup>1, 19, 20</sup>

**Figure 3.9.** Determination of  $pK_a$  based on the titration curve of terpolymer (P33: P<sub>13</sub>-B<sub>52</sub>-D<sub>35</sub>).

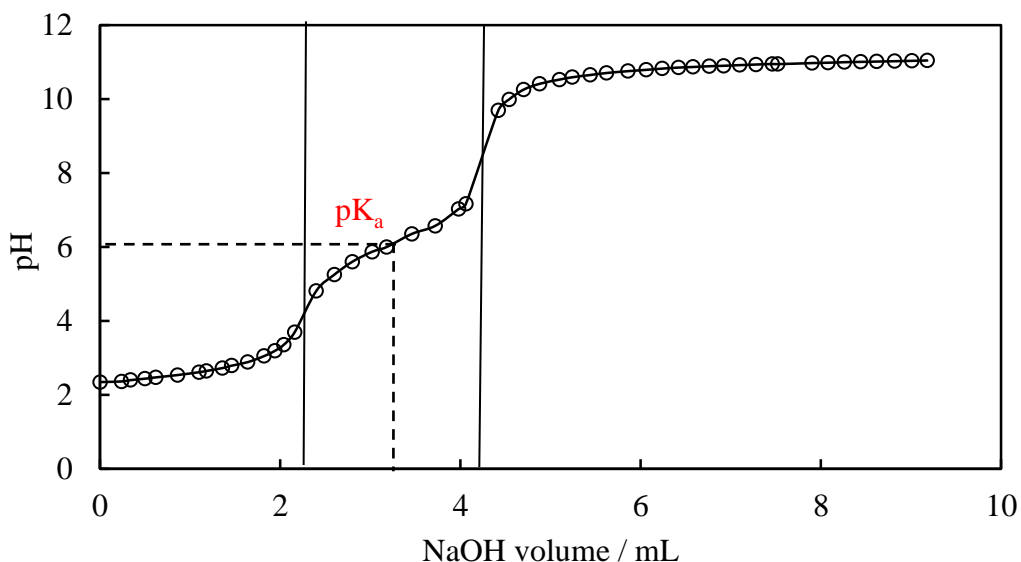
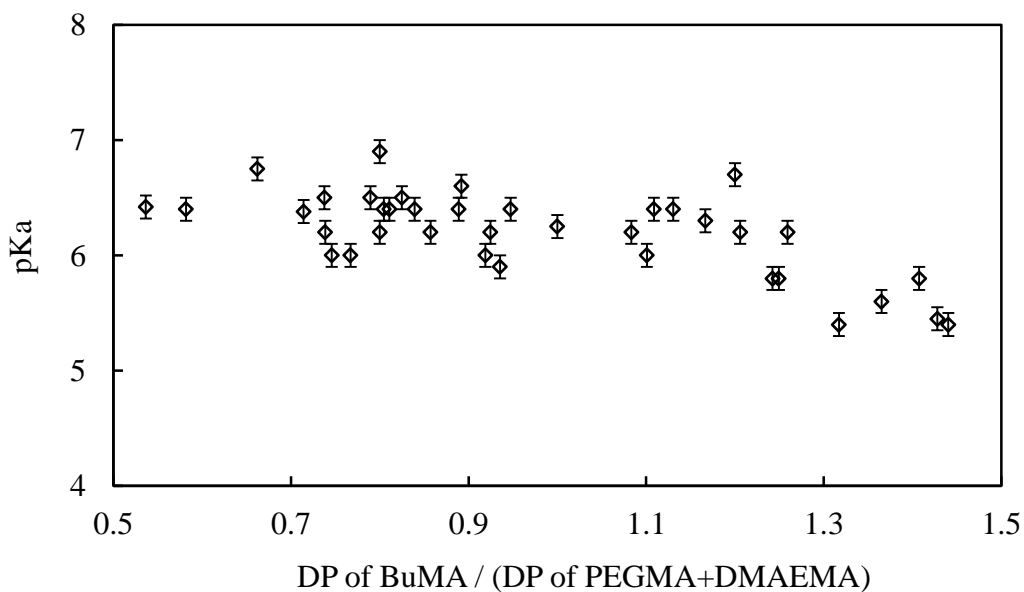


**Figure 3.10.** Effect of hydrophobicity of terpolymers on their effective  $pK_a$ s. Error bars represent the standard deviations in the  $pK_a$  values obtained from three separate measurements of the same solution.



### 3.4.5 Cloud points of terpolymers

The temperature at which a dissolved polymer is no longer soluble and the solution becomes hazy or cloudy due to a phase transition is called the cloud point. At cloud point the polymer starts to precipitate out. The cloud point is a phase transition temperature and the lower concentration that a cloud point can be observed is called lower critical solubility temperature (LCST).<sup>21</sup> The cloud point is strongly dependent on polymer molecular weight,<sup>22-24</sup> composition,<sup>22-24</sup> the pH of the solution<sup>22-24</sup> and even the architecture of the polymers (statistical versus block copolymers).<sup>25</sup>

In this study, the cloud points of 1 wt.% terpolymer solutions in water were determined by gradually increasing the temperature and observing visually if the solution was clear or not. The precipitation of PEGMA-*b*-BuMA-*b*-DMAEMA terpolymers at cloud point can be attributed to thermoresponsive behaviour DMAEMA<sup>22-24</sup> and PEGMA<sup>26-28</sup> blocks which both become more hydrophobic at higher temperatures. However, due to the poor solubility of most of the terpolymers in water, the polymers solutions were acidified slightly for a better solubilisation. The decreased pH though caused a dramatic increase of the cloud point or no observation of cloud point due to the protonation of DMAEMA groups.<sup>22, 28</sup> Table 3.3 lists the obtained cloud points for synthesised terpolymers. Unfortunately, due to acidifying the terpolymers solution, in most cases no cloud point was observed and therefore, it was difficult to find a trend based on polymer composition or molecular weight.



### 3.5 Conclusion

A series of amphiphilic terpolymers comprising of PEGMA, BuMA and DMAEMA units were successfully designed, synthesised and characterised in terms of their average molecular weight, molecular weight distribution, composition, hydrodynamic diameter, CMC, effective  $pK_a$  and cloud point.

The terpolymers design was based on varying different compositional parameters, as listed in Table 3.1. GPC and  $^1\text{H-NMR}$  results confirmed the successful synthesis of terpolymers and provided the actual composition and degree of polymerisation of terpolymers. The aqueous characterisation of terpolymers provided useful characteristics of terpolymers as summarised below:

- The actual hydrodynamic diameters of terpolymers unimer obtained from DLS were in good agreement with theoretical ones. Also, as expected, the hydrodynamic diameter increased as the average molecular weight of terpolymers increasing in a series.
- The actual micelle diameters obtained from DLS were close to the theoretical ones. However, they were mostly smaller than the calculated theoretical micelles diameter, as expected since the polymer chains are not fully stretched in solution. In addition, it was found that the micelle diameter is affected by the average molecular weight of terpolymers. As expected, terpolymers with longer hydrophilic chains provided larger micelles and vice versa.
- The CMC of terpolymers was determined using pyrene fluorescent spectroscopy method. It was observed that terpolymer composition and average molecular weight influence the CMC of the terpolymers. Increasing either the hydrophobic content (BuMA) or the average molecular weight of terpolymers results in a decrease in the CMC, similar to other reported literatures.<sup>14,15</sup>

- The effective  $pK_a$ s of terpolymers were determined by titration. As reported before, the  $pK_a$  of terpolymers was influenced by their hydrophobicity content. The higher hydrophobicity results in lowering the effective  $pK_a$  values.
- Finally, the cloud points of terpolymers were determined by visual observation of their solution as a function of temperature. However, in most cases no cloud point was observed at 20-90°C because of the acidification of the terpolymer solutions.

### 3.6 References

1. T. K. Georgiou, C. S. Patrickios, G. P. W and B. Iva'n, *Macromolecules*, 2007, **40**, 2335.
2. G. Kali, T. K. Georgiou, B. Iva'n, C. S. Patrickios, E. Loizou, Y. Thomann and J. C. Tiller, *Langmuir*, 2007, **23**, 10746.
3. G. Kali, T. K. Georgiou, B. Iva'n and C. S. Patrickios, *J. Polym. Sci., Part A: Polym. Chem.*, 2009, **47**, 4289.
4. M. R. Simmons and C. S. Patrickios, *Macromolecules*, 1998, **31**, 9075.
5. H. Schlaad, T. Krasia and C. S. Patrickios, *Macromolecules*, 2001, **34**, 7585.
6. G. Gotzamanis and C. Tsitsilianis, *Polymer*, 2007, **48**, 6226.
7. A. I. Triftaridou, M. Vamvakaki and C. S. Patrickios, *Polymer*, 2002, **43**, 2921.
8. G. T. Gotzamanis, T. Tsitsilianis, S. C. Hadjiyannakou, C. S. Patrickios, E. Lupitsky and S. Minko, *Macromolecules*, 2006, **39**, 678.
9. C. S. Patrickios, A. B. Lowe, S. P. Armes and N. C. Billingham, *J. Polym. Sci., Part A: Polym. Chem.*, 1998, **36**, 617.
10. P. C. Hiemenz, *Polymer Chemistry: The Basic Concepts*, Marcel Dekker, New York, 1984.
11. T. B. Bonne, K. Ludtke, R. Jordan and C. M. Papadakis, *Macromol. Chem. Phys.*, 2007, **208**, 1402.
12. M. A. Ward and T. K. Georgiou, *Soft Matter*, 2012, **8**, 2737.
13. M. A. Ward and T. K. Georgiou, *J. Polym. Sci., Part A: Polym. Chem.*, 2010, **48**, 775.
14. L. Xu, Z. Zhang, F. Wang, D. Xie, S. Yang, T. Wang, L. Feng and C. Chu, *J. Colloid Interface Sci.*, 2013, **393**, 174.
15. K. H. Nam, J. C. Cho and W. H. Jo, *Polym. J. (Tokyo, Jpn.)*, 1995, **27**, 904.

16. T. K. Georgiou, M. Vamvakaki, L. A. Phylactou and C. S. Patrickios, *Biomacromolecules*, 2005, **6**, 2990.
17. T. K. Georgiou, L. A. Phylactou and C. S. Patrickios, *Biomacromolecules*, 2006, **7**, 3505.
18. P. V. d. Wetering, J. Y. Cherng, H. Talsma and W. E. J. Hennink, *J. Controlled Release*, 1997, **49**, 59.
19. O. E. Philippova, N. L. Sitnikova, G. B. Demidovich and A. R. Khokhlov, *Macromolecules*, 1996, **29**, 4642.
20. A. Emileh, E. Vasheghani-Farahani and M. Imani, *Eur. Polym. J.*, 2007, **43**, 1986.
21. S. Mendrek, A. Hans-Juergen, A. Dworak and D. Kuckling, *Colloid Polym. Sci.*, 2010, **288**, 777.
22. D. Fournier, R. Hoogenboom, H. M. L. Thijs, R. M. Paulus and U. S. Schubert, *Macromolecules*, 2007, **40**, 915.
23. V. Butun, S. P. Armes and N. C. Billingham, *Polymer*, 2001, **42**, 5993.
24. W. L. J. Hinrichs, N. M. E. Schuurmans-Nieuwenbroek, P. V. Wetering and W. E. J. Hennink, *J. Controlled Release*, 1999, **60**, 249.
25. M. A. Ward and T. K. Georgiou, *J. Polym. Sci., Part A: Polym. Chem.*, 2013, **51**, 2850.
26. A. M. Kisselev and E. Manias, *Fluid Phase Equilib.*, 2007, **261**, 69.
27. R. Becer, S. Hahn, M. W. M. Fijten, H. M. L. Thijs, R. Hoogenboom and U. S. Schubert, *J. Polym. Sci., Part A: Polym. Chem.*, 2008, **46**, 7138.
28. S. Saeki, N. Kuwahara, M. Nakata and M. Kaneko, *Polymer*, 1976, **17**, 685.

## **CHAPTER 4**

### **PRELIMINARY OBSERVATIONS OF TERPOLYMERS SELF- ASSEMBLY IN AQUEOUS SOLUTION**

## 4.1 Introduction

Self-assembly of amphiphilic block copolymers has attracted considerable attention during the last decades due to having potential application in different areas.<sup>1,2</sup> Amphiphilic block copolymers can self-assemble to several different types of structures in selective solvents, such as micelles,<sup>3,4</sup> rods,<sup>5</sup> simple vesicles,<sup>6</sup> disc-like micelles,<sup>7</sup> Janus micelles with segregated faces<sup>8</sup> and toroids.<sup>9</sup> Many factors control the morphology of resultant structure, such as copolymer chemical structure, copolymer hydrophilic/hydrophobic ratio, concentration of copolymer in solution, type of used organic solvent, ratio of organic solvent/water, salt concentration, pH of solution, temperature and the preparation method.<sup>10</sup> However, among these factors, the volume ratio of the hydrophilic to hydrophobic segments seems to be the most important factor that may affect the self-assembly of amphiphilic copolymers. Usually, amphiphilic copolymers with hydrophilic/hydrophobic volume ratios greater than 1:1 tend to form spherical micelles, whereas, copolymers with hydrophilic/hydrophobic volume ratios more than 1:2 are more favourable to form vascular type structures. Although, the hydrophilic/hydrophobic volume ratio is one of the key factors in the formation of polymeric structures, this rule is not absolute and exceptions may be observed, as it is not unlikely that different polymer structures can be formed from the same amphiphilic polymers under different conditions.<sup>11</sup> Therefore, the pure geometrical considerations are not adequate to predict the final self-assembly of amphiphilic macromolecules, because polymer chain entropy and entropy loss during the formation of self-assembly can have a considerable effect on the resultant structure at the thermodynamic equilibrium.<sup>12</sup>

The aim of the present chapter is the preliminary study of the behaviour of ABC terpolymers in aqueous solution to investigate whether they form polymersomes or any other aggregation as a function of their block ratio and molecular weight. For this purpose a number of ABC terpolymers based on hydrophilic PEGMA, hydrophobic BuMA and hydrophilic DMAEMA, with varied molecular weights but same composition are used for the preparation of the polymer self-assembly using bulk and film rehydration methods. The properties of the prepared self-assemblies in terms of their morphology are studied using high

resolution microscopic techniques and DLS. Moreover, the effect of the temperature on the mean diameter of formed aggregates is investigated.

#### **4.2 Study of self-assembly of terpolymers in aqueous solution by DLS**

A series of terpolymers were assessed in terms of forming self-assembled aggregation in pure water. As discussed in Chapter 3, they all self-assemble into spherical micelles at concentrations over their CMC due to their hydrophobic middle block. The preliminary DLS results obtained from a series of terpolymers with increasing average molecular weight confirmed the existence of polymer aggregation in solution prepared by either direct dissolution of terpolymer in water or film rehydration method. Solutions prepared by direct dissolution of terpolymers in water at concentration of 1 wt.% showed the presence of aggregation with unimodal size distribution for all polymers with a size about a few tens of nm.

For polymer solutions prepared by film-rehydration method (1 wt.%) a bimodal size distribution was observed. The bimodal distribution consisted of a sharp peak with the mean diameter size of about a few tens of nanometre (corresponding to micelles) and a broad peak with much larger aggregate mean size (a few hundreds nm). The mean size of the both aggregate distributions increased as the molecular weight of the terpolymers increased at a same composition. Table 4.1 illustrates the obtained average sizes attributed to the self-assembly of the used terpolymers using both bulk rehydration and film rehydration methods. Variation of aggregation size over number average molecular weight of terpolymers is shown in Figure 4.1. As it can be seen in Table 4.1, the hydrophilic: hydrophobic ratio (obtained from sum of DP of hydrophilic blocks/DP of hydrophobic block) in this series of terpolymers is about 1:0.9 which is quite close to 1:1 ratio (assuming PEGMA, BuMA and DMAEMA monomer has a same volume). Therefore, it is expected the formed aggregations to be all spherical micelles.<sup>11</sup> As it can be seen in Table 4.1, bulk rehydration of this series of terpolymers resulted in formation of presumably spherical micelles as the obtained values were very close to the calculated theoretical sizes of spherical micelle for this series of terpolymers. However, two populations of aggregates were observed when a thin film of them was rehydrated in water. The first population which consist less than 40% of the forms self-assembled aggregations, can be attributed to formation of spherical

micelles, as the obtained mean diameters were in agreement with the theoretical ones. The larger size formed aggregation might be corresponding to more complex structures. In addition, the broad peak with large polydispersity is suggesting the existence of a range of transitional structures with a variety of diameters.

**Table 4.1.** DLS summary results corresponding to formed aggregates via bulk rehydration and film rehydration methods.

Polymer Characteristics			Bulk Rehydration	Film Rehydration			
No.	Polymer Structure	M <sub>n</sub> g/mol	Phylic/Phobic molar ratio	$\bar{d}_{agg.}(nm)$ ± 1 nm	I %	$\bar{d}_{agg.}(nm)$ ± 1 nm	I %
27	P <sub>4</sub> -B <sub>18</sub> -D <sub>17</sub>	5900	1 : 0.9	11.0	100	12.2 290.3	35.5 64.5
28	P <sub>6</sub> -B <sub>36</sub> -D <sub>32</sub>	11300	1 : 0.9	25.5	100	25.6 325.5	28.4 64.8
29	P <sub>9</sub> -B <sub>47</sub> -D <sub>47</sub>	15700	1 : 0.8	33.4	100	35.8 407.8	29.1 70.9
30	P <sub>12</sub> -B <sub>60</sub> -D <sub>62</sub>	20400	1 : 0.8	44.0	100	42.3 487.8	36.2 63.8
31	P <sub>14</sub> -B <sub>70</sub> -D <sub>73</sub>	23500	1 : 0.8	55.8	100	57.8 585.1	27.8 72.2
32	P <sub>15</sub> -B <sub>80</sub> -D <sub>85</sub>	26300	1 : 0.8	57.1	100	58.3 642.2	36.4 63.6

Increasing the temperature of the polymers solutions from 25°C to 37°C and then to 50°C, resulted in a significant decrease in diameter of the larger aggregates (see Figure 4.2). This reduction in aggregate size might be due to less solubility of DMAEMA block at higher temperatures which causes them to collapse and a decrease in the overall size of the formed aggregates. On the other hand, the second possibility is the partial dissociation of the formed aggregates which might lead to their morphology transition.



**Figure 4.1.** Variation of terpolymers aggregates size versus their number average molecular weights obtained from DLS for observed bimodal size distribution. Error bars represent the standard deviations in the diameter of formed aggregations obtained from three separate measurements of the same solution.

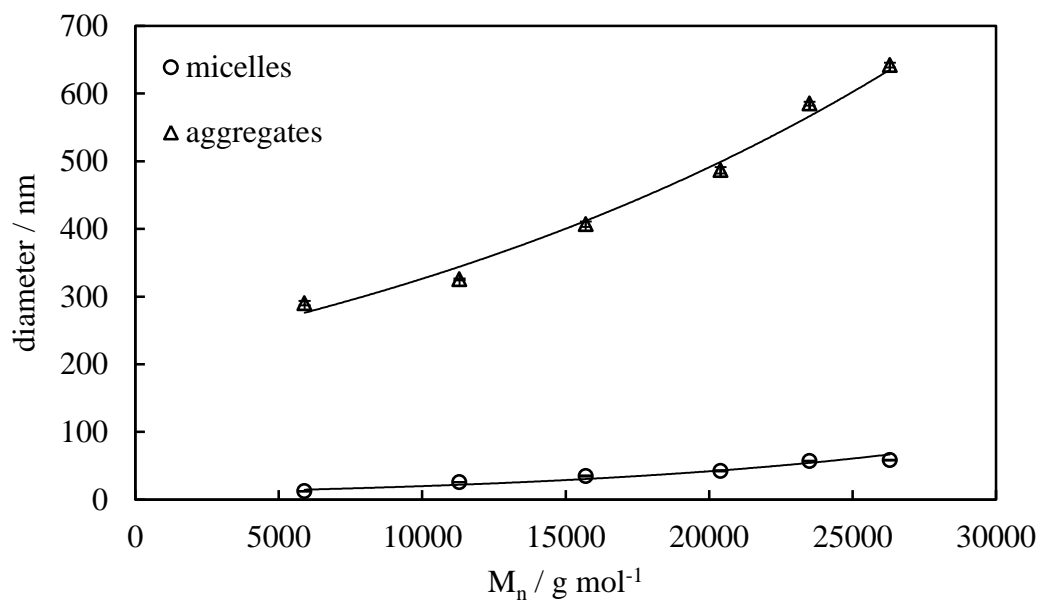
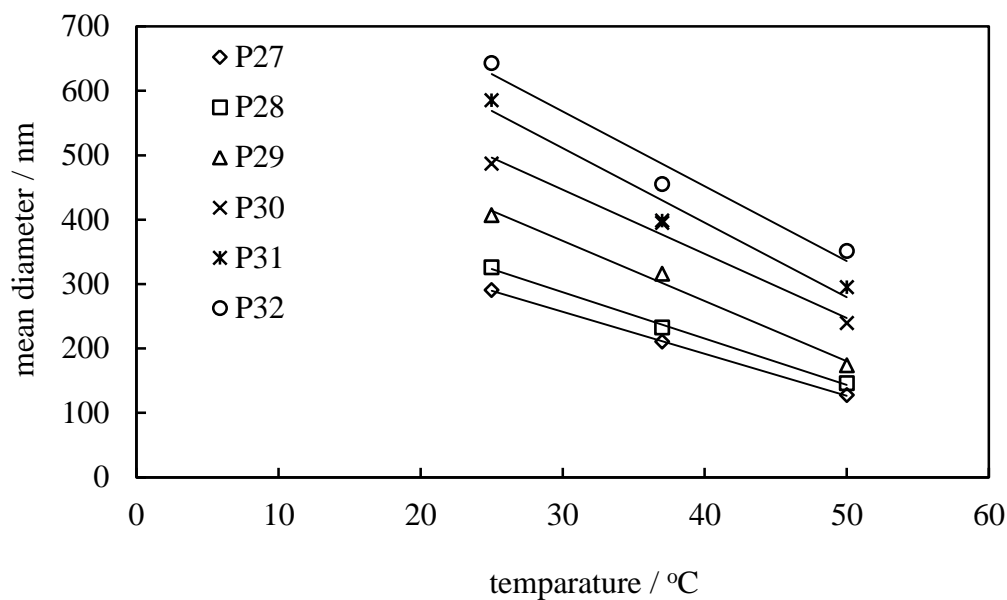


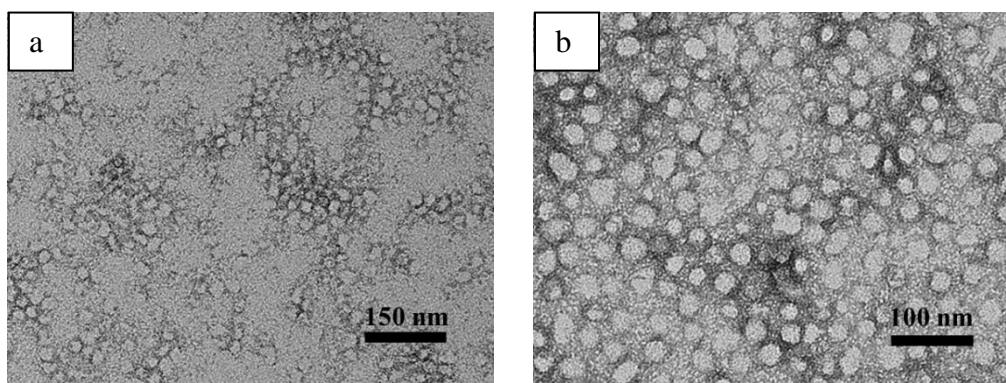
**Figure 4.2.** Effect of temperature variation on the mean aggregate size of polymer solutions prepared by film rehydration method.



### 4.3 Study of self-assembly of ABC terpolymers in aqueous solution by high resolution techniques

The morphology and size of the aggregates were determined by high resolution techniques. Preliminary TEM observations of some of the terpolymer solutions revealed that this series of terpolymers self-assemble into spherical micelles with hydrophobic BuMA core and hydrophilic PEGMA and DMAEMA coronas when hydrated in bulk. TEM images corresponding to two of the terpolymers, namely P27: P<sub>4</sub>-B<sub>18</sub>-D<sub>17</sub> and P31: P<sub>14</sub>-B<sub>70</sub>-D<sub>73</sub>, are shown in Figure 4.3 as example. Comparing the average micelles diameter of e.g. P31: P<sub>14</sub>-B<sub>70</sub>-D<sub>73</sub> terpolymer obtained from TEM images (40.2 nm) with the mean diameter obtained from DLS (56 nm), the micelle size appears to be smaller by 28%. This is because the DLS determined the hydrodynamic diameter which is the size of micelles when the polymer chains are hydrated in solution, while the TEM images are from samples in their dry state. The same trend was observed for the other terpolymers in this series in terms of their aggregate size when their size was compared in dry and hydrated states.

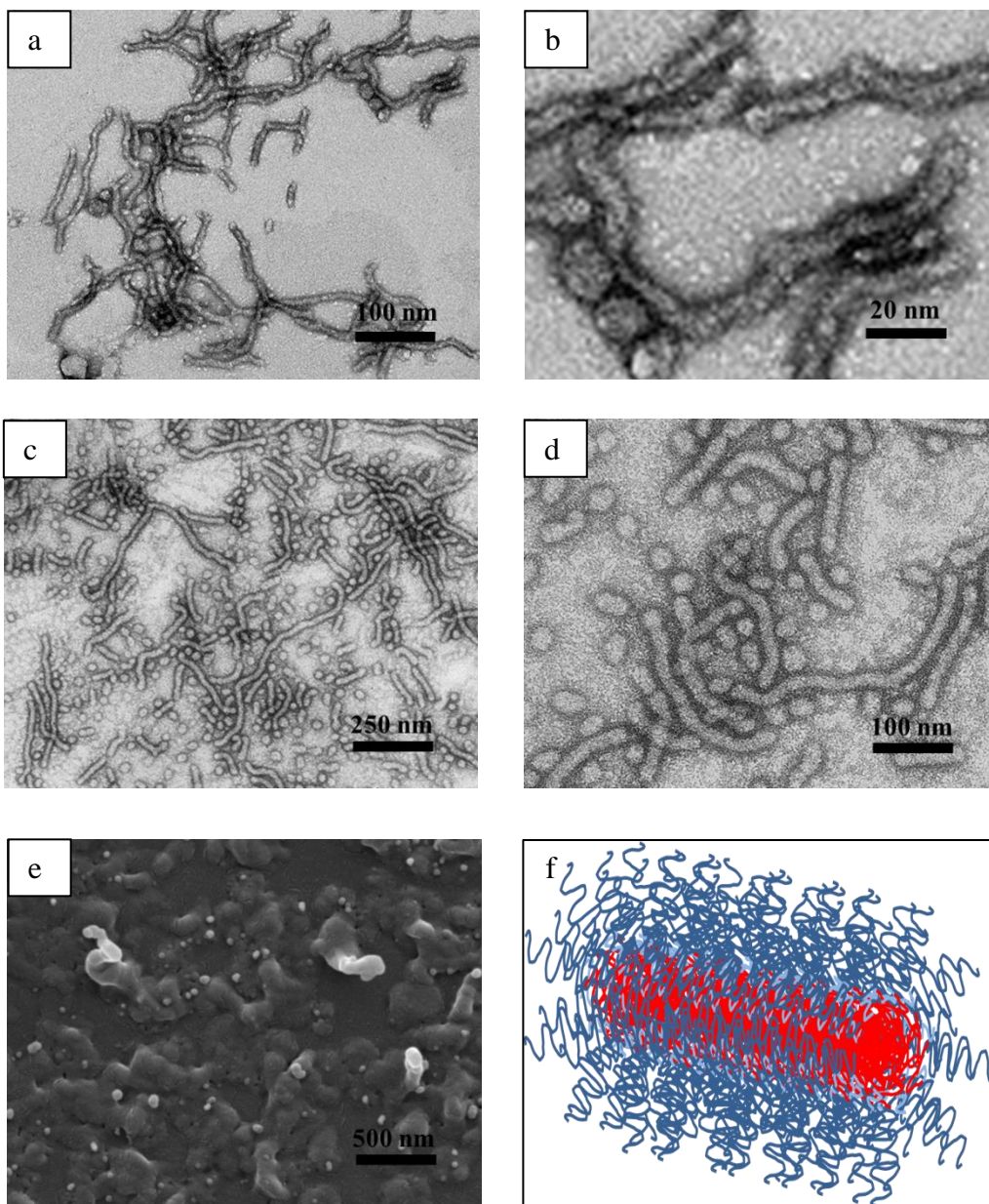
**Figure 4.3.** TEM images corresponding to bulk rehydration of 1 wt.% of (a) P27: P<sub>4</sub>-B<sub>18</sub>-D<sub>17</sub> and (b) P31: P<sub>14</sub>-B<sub>70</sub>-D<sub>73</sub> in water.



TEM images of the terpolymer solutions prepared via film rehydration method show the presence of worm-like micelles along with spherical micelles in all cases. Figure 4.4 illustrates the TEM and SEM images obtained from 1 wt.% solution of P27: P<sub>4</sub>-B<sub>18</sub>-D<sub>17</sub> and P31: P<sub>14</sub>-B<sub>70</sub>-D<sub>73</sub> terpolymers, as example. As it can be seen the size distribution of the formed worm-like micelles is quite broad which is in agreement with the obtained DLS results. The size of the formed worm-like micelles was about 20 to 500 nm in length and 9.4 nm in width for P27: P<sub>4</sub>-B<sub>18</sub>-D<sub>17</sub> and 50 to 1000 nm in length and 32.6 nm in width in the case of P31: P<sub>14</sub>-B<sub>70</sub>-D<sub>73</sub> terpolymer.

The formed worm-like micelles seems to be flexible and entangled loosely with each other. Combining the mean aggregation diameter obtained from DLS and the observed TEM images, it seems that as the polymer chains increases in length, the possibility of formation of longer and thicker worm-like micelles increases in the system. Overall, it seems that this series of examined terpolymers does not form polymersomes using conventional preparation methods and instead they all form spherical and worm-like micelles using bulk and film rehydration methods, respectively.

**Figure 4.4.** TEM images corresponding to film rehydration of (a, b) P27: P<sub>4</sub>-B<sub>18</sub>-D<sub>17</sub> and (c, d) P31: P<sub>14</sub>-B<sub>70</sub>-D<sub>73</sub> (1 wt.%) in water. Image (e) is SEM image corresponding to P31: P<sub>14</sub>-B<sub>70</sub>-D<sub>73</sub> terpolymer from the same prepared sample. Figure (f) is schematic presentation of worm-like aggregates where light blue, red and dark blue colour is corresponding to PEGMA, BuMA and DAMEMA blocks respectively.



#### 4.4 Conclusion

The self-assembly behaviour of a series of amphiphilic ABC terpolymers based on PEGMA, BuMA and DMAEMA monomers with the general structure of  $P_x-B_y-D_z$  in aqueous solution was studied. The preliminary observations revealed that this series of terpolymers with similar composition but varied molecular weights self-assemble into different types of micellar structures, based on the preparation method. Bulk rehydration of this series of terpolymers resulted in the formation of spherical micelles, whereas rehydration of their thin film led to the formation of flexible worm-like micelles. It seems that increasing the molecular weight of terpolymers enhances the formation of longer and thicker worm-like micelles. Increasing the temperature causes shrinkage in the mean diameter or probably formation of different type of self-assembly.

In summary at neutral pH, the preliminary observations of the behaviour of a number of terpolymers in water revealed that the amphiphilic polymers have the ability to self-assemble, but not to polymersome-like structure as it was desired. However, further investigations could be done at basic pHs so the DMAEMA block hydrophilicity will be significantly decreased in order to change the hydrophilic/hydrophobic ratio closer to 1: 2 or 1: 3 that has been reported in the literature to self-assemble to vascular type structures.<sup>11</sup>

## 4.5 References

1. P. Alexandridis and B. Lindman, *Amphiphilic Block Copolymers: Self-Assembly and Applications*, 1st. edn., Elsevier, Amsterdam, 2000.
2. N. Hadjichristidis, S. Pispas and G. Floudas, *Block Copolymers, Synthetic Strategies, Physical Properties, and Applications*, John Wiley & Sons Inc., Hoboken, New Jersey, 2003.
3. E. S. Read and S. P. Armes, *Chem. Commun.*, 2007, **29**, 3021.
4. R. K. O'Reilly, C. J. Hawker and K. L. Wooley, *Chem. Soc. Rev.*, 2006, **35**, 1068.
5. X. Wang, G. Guerin, H. Wang, Y. Wang, I. Manners and M. A. Winnik, *Science*, 2007, **317**, 644.
6. L. Zhang and A. Eisenberg, *J. Am. Chem. Soc.*, 1996, **118**, 3168.
7. I. K. Voets, A. d. Keizer, P. d. Waard, P. M. Frederik, P. H. H. Bomans, H. Schmalz, A. Walther, S. M. King, F. A. M. Leermakers and M. A. Cohen-Stuart, *Angew. Chem., Int. Ed.*, 2006, **45**, 6673.
8. R. Erhardt, M. F. Zhang, A. Boker, H. Zettl, C. Abetz, P. Frederik, G. Krausch, V. Abetz and A. H. E. Mueller, *J. Am. Chem. Soc.*, 2003, **125**, 3260.
9. D. J. Pochan, Z. Chen, H. Cui, K. Hales, K. Qi and K. L. Wooley, *Science*, 2004, **306**, 94.
10. P. L. Soo and A. Eisenberg, *J. Polym. Sci., Part B: Polym. Phys.*, 2004, **42**, 923.
11. J. Du and R. K. O'Reilly, *Soft Matter*, 2009, **5**, 3544.
12. J. F. L. Meins, O. Sandre and S. Lecommandoux, *Eur. Phys. J. E.*, 2011, **34**, 14.

## **CHAPTER 5**

### **WATER-IN-WATER EMULSIONS BASED ON ATPS AND STABILISED BY TERPOLYMERS – TEMPLATED POLYMERSOMES**

## 5.1 Introduction

Emulsions are dispersions of two immiscible liquids which are thermodynamically unstable, but can be kinetically stabilised by the adsorption of surfactants, amphiphilic polymers or particles at the interface. In general emulsions are consisted of two immiscible phases that are usually oil and water, thus forming dispersions of oil-in-water (o/w) or water-in-oil (w/o). However, water-in-water (w/w) emulsions can also be formed based on aqueous two phase systems (ATPSs) which are aqueous mixtures of two incompatible polymers. For instance, emulsification of an ATPS consisting of a few weight percentages of dextran and PEG results in formation of w/w emulsions with either dispersed drops of dextran rich phase in PEG rich continuous phase (d/p) or vice versa (p/d). These systems are potentially attractive, since no organic solvent is used for their preparation and the prepared emulsions are entirely aqueous. Also, they benefit from having the ability to selectively incorporate or separate different biopolymers. However, similar to conventional o/w or w/o emulsions, these systems need kinetic stabilisation, since they are thermodynamically unstable. ATPS systems have been widely used for partitioning and separation of macromolecules at which rapid phase separation is essential. However, not much work has been done on stabilisation of these systems and as a result, it is not fully understood what type of species can be adsorbed at w/w interface to provide kinetic stabilisation. As it was mentioned in introduction section, the interfacial tension of ATPSs is very low, about 0.066 mN/m for a ATPS consisting of 8 wt.% dextran and 6 wt.% PEG, compare to oil/water systems with a typical surface tension of 30-50 mN/m. Therefore, stabilisation of these systems is quite challenging. In this chapter the stabilisation of w/w emulsions using either ABA or ABC terpolymers is of interest.

As reviewed before, there is a limited number of publications on stabilisation of w/w emulsions or other related systems with block copolymers. For instance, stabilisation of oil in oil emulsions consisting of two incompatible polystyrene and polybutadiene polymers using poly(styrene-*b*-butadiene) diblock copolymers described by Molau <sup>1</sup> is one of the early works in this area. In addition, Ossenbach-Sauter and Riess described stabilisation of w/w emulsions containing mixtures of poly(vinylpyridinium chloride) (pVPC) and PEG polymers with di-block pVPC-*b*-PEG copolymers. <sup>2</sup> Jin et. al. illustrated the stabilisation of w/w emulsions based on



dextran-PEG ATPS by using sodium alginate as stabiliser.<sup>3</sup> Simon et. al. reported the formation of w/w emulsion consisting of water solvated dispersed liquid crystal disodium cromoglycate (DSCG) in continuous phase containing a range of water soluble nonionic, anionic and cationic polymers which have potential to exclude DSCG to form water solvated drops.<sup>4</sup> They found that the non-ionic polymers form quite stable w/w emulsion (30 days) via providing steric hindrance which prevent from coalescence of the droplets.

Thus, according to these studies, it seems that block copolymers with relatively high adsorption energies need to be adsorbed in order to stabilise the very low tension surfaces of water-in-water emulsions. Therefore, the block copolymer should possess an affinity towards aqueous two phases. To the best of our knowledge terpolymers have not been used before for stabilisation of w/w emulsions. In this study, the possibility of using either ABA or ABC terpolymers as effective stabilisers for stabilisation of w/w emulsions consisting of dextran and PEG polymers is investigated. Firstly, commercially available ABA terpolymers with hydrophilic terminal A blocks and hydrophobic B middle block are used where A blocks were assumed to have affinity to stay in either of aqueous two phases while hydrophobic B block remains at the interface. Similarly, in the case of using ABC terpolymers, the terminal A and C blocks both are hydrophilic and also possess different affinities towards dextran and PEG rich phases. Similar to ABA terpolymers, the middle B block is hydrophobic and will induce polymer-polymer cohesion and results in formation of a coherent hydrophobic layer around the dispersed droplets. Also the hydrophobic B block acts as a driving force to lead A and C blocks towards dextran and PEG rich phases. The process of stabilisation of w/w emulsions using terpolymers can be described in two alternative ways:

1. Kinetic stabilisation of w/w emulsions as a result of adsorption of the terpolymers at dextran-PEG interface.
2. Formation of polymersomes based on terpolymers being templated around w/w emulsions droplets.

Therefore, this research strategy is based on a combination of two concepts of terpolymer stabilised w/w emulsions and formation of polymersomes. Polymersomes have been prepared using several different methods, at which there is

the direct or indirect involvement of an organic solvent as described in Section 1.5.1. This is the main disadvantage of using current methods for preparation of polymersomes. In addition, there are a few reported studies on preparation of polymersomes using ABA or ABC terpolymers, but in most of them it remained unclear whether they form a monolayer shell, a bilayer containing hairpin folded molecules or a mixed coronas. Moreover, the encapsulation efficiency of prepared polymersomes using current methods is very low. However, there are a few new techniques such as microfluidic method at which the encapsulation efficiency of polymersomes has been improved.<sup>5</sup>

In this work we intend to investigate whether polymersomes can be formed by templating the dispersed phase of a w/w emulsion, which can be formed by emulsification of an ATPS. This novel strategy avoids the use of any organic solvent in the system. In addition, the encapsulation efficiency of prepared polymersomes based on this strategy can be increased significantly by concentrating the encapsulant within the dispersed phase prior to emulsification process. Moreover, this novel technique for preparation of polymersomes can be easily scaled up compare to more complex techniques such as microfluidics.

The specific aims of this chapters are to determine (i) whether ABA or ABC terpolymers can stabilise water-in-water emulsion based on the PEG-dextran ATPS; (ii) how the emulsion properties such as type, drop size and stability depend on the block sizes of the ABC terpolymers and (iii) how solute molecules distribute within the water-in-water emulsion (or templated polymersome) system.

## **5.2 Stabilisation of dextran-PEG ATPS using ABA terpolymers, Pluronics<sup>®</sup>**

ABA terpolymers based on poly(ethylene glycol)<sub>x</sub>-*b*-poly(propylene glycol)<sub>y</sub>-*b*-poly(ethylene glycol)<sub>x</sub>, (EO<sub>x</sub>-PO<sub>y</sub>-EO<sub>x</sub>) so called Pluronics<sup>®</sup>, where EO and PO are hydrophilic and hydrophobic in character respectively, were used for the stabilisation of dextran-PEG ATPS and possible formation of polymersomes. It was assumed that the hydrophilic terminal A blocks have the same affinity to stay in either of aqueous polymer phases (PEG or dextran) while the hydrophobic B block is adsorbed at the liquid-liquid interface. The research strategy is illustrated schematically in Figure 5.1. As it can be seen in this Figure, in the presence of encapsulant that can be selectively partitioned within one of the polymer phases, after addition of ABA

terpolymers and emulsification, they will be encapsulated within the dispersed phase and formed polymersomes. Using this strategy the encapsulation efficiency of the formed polymersomes would be equal to the fraction of encapsulant that has partitioned into the dispersed phase. Three different Pluronics<sup>®</sup>, namely, F68 (EO<sub>76</sub>-PO<sub>29</sub>-EO<sub>76</sub>), F108 (EO<sub>132</sub>-PO<sub>50</sub>-EO<sub>132</sub>) and F127 (EO<sub>100</sub>-PO<sub>65</sub>-EO<sub>100</sub>), with varied characteristics were used in this study. F68 and F108 have the same composition (80 wt.% EO and 20 wt.% PO) but different MW 8400 and 14600 g/mol respectively. It was expected longer EO chains penetrate more into aqueous polymer phases and therefore stabilise the emulsion for a longer time. F127 has a higher hydrophobic content (70 wt.% EO and 30 wt.% PO) and a relatively high molecular weight, 12600 g/mol. It was assumed that increasing the hydrophobic middle block length will increase the cohesion between the terpolymers within an adsorbed film and thereby enhances the emulsion drop stability. Figure 5.2 illustrate the schematic structure of used Pluronics<sup>®</sup>.

**Figure 5.1.** Stabilisation of APTS using ABA terpolymers in the presence of encapsulant concentrated within one of the phases.

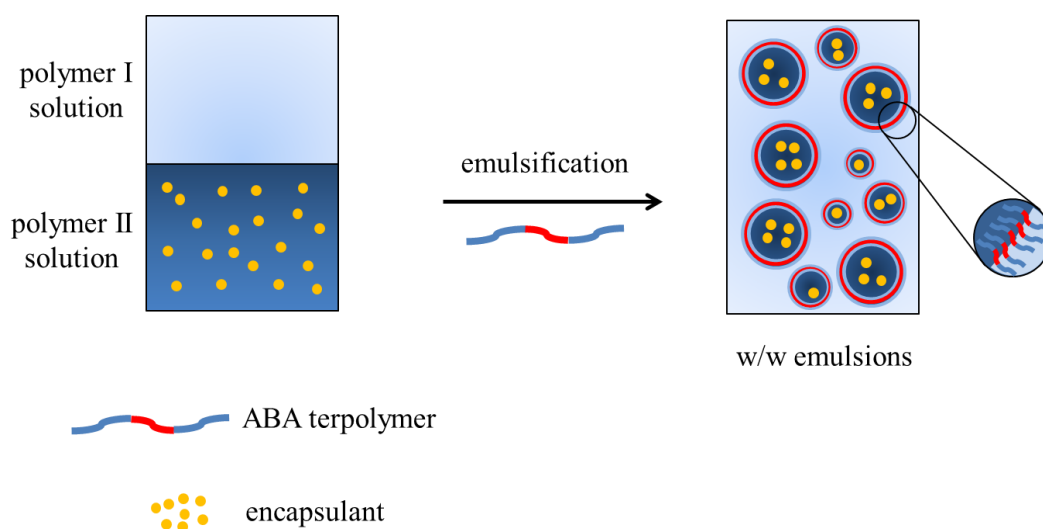
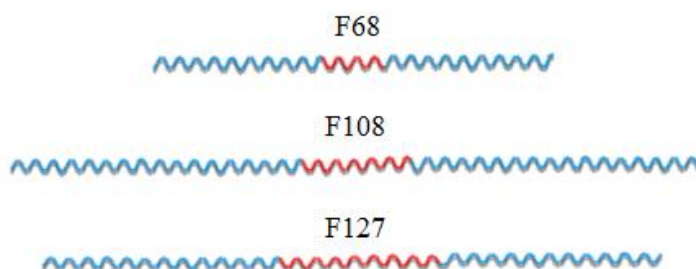


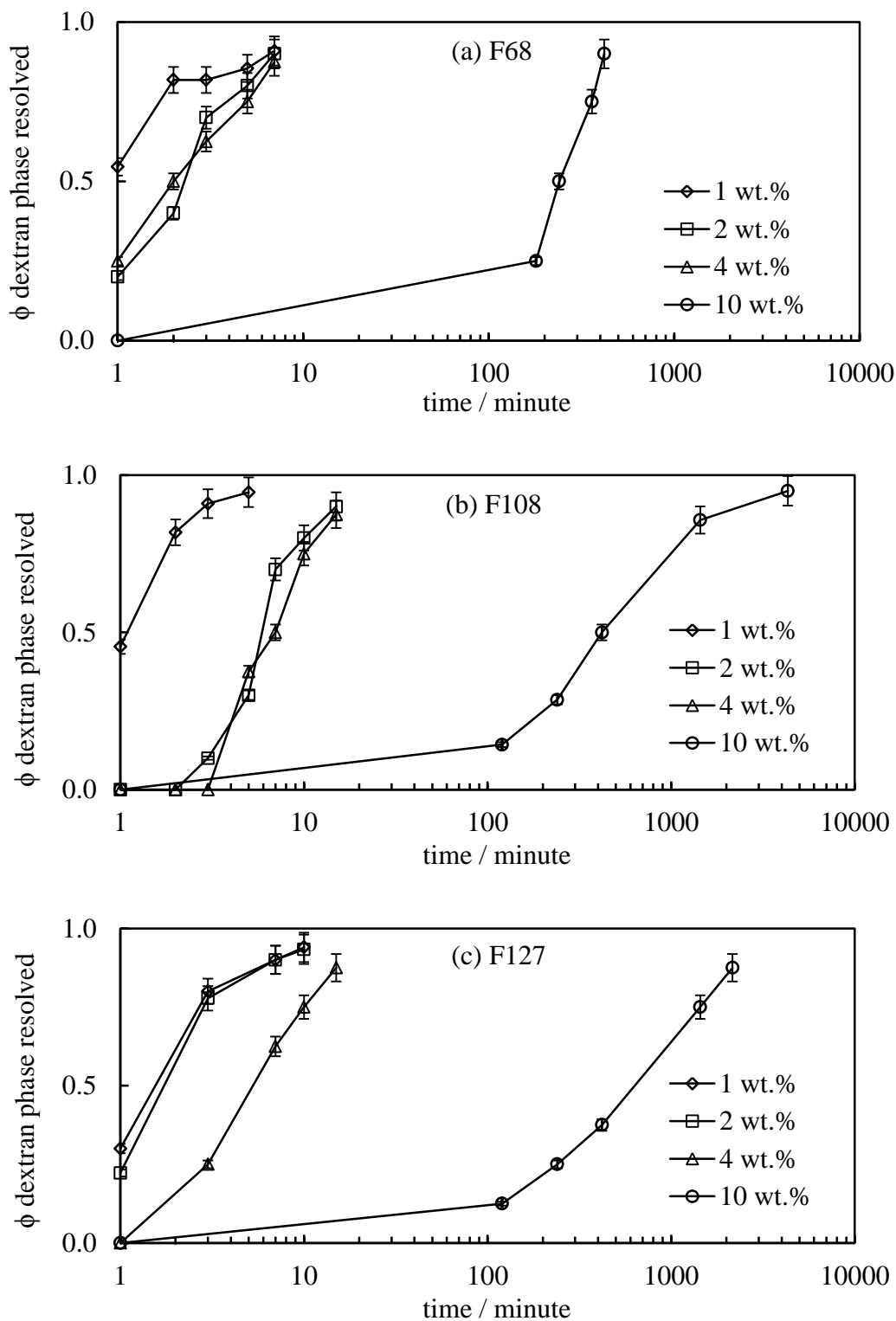
**Figure 5.2.** Schematic representation of Pluronic<sup>®</sup> terpolymers; blue and red chains are corresponding to EO and PO blocks respectively.



### ***5.2.1 Effect of Pluronic<sup>®</sup> concentration, composition and MW on stability of w/w emulsion***

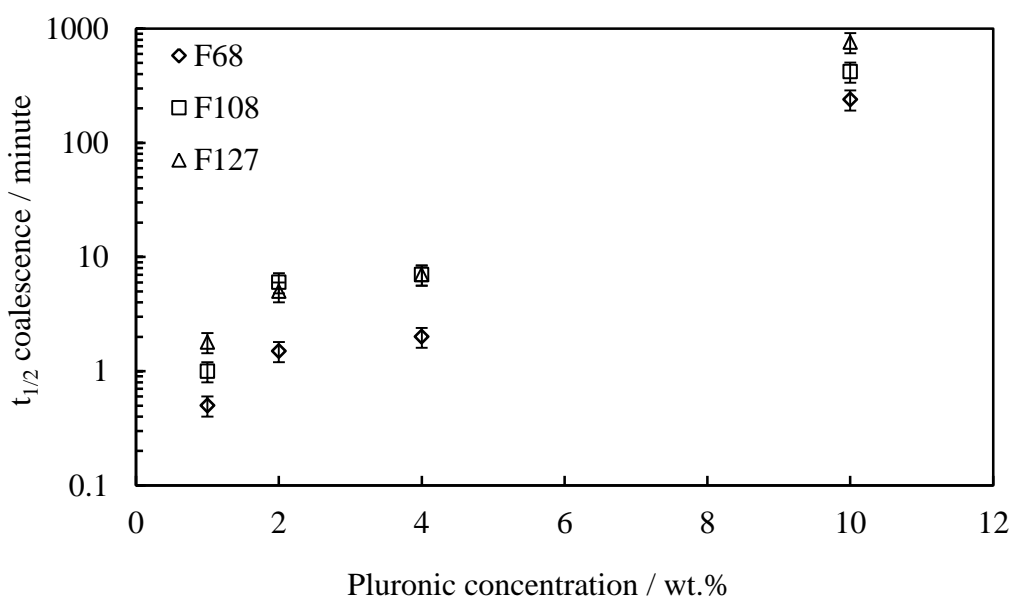
Different concentrations of Pluronic<sup>®</sup>, namely, 1, 2, 4 and 10 wt.% were used for the stabilisation of dextran-PEG APTS with equal volume fractions (0.5:0.5) and the stability of prepared emulsions was monitored over time. Emulsions were prepared via 2 minutes homogenisation at 11000 rpm at room temperature. The first observation was the instability of all prepared emulsions at low concentrations (1, 2, 4 wt.% of Pluronic<sup>®</sup>). By increasing the concentration of stabiliser to 10 wt.% the stability of emulsions increased dramatically specially in the case of using F108: EO<sub>132</sub>-PO<sub>50</sub>-EO<sub>132</sub> and F127: EO<sub>100</sub>-PO<sub>65</sub>-EO<sub>100</sub>. Figure 5.3 shows the volume fractions of resolved dextran rich phase i.e. dispersed phase, over time for the prepared emulsion using different contents of Pluronic<sup>®</sup> grades.

**Figure 5.3.** Plots of resolved dextran phase volume fraction ( $\phi$  dextran) versus time in logarithmic scale for dextran-in-PEG emulsions consisting of 0.5: 0.5 volume fractions of dextran-PEG stabilised using 1, 2, 4 and 10 wt.% of (a) F68: EO<sub>76</sub>-PO<sub>29</sub>-EO<sub>76</sub>, (b) F108: EO<sub>132</sub>-PO<sub>50</sub>-EO<sub>132</sub> and (c) F127: EO<sub>100</sub>-PO<sub>65</sub>-EO<sub>100</sub>. Emulsions were prepared via 2 minutes homogenisation at 11000 rpm at room temperature.



However, none of the used Pluronics<sup>®</sup> was able to stabilise the emulsion for a long time. Comparing the time taken for dextran rich phase (dispersed phase, bottom phase) to resolve half of its volume fraction (or height), so called  $t_{1/2}$  coalescence, the most stable emulsion ( $t_{1/2}$  ~12.5 hours) was obtained in the case of using 10 wt.% of F127: EO<sub>100</sub>-PO<sub>65</sub>-EO<sub>100</sub> (see Figure 5.4). In addition, it is obvious that emulsion stability varies as a function of polymer MW and composition. In the case of using F68 and F108 which both have same composition (20 wt.% PO and 80 wt.% EO) but varied MW, the emulsion stability doubled when MW increased from 8400 to 14600 g/mol. In the case of using F127 with higher hydrophobic content (30 wt.%), longer stability was observed in compare to F108 although its MW (12600 g/mol) is lower to that of the F108 (14600 g/mol).

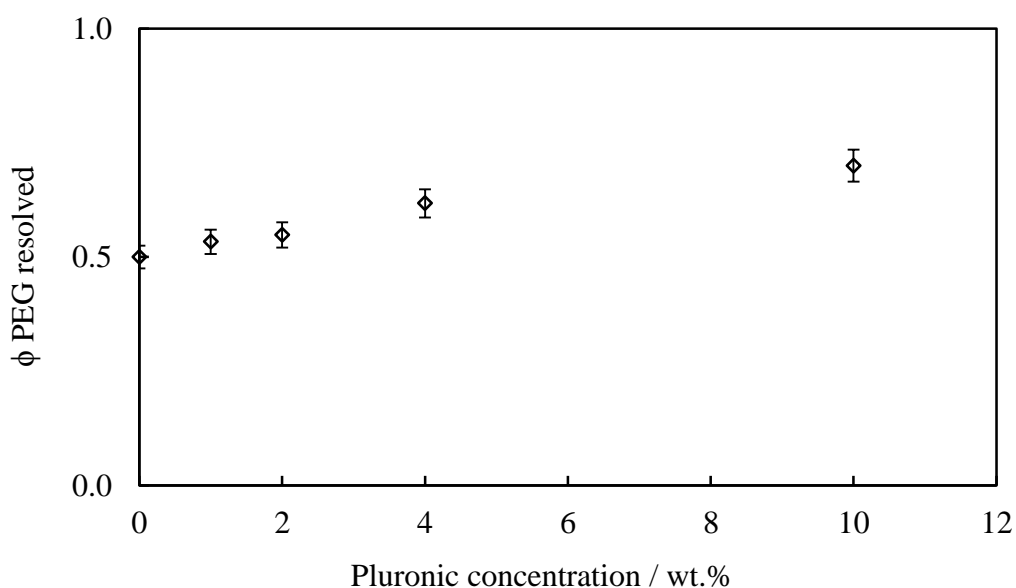
**Figure 5.4.** Variation of  $t_{1/2}$  of resolved dextran rich phase ( $t_{1/2}$  of coalescence) with concentration of used Pluronics<sup>®</sup> for stabilisation of dextran-in-PEG emulsions consisting of 0.5: 0.5 volume ratios of dextran:PEG prepared via 2 minutes homogenisation at 11000 rpm at room temperature.



Overall it seems that by increasing the hydrophobicity and the MW of the stabiliser the longer is the stability of prepared w/w emulsions. However, it should be noted that polymers with high MW when dissolved in dextran-PEG APTS system, increase the viscosity of the system and therefore, the rate of creaming or sedimentation and coalescence decreases which result in slower phase separation of the emulsion. The longer stability of the w/w emulsions when using the Pluronic<sup>®</sup>

with a longer hydrophobic chain might be due to the enhanced polymer film around the dispersed phase. However, observing the emulsions after a full phase separation revealed that all three used Pluronics<sup>®</sup> in this work have the tendency to remain in the PEG rich phase rather than dextran rich phase, as the volume fraction of PEG rich phase increased with respect to increasing the polymer concentration in the system. This increase in concentration of the Pluronics<sup>®</sup> causes a disruption in the equilibrium phase behaviour of dextran-PEG ATPS and shifts it from equal volume fraction to larger PEG and smaller dextran volume fractions (see Figure 5.5). It can be concluded that the Pluronics<sup>®</sup> have the tendency to stay in the PEG rich phase, probably due to their molecular similarity and not at the dextran-PEG interface, therefore, they are not able to effectively stabilise w/w emulsions based on dextran-PEG system and the observed short stability is probably due to the high viscosity of the system.

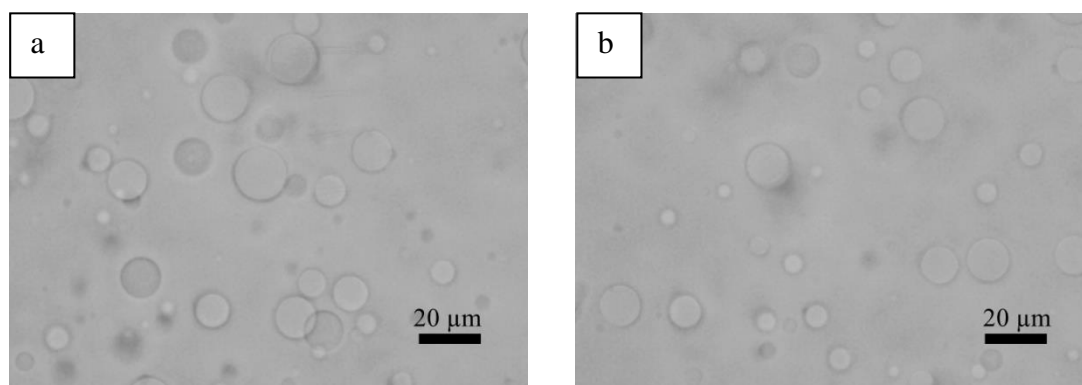
**Figure 5.5.** Variation of PEG-rich phase volume fraction after full phase separation by increasing the concentration of Pluronics<sup>®</sup> in the system.



### 5.2.2 Micrographs of w/w emulsions stabilised using Pluronics®

For the dextran-PEG system of equal volume fraction (9.24 wt.% dextran and 4.96 wt.% PEG), separation of the two polymers begins immediately after emulsification, when no stabiliser is present. As expected separation proceeds quickly, a clear interface separating a distinct top and bottom phase of equal volume fractions is seen in less than a minute. However, observing the separated top and bottom phases under microscope showed that even after a few hours, there were residual dispersed drops in both phases (see Figure 5.6). A Full phase separation occurred after 24 hours.

**Figure 5.6.** Micrographs of emulsified dextran-PEG ATPS with 0.5:0.5 volume fractions and no stabiliser. Emulsion was prepared via 2 minutes homogenisation at 11000 rpm at room temperature. Micrographs were taken 2 hours after emulsification process from (a) PEG rich phase (top phase) and (b) dextran rich phase (bottom phase).



Micrograph taken from stabilised w/w emulsions with Pluronics® showed that the unstable emulsions containing 1, 2 and 4 wt.% of either of F68 or F108 or F127 have the similar drop size residual dispersed phase. But in case of using 10 wt.% of F108 and F127 a compact emulsion containing significant amount of dispersed phase was observed (see Figure 5.8 and 5.9), while emulsion containing F68 showed discrete residual dispersed phase as it was quite unstable in compare to F108 and F127, even at 10 wt.% concentration (see Figure 5.7). The mean drop size of emulsions containing 10 wt.% of F108 (20 wt.% hydrophobicity) and F127 (30 wt.% hydrophobicity) was  $31.1 \pm 13.5$  and  $15.0 \pm 5.5$   $\mu\text{m}$  respectively, while in case



of emulsion containing 1, 2 and 4 wt.% of any of the Pluronics® the mean drop size of residual dispersed phase was about  $4.7 \pm 2.5 \mu\text{m}$ .

**Figure 5.7.** Micrographs of w/w emulsions based on dextran-PEG APTS with 0.5:0.5 volume fractions, stabilised using F68: EO<sub>76</sub>-PO<sub>29</sub>-EO<sub>76</sub> at (a) 1 wt.%, (b) 2 wt. %, (c) 4 wt.% and (d) 10 wt.% concentration. Emulsions were prepared via 2 minutes homogenisation at 11000 rpm at room temperature. Micrographs were taken immediately after preparation of emulsions. Emulsion type was dextran-in-PEG in all cases.

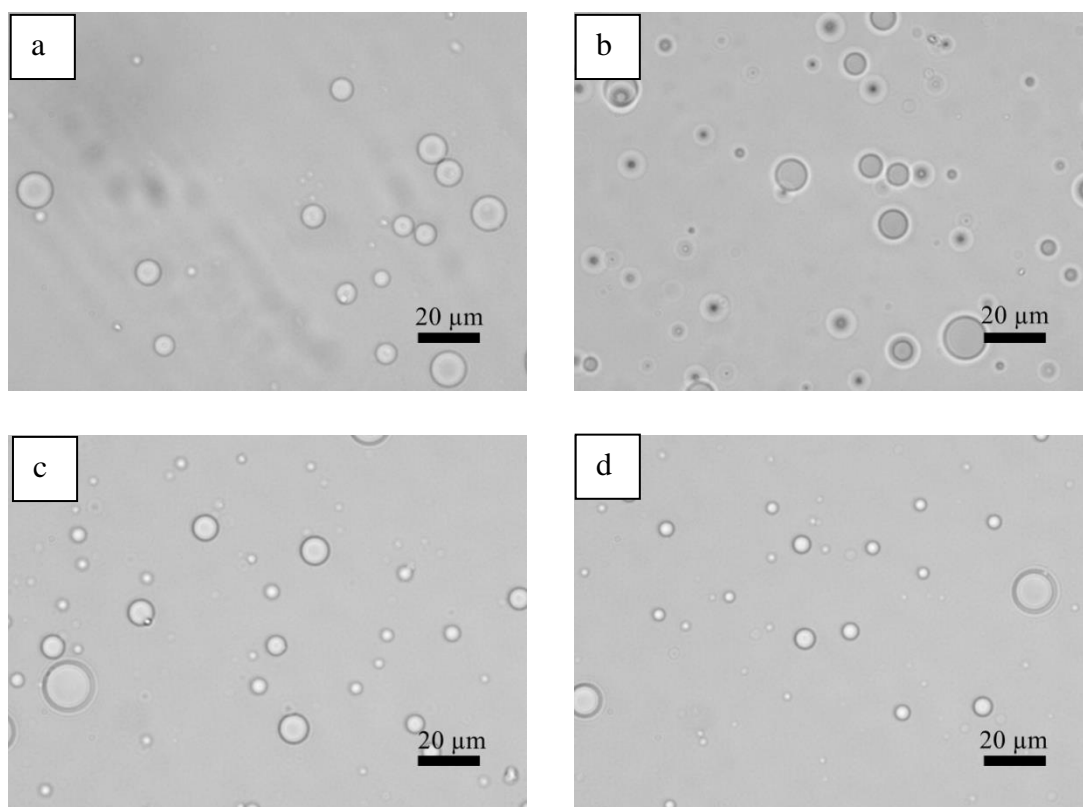


**Figure 5.8.** Micrographs of w/w emulsions based on dextran-PEG ATPS with 0.5:0.5 volume fractions, stabilised using F108: EO<sub>132</sub>-PO<sub>50</sub>-EO<sub>132</sub> at (a) 1 wt.%, (b) 2 wt.%, (c) 4 wt.% and (d) 10 wt.% concentration. Emulsions were prepared via 2 minutes homogenisation at 11000 rpm at room temperature. Micrographs were taken immediately after preparation of emulsions. Emulsion type was dextran-in-PEG in all cases.

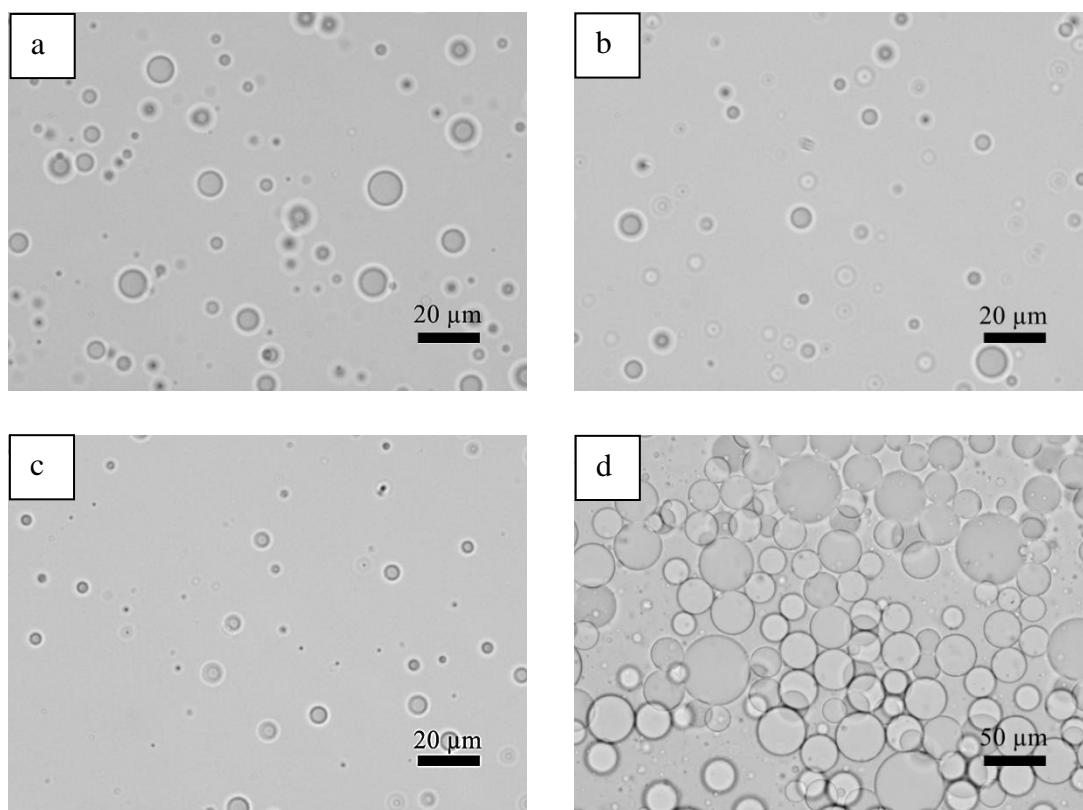
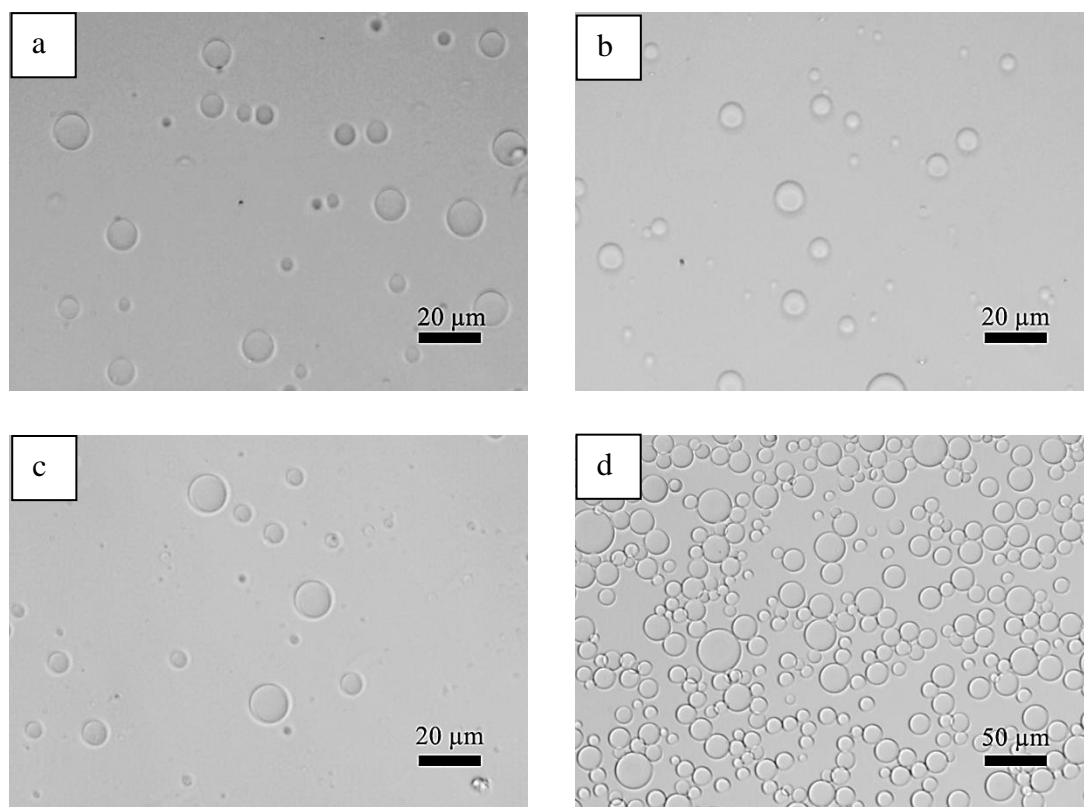


**Figure 5.9.** Micrographs of w/w emulsions based on dextran-PEG ATPS with 0.5:0.5 volume fractions, stabilised using F108: EO<sub>100</sub>-PO<sub>65</sub>-EO<sub>100</sub> at (a) 1 wt.%, (b) 2 wt.%, (c) 4 wt.% and (d) 10 wt.% concentration. Emulsions were prepared via 2 minutes homogenisation at 11000 rpm at room temperature. Micrographs were taken immediately after preparation of emulsions. Emulsion type was dextran-in-PEG in all cases.

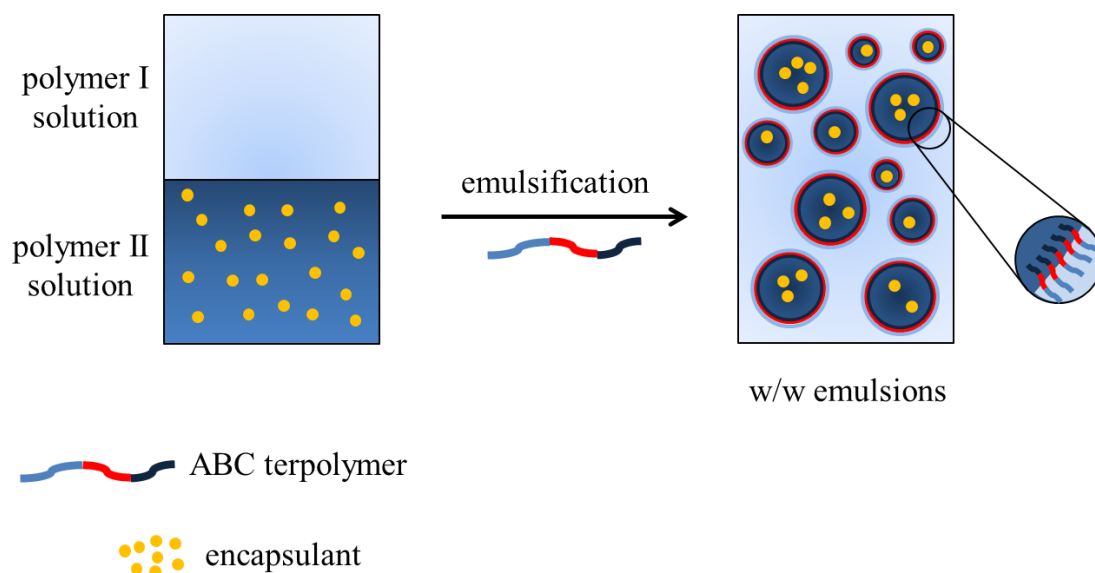


### 5.3 Stabilisation of dextran-PEG ATPS using ABC terpolymers

ABC terpolymers based on hydrophilic non-ionic monomer, PEGMA, a non-ionic hydrophobic monomer, BuMA and a hydrophilic ionisable thermo-responsive monomer, DMAEMA were used for stabilisation of dextran-PEG ATPS. The hydrophobic monomer, BuMA consists the B block, which is in the middle of the polymer where the two hydrophilic monomers PEGMA and DMAEMA form the A and C blocks, respectively. The reason behind choosing these monomers and ABC type terpolymer was firstly the possibility of contribution of the amine functional groups of DMAEMA block in formation of hydrogen bond with the dextran hydroxyl groups. Consequently, it was assumed that the DMAEMA block has tendency to remain in dextran rich phase. Secondly, it was presumed the PEGMA

with a comb like structure consisting of a polymethacrylate back bone and PEG brushes, tends to stay in PEG rich phase, due to the compatibility of PEG brushes with PEG phase. As a result this amphiphilic triblock copolymer is expected to have the ability to stabilise w/w emulsion consisting of dextran and PEG rich phases. In addition, the presence of BuMA block in the structure of this type of terpolymer enhances the possibility of polymersomes formation in such system. The research strategy is illustrated schematically in Figure 5.10 where light blue, red and dark blue chains are corresponding to PEGMA, BuMA and DMAEMA blocks respectively. As explained for ABA terpolymers, using this research strategy for stabilisation of w/w emulsions and possible formation of polymersomes, high encapsulation efficiency can be obtained. To examine this assumption a series of ABC terpolymers with general structure of  $P_x-B_y-D_z$  but different x, y and z block lengths were used as stabiliser for w/w emulsion preparation or in the other words, polymersomes preparation.

**Figure 5.10.** Stabilisation of ATPS using ABC terpolymers in the presence of encapsulant concentrated within one of the phases.

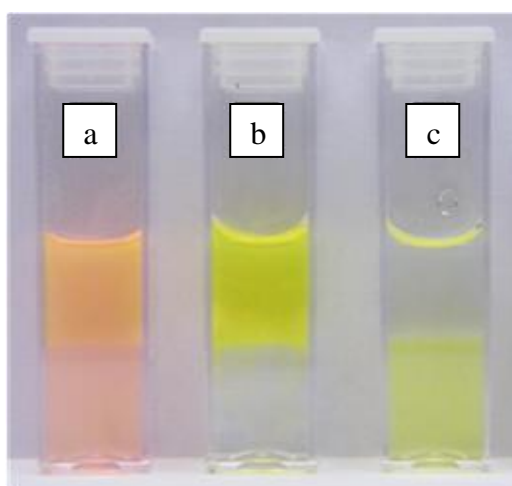


### 5.3.1 Effect of ABC terpolymer composition on emulsion type

It is well-established that the emulsion type depends on nature of the stabiliser and the relative volume fractions of the two phases.<sup>6</sup> At equal volume fractions of oil/water, surfactant with long hydrophobic tail results in water-in-oil emulsions while type of emulsion changes to oil-in-water when surfactant with big hydrophilic head and short hydrophobic tail is used. Therefore, in this work it was predicted that the type of formed emulsion would depend on the polymer composition since two DMAEMA and PEGMA terminal blocks are expected to govern the relative affinities of the terpolymer towards the dextran and PEG rich phases respectively. Terpolymers with long DMAEMA block were expected to form PEG in dextran emulsion, while those with long PEGMA block would expect to form dextran in PEG.

In order to investigate whether in ATPSs the composition of the used stabiliser can invert the emulsion type, equal volume fractions of dextran and PEG ATPS was used, hence emulsion type depends just on the nature of the stabiliser. Emulsions type was determined using fluorescence probes with affinity to stay in either dextran or PEG rich phase. As it can be seen in Figure 5.11, rhodamine and fluorescein partition preferentially to the top PEG-rich phase in the separated ATPS at equilibrium, whereas FITC-dextran partitions to the bottom dextran-rich phase.

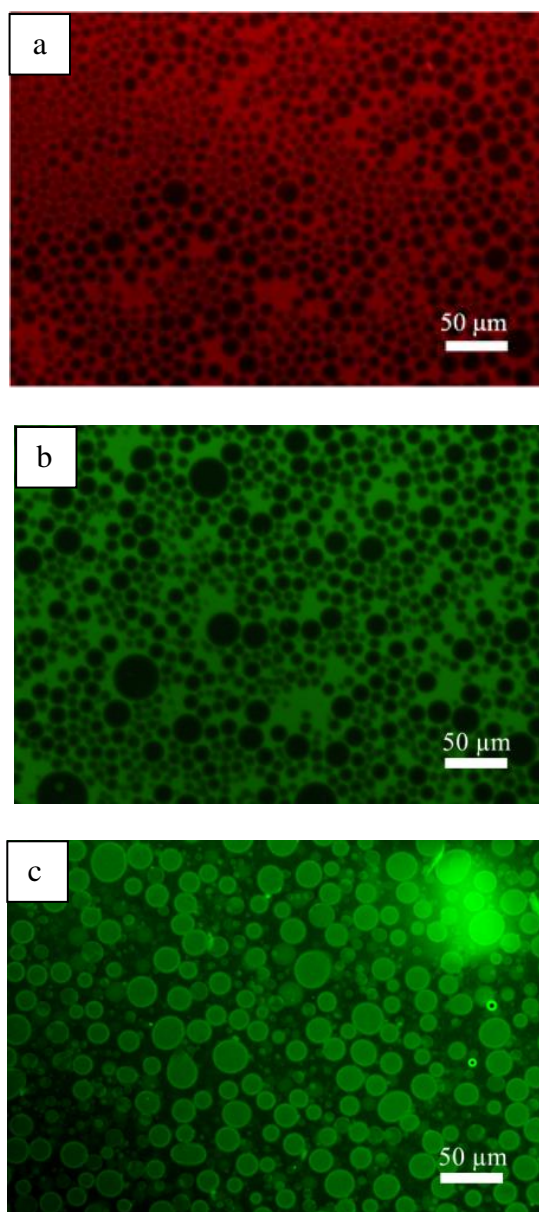
**Figure 5.11.** Aqueous two phase systems containing 9.24 wt.% dextran and 4.96 wt.% PEG giving equal volumes of dextran-rich bottom phase and PEG-rich top phase and showing the partitioning of (a) rhodamine, (b) fluorescein and (c) fluorescein isothiocyanate dextran (FITC-dextran) conjugate.



The fluorescent micrographs of w/w emulsion based on dextran-PEG ATPS with equal volume fraction and containing 1 wt.% of P36: P<sub>13</sub>-B<sub>76</sub>-D<sub>40</sub> ABC terpolymer and any of the mentioned fluorescent probes further confirmed that both rhodamine and fluorescein are preferentially located in the continuous phase (which is therefore the PEG-rich phase) and FITC-dextran is in the dispersed phase (see Figure 5.12). Therefore, the type of emulsion was determined to be dextran-in-PEG (d/p). Similar experiments revealed that all synthesised terpolymers provide dextran-in-PEG type of emulsion (when emulsion is stable), despite the degree of polymerisation of PEGMA/DMAEMA being varied from a maximum of 1.93 to a minimum of 0.05.

Formation of dextran dispersed phase in PEG continuous phase at equal volume fractions of dextran and PEG, for terpolymers containing a long DMAEMA chain revealed that the type of emulsion is independent to terpolymer composition and so called, transitional phase inversion, does not occur in these systems. This contrary result might be due to the much higher density of dextran rich phase which preferentially forms the dispersed phase rather the continuous phase at equal volume fractions of dextran and PEG. It is known that the denser phase prefers to form dispersed phase while, the less dense phase forms the continuous phase.<sup>7</sup>

**Figure 5.12.** Fluorescence micrographs of emulsions containing equal volume fractions of PEG-rich and dextran-rich phases, 1 wt.% P36: P<sub>13</sub>-B<sub>76</sub>-D<sub>40</sub> and stained with (a) 0.04 mg/mL of rhodamine, (b) 0.04 mg/mL of fluorescein and (c) 0.2 mg/mL of FITC-dextran.



### *5.3.2 Effect of relative volume fractions of the dextran-PEG phases on emulsion type*

It was discussed in previous section that all synthesised terpolymers forms dextran in PEG emulsions at equal volume fractions of dextran-PEG. Therefore, block length variations were not sufficient to cause transitional phase inversion. However, it was found that by varying the relative volume fractions of dextran and

PEG phases when a fixed stabiliser is used, so called catastrophic phase inversion occurs in w/w emulsions. Emulsions consisting of 1 wt.% of P16: P<sub>11</sub>-B<sub>60</sub>-D<sub>64</sub> but with varying volume fraction of dextran and PEG rich phases ( $\phi_{\text{dex}}$  and  $\phi_{\text{PEG}}$ ) were prepared. The reason behind choosing P16 terpolymer was fairly long stability of the system provided by this polymer. This variation in volume fractions of dextran and PEG was achieved by varying the dextran and PEG concentrations along the fixed tie-line F of dextran-PEG phase diagram as assigned in Figure 5.13 by triangle symbols. The emulsion type was determined using rhodamine fluorescent probe which has selective affinity towards PEG rich phase (see Figure 5.14). As can be seen, in this Figure emulsions containing less than 0.56 volume fraction of dextran ( $\phi_{\text{dex}} < 0.56$ ) formed dextran in PEG (d/p) emulsions, while a catastrophic phase inversion occurred when volume fraction of dextran increased above 0.62 and PEG in dextran (p/d) emulsions were obtained. The phase compositions, volume fractions of dextran-PEG and the emulsion type are summarised in Table 5.1.

**Figure 5.13.** Phase diagram of the dextran ( $M_w = 500$  kDa) and PEG ( $M_w = 6$  kDa) system at 20°C. The solid line shows the binodal and the dashed lines in the two-phase region show tie-lines terminating in the unfilled circles. The filled circle indicates the plait point. The triangle and square symbols indicate the compositions of used ATPSs on tie line F and G, respectively.

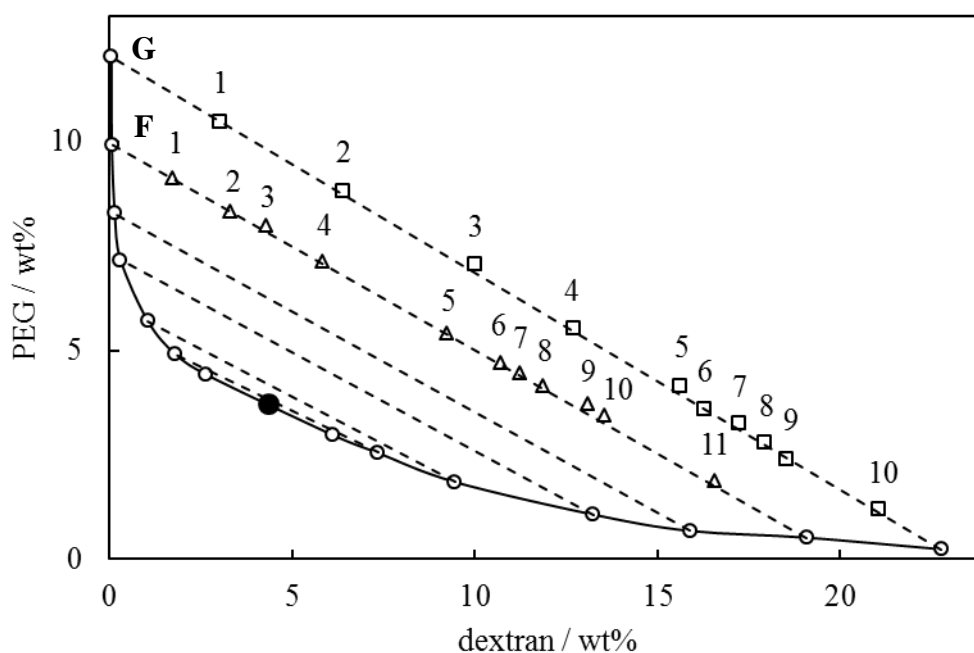




**Figure 5.14.** Fluorescence micrographs of w/w emulsions containing different volume fractions of dextran-PEG ATPS, 1 wt.% of P16: P<sub>11</sub>-B<sub>60</sub>-D<sub>64</sub> terpolymer and 0.04 mg/mL of rhodamine. Emulsions were prepared via stirring for two hours at 500 rpm. Micrographs were taken 30 minutes after stopping stirring. Each micrograph refers to one point of the phase diagram (see Table 5.1 for details).

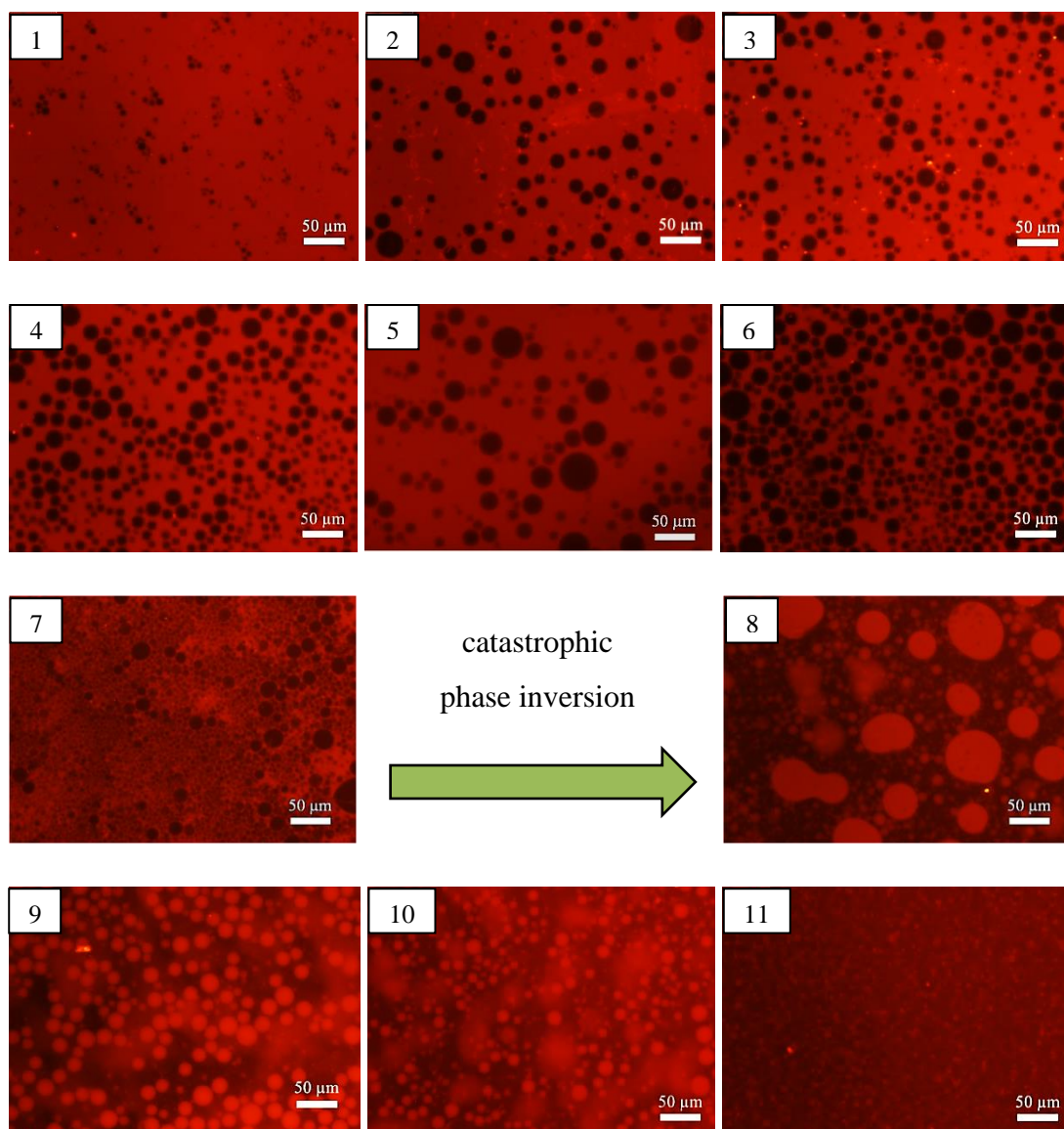


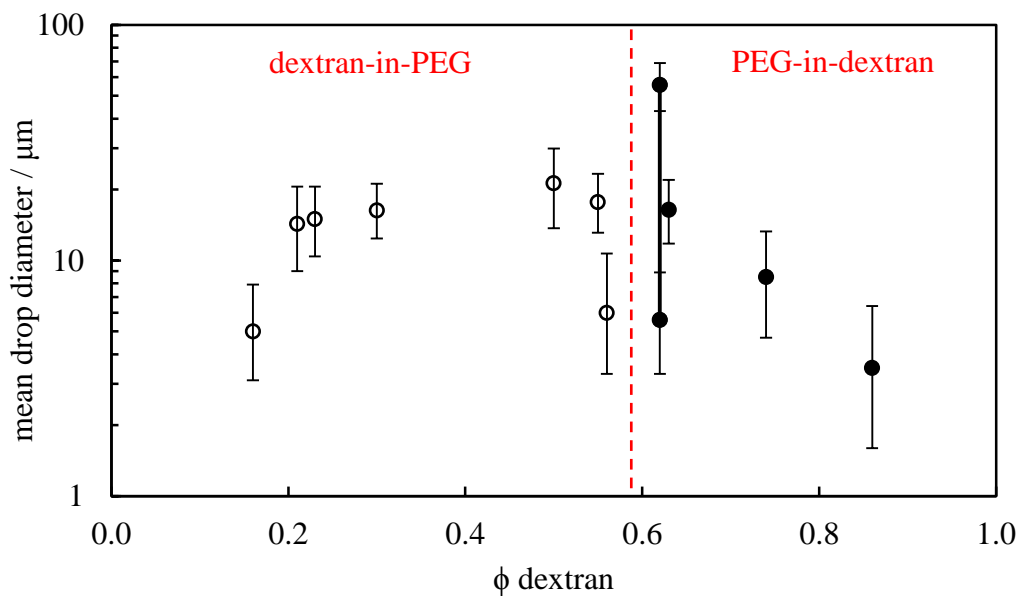
**Table 5.1.** Summary of compositions, phase volume fractions and emulsion type of emulsions formed from ATPSs containing 1 wt.% of P16: P<sub>11</sub>-B<sub>60</sub>-D<sub>64</sub> at pH 6 and different amounts of dextran and PEG, giving different volume fractions of the dextran- and PEG-rich phases.

Point	Dextran wt. %	PEG wt. %	$\phi_{\text{dextran}}$	$\phi_{\text{PEG}}$	Emulsion Type
1	1.72	9.12	0.16	0.84	Dex-in-PEG
2	3.30	8.33	0.21	0.79	Dex-in-PEG
3	4.28	8.00	0.23	0.77	Dex-in-PEG
4	5.84	7.13	0.30	0.70	Dex-in-PEG
5	9.24	4.96	0.50	0.50	Dex-in-PEG
6	10.71	4.71	0.55	0.45	Dex-in-PEG
7	11.25	4.46	0.56	0.44	Dex-in-PEG
8	11.86	4.13	0.62	0.38	PEG-in-Dex
9	13.09	4.00	0.63	0.37	PEG-in-Dex
10	13.54	3.26	0.74	0.26	PEG-in-Dex
11	16.55	1.86	0.86	0.14	PEG-in-Dex

### 5.3.3 Effect of relative volume fractions of the dextran-PEG phases on emulsions mean drop size

As it can be seen in Figure 5.14, emulsions drop size varies as a function of volume fraction of dextran and PEG phases. At point 1 where volume fraction of dextran is at the lowest ( $\phi_{\text{dextran}}$ : 0.16 and  $\phi_{\text{PEG}}$ : 0.84) there are small flocculations of drops in discrete distance with mean size of  $5.0 \pm 2.9 \mu\text{m}$ . With increasing the  $\phi_{\text{dextran}}$  in the system, emulsion drop size increased gradually and reached a maximum ( $21.3 \pm 8.6 \mu\text{m}$ ). Close to the catastrophic phase inversion point, the emulsions mean drop size falls down significantly and a bimodal drop size distribution consisting of drops with mean size of  $5.6 \pm 3.3$  and  $55.5 \pm 13.4 \mu\text{m}$  was observed. After the catastrophic phase inversion point, the mean drop size firstly increased with increasing the  $\phi_{\text{dextran}}$  and then gradually decreased to reach a minimum size ( $3.5 \pm 2.9 \mu\text{m}$ ). Figure 5.15 illustrates the variation of emulsion mean drop size as a function of increasing the  $\phi_{\text{dextran}}$  in the system.

**Figure 5.15.** Variation of initial mean drop diameter versus the volume fraction of dextran-rich phase  $\phi_{\text{dex}}$  in emulsions stabilised by 1 wt.% of P16: P<sub>11</sub>-B<sub>60</sub>-D<sub>64</sub> at pH 6. Emulsions were prepared via two hours emulsification at 500 rpm at room temperature. Drop size was determined immediately after preparation of emulsions. The vertical dashed line indicates the point of catastrophic phase inversion from dextran-in-PEG (at low  $\phi_{\text{dex}}$ ) to PEG-in-dextran (at high  $\phi_{\text{dex}}$ ). The vertical solid line connecting two data points indicates a bimodal drop size distribution with peaks at 5.6 and 55.5  $\mu\text{m}$ .

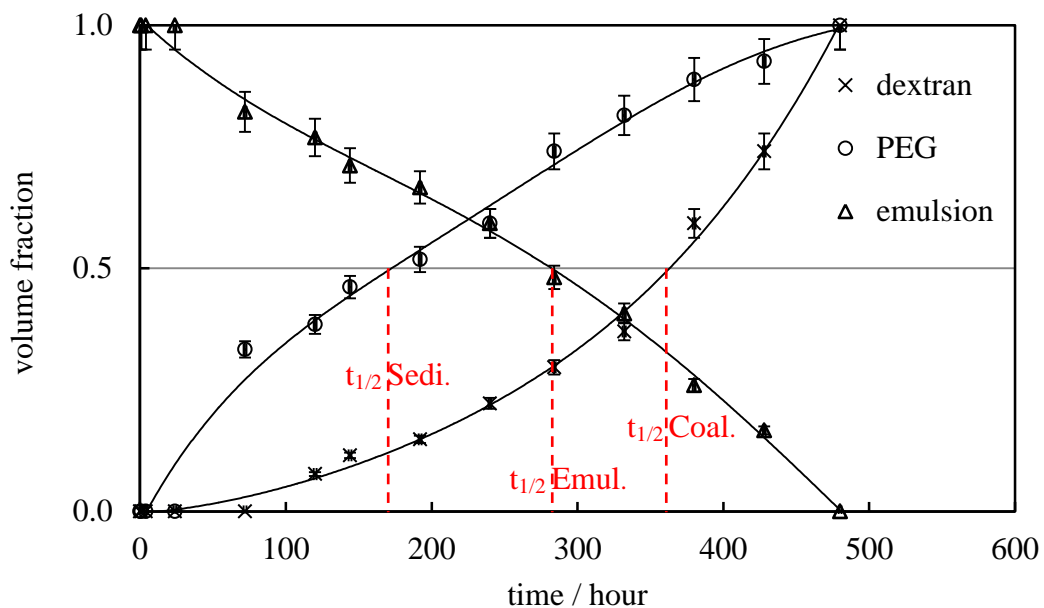


#### 5.3.4 Effect of relative volume fractions of the dextran-PEG phases on emulsion stability

The emulsions stability was assessed by recording the volume fractions of resolved PEG (upper, less dense) and dextran (lower, denser) phases and unresolved emulsion as a function of time. For emulsions of the dextran-in-PEG type, the resolution of the less dense PEG-rich phase occurs as a result of sedimentation of the emulsion drops of the denser dextran-rich phase. The resolution of the dextran-rich phase occurs as a result of coalescence of the emulsion drops of the dextran-rich phase. In contrary, for a PEG-in-dextran type of emulsion, the resolution of the PEG rich phase occurs as a result of coalescence of the emulsion drops, while the resolving of dextran rich phase is due to creaming of PEG rich dispersed phase. Half-lives of coalescence, creaming or sedimentation and emulsion, namely,  $t_{1/2}$

coalescence,  $t_{1/2}$  creaming or sedimentation and  $t_{1/2}$  emulsion, were obtained by plotting the recorded volume fractions of dextran rich phase, PEG rich phase in the case of dextran-in-PEG type of emulsion (in the case of PEG-in-dextran emulsion, resolved PEG and dextran rich phases were recorded respectively) and emulsion region versus time respectively, where the corresponding regions reach to half of their initial volumes fractions. Figure 5.16 illustrates a typical graph of variation of each region over time and determination of the corresponding half-lives.

**Figure 5.16.** Determination of  $t_{1/2}$  coalescence,  $t_{1/2}$  sedimentation and  $t_{1/2}$  emulsion based on resolved volume fractions of dextran, PEG and remaining emulsion region over time, respectively. Emulsions were prepared by emulsifying a mixture of dextran-PEG ATPS with 0.5: 0.5 volume fractions stabilised by 1 wt.% P19: P<sub>4</sub>-B<sub>65</sub>-D<sub>84</sub> terpolymer at room temperature for duration of two hours at 500 rpm. Emulsion type is dextran-in-PEG. The curved best fit solid lines are guides for the eye and the red vertical dashed lines indicate the  $t_{1/2}$ s of sedimentation, coalescence and emulsion.



The stability of the emulsions containing 1 wt.% P16: P<sub>11</sub>-B<sub>60</sub>-D<sub>64</sub> with respect to  $t_{1/2}$  coalescence,  $t_{1/2}$  creaming and  $t_{1/2}$  emulsion was monitored over time, as function of dextran volume fraction in the system. It was found that the emulsion stability varies as a function of  $\phi_{dex}$ . A slight maximum was observed close to the phase inversion point where the drop size also decreased significantly. Figure 5.17 shows the variation of emulsion stability by plotting the obtained  $t_{1/2}$  coalescence of

emulsions over the  $\phi_{\text{dex}}$ . The observed mean initial drop diameter and stability parameters of emulsions containing 1 wt.% P16: P<sub>11</sub>-B<sub>60</sub>-D<sub>64</sub> with varied volume fractions of dextran-PEG are summarised in Table 5.2.

It is known that in surfactant-stabilised emulsions, the catastrophic phase inversion is associated with hysteresis and with the formation of multiple emulsions where emulsion drops increase in size and become less stable as the inversion point is approached.<sup>8</sup> In case of particle-stabilized emulsions, no hysteresis is normally observed and there is some increase in drop size at inversion point where a maximum stability with respect to sedimentation/creaming occurs.<sup>9</sup>

**Figure 5.17.** Variation of half-life for drop coalescence versus the volume fraction of dextran rich phase in emulsions with dextran-PEG composition varied along tie-line F and stabilised by 1 wt.% of P<sub>11</sub>-B<sub>60</sub>-D<sub>64</sub> at pH 6. Emulsions were prepared via two hours emulsification at 500 rpm at room temperature. Emulsions were kept at room temperature during their assessment. The vertical dashed line indicates the point of catastrophic phase inversion from dextran-in-PEG to PEG-in-dextran.

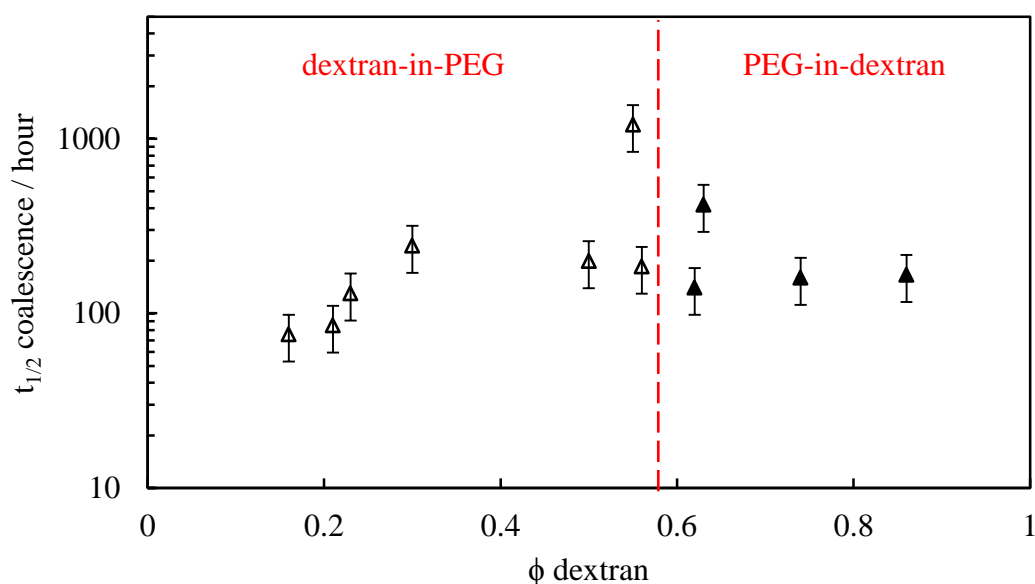


**Table 5.2.** Summary of phase volume fractions, emulsion type, stability parameters and droplet sizes for emulsions formed from aqueous two phase systems containing 1 wt.% of P<sub>11</sub>-B<sub>60</sub>-D<sub>64</sub> at pH 6 and different volume fractions of the dextran- and PEG-rich phases along tie-line F.

Tie-line F							
Point	$\phi_{\text{dex}}$	$\phi_{\text{PEG}}$	Emulsion Type	$t_{1/2}$ Coal. (hour)	$t_{1/2}$ Crea. or Sed. (hour)	$t_{1/2}$ Emul. (hour)	Mean drop diameter ( $\mu\text{m}$ )
1	0.16	0.84	d/p	75.5	5	8	$5.0 \pm 2.9$
2	0.21	0.79	d/p	85	11	13.5	$14.3 \pm 6.3$
3	0.23	0.77	d/p	130	400	370	$15.0 \pm 5.6$
4	0.30	0.70	d/p	244	32	58	$16.3 \pm 4.9$
5	0.50	0.50	d/p	199	68	120	$21.3 \pm 8.6$
6	0.55	0.45	d/p	1200	1030	1150	$17.7 \pm 5.6$
7	0.56	0.44	d/p	185	235	200	$6.0 \pm 4.7$
8	0.62	0.38	p/d	140	153	153	$5.6 \pm 3.3$ $55.5 \pm 13.4$
9	0.63	0.37	p/d	418	280	350	$16.4 \pm 5.6$
10	0.74	0.26	p/d	160	132	144	$8.5 \pm 4.8$
11	0.86	0.14	p/d	166	128	132	$3.5 \pm 2.9$

### 5.3.5 Effect of shifting to a higher tie-line in dextran-PEG ATPS phase diagram on emulsion stability and type

Different compositions of dextran-PEG ATPS with varied volume fractions of both phases along a higher tie-line of dextran-PEG phase diagram, namely tie-line G (see Figure 5.13), were attempted to be stabilised using the same terpolymer (P16: P<sub>11</sub>-B<sub>60</sub>-D<sub>64</sub>) which was used for stabilisation of dextran-PEG ATPSs on tie line F. The prepared ATPSs on this tie-line have a higher viscosity as a higher mass of dextran and PEG polymers were used for their preparation. Shifting to a higher tie-line provides ATPS systems with larger interfacial tension, which is expected to enhance the adsorption of terpolymers at the interface. Table 5.3 illustrates the summary results of emulsion characteristics in terms of the stability parameter and drop size. Comparing the  $t_{1/2}$  of emulsions drop coalescence versus dextran-rich phase volume fraction, for ATPS systems along tie-line F and G, showed that the stability of emulsions significantly increases (about 10 times in logarithmic scale) by

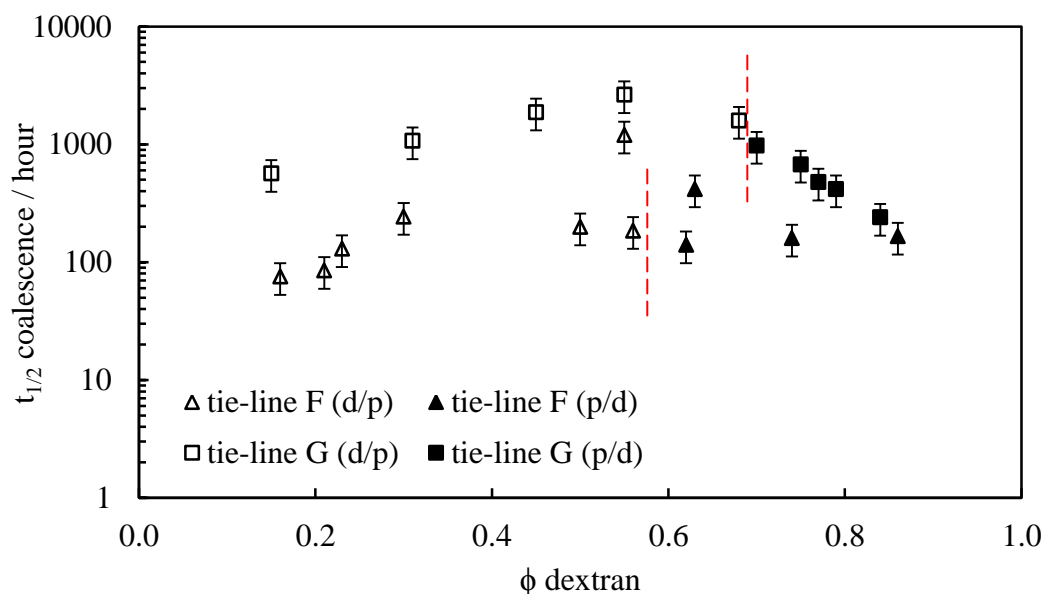
shifting the dextran-PEG ATPS composition from tie-line F to tie-line G (see Figure 5.18) In addition, the size of the droplets of the prepared emulsions along tie-line G was considerably smaller than those on tie-line F.

**Table 5.3.** Summary of phase volume fractions, emulsion type, stability parameters and droplet sizes for emulsions formed from aqueous two phase systems containing 1 wt.% of P16: P<sub>11</sub>-B<sub>60</sub>-D<sub>64</sub> at pH 6 and different volume fractions of the dextran- and PEG-rich phases along tie-line G.

Tie-line G							
Point	$\phi_{\text{dex}}$	$\phi_{\text{PEG}}$	Emulsion Type	$t_{1/2}$ Coal. (hour)	$t_{1/2}$ Crea. or Sed. (hour)	$t_{1/2}$ Emul. (hour)	Mean drop diameter ( $\mu\text{m}$ )
1	0.15	0.85	d/p	566	38	60	$1.3 \pm 1.1$
2	0.31	0.69	d/p	1071	139	170	$3.2 \pm 2.9$
3	0.45	0.55	d/p	1875	250	375	$6.5 \pm 5.1$
4	0.55	0.45	d/p	2633	345	626	$7.8 \pm 4.9$
5	0.68	0.32	d/p	1594	567	986	$5.3 \pm 8.1$
6	0.70	0.30	p/d	979	841	939	$18.7 \pm 7.6$ $3.9 \pm 2.7$
7	0.75	0.25	p/d	677	292	248	$3.2 \pm 2.4$
8	0.77	0.23	p/d	478	174	174	$2.8 \pm 2.2$
9	0.79	0.21	p/d	418	280	350	$2.1 \pm 1.4$
10	0.84	0.06	p/d	240	24	72	$1.5 \pm 0.9$

The longer stability of the prepared emulsions on tie-line G might arise from the higher viscosity of the systems which prevent from creaming or sedimentation of the drops. In addition, as mentioned before, ATPS systems along tie-tine G possess larger interfacial tensions which enhance the adsorption of terpolymers at the interface.

**Figure 5.18.** Variation of  $t_{1/2}$  of drop coalescence versus the volume fraction of dextran rich phase along tie-line F and G in emulsions stabilised by 1 wt.% of P16: P<sub>11</sub>-B<sub>60</sub>-D<sub>64</sub> at pH 6. Emulsions were prepared via two hours emulsification at 500 rpm at room temperature. Emulsions were kept at room temperature during their assessment. The vertical dashed lines indicate the point of catastrophic phase inversion from dextran-in-PEG to PEG-in-dextran.



### 5.3.6 Effect of terpolymer composition on emulsion stability

ATPSs consisting of 9.24 wt.% dextran and 4.96 wt.% PEG with equal volume fractions were attempted to stabilise by all the 38 synthesised terpolymers of varying compositions and block lengths. The stabilities of the emulsions were assessed by recording the fractional resolution of the dextran- and PEG-rich phases and remaining emulsion region from the emulsions as a function of time (as explained in previous section). Table 5.4 illustrates the obtained  $t_{1/2}$  of coalescence, sedimentation and emulsion for emulsions containing equal volume fractions of dextran and PEG phases which were stabilised with 1 wt.% of P<sub>x</sub>-B<sub>y</sub>-D<sub>z</sub> terpolymers of different x, y and z block length.



**Table 5.4.** Summary of the P<sub>x</sub>-B<sub>y</sub>-D<sub>z</sub> terpolymer structures, emulsion type and stability parameters in emulsions formed from aqueous two phase systems containing 9.24 wt.% dextran, 4.96 wt.% PEG (giving equal volumes of dextran-rich and PEG-rich phases) and 1 wt.% of P<sub>x</sub>-B<sub>y</sub>-D<sub>z</sub> at pH 6.

No.	Polymer Structure	M <sub>n</sub> g/mol	Emul. type	t <sub>1/2</sub> Coal. hours	t <sub>1/2</sub> Sedi. hours	t <sub>1/2</sub> Emul. hours	t <sub>sep.</sub> hours
1	P <sub>16</sub> -B <sub>32</sub> -D <sub>39</sub>	14000	d/p	0.38	0.12	0.31	0.5
2	P <sub>19</sub> -B <sub>49</sub> -D <sub>55</sub>	18800	d/p	40	19.5	28	42
3	P <sub>18</sub> -B <sub>66</sub> -D <sub>48</sub>	19800	d/p	96	41	73	120
4	P <sub>23</sub> -B <sub>40</sub> -D <sub>33</sub>	16000	d/p	1	0.3	0.4	0.5
5	P <sub>41</sub> -B <sub>56</sub> -D <sub>32</sub>	22000	d/p	0.045	0.04	0.04	0.25
6	P <sub>8</sub> -B <sub>45</sub> -D <sub>53</sub>	15300	d/p	75	43	60.5	96
7	P <sub>22</sub> -B <sub>44</sub> -D <sub>60</sub>	19300	d/p	114	90	108	144
8	P <sub>8</sub> -B <sub>38</sub> -D <sub>19</sub>	9800	d/p	0.385	0.1	0.28	0.5
9	P <sub>28</sub> -B <sub>49</sub> -D <sub>25</sub>	17900	d/p	0.13	0.03	0.065	1
10	P <sub>27</sub> -B <sub>54</sub> -D <sub>14</sub>	16800	d/p	0.15	1	0.36	0.5
11	P <sub>14</sub> -B <sub>29</sub> -D <sub>17</sub>	9100	d/p	0.64	0.19	0.33	1
12	P <sub>13</sub> -B <sub>34</sub> -D <sub>24</sub>	11300	d/p	1.41	0.5	0.85	1
13	P <sub>10</sub> -B <sub>33</sub> -D <sub>27</sub>	10700	d/p	1.42	0.75	1.25	2
14	P <sub>8</sub> -B <sub>32</sub> -D <sub>28</sub>	10000	d/p	2.34	1.22	1.64	2
15	P <sub>7</sub> -B <sub>33</sub> -D <sub>33</sub>	10600	d/p	15.8	7.2	10.5	20
16	P <sub>11</sub> -B <sub>60</sub> -D <sub>64</sub>	17800	d/p	199	68	120	200
17	P <sub>4</sub> -B <sub>30</sub> -D <sub>34</sub>	9400	d/p	68	41	55	75
18	P <sub>8</sub> -B <sub>91</sub> -D <sub>114</sub>	28500	d/p	2.5	46.5	35	72
19	P <sub>4</sub> -B <sub>65</sub> -D <sub>84</sub>	20600	d/p	360	175	271	480
20	P <sub>2</sub> -B <sub>13</sub> -D <sub>10</sub>	3400	d/p	0.014	0.046	0.035	0.16
21	P <sub>3</sub> -B <sub>21</sub> -D <sub>15</sub>	5700	d/p	0.024	0.048	0.04	0.16
22	P <sub>4</sub> -B <sub>26</sub> -D <sub>19</sub>	7200	d/p	0.016	0.45	0.39	0.16
23	P <sub>5</sub> -B <sub>34</sub> -D <sub>22</sub>	9100	d/p	0.48	0.28	0.36	1
24	P <sub>6</sub> -B <sub>41</sub> -D <sub>28</sub>	11300	d/p	2.05	2.5	2.4	5
25	P <sub>7</sub> -B <sub>48</sub> -D <sub>33</sub>	13000	d/p	4	3.4	3.7	6
26	P <sub>7</sub> -B <sub>51</sub> -D <sub>39</sub>	14300	d/p	4.2	3.8	4.05	7
27	P <sub>4</sub> -B <sub>18</sub> -D <sub>17</sub>	5900	d/p	0.066	0.033	0.05	0.33
28	P <sub>6</sub> -B <sub>36</sub> -D <sub>32</sub>	11300	d/p	0.34	0.1	0.21	0.75
29	P <sub>9</sub> -B <sub>47</sub> -D <sub>47</sub>	15700	d/p	35.5	24	30	72
30	P <sub>12</sub> -B <sub>60</sub> -D <sub>62</sub>	20400	d/p	60	22.5	48	96
31	P <sub>14</sub> -B <sub>70</sub> -D <sub>73</sub>	23500	d/p	658	616	638	912
32	P <sub>15</sub> -B <sub>80</sub> -D <sub>85</sub>	26300	d/p	>5800	3800	>5800	>5800
33	P <sub>13</sub> -B <sub>52</sub> -D <sub>35</sub>	14600	d/p	370	60	200	456
34	P <sub>13</sub> -B <sub>65</sub> -D <sub>38</sub>	17300	d/p	430	100	330	576

No.	Polymer Structure	M <sub>n</sub> g/mol	Emul. type	t <sub>1/2</sub> Coal. hours	t <sub>1/2</sub> Sedi. hours	t <sub>1/2</sub> Emul. hours	t <sub>sep.</sub> hours
35	P <sub>13</sub> -B <sub>67</sub> -D <sub>36</sub>	17200	d/p	380	50	200	456
36	P <sub>13</sub> -B <sub>76</sub> -D <sub>40</sub>	19300	d/p	330	50	110	432
37	P <sub>11</sub> -B <sub>58</sub> -D <sub>36</sub>	15300	d/p	82	26	58	360
38	P <sub>14</sub> -B <sub>81</sub> -D <sub>43</sub>	20400	d/p	3290	800	2000	>3600

By plotting the t<sub>1/2</sub> of coalescence, sedimentation or emulsion versus the polymer compositional variation, the following results were obtained:

By plotting the stability of emulsions in terms of their t<sub>1/2</sub> of drop coalescence versus the length of PEGMA block, two different trends in contrary were observed as can be seen in Figure 5.19. Terpolymers with PEGMA blocks consisting of less than 15 repeated units (or degree of polymerisation) showed an increase in emulsion stability by increasing the PEGMA length. Oppositely, in case of terpolymers with more than 15 PEGMA units in their chain, increasing the PEGMA content resulted in less stability of the emulsions over time. Similar result was obtained when t<sub>1/2</sub> of sedimentation or t<sub>1/2</sub> of emulsion was plotted over PEGMA length (see Appendix). More specifically, by comparing P25: P<sub>7</sub>-B<sub>48</sub>-D<sub>33</sub>, P33: P<sub>13</sub>-B<sub>52</sub>-D<sub>35</sub> and P5: P<sub>41</sub>-B<sub>56</sub>-D<sub>32</sub> with relatively constant BuMA and DMAEMA block but increasing PEGMA block length (see Figure 5.20), the half-lives of emulsion drop coalescence is first increase from 4 to 370 hours for P25 and P33 and then drops down for P5 with longest PEGMA chain to a few minutes. Overall, maximum emulsion stability was observed for terpolymers with 13-15 PEGMA repeated units in their chain.

**Figure 5.19.** Variation of  $t_{1/2}$  for dextran phase resolution (resulting from drop coalescence) with the PEGMA block length for terpolymers at equal volume fractions of dextran-PEG phases. Emulsions were prepared via two hours stirring at 500 rpm at pH 6.

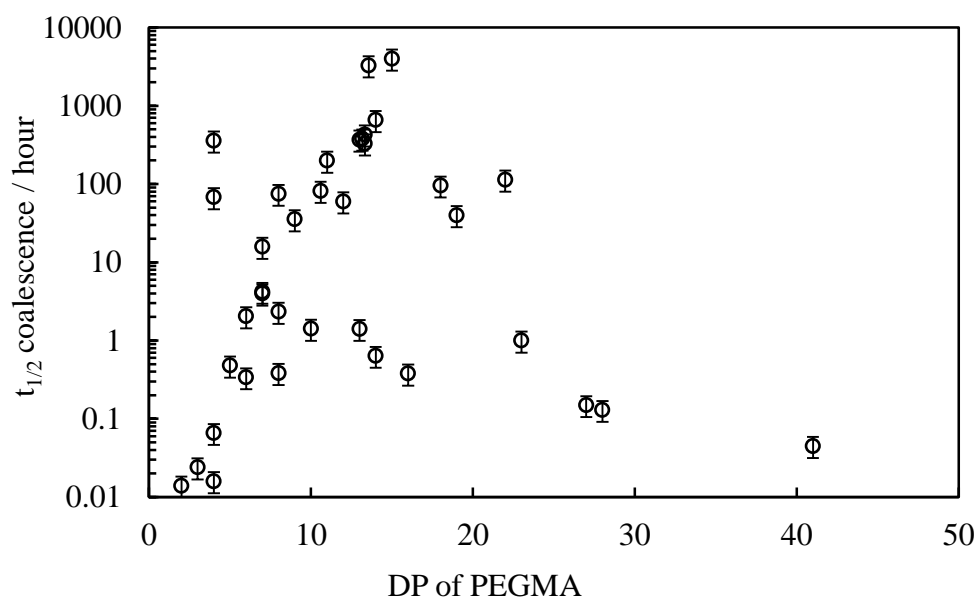
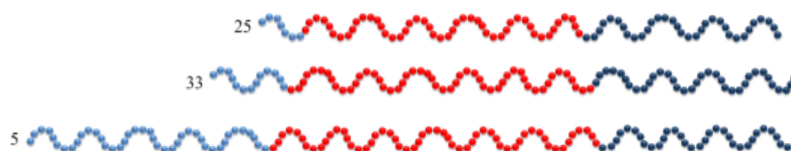


**Figure 5.20.** Schematic presentation of P25: P<sub>7</sub>-B<sub>48</sub>-D<sub>33</sub>, P33: P<sub>13</sub>-B<sub>52</sub>-D<sub>35</sub> and P5: P<sub>41</sub>-B<sub>56</sub>-D<sub>32</sub> with relatively constant BuMA and DMAEMA block but increasing PEGMA block length.



Plotting the stability of emulsions in terms of their  $t_{1/2}$  of drop coalescence versus the length of hydrophobic BuMA block, showed the drop coalescence stability increases with increasing hydrophobic BuMA block length (See Figure 5.21). Similar result was obtained when  $t_{1/2}$  of sedimentation or  $t_{1/2}$  of emulsion was plotted over BuMA length (see Appendix). More specifically, comparing P33: P<sub>13</sub>-B<sub>52</sub>-D<sub>35</sub> and P34: P<sub>13</sub>-B<sub>65</sub>-D<sub>38</sub> terpolymers with relatively constant hydrophilic PEGMA and DMAEMA blocks but increasing BuMA block length (see Figure 5.22), the  $t_{1/2}$  of drop coalescence increases 60 hours by addition of 13 more BuMA unites in terpolymer structure. This is presumably due to increased cohesion within the stabilising polymer film driven by hydrophobic attraction. Maximum stability

(corresponding to a  $t_{1/2}$  coalescence value of about 6000 hours or about 8 months) is seen for a BuMA block length of about 80 repeated units.

**Figure 5.21.** Variation of  $t_{1/2}$  for dextran phase resolution (resulting from drop coalescence) with the BuMA block length for terpolymers at equal volume fractions of dextran-PEG phases. Emulsions were prepared via two hours stirring at 500 rpm at pH 6.

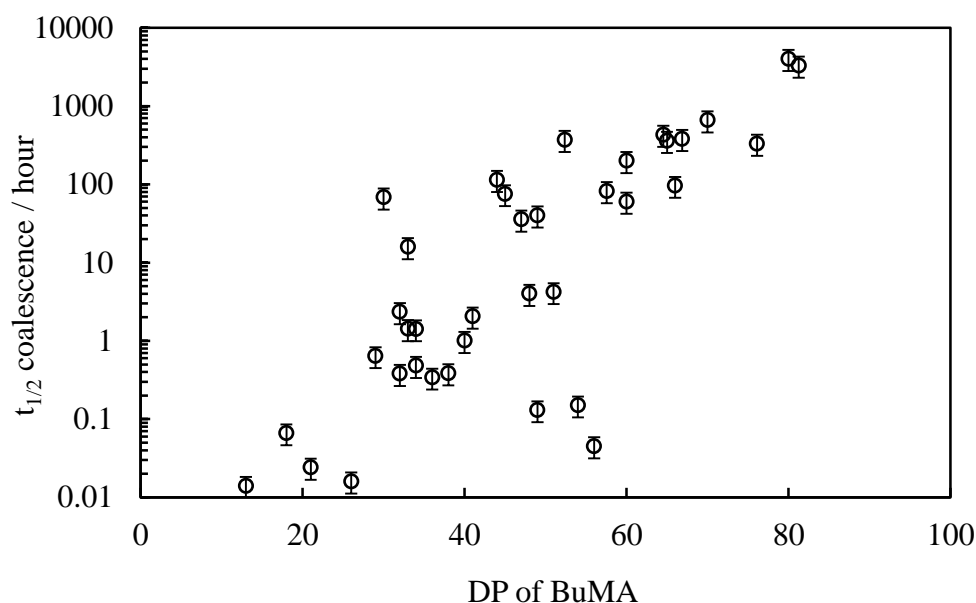


**Figure 5.22.** Schematic presentation of P33: P<sub>13</sub>-B<sub>52</sub>-D<sub>35</sub> and P34: P<sub>13</sub>-B<sub>65</sub>-D<sub>38</sub> with relatively constant PEGMA and DMAEMA block but increasing BuMA block length.



Plotting the stability of emulsions in terms of their  $t_{1/2}$  of drop coalescence versus the length of DMAEMA block, showed a similar result to that of the BuMA block. As it can be seen in Figure 5.23, the drop coalescence stability increased with increasing the DMAEMA block length. Same result was obtained when  $t_{1/2}$  of sedimentation or  $t_{1/2}$  of emulsion was plotted over DMAEMA length (see Appendix). More specifically, comparing P35: P<sub>13</sub>-B<sub>67</sub>-D<sub>36</sub> and P31: P<sub>14</sub>-B<sub>70</sub>-D<sub>73</sub> terpolymers with relatively constant PEGMA and BuMA blocks but increasing DMAEMA block length (see Figure 5.24), the  $t_{1/2}$  of drop coalescence increases more than 250 hours

only by addition of 37 more DMAEMA unites in terpolymer structure. This could be due to increased penetration of DMAEMA blocks into the dextran rich dispersed phase which enhances the segregation of terpolymers block at the dextran-PEG interface. Maximum stability (corresponding to a  $t_{1/2}$  coal. value of about 6000 hours or about 8 months) is seen for a DMAEMA block length of about 85 repeated units. However, it should be noted that too long DMAEMA chain causes the gelation of w/w emulsions due to the entanglement of DMAEMA chains. This was observed when P18:P<sub>8</sub>-B<sub>91</sub>-D<sub>114</sub> terpolymer, with longest DMAEMA chain among the whole terpolymers series, was used for the stabilisation of emulsion. Although the emulsion turned into a gel-like mixture, it was less stable than the emulsions stabilised by terpolymers containing fewer DMAEMA units.

**Figure 5.23.** Variation of  $t_{1/2}$  for dextran phase resolution (resulting from drop coalescence) with the DMAEMA block length for terpolymers at equal volume fractions of dextran-PEG phases. Emulsions were prepared via two hours stirring at 500 rpm at pH 6.

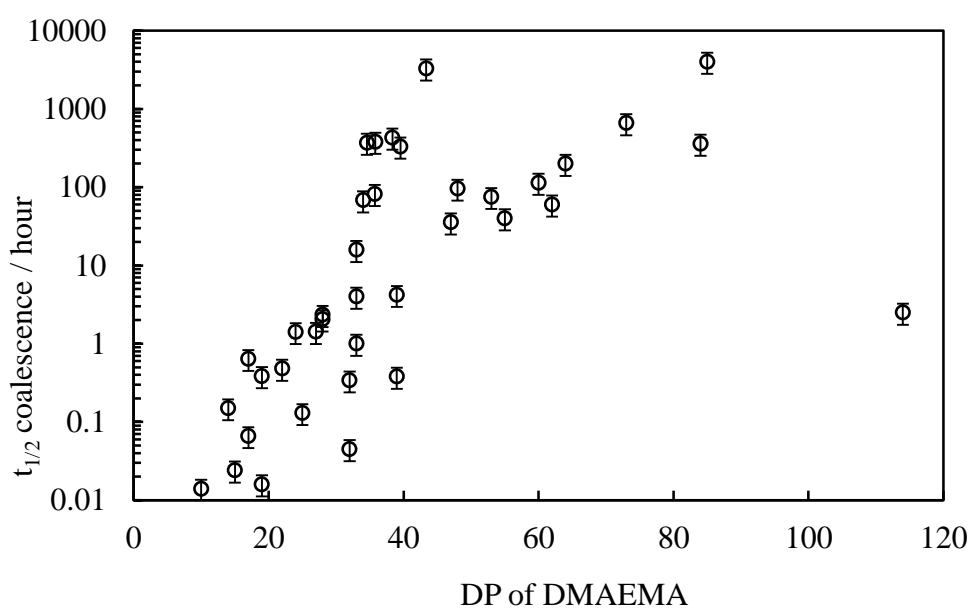
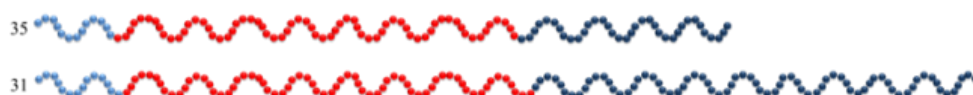


**Figure 5.24.** Schematic presentation of P35: P<sub>13</sub>-B<sub>67</sub>-D<sub>36</sub> and P31: P<sub>14</sub>-B<sub>70</sub>-D<sub>73</sub> with relatively constant PEGMA and BuMA block but increasing DMAEMA block length.



In order to find out the optimum PEGMA/DMAEMA block ratio,  $t_{1/2}$  of drop coalescence of the emulsions was plotted over PEGMA/DMAEMA ratio. As can be seen in Figure 5.25 no specific trend in stability of emulsions is observed for terpolymers with PEGMA/DMAEMA block ratio less than 0.5. By increasing the PEGMA/DMAEMA ratio over 0.5 in terpolymers, it seems that the ability to stabilise dextran-PEG ATPS decreases dramatically and reaches to a minimum. For instance, comparing P10: P<sub>27</sub>-B<sub>54</sub>-D<sub>14</sub> and P26: P<sub>7</sub>-B<sub>51</sub>-D<sub>39</sub> with relatively constant hydrophobic BuMA blocks and similar total degree of polymerisation, but varied PEGMA/DMAEMA block ratio of 1.92 to 0.18, the  $t_{1/2}$  of emulsion drop coalescence increases from 0.15 to 4.2 hours (see Figure 5.26).

**Figure 5.25.** Variation of  $t_{1/2}$  for dextran phase resolution (resulting from drop coalescence) with the PEGMA/DMAEMA block ratio for terpolymers at equal volume fractions of dextran-PEG phases. Emulsions were prepared via two hours stirring at 500 rpm at pH 6.

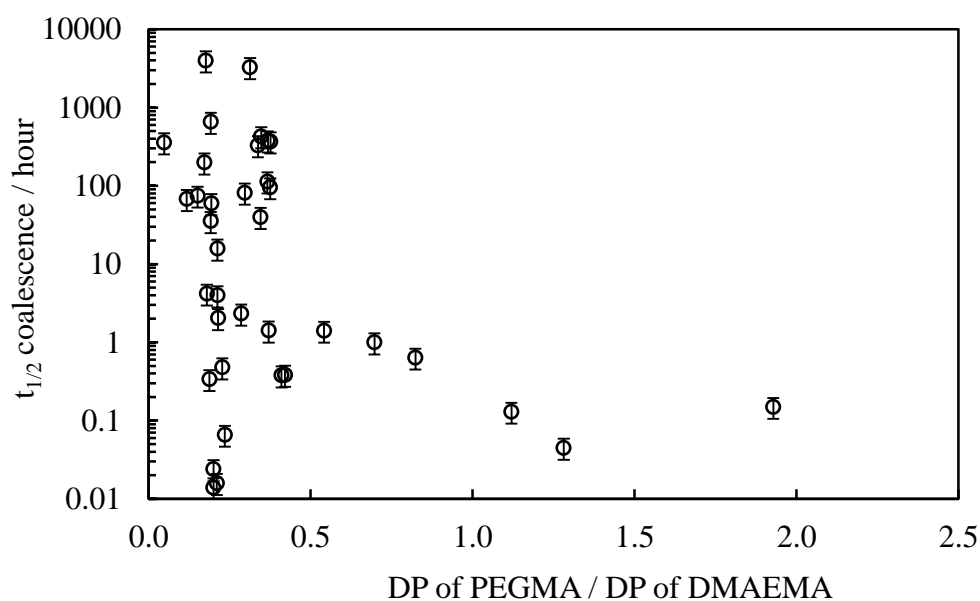
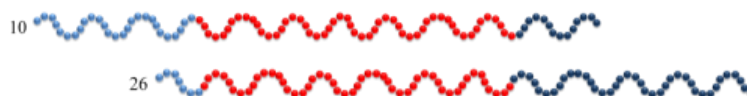


**Figure 5.26.** Schematic presentation of P10: P<sub>27</sub>-B<sub>54</sub>-D<sub>14</sub> and P26: P<sub>7</sub>-B<sub>51</sub>-D<sub>39</sub> with relatively constant BuMA block but decreasing PEGMA/DMAEMA block ratio.



### 5.3.7 Effect of terpolymer molecular weight on emulsion stability

The variation of  $t_{1/2}$  of drop coalescence with the  $M_n$  of terpolymers at a constant composition showed a linear increase with increasing the molecular weight of terpolymers. This trend was observed when the  $t_{1/2}$  of drop coalescence of P27: P<sub>4</sub>-B<sub>18</sub>-D<sub>17</sub>, P28: P<sub>6</sub>-B<sub>36</sub>-D<sub>32</sub>, P29: P<sub>9</sub>-B<sub>47</sub>-D<sub>47</sub>, P30: P<sub>12</sub>-B<sub>60</sub>-D<sub>62</sub>, P31: P<sub>14</sub>-B<sub>70</sub>-D<sub>73</sub> and P32: P<sub>15</sub>-B<sub>80</sub>-D<sub>85</sub> with same composition (PEGMA: BuMA: DMAEMA = 0.16: 0.40: 0.44) but increasing molecular weights were plotted over their  $M_n$  (see Figure 5.27 and 5.28).

**Figure 5.27.** Schematic presentation of P27: P<sub>4</sub>-B<sub>18</sub>-D<sub>17</sub>, P28: P<sub>6</sub>-B<sub>36</sub>-D<sub>32</sub>, P29: P<sub>9</sub>-B<sub>47</sub>-D<sub>47</sub>, P30: P<sub>12</sub>-B<sub>60</sub>-D<sub>62</sub>, P31: P<sub>14</sub>-B<sub>70</sub>-D<sub>73</sub> and P32: P<sub>15</sub>-B<sub>80</sub>-D<sub>85</sub>.

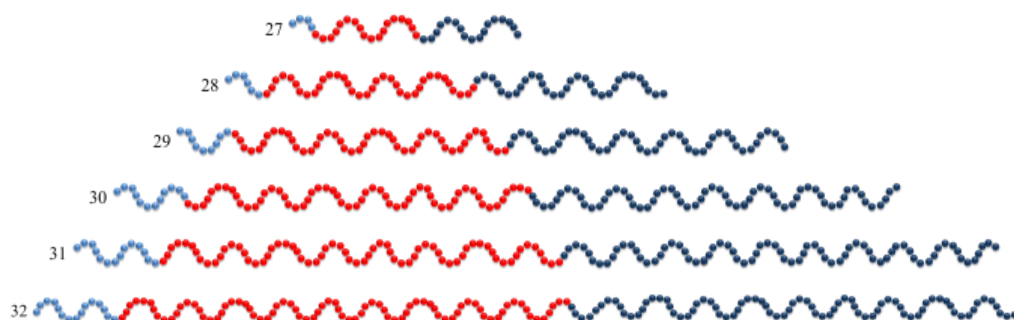
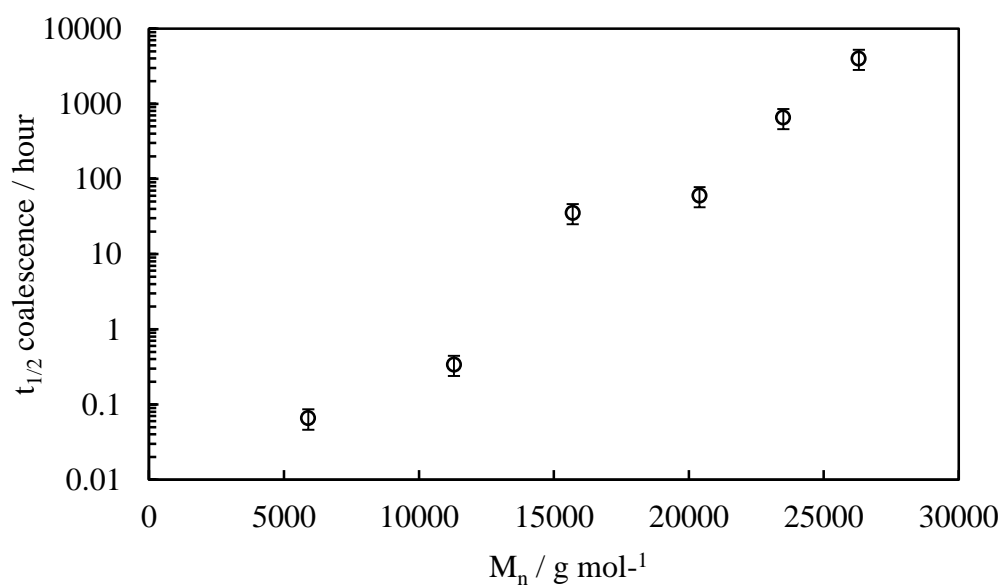
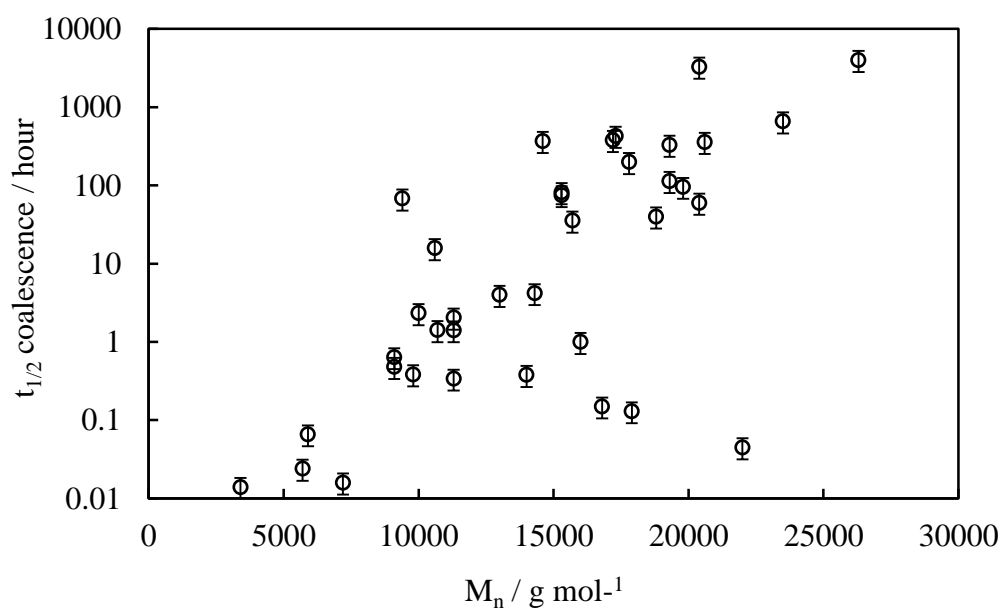


**Figure 5.28.** Variation of  $t_{1/2}$  for dextran phase resolution (resulting from drop coalescence) with the number average molecular weight of terpolymers with a constant composition, at equal volume fractions of dextran-PEG phases. Emulsions were prepared via two hours stirring at 500 rpm at pH 6.



Overall, increasing the molecular weight of terpolymers even with varied compositions resulted in an increase in the stability of the resulted emulsions (see Figure 5.29). This effect might be corresponding to the higher viscosity of the system which prevent from drop coalescence as well as reducing the sedimentation rate. However, as can be seen in this Figure, there are a number of terpolymers with quite high molecular weights which were not able to stabilise the dextran-PEG system for a long time. Therefore, in addition to the MW, the composition of terpolymers plays an important role in the stabilisation of such systems.

**Figure 5.29.** Variation of  $t_{1/2}$  for dextran phase resolution (resulting from drop coalescence) with the number average molecular weight of terpolymers, at equal volume fractions of dextran-PEG phases. Emulsions were prepared via two hours stirring at 500 rpm at pH 6.



### 5.3.8 Effect of emulsion stability on emulsion drop size

Studying the droplet size of prepared emulsions showed that the relatively stable emulsions generally form small drops with diameter of a few  $\mu\text{m}$  while in the relatively unstable ones, the emulsion drop size dramatically increases to a few tens of  $\mu\text{m}$ . For instance, as it can be seen in Figure 5.30 which shows the transmission optical micrographs taken immediately after preparation of four representative examples of the dextran in PEG emulsions, the obtained drop size for relatively stable emulsions stabilised by P31: P<sub>14</sub>-B<sub>70</sub>-D<sub>73</sub> and P16: P<sub>11</sub>-B<sub>60</sub>-D<sub>64</sub> were  $4.5 \pm 1.2$



$\mu\text{m}$  and  $5.9\pm 1.6 \mu\text{m}$  respectively, while much larger drop size  $40\pm 34 \mu\text{m}$  and  $53\pm 31 \mu\text{m}$  were observed for relatively unstable emulsions containing P28: P<sub>6</sub>-B<sub>36</sub>-D<sub>32</sub> or P27: P<sub>4</sub>-B<sub>18</sub>-D<sub>17</sub> respectively. The derived cumulative drop size distribution of these four examples is shown in Figure 5.31 for a better presentation of their overall pattern which shows the distributions are mono-modal.

**Figure 5.30.** Transmission micrographs of dextran-in-PEG emulsions containing equal volume fractions of PEG-rich and dextran-rich phases and 1 wt.% (a) P27: P<sub>4</sub>-B<sub>18</sub>-D<sub>17</sub>, (b) P28: P<sub>6</sub>-B<sub>36</sub>-D<sub>32</sub>, (c) P16: P<sub>11</sub>-B<sub>60</sub>-D<sub>64</sub> and (d) P31: P<sub>14</sub>-B<sub>70</sub>-D<sub>73</sub>. Emulsions were prepared via two hours stirring at 500 rpm at pH 6. Micrographs were taken immediately after emulsion preparation.

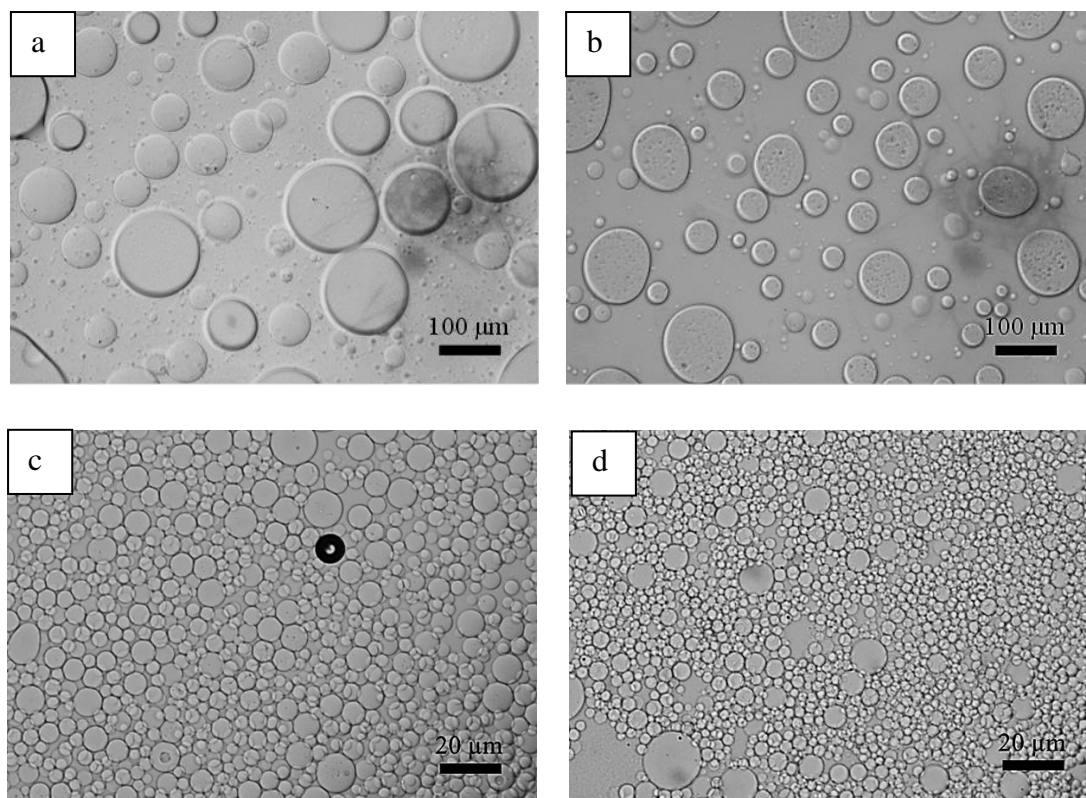
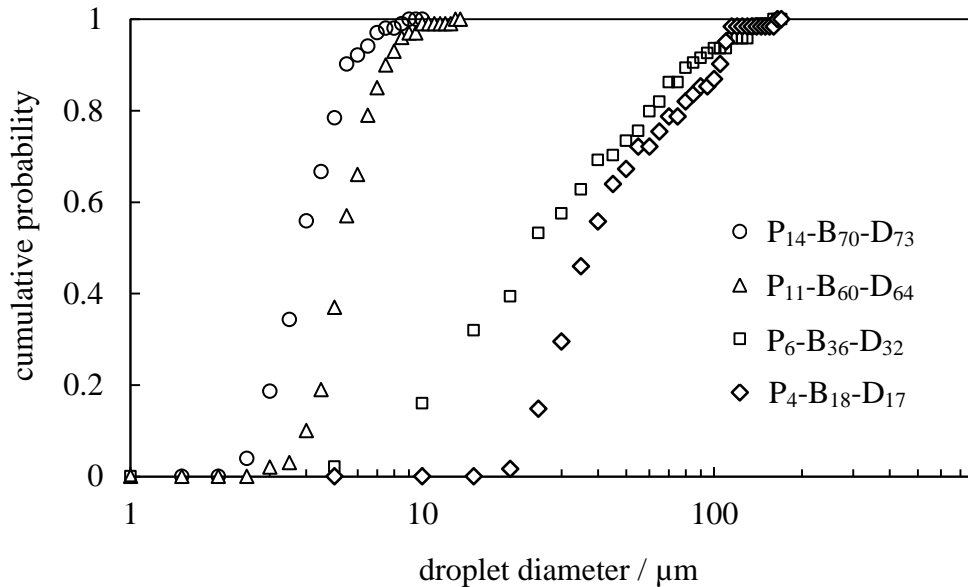


**Figure 5.31.** Initial cumulative droplet size distributions for dextran-in-PEG emulsions formed from aqueous two phase systems containing equal volume fractions of dextran and PEG plus 1 wt.% of four different  $P_x-B_y-D_z$  terpolymers (indicated in key) at pH 6. Emulsions were prepared via two hours stirring at 500 rpm.



### 5.3.9 Variation of emulsion drop size over time

The mean drop diameter of an emulsion containing equal volume fractions of dextran-PEG and 1 wt.% of P16: P<sub>11</sub>-B<sub>60</sub>-D<sub>64</sub> was measured as a function of time as shown in Figure 5.32. For this system for which  $t_{1/2}$  of drop coalescence: 199 hours,  $t_{1/2}$  drop sedimentation: 68 hours and  $t_{1/2}$  of emulsion: 120 hours, the mean drop diameter in the residual emulsion increases almost linearly from approximately 6 to 10  $\mu\text{m}$  over 290 hours. Also, over time the standard deviation of drop size increases significantly which suggesting an increase in polydispersity of the system over time as shown in Figure 5.33.

**Figure 5.32.** Transmission micrographs of emulsion consisting of equal volume fractions of dextran-PEG and 1 wt.% P16: P<sub>11</sub>-B<sub>60</sub>-D<sub>64</sub> at pH 6. Emulsion was prepared via two hours emulsification at 500 rpm. Micrographs were taken (a) 0.5, (b) 3, (c) 24, (d) 48, (e) 96, (f) 144, (g) 168, (h) 216 and (i) 288 hours after emulsion preparation.

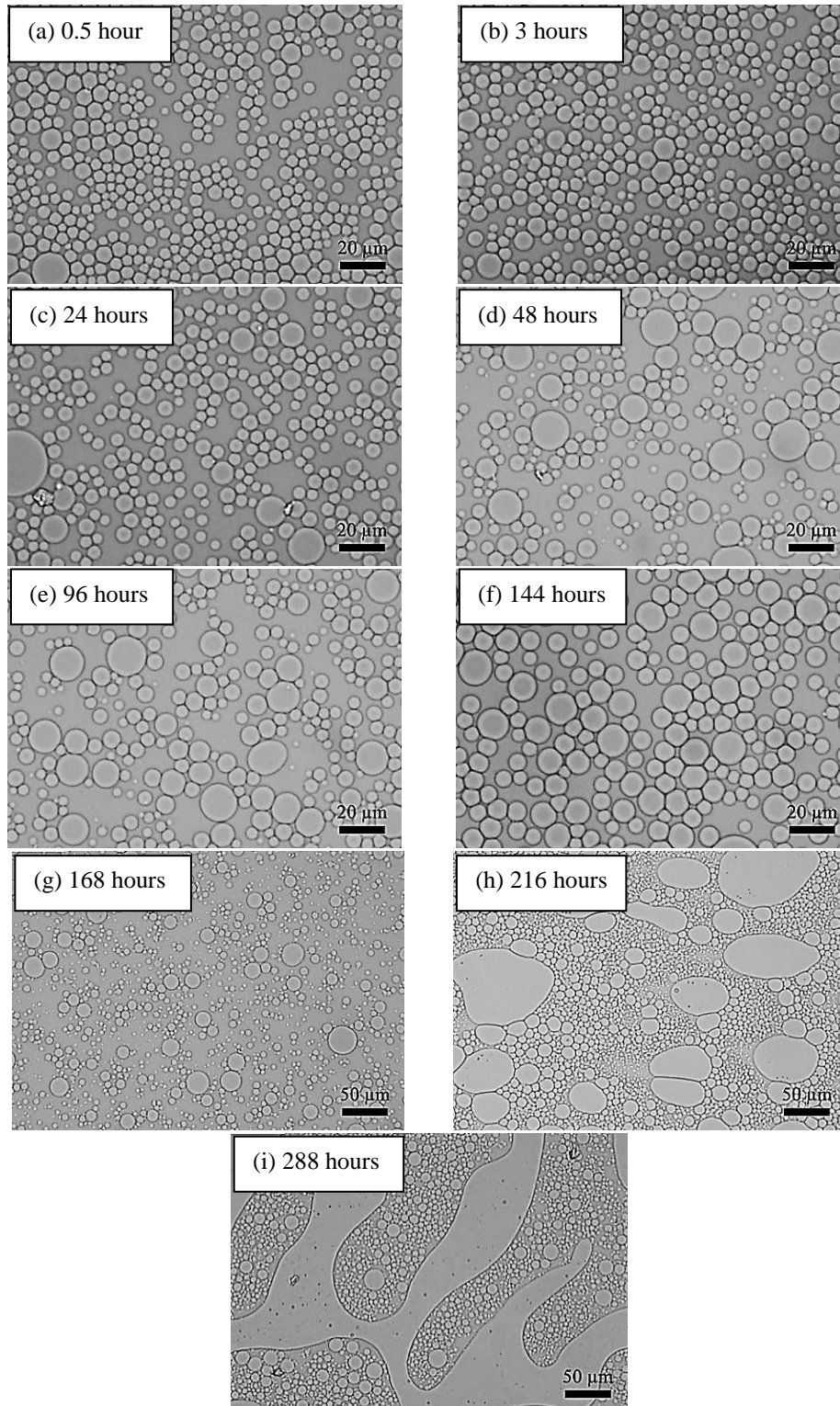
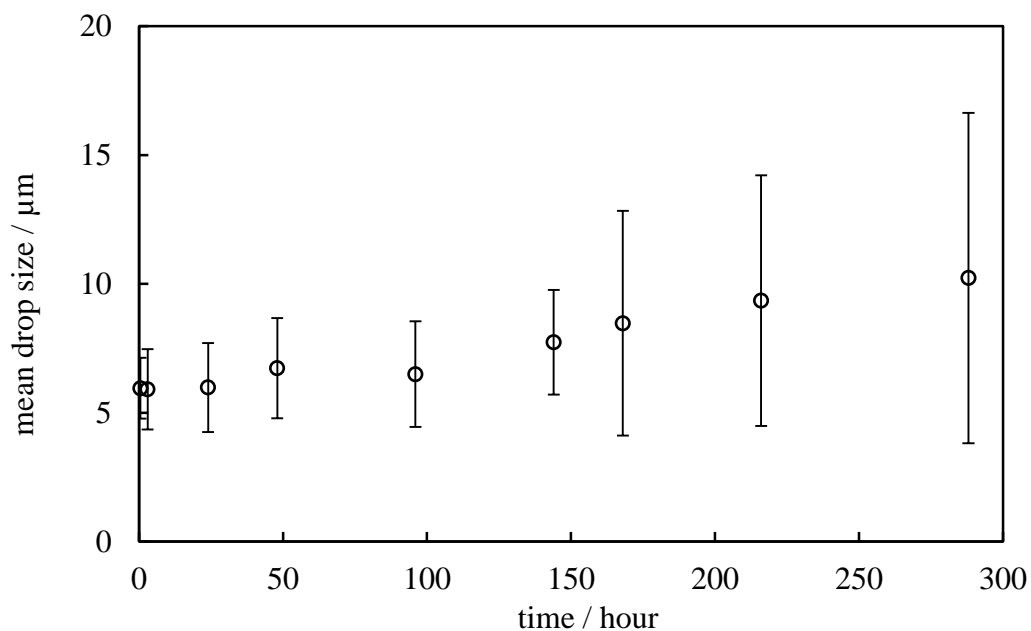


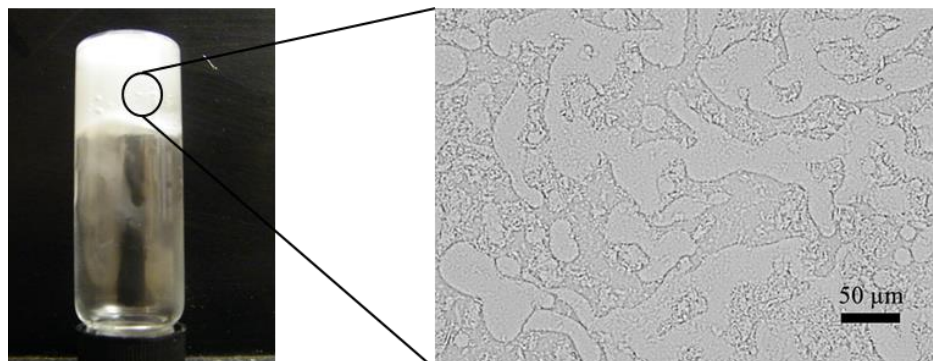
**Figure 5.33.** Variation of emulsion mean drop size over time for an emulsion with equal volume fractions of dextran-PEG and 1 wt.% P16: P<sub>11</sub>-B<sub>60</sub>-D<sub>64</sub>. Emulsion was prepared via two hours stirring at 500 rpm at pH 6. Error bars are corresponding to the standard deviations of obtained mean drop size.



### ***5.3.10 Effect of increasing terpolymer concentration on emulsions***

It was attempted to increase the concentration of terpolymers for preparation of w/w emulsions. Higher concentrations of P16: P<sub>11</sub>-B<sub>60</sub>-D<sub>63</sub>, namely, 2, 3 and 4 wt.% were attempted. But it was found out that the higher concentrations of terpolymer causes the mixtures to become viscoelastic. Emulsification yielded some emulsion drops but also regions of non-dispersed, gelled polymer solution (see Figure 5.34).

**Figure 5.34.** *left:* Camera picture taken from a gelled dextran-PEG ATPS with equal volume fractions which is containing 2 wt.% of P16: P<sub>11</sub>-B<sub>60</sub>-D<sub>63</sub> terpolymer. *Right:* corresponding transmission electron micrograph.



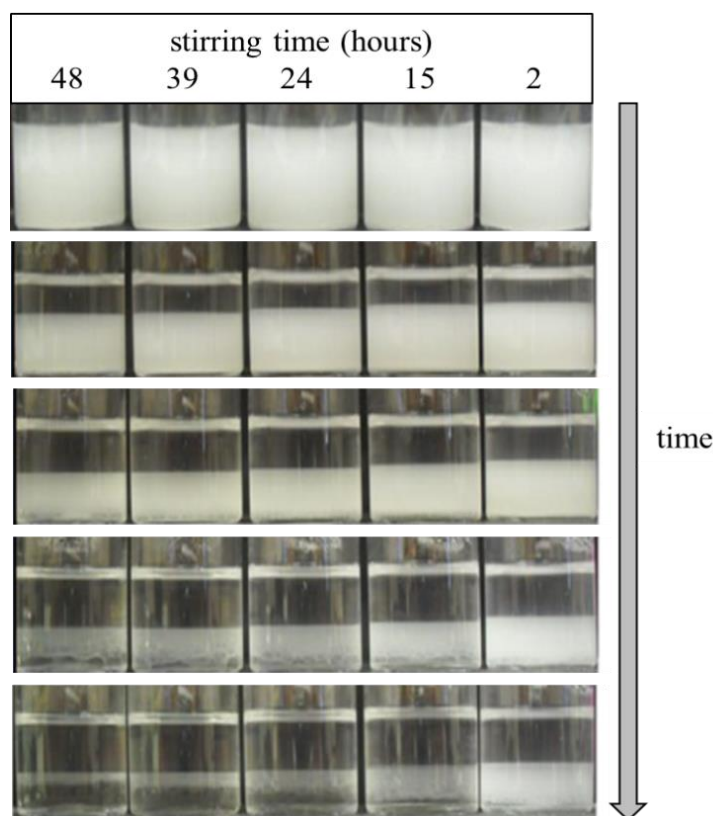
### ***5.3.11 Effect of varying pH on emulsions stability***

The pH of emulsions was varied between 4 to 7 in order to investigate the effect of pH on the stability of emulsions. At pHs greater or equal to 7 ( $\text{pH} \geq 7$ ) some of the terpolymers were insoluble in the system. It was found that the emulsions stabilities were virtually independent of pH over the range 4-6. However, the stability of emulsions varied slightly by decreasing the pH, but not a specific trend was observed. Overall, the maximum emulsion stability with respect to  $t_{1/2}$  of coalescence was observed at pH 6.

### ***5.3.12 Effect of emulsification duration and method on the stability of emulsion***

In this work, emulsions were prepared either by gentle stirring using a stirrer bar at 500 rpm for two hours or homogenisation using a homogenising head at 11000 rpm for duration of two minutes. It was found that emulsions prepared via gentle stirring are much more stable than those prepared under vigorous homogenisation. In addition, increasing the homogenisation or stirring time significantly decreases the stability of the prepared emulsions. In an experiment, a large batch of ATPS containing equal volume fractions of dextran-PEG and 1 wt.% of P3: P<sub>18</sub>-B<sub>66</sub>-D<sub>48</sub> was prepared and after pH adjustment (pH 6), the prepared mixture was divided into 5 small batches and each was stirred for a different duration of time. Figure 5.35 shows the stability behaviour of these emulsions over time.

**Figure 5.35.** Effect of stirring time on the stability of emulsions consisting of 0.5: 0.5 volume fractions of dextran-PEG and 1 wt.% of P3: P<sub>18</sub>-B<sub>66</sub>-D<sub>48</sub> at pH 6 over time. A big batch of emulsion was divided into 5 separate emulsions and each was stirred for 2, 15, 24, 39 and 48 hours respectively.



Considering that all five prepared emulsions were in the same conditions (concentration of stabiliser, pH and temperature) and the only variable was the stirring time, it can be resulted that the longer the emulsions are stirred for, the less stable they are over time. In other words, the more energy input is applied to the system the less stable it will be over time. This result is in agreement with the previous results when the stirring and homogenisation methods were compared, as the homogenisation method prepared less stable emulsions in compare to stirring method, knowing that homogenisation applies more energy to the system. The reason behind this behaviour is still unclear. However, a possible reason might be the longer time needed for terpolymers to be adsorbed at the dextran-PEG interface with a relatively low interfacial tension. Homogenisation for a short time might not provide enough time for the adsorption of terpolymers, while stirring the system for an appropriate period of time might increase the possibility of the slow adsorption of

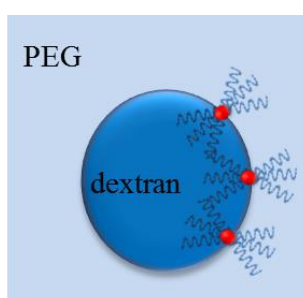
terpolymers at the interface which leads to formation of more stable emulsion. Stirring the system for longer time might result in the formation of self-assemblies (aggregations) of terpolymers in the system in equilibrium with the adsorption and desorption process of terpolymers at the interface; therefore the decreases stability of emulsions can be attributed to the presence of less free terpolymers in the system.

### 5.3.13 Effect of polymer architecture on emulsion stability

In addition to  $P_x-B_y-D_z$  terpolymers,  $P_x-B_y$  and  $B_y-D_z$  diblock copolymers were also used as stabiliser for formation of stable w/w emulsions or possibly bilayer type of polymersomes.  $P_{16}-B_{42}$  was not soluble in the system while  $B_{59}-D_{83}$  gave reasonable emulsion stabilisation ( $t_{1/2}$  coalescence: 480 hours). Although only a very limited comparison is possible, we note that the best tri-block stabiliser used here can stabilise the emulsions for more than 8 months and is considerably more effective than the  $B_{59}-D_{83}$  diblock copolymer.  $P_x-D_z$  diblock copolymers were not attempted in this work, as one of the main aims was to template w/w emulsions for polymersomes formation and one of the main features of polymersomes is their hydrophobic membrane structure.

Moreover, star polymers consisting of flexible PEGMA and DMAEMA chains and cross-linked core were synthesised in order to be used for stabilisation of dextran-PEG ATPS (see Figure 5.36). In spite of quite long PEGMA and DMAEMA chains (30 degree of polymerisation for each), the formed emulsions were very unstable and phase separated in less than a few minutes. This control experiment revealed the key role of hydrophobic BuMA block which enhances the cohesion between formed polymeric film around the emulsion drops.

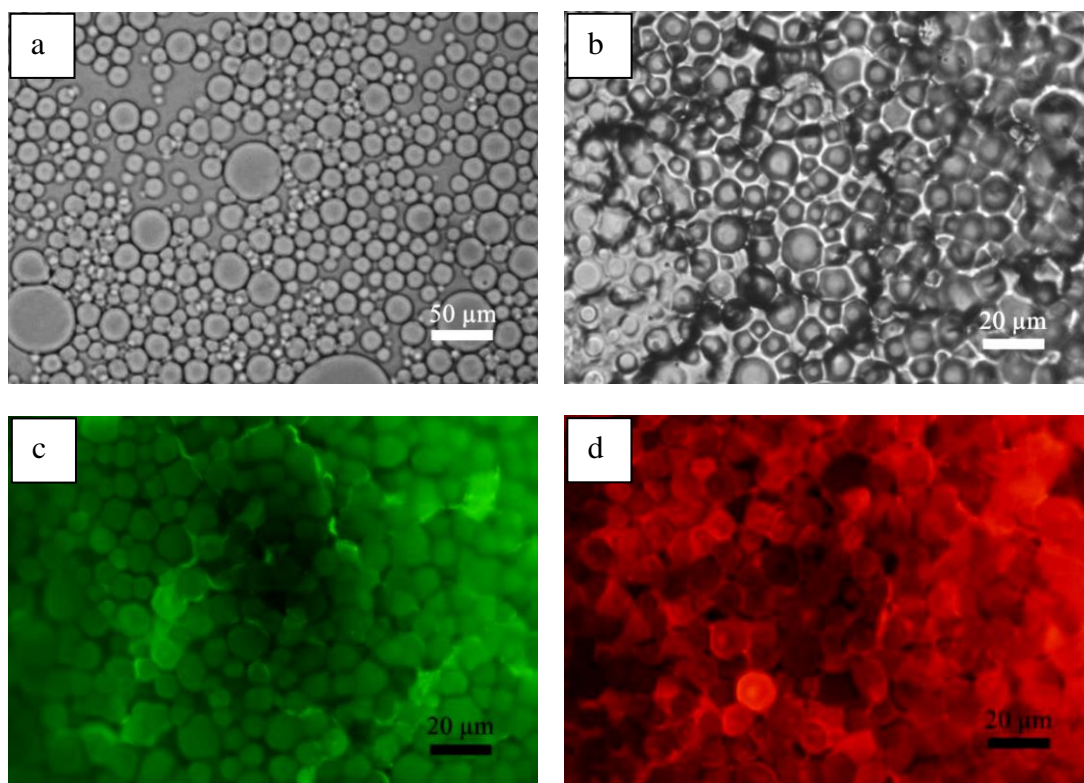
**Figure 5.36.** Schematic presentation of using PEGMA (light blue chains) and DMAEMA (dark blue chains) star polymers with cross linked core (red circles) for stabilisation of dextran-PEG ATPS.



### 5.3.14 Drying the templated polymersomes

A dextran-in-PEG emulsion containing equal volumes of dextran and PEG rich phases, rhodamine and FITC-dextran fluorescent dyes and 1 wt.% of P28: P<sub>6</sub>-B<sub>36</sub>-D<sub>32</sub> was allowed to dry out on a microscope slide. Transmission and fluorescent optical micrographs of the dried residue indicated that the polymersome-like structure is retained on drying (see Figure 5.37). However, as it can be seen, the size of the polymersomes shrank compare to that of the wet ones due to the evaporation of water.

**Figure 5.37.** Transmission and fluorescent optical micrographs of a dextran-in-PEG emulsion containing equal volume fractions of dextran and PEG rich phases, rhodamine and FITC-dextran fluorescent dyes, stabilised by 1 wt.% of P28: P<sub>6</sub>-B<sub>36</sub>-D<sub>32</sub> (a) before drying, (b), (c) and (d) after drying. Note that no cover slip was used for microscopy sample preparation, therefore drop sizes are smaller than those reported before.



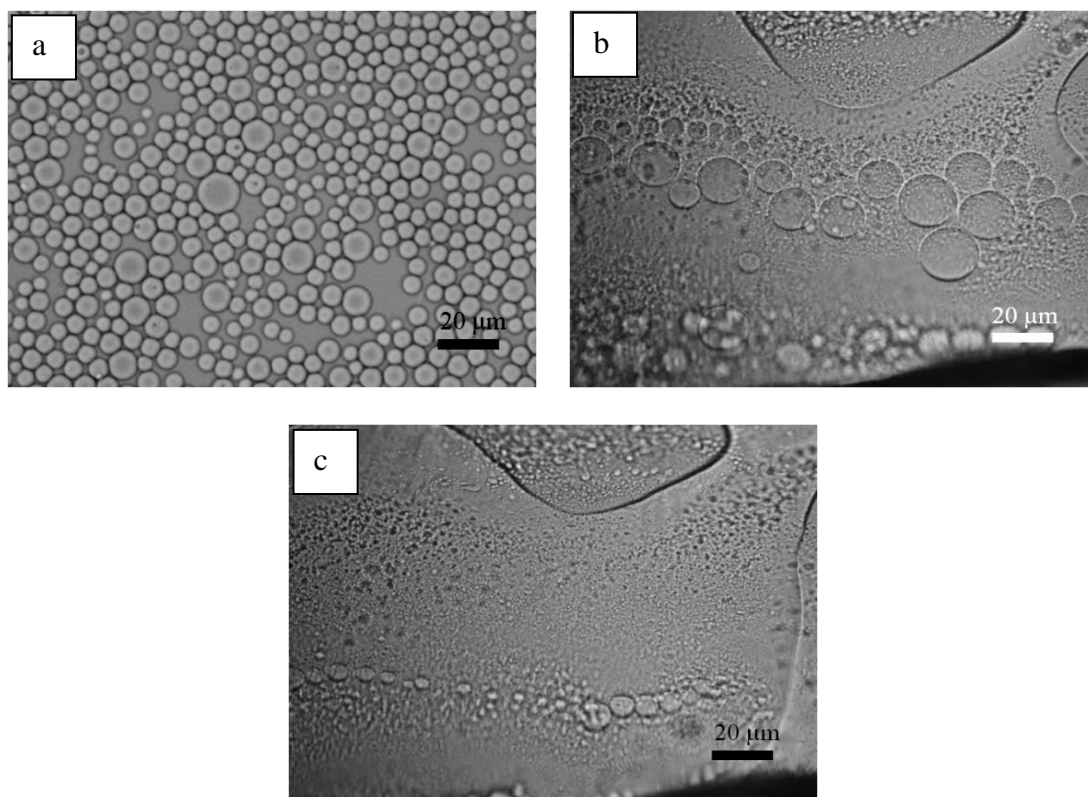


### 5.3.15 Dilution of the templated polymersomes

Dilution of the w/w emulsion with pure water led to mass transport of the dextran and PEG between the dispersed drops and continuous phase and causes the formation of a single phase solution. Thereby, emulsion structure collapses, as expected from the dextran-PEG phase diagram shown in Figure 5.13. A relatively stable emulsion containing equal volume fractions of dextran-PEG and 1 wt.% P30: P<sub>12</sub>-B<sub>60</sub>-D<sub>62</sub> was diluted with pure water 5 times, either at one addition or gradually to give a final composition within the one phase region of dextran-PEG system.

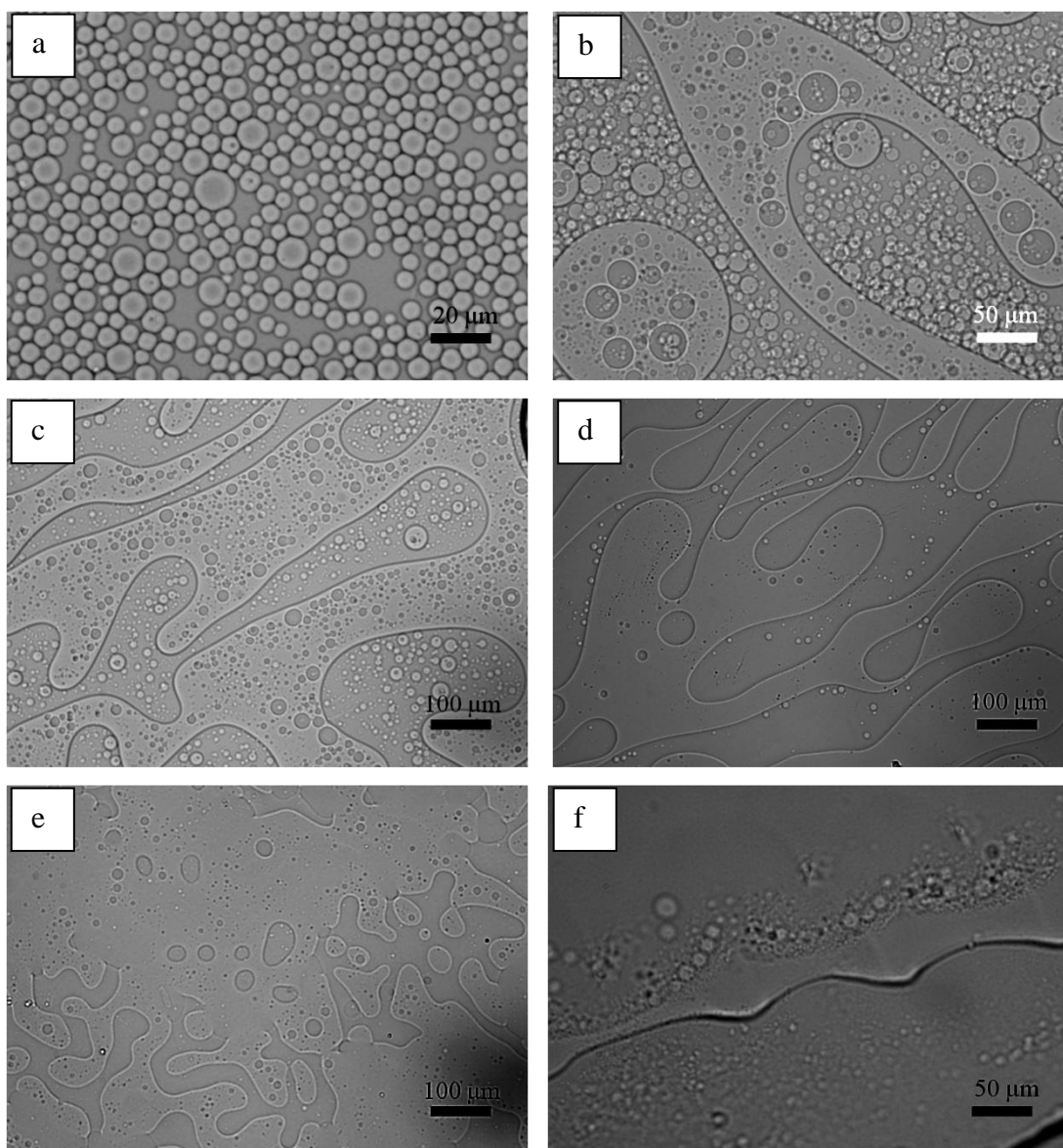
As it can be seen in Figure 5.38, diluting the system with 5 fold pure water at one addition triggers the collapse of the emulsion which was virtually completed within a few minutes.

**Figure 5.38.** Optical micrographs of w/w emulsion initially containing 9.24 wt.% dextran, 4.96 wt.% PEG (equal volume fractions) and 1 wt.% P30: P<sub>12</sub>-B<sub>60</sub>-D<sub>62</sub> (a) before dilution, (b) 1 minute after 5 folds dilution, (c) 2 minutes after 5 folds dilution.



Similarly, gradual dilution of the same emulsion caused the continuing destabilisation of the system. Despite diluting the system to a concentration at which one single phase is visually observed, the microscopic observation of the system immediately after dilution, revealed that there are still some remaining drops in the system which disappear in a few minutes (see Figure 5.39).

**Figure 5.39.** Optical micrographs of a w/w emulsion initially containing 9.24 wt.% dextran, 4.96 wt.% PEG (equal volume fractions) and 1 wt.% P30: P<sub>12</sub>-B<sub>60</sub>-D<sub>62</sub> containing (a) 85.8 wt.%, (b) 87.34 wt.%, (c) 88.32 wt.%, (d) 89.15 wt.%, (e) 89.87 wt.% and (f) 93.92 wt.% of water. Micrographs were taken immediately after dilution.

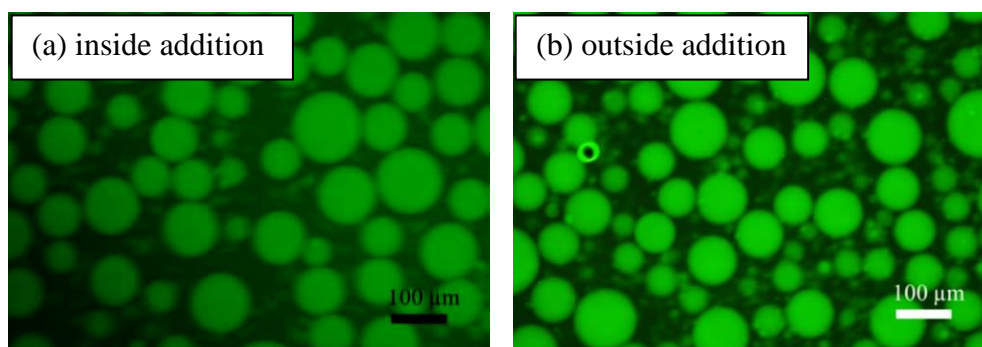


#### 5.4 Encapsulation/segregation of solutes within templated polymersomes

As illustrated before in Figure 5.11 fluorescent dye solutes selectively partition into the dextran- and PEG-rich phases of the APTS and hence partition similarly between the dispersed dextran drops and PEG continuous phase of the emulsions. For dextran-in-PEG emulsion drops stabilised by an adsorbed film of a  $P_x-B_y-D_z$  terpolymer, or in other words templated polymersomes, the permeation of solute molecules through the adsorbed polymer film was investigated. In addition, the rate of solute permeation in terms of being kinetically trapped in either the drops or the continuous phase of the emulsions was studied. Two small solute molecules, namely, fluorescein and rhodamine and one large molecule, namely, FITC-dextran were used in this study using two different approaches.

In the first approach, fluorescence micrographs obtained for systems of identical compositions but which differ only in the order of addition of the components were compared. In the “inside addition” method, the water, PEG, dextran and solute were first mixed to ensure partitioning of the solute. The terpolymer stabiliser was added afterwards followed by emulsification of the system. In the “outside addition” method, the mixture containing all ingredients except for the fluorescent dye solute was first emulsified and the dye was then added into the continuous phase of the preformed emulsion and the system lightly stirred for 30 minutes. As mentioned before, both small solute molecules (fluorescein and rhodamine) partition preferentially into the PEG-rich continuous phase and hence, as expected, no difference is observed between fluorescence micrographs of samples prepared by the “inside” or “outside” addition methods. Fluorescent micrographs were also obtained for FITC-dextran within dextran-in-PEG emulsions containing equal volume fractions of dextran-and PEG-rich phases stabilised by 1 wt.% of P28:  $P_6-B_{36}-D_{32}$ . FITC-dextran partitions preferentially into the dextran-rich phase which forms the droplets of the emulsion. Hence, if the FITC-dextran is slow to permeate the emulsion drop interface, the micrographs for “inside” and “outside” addition should be different. However, they were observed to be identical as it can be seen in Figure 5.40. Hence, the conclusion is that the FITC-dextran dye is able to permeate emulsion drop surfaces stabilised by the terpolymer adsorbed film freely on a timescale of 30 minutes or less.

**Figure 5.40.** Fluorescent micrographs obtained of dextran-in-PEG emulsions containing equal volume fractions of dextran-and PEG-rich phases and FITC-dextran (0.2 mg/mL) stabilised by 1 wt.% of P28: P<sub>6</sub>-B<sub>36</sub>-D<sub>32</sub>. The order of addition of FITC-dextran was (a) before addition of terpolymer and (b) after addition of terpolymer in the system.



In the second approach, the distribution of the negatively-charged FITC-dextran, which normally partitions to the dextran-rich phase, was altered by the addition of positively-charged rhodamine (which normally partitions to the PEG-rich phase). Addition of rhodamine to the systems containing FITC-dextran initially located in the dextran-rich drops of the emulsion causes the FITC-dextran to slightly partition to the PEG-rich continuous phase. This is presumably due to the formation of a rhodamine-FITC-dextran ion pair which distributes preferentially to the PEG-rich phase. For the experiment shown in Figure 5.41, a dextran-in-PEG emulsion containing FITC-dextran was first prepared and rhodamine added into the continuous phase. The intensities of green light emission from the FITC-dextran from both the emulsion drops ( $I_{\text{drop}}$ ) and continuous phase ( $I_{\text{cont}}$ ) were monitored over 1 minute. Both intensities decrease as a result of photo-bleaching. However, the ratio  $I_{\text{drop}}/I_{\text{cont}}$  decreases from greater than 1 initially to a plateau value of less than 1. This change indicates that the FITC-dextran is preferentially located in the dextran rich drops initially and the rhodamine addition extracts a fraction of the FITC-dextran into the PEG-rich continuous phase. The plot of  $I_{\text{drop}}/I_{\text{cont}}$  versus time shows that the permeation of the FITC-dextran through the adsorbed layer of P28:P<sub>6</sub>-B<sub>36</sub>-D<sub>32</sub> coating the drops occurs on a timescale of less than 1 minute. Control measurements of the fluorescence intensities of FITC-dextran in the absence of added rhodamine showed similar rates of photo-bleaching but the ratio  $I_{\text{drop}}/I_{\text{cont}}$  remained constant and greater than 1 over time (see Figure 5.42).

**Figure 5.41.** Dextran-in-PEG emulsions containing equal volumes of dextran-and PEG-rich phases stabilised by 1 wt.% of P28: P<sub>6</sub>-B<sub>36</sub>-D<sub>32</sub> emulsified with FITC-dextran (0.2 mg/mL) to which rhodamine (0.01 mg/mL) was subsequently added. The upper images show the fluorescence images immediately after preparation. The bellow plots show (a) the green fluorescence intensities from FITC-dextran in the drops and continuous phases and the (b) ratio  $I_{\text{drop}}/I_{\text{cont}}$  versus time.

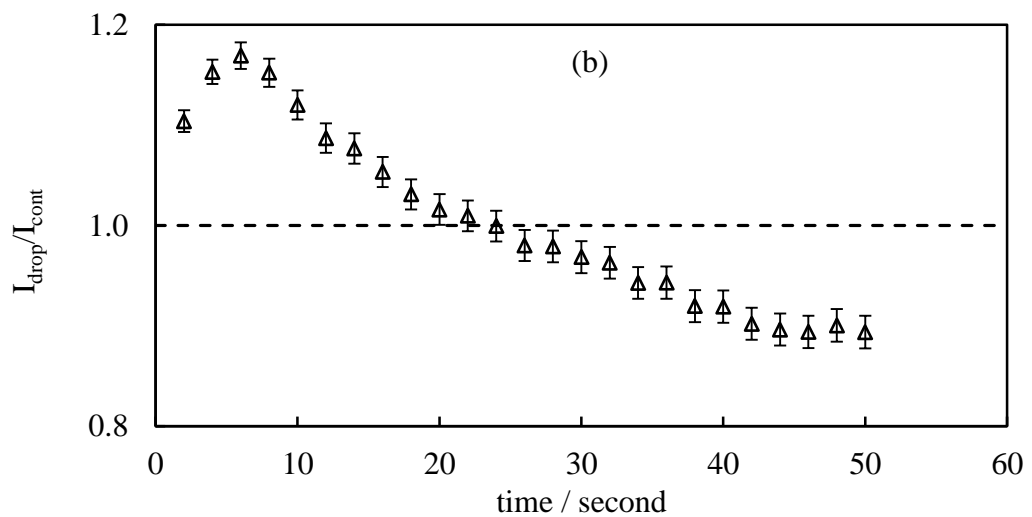
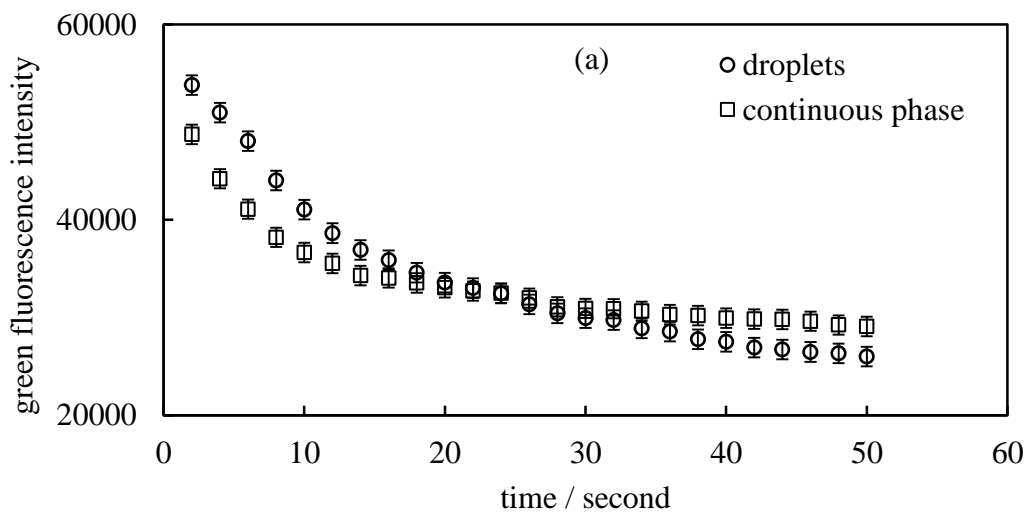
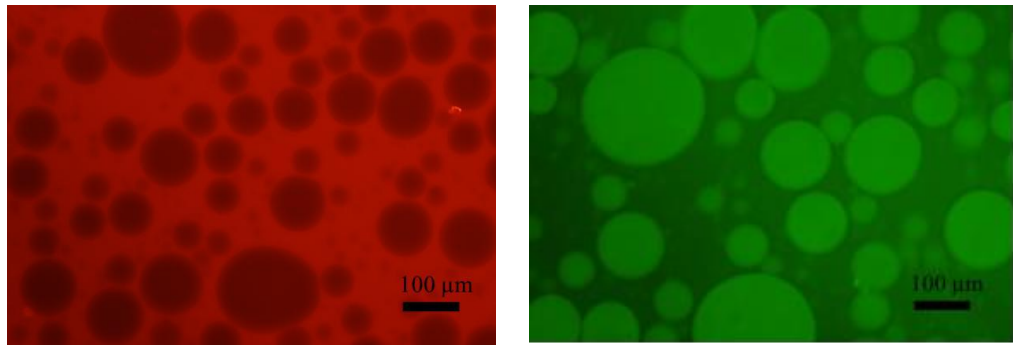
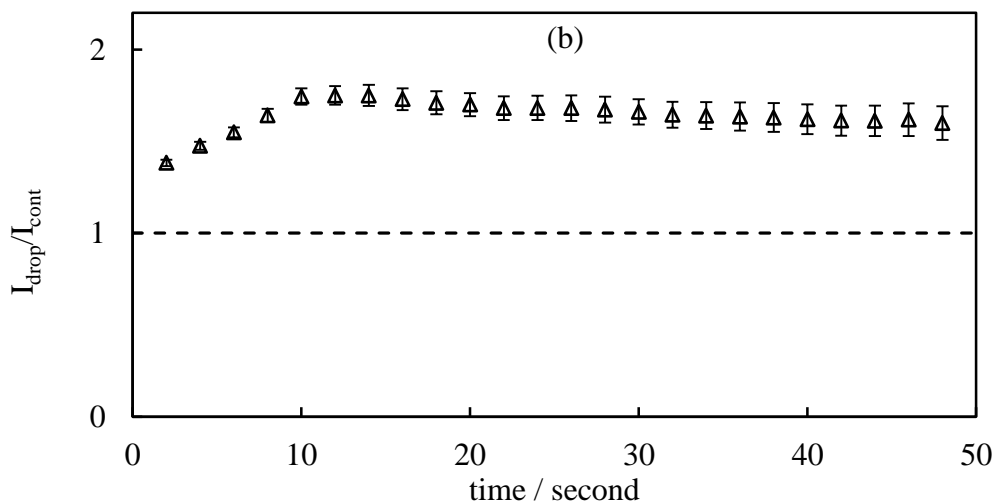
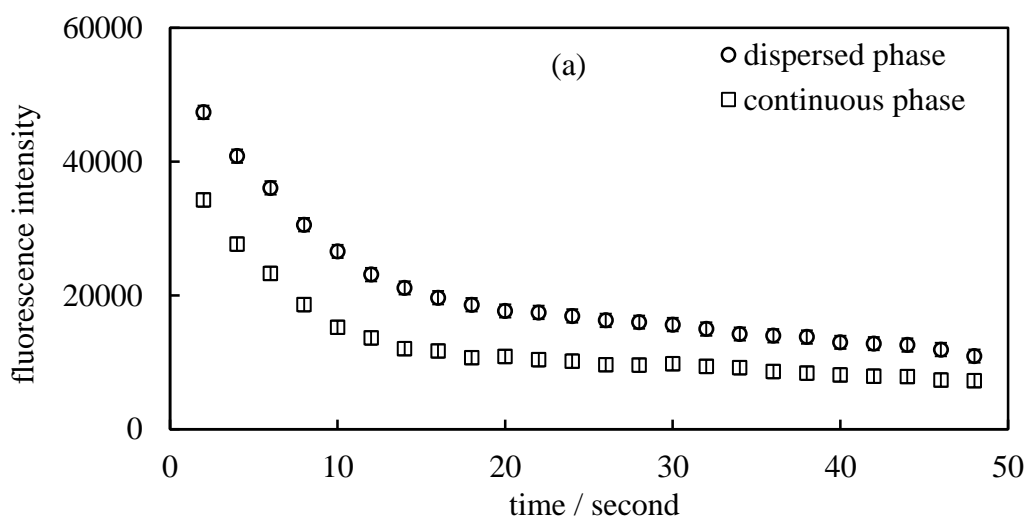
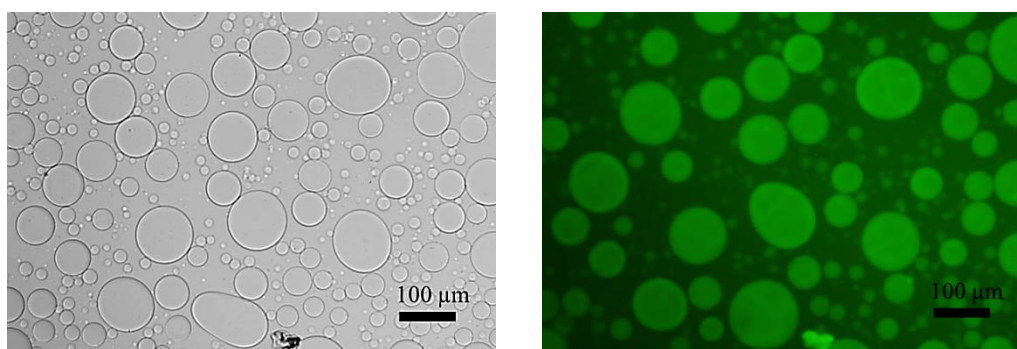


**Figure 5.42.** Dextran-in-PEG emulsion containing equal volumes of dextran-and PEG-rich phases stabilised by 1 wt.% of P28:P<sub>6</sub>-B<sub>36</sub>-D<sub>32</sub> emulsified with FITC-dextran (0.2 mg ml<sup>-1</sup>). The upper images show the FITC-dextran transmission and fluorescence images immediately after preparation. The bellow plots show (a) the green fluorescence intensities from FITC-dextran in the drops and continuous phases and (b) the ratio  $I_{\text{drop}}/I_{\text{cont}}$  versus time.



We have shown that the fluorescent dye solutes can permeate through the stabilising film of P28: P<sub>6</sub>-B<sub>36</sub>-D<sub>32</sub> on a short timescale. Additional experiments (not shown here) indicate that other terpolymers from Table 5.4 behave similarly. Because mass transport in/out of the emulsion drops can occur on a short timescale, it is predicted that dilution of the water-in-water emulsions with pure water (such that the diluted emulsion composition lies within the one phase region of the phase diagram in Figure 5.13) should lead to mass transport of the dextran and PEG between the drops and continuous phase to form a single phase mixed solution and thereby collapse the emulsion structure on the same timescale. As shown in Section 5.3.16 this dilution triggers the collapse of the emulsion which is virtually complete within a few minutes thus it is in agreement with the permeation rate observed for fluorescent probes.

### **5.5 Applications of templated polymersomes based on w/w emulsion**

Although polymersomes prepared by templating w/w emulsion have some similarity to conventional polymersomes, there are significant differences. Conventional polymersomes are kinetically stable entities which retain their structure upon dilution and retain encapsulated solutes. Encapsulated materials within a conventional polymersome are *kinetically* retained. In other words, the permeation rate of the encapsulant through the polymersome membrane is slow.<sup>10</sup> In addition, generally the encapsulants do not have any specific affinity to stay either inside or outside of the conventional polymersomes because both interior and exterior environment are the same in character. Therefore, in order to load solutes within the polymersomes using conventional methods, generally additional loading steps are required which leads to very low encapsulation efficiencies.<sup>11</sup> Moreover, most of the times, extra steps are required to separate and remove the unencapsulated species from the encapsulated ones.

The prepared polymersomes based on templating w/w emulsions show solute mass transport on a timescale of a few minutes, therefore encapsulant can move freely between the interior and exterior of these structures based on their affinity towards outside or inside. In addition, encapsulant can be trapped within the formed polymersomes based on their affinity for required timescale and easily released by

dilution of the system with water which triggers collapsing the polymersome structure and destabilisation of the system.

Based on the mentioned key differences between conventional and templated polymersomes, one can result that these structures have both advantages and disadvantages for potential applications. Because of the fast mass transport and lack of kinetic trapping of encapsulated species within these structures, they are not suitable for application such as drug delivery where dilution of the system (for example with blood serum) causes the destabilisation of the system. However, the specific properties of these structures can be advantageous where spontaneous self-loading of the species is required. Encapsulant with specific affinities towards dispersed benefit from retaining their segregation (partition) indefinitely, since they are trapped thermodynamically rather than kinetically. The self-loading and fast mass transport of the encapsulant makes these structures potentially appropriate for application in the segregation of reactive species within a formulated product (e.g. household cleaning products) in which mixing and reaction of the active species could be triggered in use by dilution with water. The templated polymersomes can be also be used in application where slow mass transport of the encapsulant is need by slight modification of the formed polymer film. The constituent terpolymers contain DMAEMA block which can be potentially cross-linked using appropriate cross-linker (e.g. 1,2-bis(2-iodoethoxy)ethane).<sup>12</sup> By adjusting the degree of crosslinking, the mass transportation of encapsulant triggered by diluting can be controlled.

## **5.6 Conclusion**

A fundamentally different strategy for polymersome formation based on an ATPS of dextran-PEG were proposed and studied. At first the effect of a three commercially available ABA terpolymers, namely, Pluronic<sup>®</sup> with different hydrophilic-hydrophobic ratios and molecular weights, on stabilising the aqueous two phase polymer system of dextran-PEG was investigated. Unfortunately, none of the used commercially available triblock copolymers was able to stabilise this system for a long time. However, the behaviour of the prepared systems was different in terms of the separation rate of each phase, as well as the volume fraction of phases. Experimental results of using F68 and F108 Pluronic<sup>®</sup> grades as the stabiliser showed that the higher the molecular weight of the stabiliser the more is



the stability of the emulsion. However, this was presumed to be due to the high viscosity of system which leads to a slow rate of phase separation.

Being unsuccessful to stabilise the aqueous two phase system of dextran-PEG using commercially available amphiphilic copolymers, led the project strategy to used in-house synthesised ABC amphiphilic terpolymers. ABC terpolymers of different compositions ( $P_x-B_y-D_z$ ) based on the non-ionic hydrophilic PEGMA, non-ionic hydrophobic BuMA, the ionisable hydrophilic and thermoresponsive DMAEMA were used for the stabilisation of w/w emulsion and possible formation of templated polymersomes. We have demonstrated that large polymersome-like structures can be formed by using these terpolymers templating water-in-water emulsions based on PEG-dextran ATPS. Based on the fluorescence microscopic observation, it was found that the type of formed emulsion is not strongly affected by the composition of terpolymers in a way that could results in transitional phase inversion of the system. However, it was shown that by varying the volume fraction of dextran-PEG ATPS, it is possible to have the catastrophic phase inversion of the system.

The type of emulsions containing equal volume fractions of dextran-PEG stabilised using a range of terpolymers with varied compositional design, was determined to be all dextran in PEG. The emulsion drop sizes (or polymersomes size) can be varied based on the choice of precursor terpolymer and it is in range of 1-100  $\mu\text{m}$  in diameter. Overall, it was resulted that emulsions with higher stability contain smaller drops.

Comparing the  $t_{1/2}$  of coalescence of the dispersed phase obtained from emulsions which were stabilised using a range of terpolymers with varied composition, pointed out a number compositional requirement in order to optimise the final structure of terpolymers based on the final application of these systems. Overall, terpolymers with relatively long BuMA and DMAEMA block and PEGMA block consisting of about 15 unites were able to provide stable system for more than 8 months.

In addition, the effect of varying the concentration of terpolymers, pH, temperature and stirring rate on the system was studied. Also, the behaviour of formed polymersomes upon drying and diluting the system was investigated. It was

shown that the formed polymersomes keep their structure upon drying the system, while they dissociate by diluting up the system with pure water.

Moreover, it was demonstrated that both low and high molar mass fluorescent solutes spontaneously segregate within the dextran-PEG ATPS and can be self-loaded into the dispersed or continuous phases of water-in-water emulsions. The solutes molecules can freely permeate across the emulsion droplet interface within a few minutes and therefore they are not kinetically trapped within the formed polymersomes. However, they could be thermodynamically self-loaded into the dispersed phase and retain for relatively long time. The encapsulated species can be released by collapsing the system triggered by dilution.

There are a number of distinctive features of these systems which could be highlighted as following:

- Using very low energy input (gentle stirring) is adequate for the formation of templated polymersomes.
- There is no organic solvent in the system which makes them potentially useful for environmentally friendly applications.
- Their size is bigger than the conventional polymersomes (1-100  $\mu\text{m}$ ).
- The interior of polymersomes can be converted from dextran rich to PEG rich solution simply by varying the volume fractions of the ATPS, therefore, based on the segregation ability of different species they can be encapsulated within the desired solution.
- The segregation of encapsulants within the emulsions is an equilibrium effect; it does not vary further with time unlike the conventional polymersomes which trap encapsulants kinetically.
- Collapse of the formed polymersomes structure occurs within a few minutes triggered by dilution of the emulsions with pure water.

In spite of all the work has been done on these systems, there are still some unresolved questions. Firstly it is still unclear whether the stabilisation of the system is as a result of adsorbed terpolymer film around the dispersed phase or whether part of the stabilisation results from other effects, such as viscosifying the continuous phase. Secondly, we are uncertain about the structure of the presumably adsorbed polymer film around the dispersed drops. In the proposed research strategy terpolymers straddles the water-water interface with PEGMA blocks located one side and DMAEMA at the other side. However, there could be mixed PEGMA and DMAEMA coronas in both sides or possibility of formation of bilayer hairpin configuration or more complex configurations. The phase separation of PEGMA and DMAEMA homopolymer has been observed in a separate experiment. Therefore, it is likely that the partial segregation of PEGMA and DMAEMA block occurs in the system, although further experiments using high resolution structural determination methods such as neutron scattering are required to elucidate these unresolved aspects.

## 5.7 References

1. G. E. Molau, *Kolloid Zeit. Zeit. Polymere*, 1970, **238**, 493.
2. M. Ossenbach-Sauter and G. Riess, *C. R. Academie. Sci. Paris Ser. C*, 1976, **283**, 269.
3. T. Jin, L. Chen, H. Zhu, *Stable polymer aqueous/aqueous emulsion system and uses thereof*. US Patent 6,805,879 B2, 12 Oct. 2004.
4. K. A. Simon, P. Sejwal, R. B. Gerech and Y. Y. Luk, *Langmuir*, 2007, **23**, 1453.
5. H. C. Shum, J. W. Kim and D. A. Weitz, *J. Am. Chem. Soc.*, 2008, **130**, 9543.
6. J. L. Salager, L. Marquez, A. A. Pena, M. Rondon, F. Silva and E. Tyrode, *Ind. Eng. Chem. Res.*, 2000, **39**, 2665.
7. B. P. Binks, *Modern Aspects of Emulsion Science*, Royal Society of Chemistry, Cambridge, 1998.
8. F. Xie and B. W. Brooks, *Colloid Surf. A-Physicochem. Eng. Asp.*, 2005, **252**, 27.
9. B. P. Binks and S. O. Lumsdon, *Langmuir*, 2000, **16**, 2539.
10. G. Battaglia, A. J. Ryan and S. Tomas, *Langmuir*, 2006, **22**, 4910.
11. A. J. Parnell, N. Tzokova, P. D. Topham, D. J. Adams, S. Adams, C. M. Fernyhough, A. J. Ryan and R. A. L. Jones, *Faraday Discuss.*, 2009, **143**, 29.
12. J. Du, L. Fan and Q. Liu, *Macromolecules*, 2012, **45**, 8275.

## **CHAPTER 6**

### **STABILISATION OF W/W EMULSIONS BY MODIFIED SILICA NANOPARTICLES**

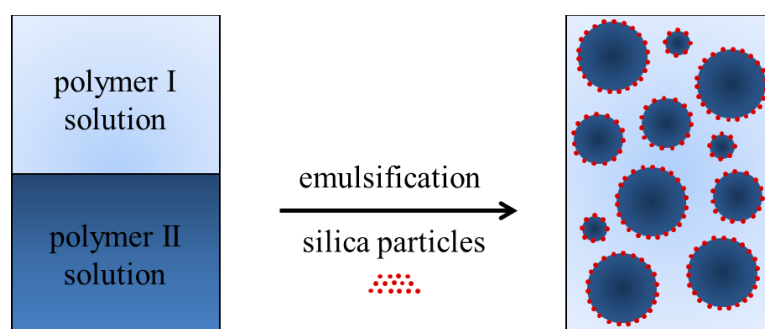
## 6.1 Introduction

It is well established that solid particles of suitable wettability will adsorb at a fluid interface with an adsorption energy which is typically larger than alternative stabilisers such as surfactants and polymers.<sup>1</sup> In particle stabilised emulsion systems colloidal particles can accumulate at the liquid-liquid interface to form a steric barrier against coalescence. However, in ATPSs due to their small interfacial tension, the adsorption of particles at the interface is quite challenging. As it was mentioned in Chapter 1 only a limited number of publications have investigated the stabilisation of w/w emulsions by particles. Preliminary, Poortinga reported the formation of microcapsules consisting of a shell of aggregated colloids based on w/w emulsion as a template consisting of either two polysaccharides or one polysaccharide and one protein stabilised for a short time (a few days) by fat particles.<sup>2</sup> Firoozmand and co-workers<sup>3</sup> described the formation of w/w emulsion based on gelatine-starch ATPS which could be stabilised for a short time using amphoteric polystyrene latex particles. He reported that the gelatin-dextran ATPS phase separates quickly, but upon addition of latex particles the phase separation slowed down although still phase separation occurred. Recently, Nicolai et al. reported formation of w/w emulsion based on dextran-PEG ATPS stabilised using fluorescent spherical latex particles<sup>4</sup> and globular whey protein  $\beta$ -lactoglobulin ( $\beta$ -lg) particles<sup>5</sup> which can be adsorbed at the dextran-PEG interface. In some cases the stability of the prepared emulsions was in a period of weeks.

As mentioned before, w/w emulsions have extremely low interfacial tensions and as such the challenge in stabilising these systems with particles relies on finding or modifying particles so that they will adsorb at the interface. In such systems, the amphiphilic properties of particles as well as their wettability towards one of the phases are important characteristics which might govern them to be adsorbed at the interface.

In this work solid silica nanoparticles with modified characteristics were used to attempt stabilisation of an ATPS comprising of PEG and dextran. The research strategy is illustrated as following (Figure 6.1):

**Figure 6.1.** Stabilisation of w/w emulsion using silica nanoparticles.



Silica is one of the most commonly used materials in particle stabilised emulsions.<sup>6-11</sup> Silica particles can simply be considered as very small, porous glass spheres. They are readily prepared from relatively cheap precursors, in technically simple procedures, where desired size and physiochemical properties i.e. pore size, surface hydrophobicity and surface coating's properties can be easily tailored.<sup>12, 13</sup>

In this work, two series of silica nanoparticles with specific characteristics were used: (1) silica nanoparticles with different extent of hydrophobicity and (2) PEGylated (PEG-philic) silica nanoparticles with different sizes. To the best of our knowledge silica nanoparticles have not been used for preparation and stabilisation of w/w emulsion. The reason behind choosing the earlier type of silica nanoparticles, namely hydrophobised ones, was their hydrophobicity which might direct them to be adsorbed at the dextran-PEG interface at an entirely aqueous solution and therefore stabilise the formed emulsion. The later PEGylated silica nanoparticles, with modified affinity towards PEG rich phase were envisaged in terms of their wettability by the PEG rich phase rather than the dextran phase which makes them to potentially adsorb at the PEG-dextran interface and stabilise the emulsion.

This chapter can be divided in two main sections. In the first section, the possibility of stabilisation of w/w emulsion based on dextran-PEG ATPS using hydrophobised silica nanoparticles is investigated to determine whether hydrophobicity of silica nano-particles can act as a driving force for the silica nano-particles to be adsorbed on the low energy interface of dextran-PEG ATPS. In addition, the effects of hydrophobicity extent of the used silica nanoparticles as well as their content in the system on stability of prepared w/w emulsion are studied. In the second section, the synthesis, characterisation and evaluation as dextran-PEG

ATPS stabilisers of PEGylated (coated with PEG) silica nanoparticles are described. The stability of emulsions are also studied as a function of PEG content and particles size.

## **6.2 Stabilisation of w/w emulsion by hydrophobised silica nanoparticles**

### ***6.2.1 Silica nanoparticles characteristics***

Silica nanoparticles with different hydrophobicities (0%, 20%, 33%, 50% and 58%) with smooth surface and primary size ranging from 10-30 nm were used, although silica nanoparticles easily aggregate or fuse to form larger non-spherical aggregation of size about 100 nm. Hydrophobisation of silica particles was done by silylation of silanol groups (SiOH) to different extent through reaction with dimethyl dichlorosilane. The hydrophobicity extent of silica nanoparticles is defined as the percentage of dimethylsilane groups on their surface.

### ***6.2.2 Effect of hydrophobicity extent of silica nanoparticle on emulsion stability***

The stability of w/w emulsions prepared using 2 wt.% of silica nanoparticles was investigated as a function of their hydrophobicity ranging from 0 to 58%. It was found that the emulsion stability, with respect to coalescence, varies significantly when varying the hydrophobicity of the silica nanoparticles. This result is summarised in Figure 6.2 for emulsions prepared based on using 0.5: 0.5 volume fractions of dextran-PEG ATPS. This Figure gives the volume fractions of resolved dextran rich phase i.e. dispersed phase, over time for the prepared emulsion using silica nanoparticles with different extent of hydrophobicity. As it can be seen in this graph, when 100% hydrophilic unmodified silica nanoparticles were used, the prepared emulsion was very unstable and similar to a reference ATPS (no stabiliser) coalesce immediately after preparation. The presence of silica nanoparticles dispersed in PEG rich phase after a full phase separation suggests the higher wettability of hydrophilic silica particles by PEG rich phase rather than dextran rich phase. With slight increase in the hydrophobicity of used particles (20%), emulsions show no sign of phase separation for at least 1 hour and rate of coalescence decreased by magnitude of 3 in logarithmic scale. Silica nanoparticles with 33% hydrophobicity provided the most stable emulsions among the others and the formed emulsion was stable for a week. In addition, it was found that particles with 50% hydrophobicity provided less stable emulsions compared to the 20% or 33%



hydrophobic silica particles. This might be due to the reduced wettability of particles with neither of the dextran and PEG rich phases. In the case of using silica particles with 58% hydrophobicity extent, particles were not dispersible in the system due to their high hydrophobicity and they remained mostly on the interior walls of the glass vessels. This phenomenon was observed for all used hydrophobised particles and raised with increase in hydrophobicity of the used particles (see Figure 6.3).

**Figure 6.2.** Plot of resolved dextran volume fraction ( $\phi$  dextran) versus time in logarithmic scale for emulsions consisting of 0.5: 0.5 volume fractions of dextran-PEG stabilised using 2 wt.% of silica nanoparticles with different hydrophobicities extent. Emulsions were prepared via two minutes homogenisation at 11000 rpm.

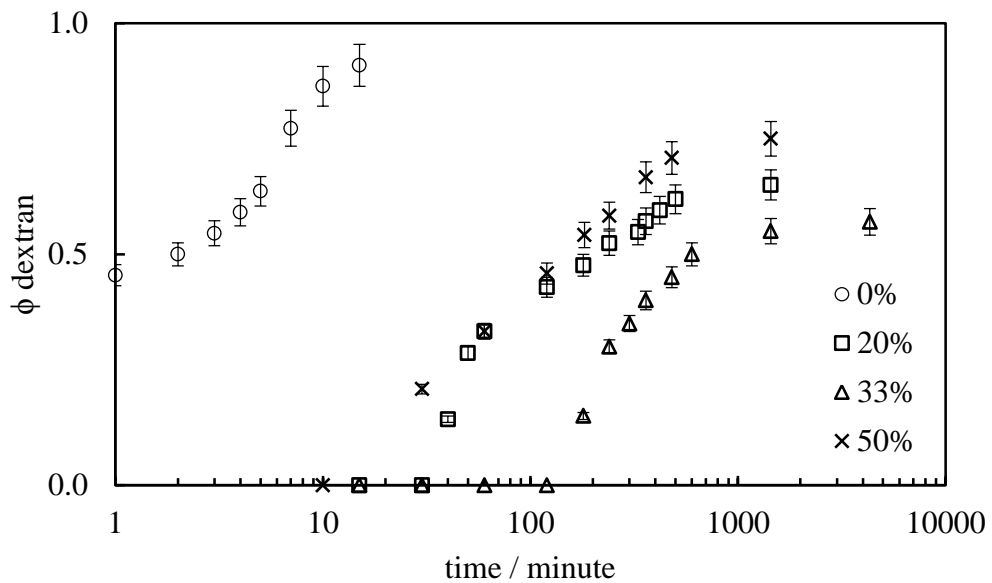
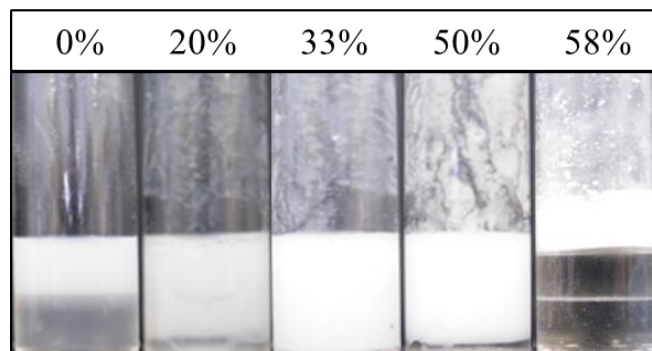
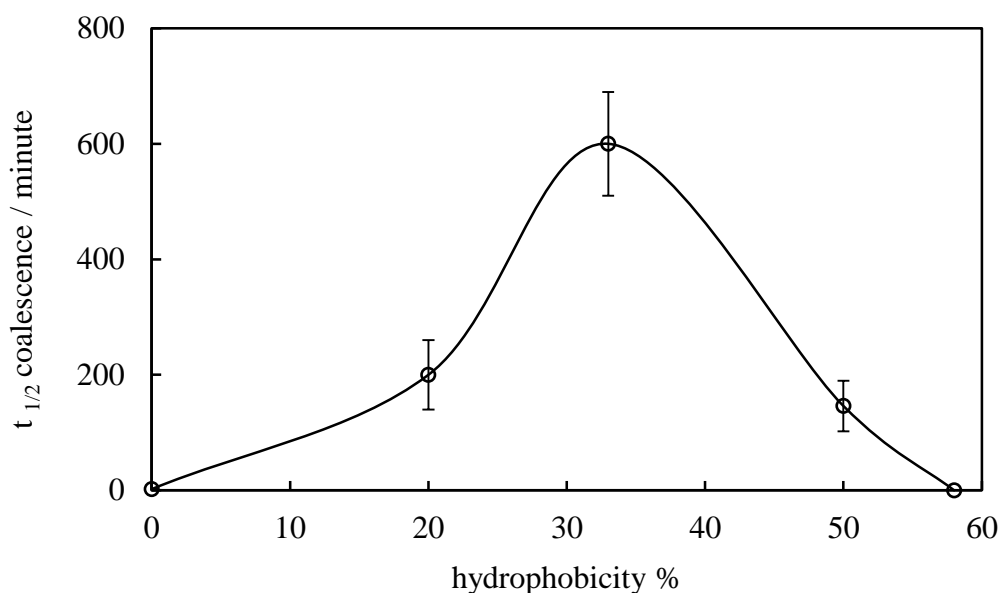


**Figure 6.3.** Digital images taken after 1 hour of preparation, from emulsions containing 0.5: 0.5 dextran-PEG volume fractions and 2 wt.% of hydrophobised silica nanoparticles with varied hydrophobicities. Emulsions were prepared via two minutes homogenisation at 11000 rpm.



By extracting the half-lives ( $t_{1/2}$ ) of coalescence for each emulsion, defined as time taken for dextran rich phase to resolve 50% of its volume fraction from the emulsion and plotting them as a function of hydrophobicity of silica nanoparticles, one can conclude that the maximum stability of emulsions in terms of coalescence, occurs when the hydrophobicity of silica nanoparticles is 33% (see Figure 6.4). Extreme degrees of hydrophilicity or hydrophobicity results in either dispersion of particles in one phase or film climbing effect respectively.

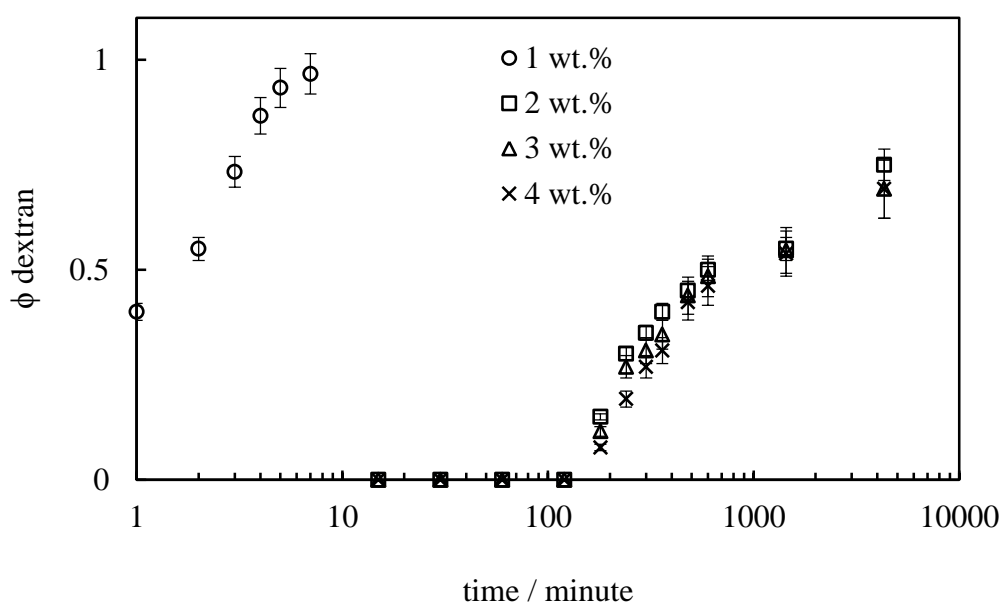
**Figure 6.4.** Plot of half-lives of coalescence versus the degree of hydrophobicity of silica nanoparticles used for the stabilisation of ATPS system consisting of 0.5:0.5 volume fractions of dextran and PEG. Emulsions were prepared via two minutes homogenisation at 11000 rpm.



### 6.2.3 Effect of silica nanoparticles concentration on emulsion stability

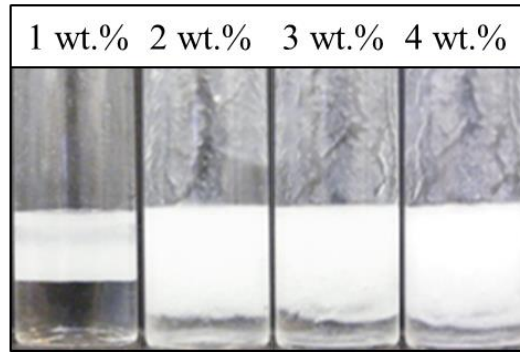
Different content (1, 2, 3 and 4 wt.%) of silica nanoparticles with 33% hydrophobicity were used for the stabilisation of ATPS consisting of 0.5: 0.5 volume fractions of dextran-PEG. The results were summarised in Figure 6.5, by plotting the volume fractions of resolved dextran phase over time for emulsions stabilised with different content of silica nanoparticles while their degree of hydrophobicity was 33%.

**Figure 6.5.** Plot of resolved dextran volume fraction ( $\phi$  dextran) versus time in logarithmic scale for emulsions consisting of 0.5: 0.5 volume fractions of dextran-PEG stabilised using 1, 2, 3 and 4 wt.% of silica nanoparticles with 33% hydrophobicity. Emulsions were prepared via two minutes homogenisation at 11000 rpm.



As it can be seen in Figure 6.5, the critical concentration of silica nanoparticles in order to cover the dextran-PEG interface and prevent coalescence is about 2 wt.%. At lower concentrations (1 wt.%), the formed emulsion is very unstable and droplets coalesce so quickly that emulsion phase separated in a few minutes. By increasing the concentration of silica nanoparticles in the system, emulsion stability is enhanced significantly and remains constant even though beyond addition of 3 or 4 fold more particles (see Figure 6.6). This result is in agreement with literature where Frelichowska et al.<sup>14</sup> proved the same effect for using hydrophobic silica nanoparticles for stabilisation of o/w emulsion. Also, they discussed that emulsion droplet size remains with no change as the concentration of used silica nanoparticles is increased beyond a certain concentration. The same result was obtained in w/w emulsions when they were observed under the microscope. Micrographs taken from emulsions region of w/w emulsions containing different concentration of silica nanoparticles with 33% hydrophobicity immediately after preparation, is shown in Figure 6.7.

**Figure 6.6.** Digital images taken after 3 days from emulsions based on 0.5: 0.5 volume fractions of dextran-PEG stabilised with different concentration of silica nanoparticle as noted on each sample vessel with 33% hydrophobicity. Emulsions were prepared via two minutes homogenisation at 11000 rpm.



Analysis of the drops size of emulsions for different concentrations of silica nanoparticles revealed that at low concentration of silica, emulsion drop size is relatively large and emulsion tend to phase separate quickly. Upon increasing the concentration of silica particles in the system, the mean diameter of the droplets decreases dramatically. For a better representation of this result, the mean diameters of emulsions drops were plotted over the concentration of used silica nanoparticles in the system. As it can be observed above 2 wt.% of silica particles in the system, the emulsion drop size remains relatively unchanged (see Figure 6.8). It has been suggested that the decrease of the droplet diameter with respect to silica content in the system is corresponded to increasing interfacial area.<sup>15-18</sup> As the silica content increases in the system, the interfacial area increases linearly causes the droplet diameter decreases inversely with respect to silica content. The mean droplet diameter,  $D$ , can be related to the interfacial area via following Equation 6.1:<sup>14</sup>

$$D = \frac{6 \phi_{dis} V}{A} \quad \text{Eq. 6.1}$$

Where,  $D$  is the mean droplet diameter,  $\phi_{dis}$  is the volume fraction of dispersed phase,  $V$  is volume of emulsion and  $A$  is the interfacial area per unit volume of emulsion. As it can be seen in this equation, the mean diameter of emulsion drops decreases linearly, with respect to the increase in the interfacial area. At the plateau where emulsion mean drop size does not change as a function of silica

content, it might be attributed to lack of efficiency of the emulsification process.<sup>19</sup> However, more investigation seems to be required as w/w emulsions based on ATPS have a very low interfacial tension and in theory the breakage of droplets should be easy.

**Figure 6.7.** Micrographs taken immediately after preparation of w/w emulsion based on 0.5:0.5 volume fractions of dextran-PEG stabilised using (a) 1 wt.%, (b) 2 wt.%), (c) 3 wt.% and (d) 4 wt.% of silica nanoparticles with 33% hydrophobicity. Emulsions were prepared via two minutes homogenisation at 11000 rpm.

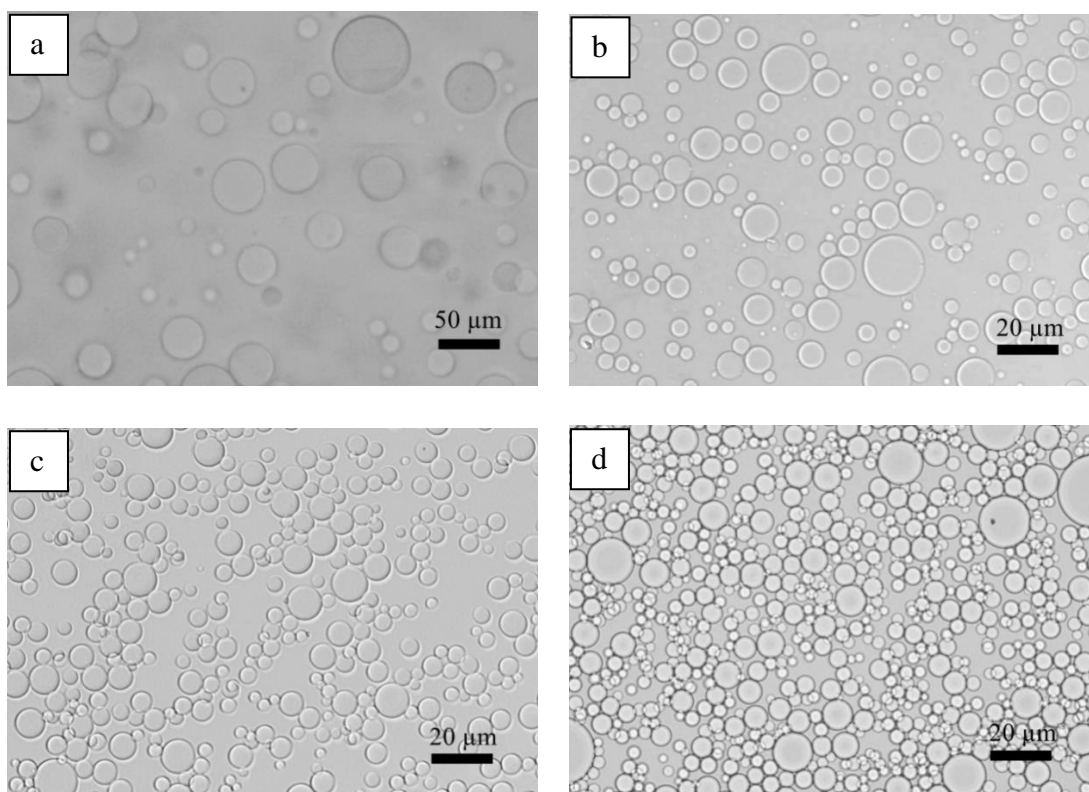
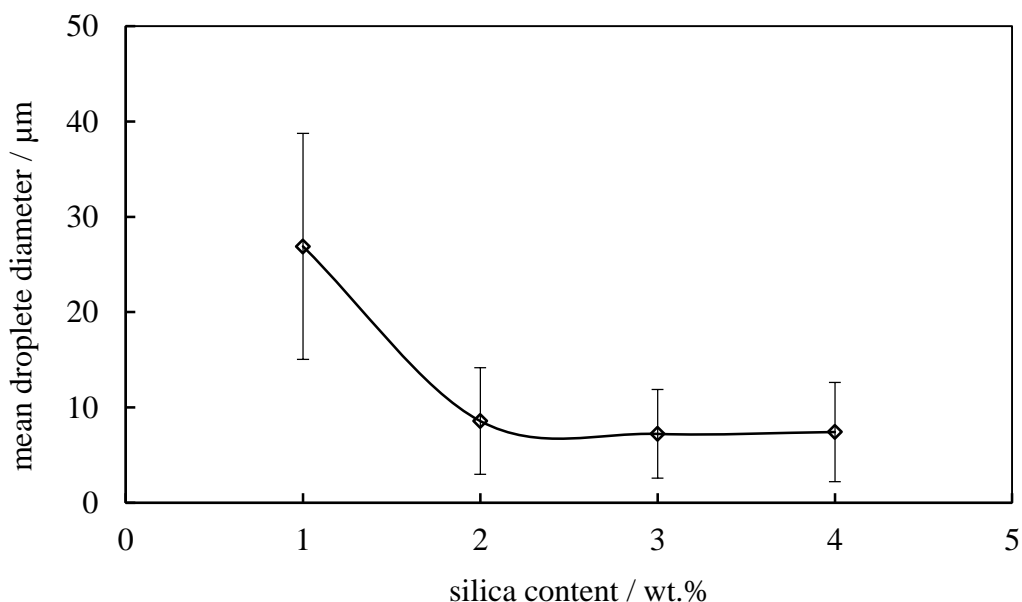


**Figure 6.8.** Diameter of the w/w emulsion droplets consisting of 0.5: 0.5 volume fractions of dextran-PEG as a function of silica concentration (33% hydrophobicity). Emulsions were prepared via two minutes homogenisation at 11000 rpm. Error bars are corresponding to standard deviations of mean droplet diameter.

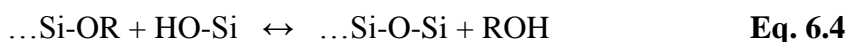
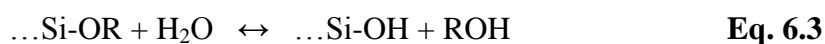
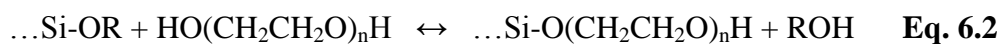


### 6.3 Stabilisation of w/w emulsion by PEGylated silica nanoparticles

#### 6.3.1 PEGylated silica nanoparticles synthesis and characteristics

Silica nanoparticles were modified in order to enhance their wettability by PEG rich phase. Such that particles are assumingly wetted more by the PEG aqueous phase, rather than the dextran aqueous phase. This effect is analogous to hydrophobic-hydrophilic wetting phenomena at an oil-water interface which will be replicated here, allowing these modified particles to be held at the dextran-PEG interface.

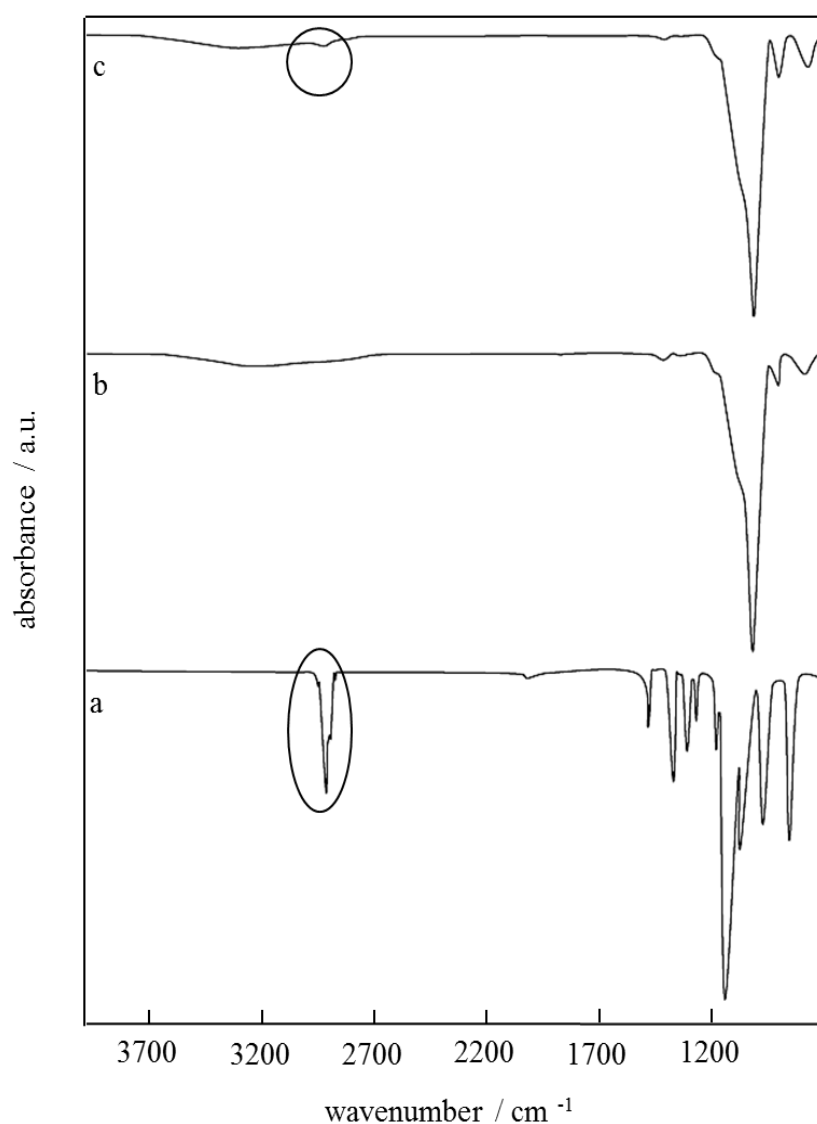
For this work coated silica nanoparticles were synthesised by a base-catalysed polymerisation of a silicon alkoxide and tetramethyl orthosilicate (TMOS) in alcohol/water mixture. By this method it is possible to obtain spherical silica particles of different sizes. Xu et al.<sup>13</sup> proposed the reaction mechanism of PEGylated silica particles as following:



Equation 6.2 shows the trans-esterification reaction between TMOS and PEG, which is in direct competition with the hydroxylation of the silicon alkoxide (Equation 6.3) and the following condensation step (Equation 6.4) yielding the formation of a silica network. It is important to note that Equation 6.3 and 6.4 are predominant over Equation 6.2.<sup>20</sup>

The synthesised PEGylated silica nanoparticles were characterised in terms of their PEG content using FT-IR spectroscopy. Figure 6.9 gives the IR spectrums of pure PEG, pure silica nanoparticles and PEGylated silica nanoparticles. In Figure 6.9a, there are many peaks characteristic to PEG but among them the two strong overlapped peaks at 2886 and 2960  $\text{cm}^{-1}$  which can be assigned to the  $-\text{CH}_2\text{CH}_2-$  stretching and implying the presence of saturated carbon  $-(\text{CH}_2\text{CH}_2)_n-$ <sup>13, 21</sup> were chosen for comparison with PEGylated silica nanoparticles. Figure 6.9b shows the IR absorption spectrum of pure silica nanoparticles, prepared by the same procedure, but without the addition of PEG polymer. A number of peaks characteristic to the silica nanoparticles can be seen at 797, 945, 1055, 1450, 1626 and 3250  $\text{cm}^{-1}$ . It is speculated that the very broad peak between around 3000 and 3600  $\text{cm}^{-1}$ , likely indicates the presence of exchangeable protons, mostly from hydroxyl groups on the surface of the silica particles. The spectrum for PEGylated silica (Figure 6.9c) gave new absorption peaks that were not present in the pure silica spectrum, at 2886 and 2960  $\text{cm}^{-1}$ , (shouldering the broad peak between 3000 and 3600  $\text{cm}^{-1}$ ). These peaks are at the same position as the characteristic peaks in the pure PEG spectrum meaning these signals are representative of chemically-bound PEG to the prepared PEGylated silica nanoparticles.

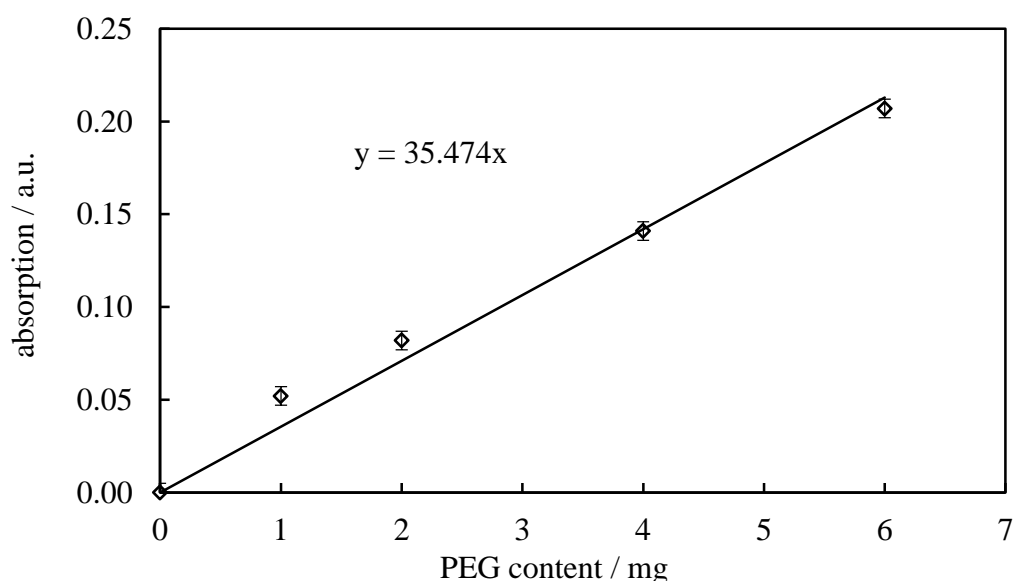
**Figure 6.9.** FT-IR spectrum corresponding to (a) pure PEG, (b) pure silica nanoparticles and (c) PEGylated silica nanoparticles.



The PEG content (wt.%) of synthesised silica nanoparticles was quantified using a calibration curve obtained by plotting the absorption at  $2886\text{ cm}^{-1}$  of samples containing different amount of PEG embedded in silica versus PEG concentrations (see Figure 6.10). From the calibration equation the PEG content (wt.%) in the PEGylated silica nanoparticles was determined to be  $2.0 \pm 0.5$  wt.% in all three PEGylated silica samples.

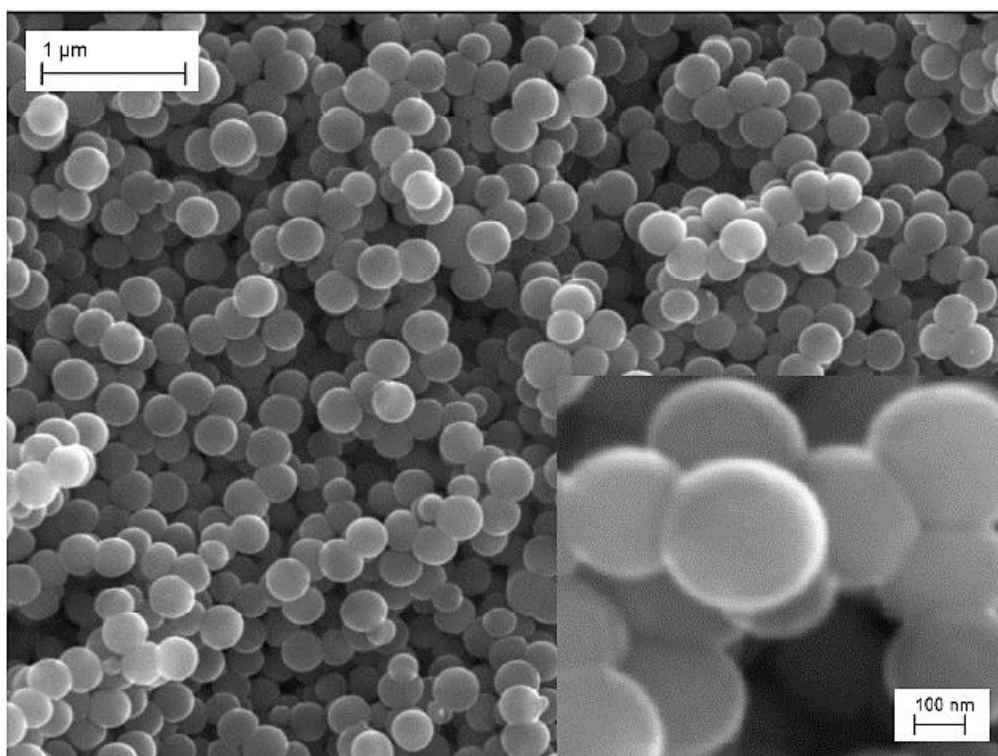


**Figure 6.10.** Calibration curve corresponding to IR absorption of PEG at  $2886\text{ cm}^{-1}$  versus PEG content.



The synthesised PEGylated silica nanoparticles were characterised in terms of their size and shape using SEM. A typical SEM image of the solid PEGylated silica particles (Sample 2) can be seen in Figure 6.11. As it can be seen particles are quite smooth and spherical with low polydispersity. Closer inspection of the images does however show some fusion of particles. At lower magnification, agglomerates made up of tens of nanoparticles can clearly be seen. This is an important observation, since it is tough to break fused large agglomerates of particles in order to stabilise emulsion droplets. But at the same time it must be stressed that SEM images were taken from the dried solid powder and give no indication of how particles will be dispersed once in water. These observations are consistent for all the PEGylated silica samples and the pure silica nanoparticles. The SEM images were used to obtain particle mean diameter of all prepared PEGylated silica samples and non-PEGylated silica nanoparticles in their dry state.

**Figure 6.11.** SEM image of PEGylated silica nanoparticles (sample 2).



PEGylated silica nanoparticles were also characterised in terms of their size and polydispersity using DLS technique. DLS revealed a bimodal size distribution pointing out that two kinds of species are present in the examined systems. The first peak with >95 % intensity was attributed to single rehydrated particles in solution comparable with the sizes obtained from SEM size measurement. The second peak with < 5% intensity and much larger hydrodynamic radius can be assigned to particle aggregates in the sample which is consistent with observations from the SEM. Table 6.1 summarises the characteristics of synthesised PEGylated silica nanoparticles in terms of their size and polydispersity, determined by SEM and DLS, as well as their PEG content, measured by FT-IR.

**Table 6.1.** Characteristics of PEGylated silica nano-particles.

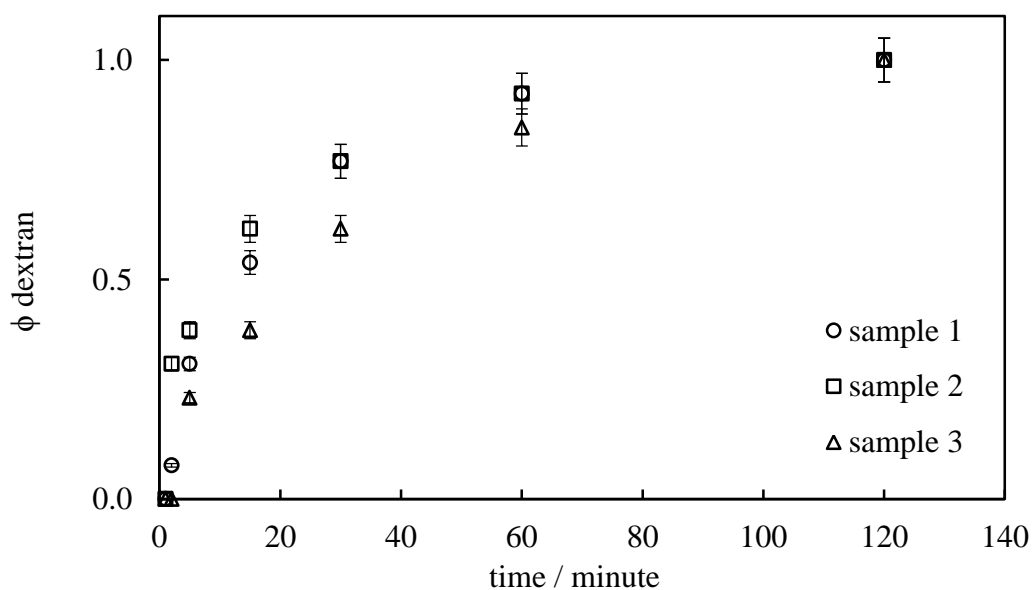
Sample	Particle size by SEM (nm)	Particle size by DLS (nm)	PEG content by FT-IR (wt.%)
1	244.6 ± 15.7	267.5 ± 11.1	1.8 ± 0.4
2	289.5 ± 18.6	298.0 ± 13.2	2.2 ± 0.4
3	304.0 ± 16.9	336.6 ± 15.7	2.2 ± 0.4

The larger particle sizes measured by DLS in compare to results gained from SEM can be explained, since the collapsed dried PEG on the surface of silica nanoparticles become rehydrated in the solution which results in observing particles with a larger size.

### 6.3.2 Effect of PEGylated nanoparticle size on emulsion stability

ATPSs with 0.5: 0.5 volume fractions were attempted to be stabilised using the synthesised PEGylated silica nanoparticles (1 wt.%) with different sizes as stabiliser. The stability of prepared w/w emulsions was studied as a function of the particle size. Three different sizes of PEGylated silica nanoparticles were used with size of  $267.5 \pm 11.1$ ,  $298.0 \pm 13.2$  and  $336.6 \pm 15.7$  nm. It was found that the emulsion stability (coalescence rate of dextran rich phase), does not change significantly with respect to particle size as shown in Figure 6.12. In addition when higher concentrations of PEGylated silica nanoparticles were used in the system, same trend was observed and extra particles sediment at the bottom of the glass vessel. In the case of using particles with the smallest size, the extra particles remained on the dextran-PEG interface after a full separation.

**Figure 6.12.** Plot of resolved dextran volume fraction ( $\phi$  dextran) versus time for emulsions consisting of 0.5: 0.5 volume fractions of dextran-PEG stabilised using 1 wt.% of PEGylated nanoparticles with varied sizes. Emulsions were prepared via two minutes homogenisation at 11000 rpm.



This result is in contrary with the bellow equation:

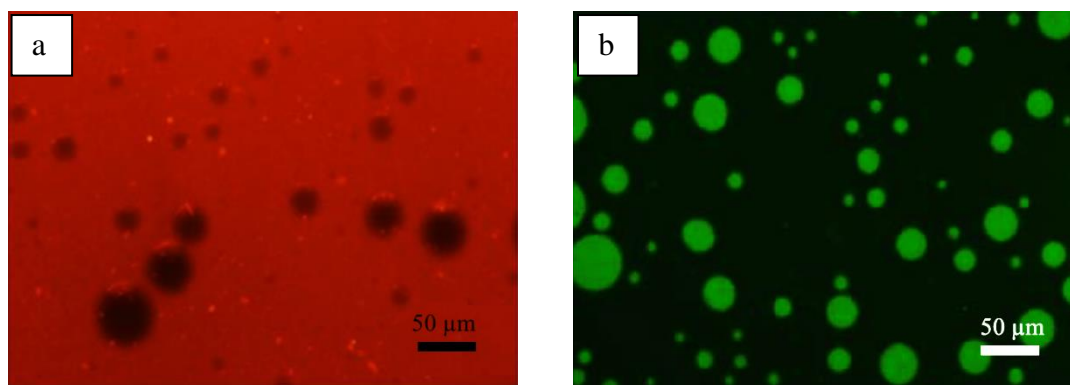
$$\Delta G_d = \pi \gamma r^2 (1 \pm \cos \theta)^2 \quad \text{Eq. 6.5}$$

Where  $\Delta G_d$  is the free energy required to detach a particle from a liquid interface,  $\gamma$  is the interfacial tension,  $r$  is the radius of particles and  $\theta$  is the contact angle. As it can be seen in this equation,  $\Delta G_d$  increases with the square of the particle radius. Therefore, it was expected to see an increase in the stability of the emulsions as the particle size increases. From these observations it can be summarised that PEGylated particles were unable to sufficiently adsorb at the dextran-PEG interface dextran and therefore emulsions were not stable for a long time. In order to stabilise an emulsion particles must provide close to complete coverage of the emulsion drops. As it was mentioned before, the stability of particle stabilised systems are extremely sensitive to particle wettability. It may simply be the case that PEGylated particles were either too PEG-philic or equally not PEG-philic enough ( $\theta_{dp} = 0$  or  $180^\circ$ ) to be adsorbed at the dextran-PEG interface and prevent coalescence process. Thus it was difficult to determine whether the size of particles have significant effect on the emulsion stability at equal volumes of dextran and PEG.

Fluorescence micrographs taken immediately after preparation of the emulsions containing fluorescent probes, namely rhodamine 6G and FITC dextran with tendency to stay in PEG and Dextran rich phase respectively, revealed the type of emulsion was dextran in PEG (d/p) (see Figure 6.13). It has been proved for water-oil emulsions that when the volume fractions of both phases are equal, the hydrophilic particles (contact angle  $< 90^\circ$ ) provide oil/water emulsions while hydrophobic particles (contact angle  $> 90^\circ$ ) would preferentially make water/oil emulsions this phenomenon is known as transitional phase inversion.<sup>22</sup> In dextran-PEG system, the PEGylated silica nanoparticles are expected to have a contact angle lower than  $90^\circ$  with PEG phase and consequently a higher wettability with PEG rich phase which provide dextran/PEG emulsions at 0.5: 0.5 volume fractions. Consequently, the obtained result was in agreement with literature. However, in a control experiment, when dextran-PEG ATPS with no stabiliser was stirred, the denser phase, which is dextran rich phase in this case, formed the dispersed phase in the PEG reach continuous phase as fluorescence microscopy revealed. Therefore, it might be just the influence of dextran rich phase density on the determination of

emulsion type even though PEGylated particles have been used for stabilisation of emulsions with equal volume fractions of two phases. In addition, if dextran-philic silica nanoparticles (particles coated with dextran) were available to be used for stabilisation of dextran-PEG systems, this result was much more reliable. In fact, it was attempted to synthesis dextran coated silica nanoparticles but it was unsuccessful.

**Figure 6.13.** Fluorescent micrographs of w/w emulsion based on dextran-PEG ATPS with 0.5: 0.5 volume fractions containing (a) rhodamine 6G and (b) FITC dextran, stabilised using 2 wt.% PEGylated silica nanoparticles with size  $289.5 \pm 18.6$  nm (sample 2).

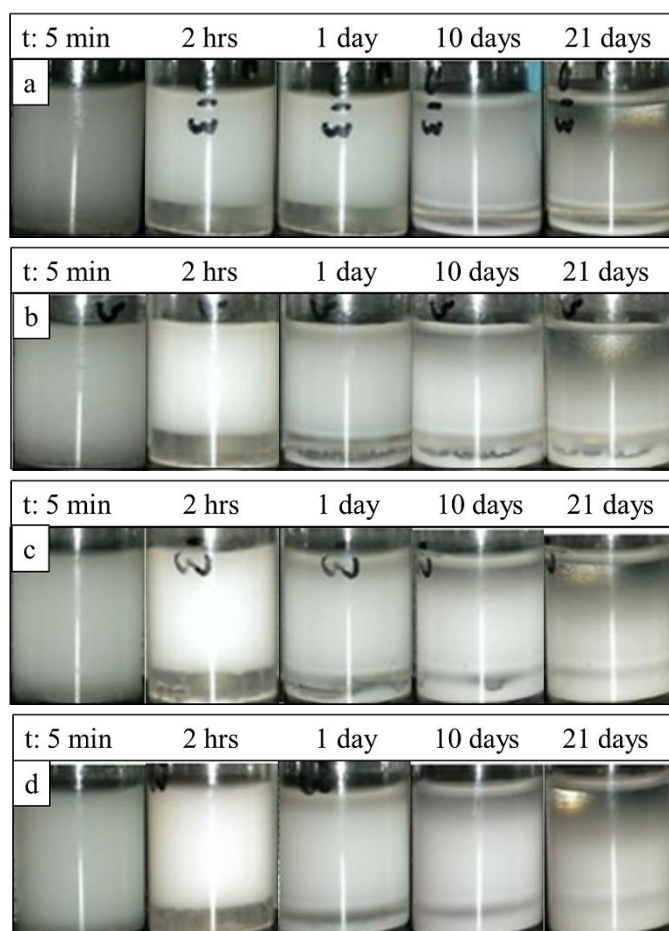


### **6.3.3 Effect of varying dextran-PEG volume fractions on emulsion stability**

Similar to ATPS consisting of 0.5: 0.5 volume fractions of dextran-PEG, in the absence of any stabiliser the dextran-PEG ATPS with 0.25: 0.75 volume fractions undergoes phase separation after mixing, within a few minutes. However, a complete phase separation might take up to 2 hours. Interestingly, when ATPS consisting of 0.25: 0.75 dextran-PEG was attempted to be stabilised using the same PEGylated silica nanoparticles with varied sizes, the prepared emulsions were stable for over 3 weeks in all cases. The type of emulsion using fluorescence microscopy was determined to be dextran in PEG (d/p). Further experiments by varying the particle content in the system namely, 1, 2, 3 and 4 wt.%, revealed no real apparent trend between particle concentration and emulsion stability. In each case a resolved dextran-rich phase can be observed within the first 30 minutes of separation and this grows only very slightly from this point, before remaining constant. The PEG-rich phase is resolved at a far smaller rate and a clear resolved PEG-rich phase can be

seen only after at least 24 hours of separation. Indeed, the PEG-rich phase is only fully resolved (transparent) after around 4 weeks. Moreover, it was noticed that the particles sediment even at low concentration (1 wt. %). The sedimentation of particles increases with time in all samples, over the three weeks. But consistently at each concentration the majority of particles had sediment within about a week. As particle concentration was increased the amount of particle sediment appeared to increase more comparably (see Figure 6.14). It is evident from that all these emulsions, by decreasing the volume fraction of dispersed phase, the stability of prepared emulsions increases significantly. This might be explained as a lower volume fraction of dispersed phase (dextran) promotes the formation of smaller and more isolated dispersed droplets of dextran and as a result the rate of coalescence decreases effectively.

**Figure 6.14.** Camera pictures taken of w/w emulsions prepared based on ATPS consisting of 0.25: 0.75 dextran-PEG and stabilised using (a) 1 wt.%, (b) 2 wt.%, (c) 3 wt.% and (d) 4 wt.% of PEGylated silica nanoparticles with size  $289.5 \pm 18.6$  nm (sample 2). Emulsions were prepared via two minutes homogenisation at 11000 rpm.



## 6.4 Conclusion

In this chapter, the stability of w/w emulsions based on dextran-PEG ATPS in the presence of modified silica nanoparticles was investigated. Two types of modified silica nanoparticles were used, namely, hydrophobised silica nanoparticles and PEGylated silica nanoparticles. The later ones were synthesised in-house and well-characterised in terms of their PEG content and size.

In the case of using hydrophobised silica nanoparticles, the effect of hydrophobicity of particles on the emulsion stability was studied. It was found that particles with 33% hydrophobicity were able to stabilised w/w emulsions for relatively long time. Extreme hydrophilicity and hydrophobicity resulted in very unstable emulsions. In addition the effect of particle content in the system on stability of w/w emulsions was investigated and it was resulted that 2 wt.% silica particles was necessary for stabilisation of emulsion. Moreover, it was found that the emulsion drop size does not vary when higher concentrations of particles were used in the system. In the case of using less than 2 wt.% of hydrophobised silica nanoparticles the drop size was much larger in compare to those containing more than 2 wt.% of particles and the prepared emulsion was very unstable.

In the case of using PEGylated silica nanoparticles, emulsions with equal volume fractions of dextran and PEG gave unstable emulsions irrespective of the particle size which was unexpected. This might be due to the low wettability of PEGylated silica nanoparticles as a result of their low content of PEG (about  $2.0 \pm 0.5$  wt.%). In addition it was observed that when the volume fraction of dispersed phase decreases, much more stable emulsions were formed which were stable for weeks. This might be explained as the lower volume fraction of dispersed phase (dextran) promotes the formation of smaller and more isolated dispersed droplets of dextran and as a result the rate of coalescence decreases effectively. However, this result showed that PEGylated silica nanoparticles should be at least weakly adsorbed at the dextran-PEG interface since they provided stable emulsion for a few weeks. In summary it can be concluded that more studies are necessary to achieve a better understanding of particle stabilised w/w emulsions.

## 6.5 References

1. B. P. Binks, *Curr. Opin. Colloid Interface Sci.*, 2002, **7**, 21.
2. A. T. Poortinga, *Langmuir*, 2008, **24**, 1644.
3. H. Firoozmand, B. S. Murray and E. Dickinson, *Langmuir*, 2009, **25**, 1300.
4. G. Balakrishnan, T. Nicolai, L. Benyahia and D. Durand, *Langmuir*, 2012, **28**, 5921.
5. B. T. Nguyen, T. Nicolai and L. Benyahia, *Langmuir*, 2013, **29**, 10658.
6. B. Braisch, K. Köhler, H. P. Schuchmann and B. Wolf, *Chem. Eng. Technol.*, 2009, **32**, 1107.
7. B. P. Binks and S. O. Lumsdon, *Phys. Chem. Chem. Phys.*, 1999, **1**, 3007.
8. B. P. Binks and S. O. Lumsdon, *Langmuir*, 2000, **16**, 2539.
9. B. P. Binks and S. O. Lumsdon, *Langmuir*, 2000, **16**, 3748.
10. B. P. Binks and S. O. Lumsdon, *Phys. Chem. Chem. Phys.*, 2000, **2**, 2959.
11. B. P. Binks and S. O. Lumsdon, *Langmuir*, 2000, **16**, 8622.
12. I. M. Rio-Echevarria, F. Selvestrel, D. Segat, G. Guarino, R. Tavano, V. Causin, E. Reddi, E. Papini and F. Mancin, *J. Mater. Chem.*, 2010, **20**, 2780.
13. H. Xu, F. Yan, E. E. Monson and R. Kopelman, *J. Biomed. Mater. Res., Part A*, 2003, **66**, 870.
14. J. Frelichowska, M. A. Bolzinger and Y. Chevalier, *J. Colloid Interface Sci.*, 2010, **351**, 348.
15. B. P. Binks and C. P. Whitby, *Langmuir*, 2004, **20**, 1130.
16. S. Arditty, C. P. Whitby, B. P. Binks, V. Schmitt and F. Leal-Calderon, *Eur. Phys. J. E*, 2003, **11**, 273.
17. S. Arditty, V. Schmitt, J. Giermanska-Kahn and F. Leal-Calderon, *J. Colloid Interface Sci.*, 2004, **275**, 659.
18. S. Arditty, V. Schmitt, F. Lequeux and F. Leal-Calderon, *Eur. Phys. J. E*, 2005, **44**, 381.



19. B. R. Midmore, *J. Colloid Interface Sci.*, 1999, **213**, 352.
20. G. Vigil, Z. Xu, S. Steinberg and J. Israelachvili, *J. Colloid Interface Sci.*, 1994, **165**, 367.
21. H. Matsuura and T. Miyazawa, *J. Polym. Sci., Part A: Polym. Chem.*, 1969, **7**, 1735.
22. R. Aveyard, B. P. Binks and J. H. Clint, *Adv. Colloid Interfac. Sci.*, 2003, **100**, 503.

## **CHAPTER 7**

### **CONCLUSION AND FUTURE WORK**

## 7.1 Summary of main findings

The main focus of this thesis was to investigate a novel alternative approach for formation of polymer-based vesicles, so called polymersomes. Specifically, to develop a fundamentally different strategy for encapsulation of different species, based on coupling the separation properties of ATPSs, with templated self-assembly of polymersomes. A series of in-house synthesised amphiphilic terpolymers containing particular blocks with specific affinity towards ATPSs' two phases were used as constructing blocks for polymersomes formation. Chapter 3 describes the design, synthesis and characterisation of these terpolymers. The employed characterisation methods illustrated the successful synthesis of terpolymers, as terpolymers with narrow polydispersity indices, compositions very close to theoretical compositions and number average molecular weight similar to theoretical molecular weights were obtained. In addition, in this chapter, the effect of varying terpolymers composition and molecular weights on their hydrodynamic diameter, CMC and  $pK_a$  values were studied in detail.

Chapter 4 summarised some preliminary observations of terpolymers solutions when hydrated in bulk or as thin film. The main aim of this chapter was to investigate whether a selection of synthesised ABC terpolymers with constant composition but varied molecular weight are able to form polymersomes using a couple of conventional methods (bulk rehydration and thin film rehydration). The initial observations revealed that this series of terpolymers can self-assemble into two different types of micellar structures, based on the preparation method. Bulk rehydration of this series of terpolymers resulted in the formation of spherical micelles whereas rehydration of their thin film led to in the formation of flexible worm-like micelles. DLS results suggested that by increasing the molecular weight of terpolymers, the average size of these worm-like micelles increases. Increasing the temperature causes shrinkage in the mean diameter or probably formation of different type of self-assembly. In conclusion, although this series of terpolymers do not form polymersomes based on the conventional techniques, they can self-assemble to a different type of micellar structure, namely worm-like micelles which also have potential in different applications. <sup>1</sup> More investigations are needed to characterise such structures in details for obtaining more conclusive result.

Chapter 5 describes a fundamentally different strategy for polymersome formation based on templating a dispersed APTS of dextran-PEG. At the beginning of this chapter, the possibility of stabilisation of dextran-PEG APTS using three commercially available ABA terpolymers, namely Pluronics<sup>®</sup>, with general structure of  $EO_x-PO_y-EO_z$  and different hydrophilic-hydrophobic ratios and molecular weights was studied. As results showed, none of the Pluronics<sup>®</sup> was able to stabilise such system for a long time. However, the behaviour of the prepared systems was different in terms of the separation rate of each phase, as well as the volume fraction of phases. Experimental results of using F68 and F108 Pluronic<sup>®</sup> grades as the surfactant showed that the higher the molecular weight of the surfactant, the more is the stability of the emulsion. However, this was presumed to be due to the high viscosity of system at high concentration of polymer, which slows down the phase separation process.

In the second part of this chapter, a series of ABC terpolymers of different compositions ( $P_x-B_y-D_z$ ) based on the hydrophilic PEGMA, hydrophobic BuMA and hydrophilic DMAEMA were used for the stabilisation of w/w emulsion and possible formation of templated polymersomes. We demonstrated that stable micron size polymersome-like structures consisting of  $P_x-B_y-D_z$  building blocks can be formed templating water-in-water emulsions based on PEG-dextran APTS. The fluorescence microscopic observation showed that the type of formed emulsion is not strongly dependent on the composition of the used terpolymers (stabiliser) as all terpolymers with varied compositional design provided dextran-in-PEG type of emulsion (where the prepared emulsion was stable). However, it was shown that by varying the volume fraction of dextran-PEG APTS, it is possible to induce catastrophic phase inversion of the system. Therefore, templated polymersomes with either dextran or PEG rich interior can be formed by simply varying the composition of the used APTS. Moreover, we showed the emulsion drop size (or polymersomes size) can be varied in range of 1-100  $\mu\text{m}$  in diameter, based on the choosing the appropriate terpolymer as building block for polymersome formation or stabilisation of w/w emulsion. Overall it was shown that emulsions with longer stability contain smaller drops.

A number of compositional requirements for optimisation of the final structure of terpolymers were achieved by analysing the relative stability of the emulsions stabilised by a series of terpolymers with varied compositions. Overall, terpolymers consisting of relatively long (70-80 repeated units) BuMA and DMAEMA blocks with equal block length and PEGMA block consisting of about 15 unites were able to provide stable system for more than 8 months.

In additions, the effect of varying the concentration of terpolymers, pH, temperature and stirring rate on the behaviour of these systems was studied. Also, the behaviour of formed polymersomes upon drying and diluting the system was investigated. It was shown that although the formed polymersomes keep their structure upon drying the system, they dissociate by diluting up the system with pure water.

At the end of this chapter, we showed how solute molecules distribute and self-loaded within the water-in-water emulsion (or templated polymersome) system. The investigation revealed that the solutes molecules can freely permeate across the emulsion droplet interface within a few minutes and therefore they are not kinetically trapped within the formed polymersomes. However, they could be thermodynamically self-loaded into the dispersed phase and retain for relatively long time. The encapsulated species can be released by collapsing the system triggered by dilution. To summarise this chapter, the distinctive features of these systems can be highlighted as following:

- Very low energy input (gentle stirring) is needed for the formation of such systems.
- There is no use of organic solvent in such systems and they are entirely aqueous systems.
- The templated polymersomes (1-100  $\mu\text{m}$ ) are larger than the conventional ones (50 nm-5 $\mu\text{m}$ ).

- The interior of polymersomes can be converted from dextran rich to PEG rich solution simply by varying the composition of the ATPS. Therefore, based on the partitioning of different species they can be firstly concentrated in the desired phase and being encapsulated by addition of appropriate terpolymer and mixing of the system.
- The segregation of encapsulants within the emulsions or templated polymersomes is an equilibrium effect; it does not vary further with time unlike the conventional polymersomes which trap encapsulants kinetically.
- Collapse of the formed polymersomes structure occurs within a few minutes triggered by dilution of the emulsions with pure water.

The work on stabilisation of w/w emulsions was further extended in Chapter 6 by using two types of modified silica nanoparticles with specific characteristics, as stabiliser. This chapter explains how the characteristics of these nanoparticles affect emulsion properties. In the first section of this chapter, hydrophobised silica nanoparticles with varied hydrophobicity extent were used for the stabilisation of dextran-PEG ATPS. Comparing the emulsion stability versus their hydrophobicity extent showed that particles with 33% hydrophobicity extent were able to stabilised w/w emulsions for relatively long time (one week). Extreme hydrophilicity and hydrophobicity of the particles resulted in very unstable emulsions. In addition the effect of particle content in the system on stability of w/w emulsions was investigated. It was shown that 2 wt.% silica particles (33% hydrophobicity) was necessary for stabilisation of emulsion, as when less than 2 wt.% of hydrophobised silica nanoparticles was used in the system, the emulsion drop size was much bigger and the prepared emulsion was very unstable. Moreover, it was found that the emulsion drop size does not vary when more than 2 wt.% of particle were used in the system and the unadsorbed particles precipitated at the bottom of sample vial.

In the second part of this chapter, PEGylated silica nanoparticles were synthesised in-house and well-characterised in terms of their PEG content and mean size. The PEGylated silica nanoparticles were spherical in shape with a relatively smooth surface. Their mean diameter was determined between 250 to 300 nm and they contain about  $2 \pm 0.5$  wt.% PEG. Addition of these PEGylated silica nanoparticles to dextran-PEG ATPS with equal volume fractions resulted in unstable systems

disrespectful of the particle size, as it was expected larger size particles form more stable emulsion. This might be due to the low wettability of PEGylated silica nanoparticles as a result of their low content of PEG (about  $2.0 \pm 0.5$  wt.%) by either of dextran or PEG system. However, it was observed that when the volume fraction of dispersed phase decreases, much more stable emulsions (more than 20 days) can be obtained. This result showed that PEGylated silica nanoparticles should be at least weakly adsorbed at the dextran-PEG interface since they provided relatively stable emulsions. This might be explained as a lower volume fraction of dispersed phase (dextran) promotes the formation of smaller and more isolated dispersed droplets of dextran and as a result the rate of coalescence decreases effectively. Virtually, compared to terpolymer stabilised w/w emulsions, the particle stabilised w/w emulsions were stable for much shorter duration. All in all more experiment would be beneficial to give a better understanding of the particle stabilised w/w emulsions.

## 7.2 Future work

Amphiphilic terpolymers with specific affinity towards dextran-PEG ATPS illustrated promising results in terms of providing stable w/w emulsion or in other words, templated polymersomes. From the synthetic point of view, synthesis of a new series of ABC terpolymers based on PEGMA-*b*-BuMA-*b*-Dextran composition would be of major benefit as this type of terpolymers would ensure the segregation of amphiphilic terpolymer towards dextran and PEG rich phase. This synthesis could be accomplished by addition of dextran homopolymer with a terminal azide moiety to PEGMA-*b*-BuMA diblock copolymer containing a triple bond at the BuMA terminal based on click chemistry.<sup>2</sup> Dextran containing azide moiety can be synthesised by the reaction of 1-azido-2,3-epoxypropane with dextran under alkaline conditions.<sup>3</sup> PEGMA-*b*-BuMA diblock copolymer containing propargyl methacrylate (PMA) functional group which contains a triple bond at the end of the polymer chain has been already synthesised in course of this work. Coupling these two macromolecules via click chemistry will produce PEGMA-*b*-BuMA-*b*-Dextran with potential application in formation of templated polymersomes which might be more developed in biomedical applications.

The preliminary work has been done in Chapter 4 can be more extended by studying the self-assembly behaviour of all synthesised terpolymers with varied compositions and block lengths to obtain more conclusive result. Unfortunately, because of lack of time just a limited series of synthesised terpolymers were studied in terms of self-assembly behaviour in this chapter.

Chapter 5 can be more developed by deeper investigations on a number of unresolved questions in this work. In spite of all the work being done on w/w emulsions, it is still unclear whether the stabilisation of the system is as a result of adsorbed terpolymer film around the dispersed phase or a part of the stabilisation results from other effects, such as viscosifying the continuous phase. Therefore, it would be helpful to measure and compare the viscosity of the dextran-PEG APTS stabilised with different terpolymers to find out how viscosity influences the stability of the emulsions. In addition, providing phase diagram of PEGMA block and dextran rich phase as well as DMAEMA block with both PEG and dextran rich phases would make it more clear how these polymers interact with each other in aqueous solution.

Secondly, we are uncertain about the structure of the presumably adsorbed polymer film around the dispersed drops. In the proposed research strategy terpolymers straddles the water-water interface with PEGMA blocks located one side and DMAEMA at the other side. However, there could be mixed PEGMA and DMAEMA coronas in both sides or possibility of formation of bilayer hairpin configuration or more complex configurations. Therefore, further experiments using high resolution structural determination methods such as neutron scattering and cryo-TEM are required to elucidate these unresolved aspects.

The templated polymersomes can be also more developed in application where slow mass transport of the encapsulant is needed, such as drug delivery applications, by slight modification of the formed polymer film. It is well-established that the constituent terpolymers containing DMAEMA block can be potentially cross-linked using appropriate cross-linker (e.g. 1,2-bis(2-iodoethoxy)ethane).<sup>4</sup> By adjusting the degree of crosslinking, the mass transportation of encapsulant triggered by diluting can be well-controlled.



The investigation into stabilisation of ATPSs could be expanded by choosing different polymer pairs and stabilisers. These systems have huge potential for formation of entirely aqueous emulsions which could change the insight towards applications of emulsions in different industries.

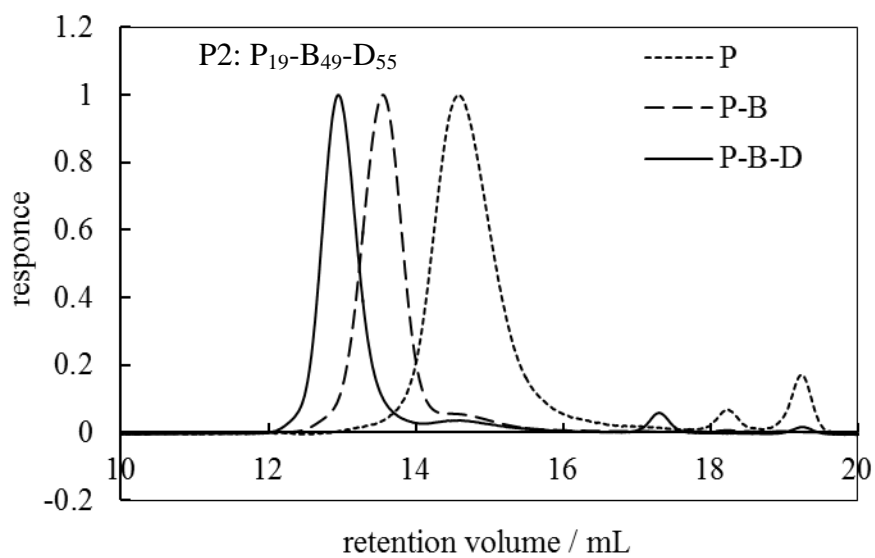
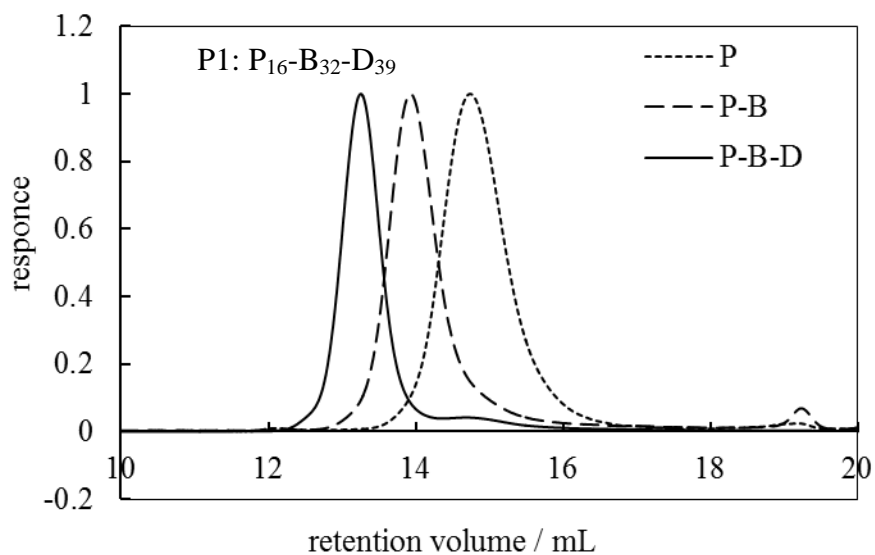
Chapter 6 can be improved by measuring the contact angle of the used modified silica nanoparticles with dextran and PEG rich phases, in order to have a better understanding of the adsorption energy towards the dextran-PEG interface. In case of using PEGylated silica nanoparticles for the stabilisation of dextran-PEG ATPS, by developing the synthesis route of the PEGylated silica nanoparticles, particles with higher content of PEG could be obtained which presumably would enhance the adsorption of particles at the dextran-PEG interfaces. In addition, modifying the synthesis route towards preparation of silica-nanoparticles coated with both dextran and PEG would be of major benefit.

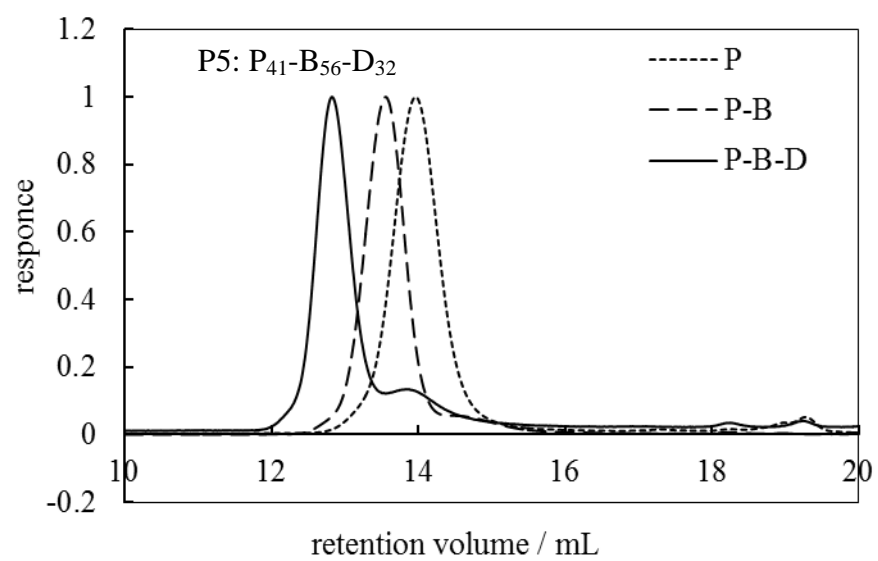
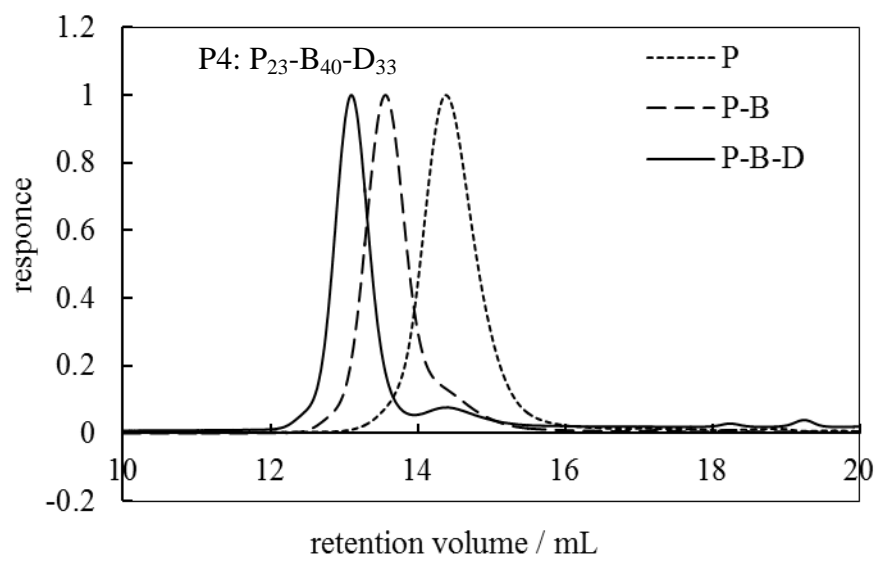
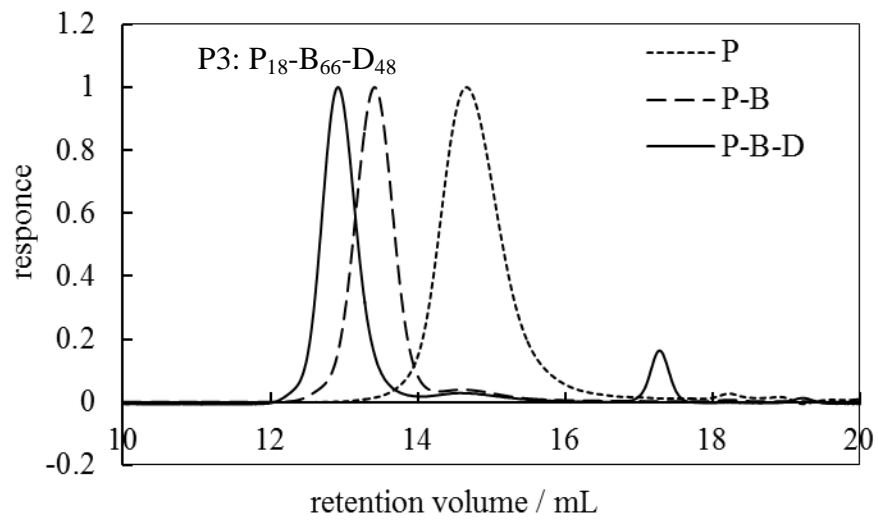
### 7.3 References

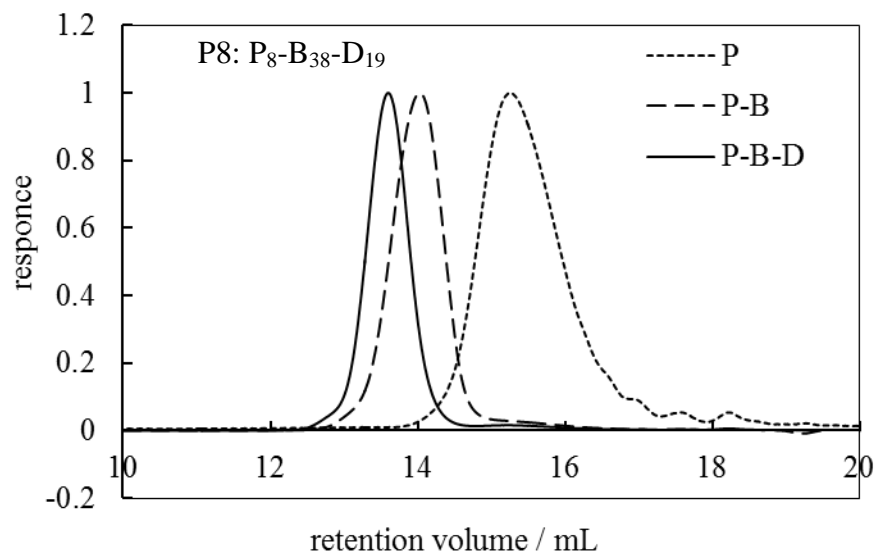
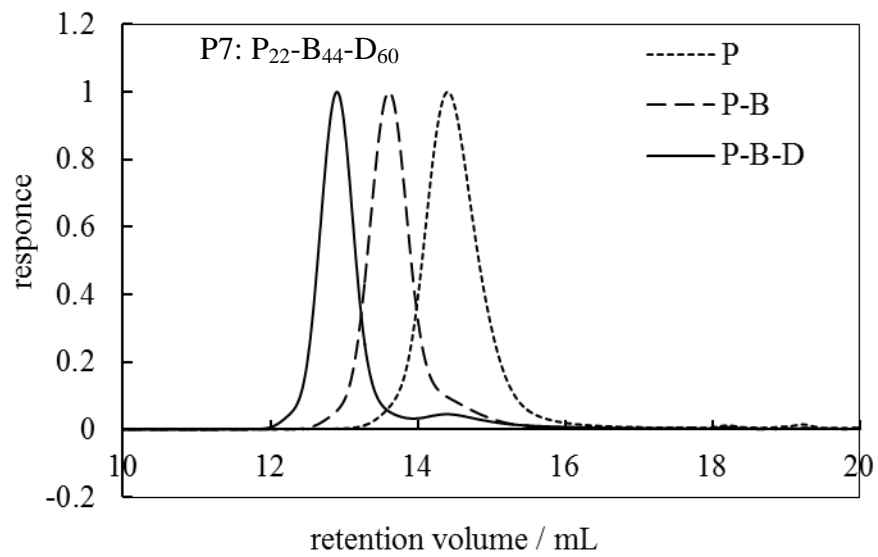
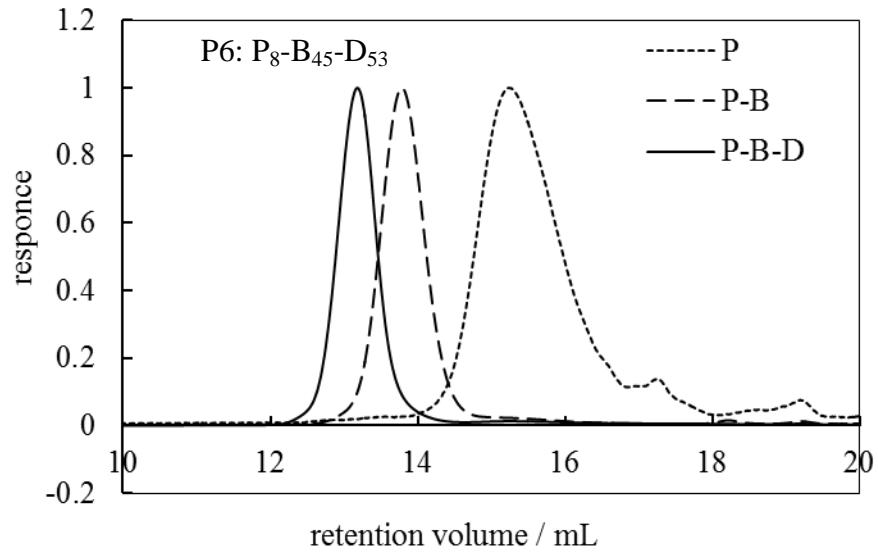
1. J. P. Rothstein, *Rheol. Rev.*, 2008, **1**, 1.
2. H. C. Kolb, M. G. Finn and K. B. Sharpless, *Angew. Chem., Int. Ed.*, 2001, **40**, 2004.
3. N. Pahimanolis, A. H. Vesterinen, J. Rich and J. S. m. 78–82., *Carbohydr. Polym.*, 2010, **82**, 78.
4. J. Du, L. Fan and Q. Liu, *Macromolecules*, 2012, **45**, 8275.

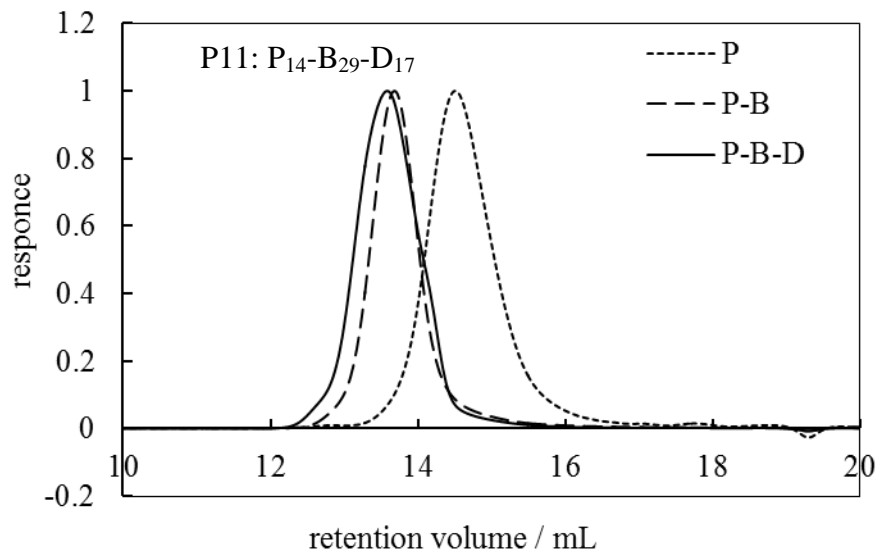
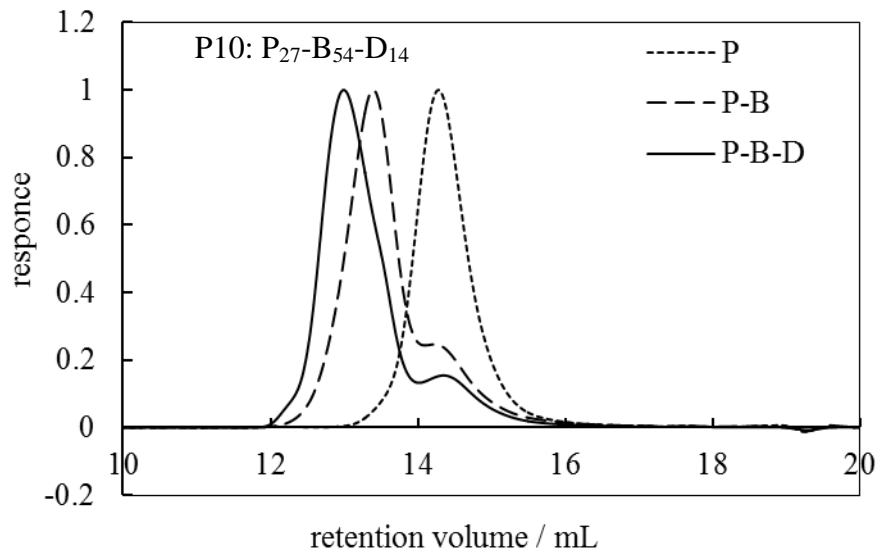
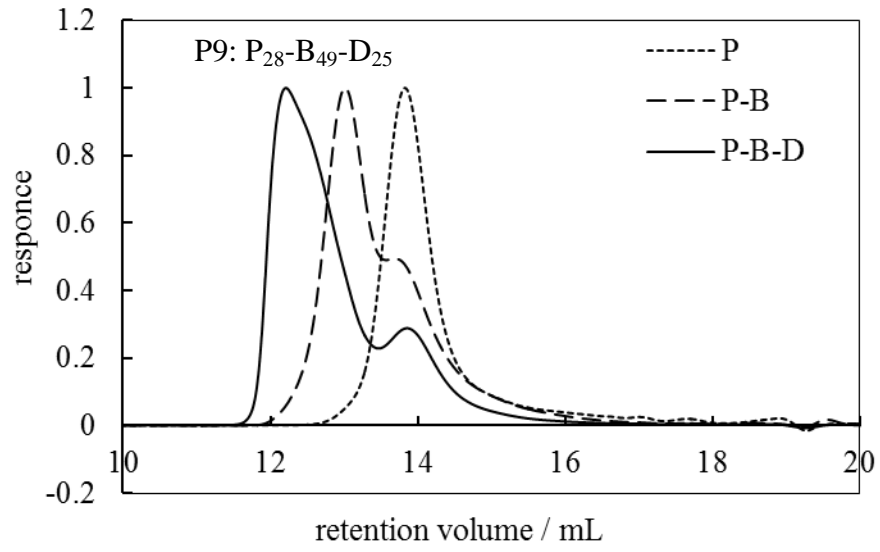
## **APPENDIX**

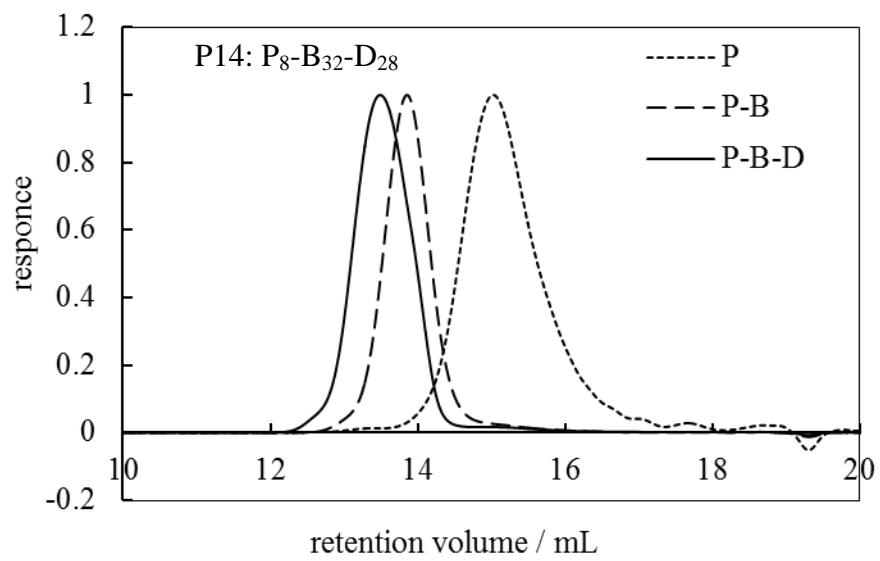
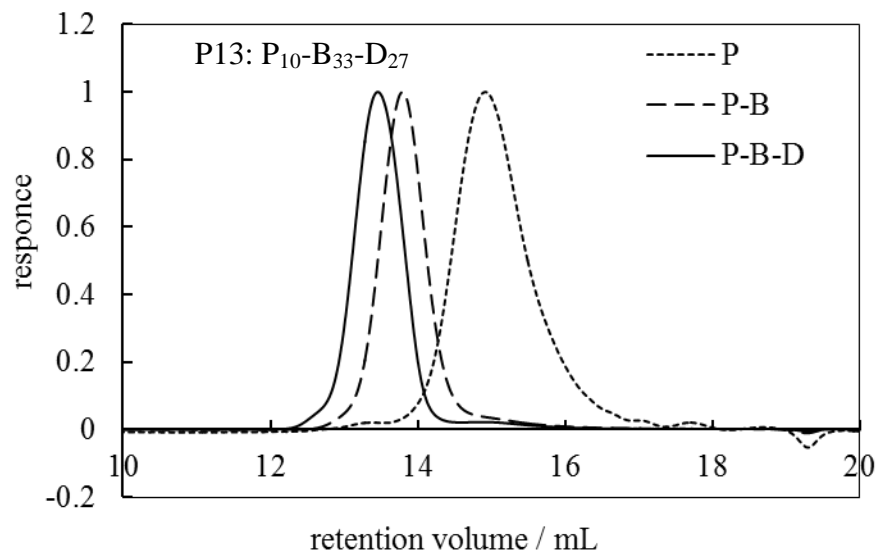
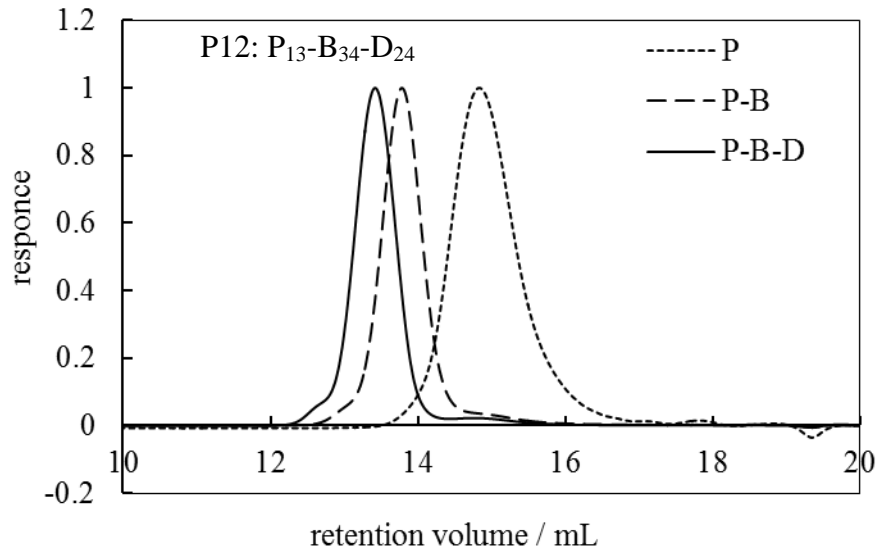
**A.1.** GPC chromatographs corresponding to synthesised  $P_x$ - $B_y$ - $D_z$  terpolymers and their precursors  $P_x$ - $B_y$  and  $P_x$ .



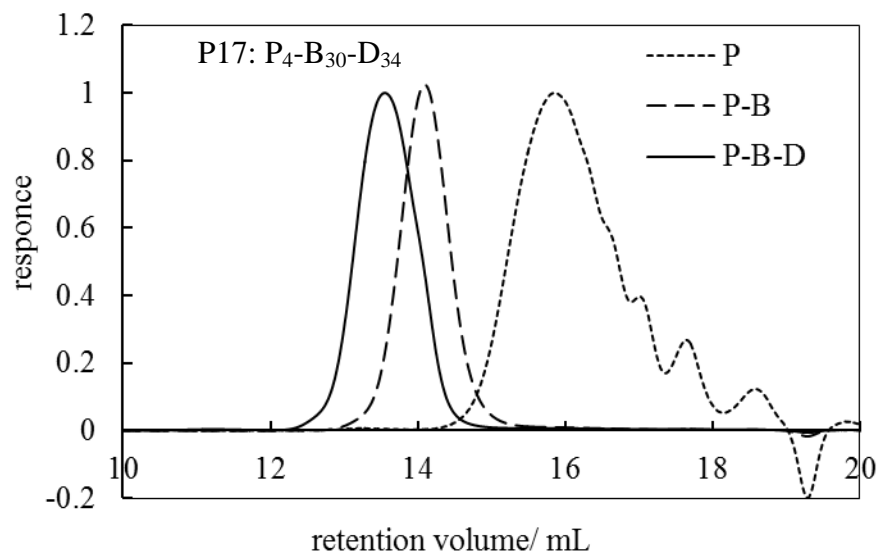
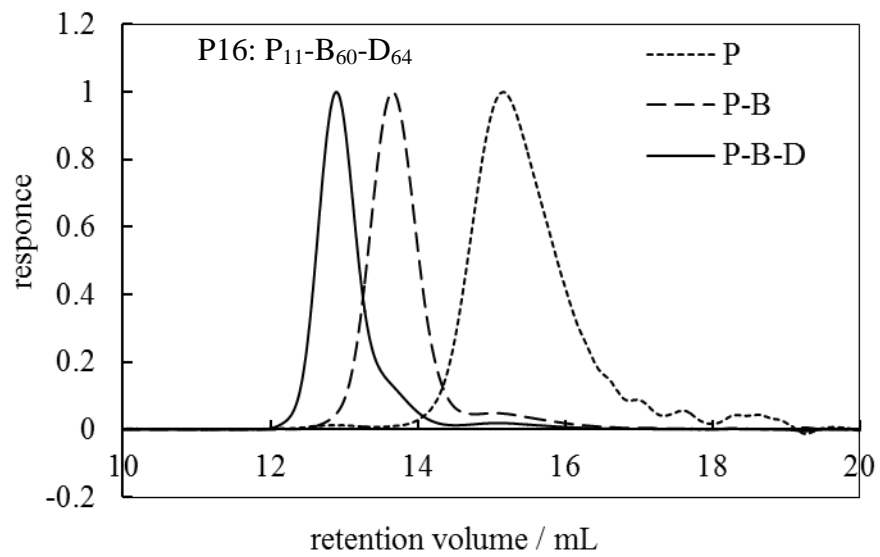
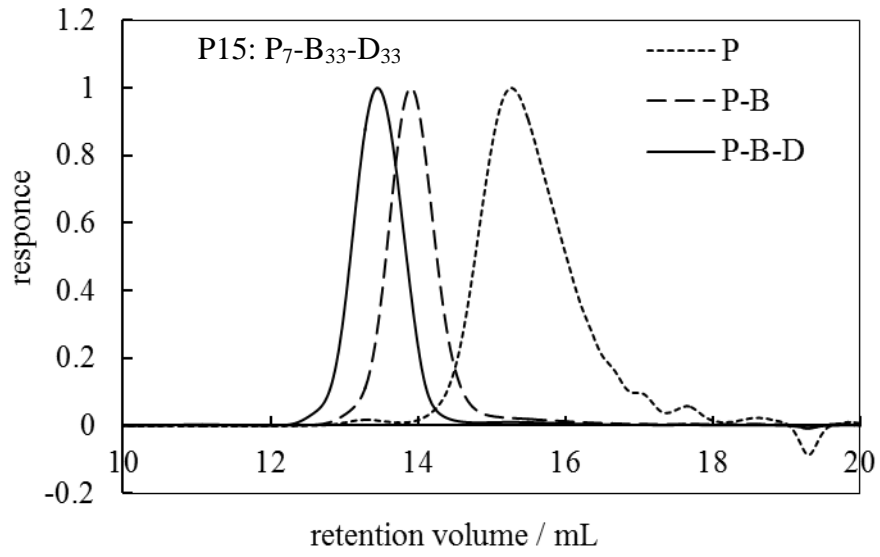


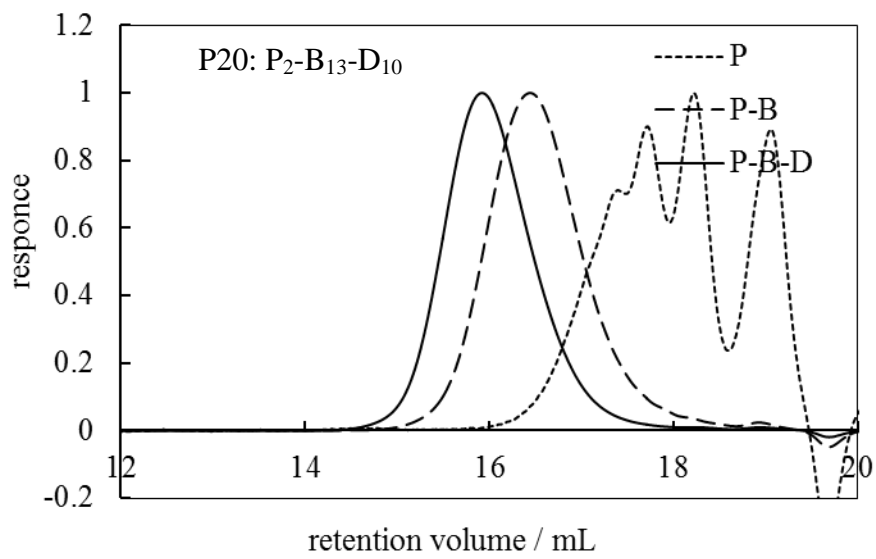
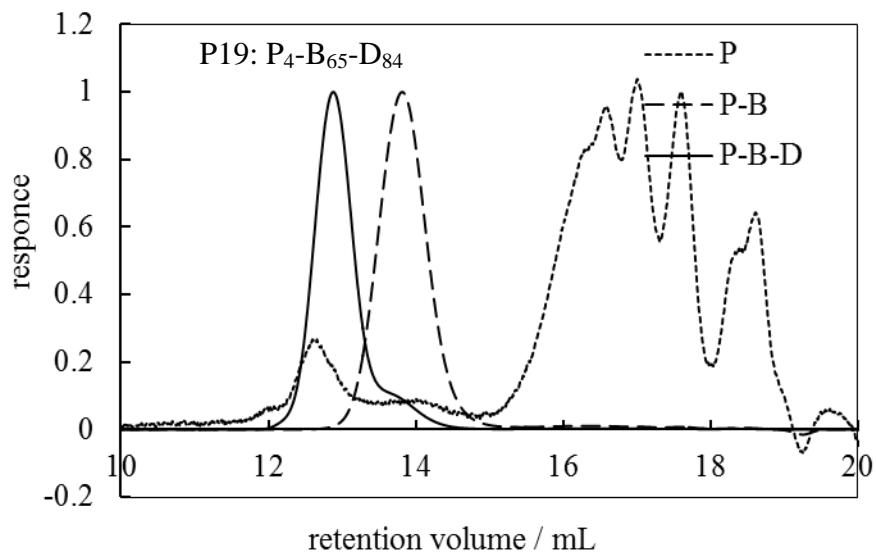
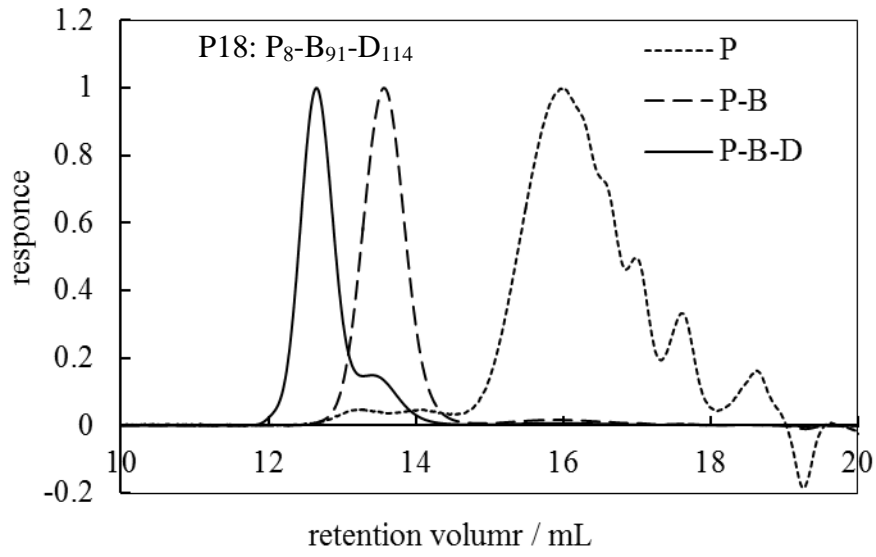


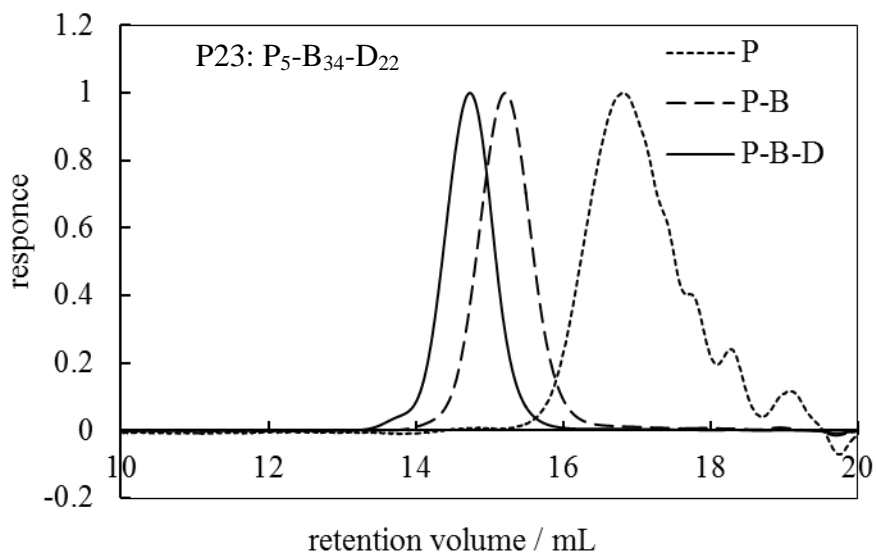
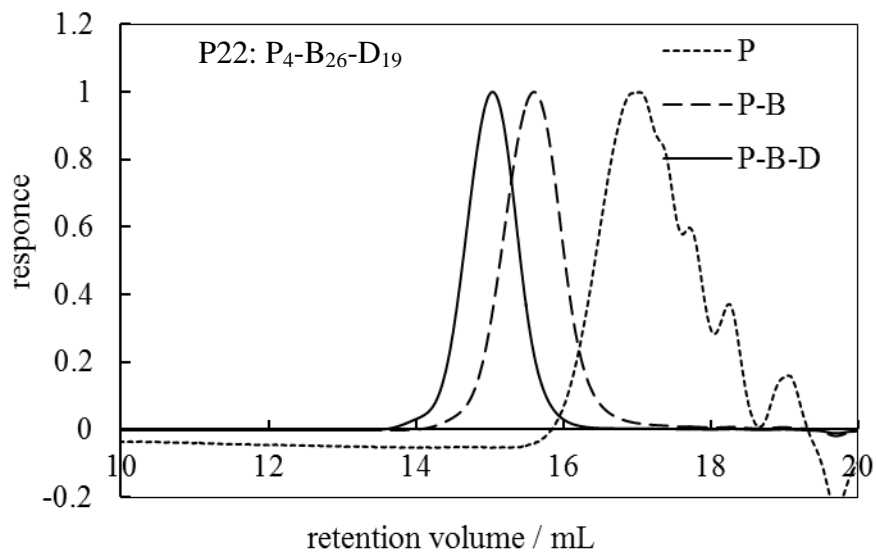
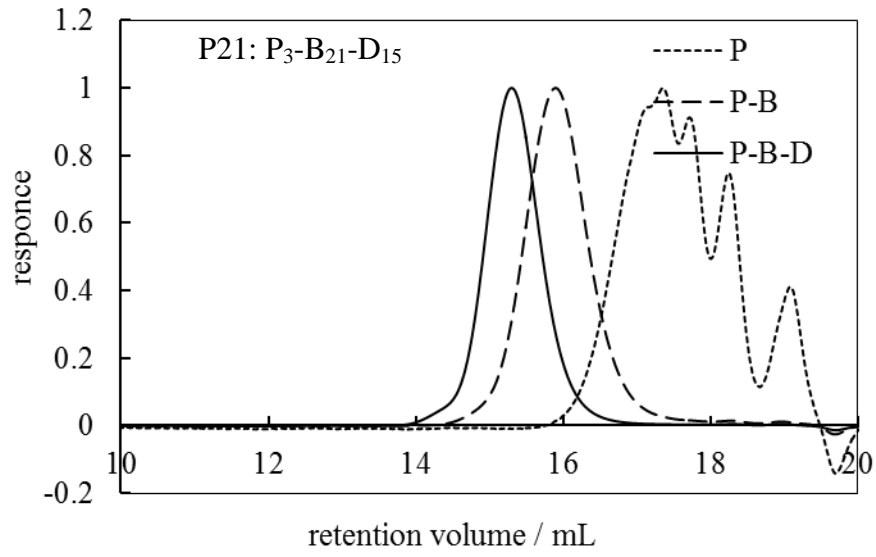


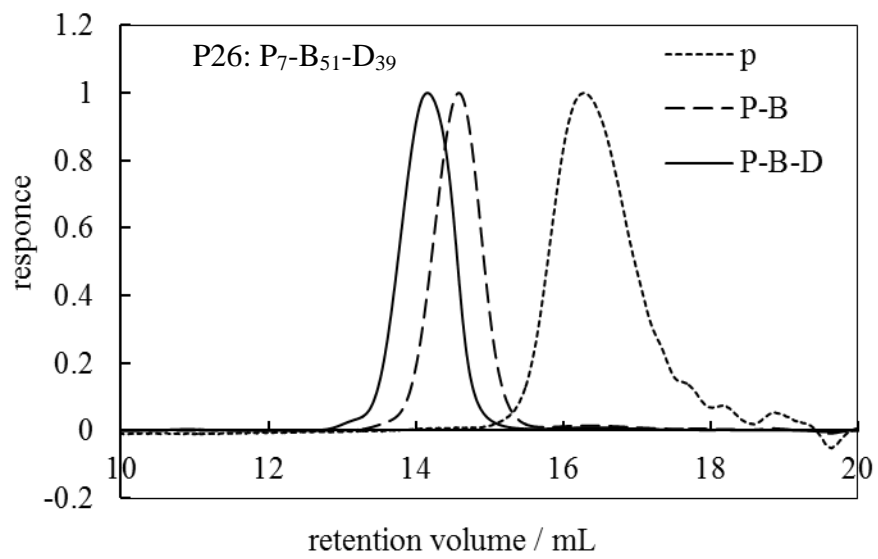
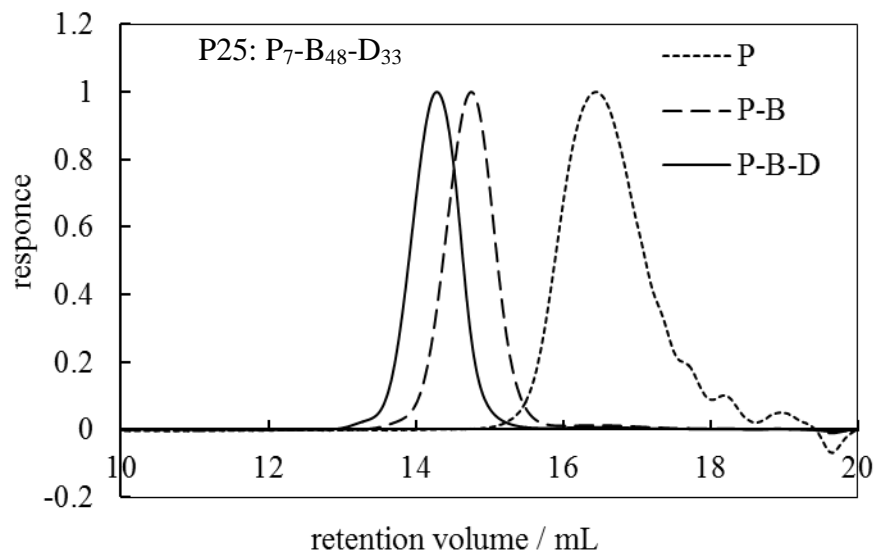
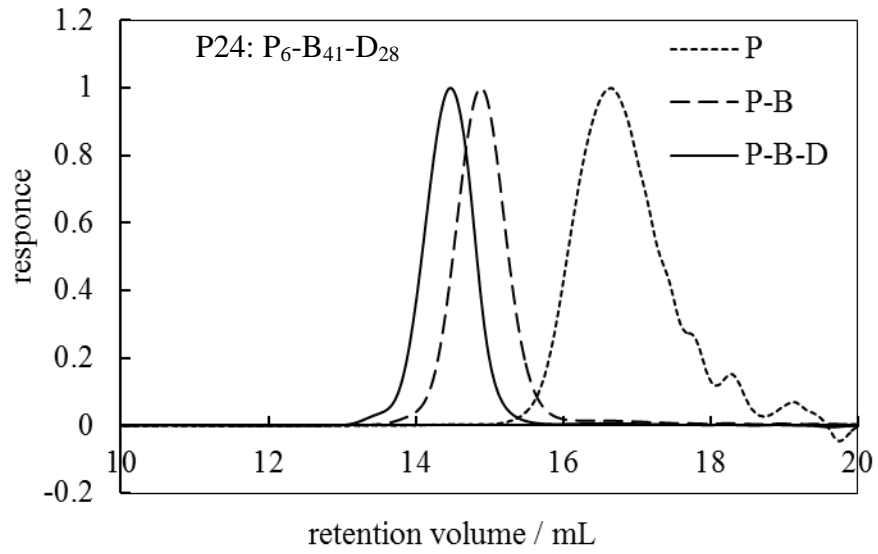


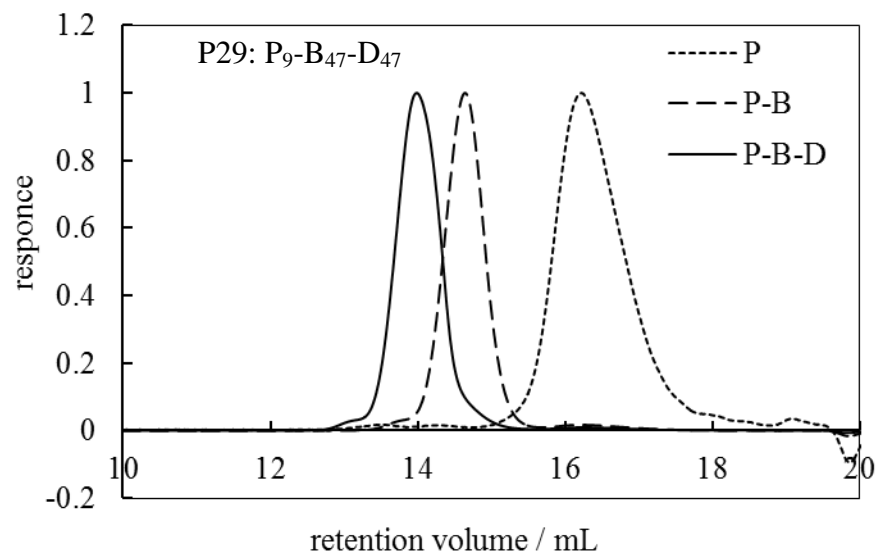
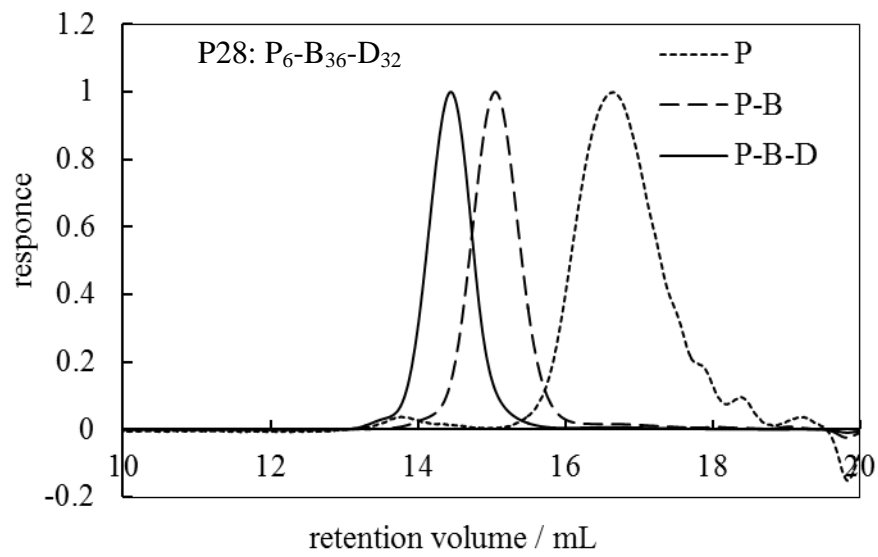
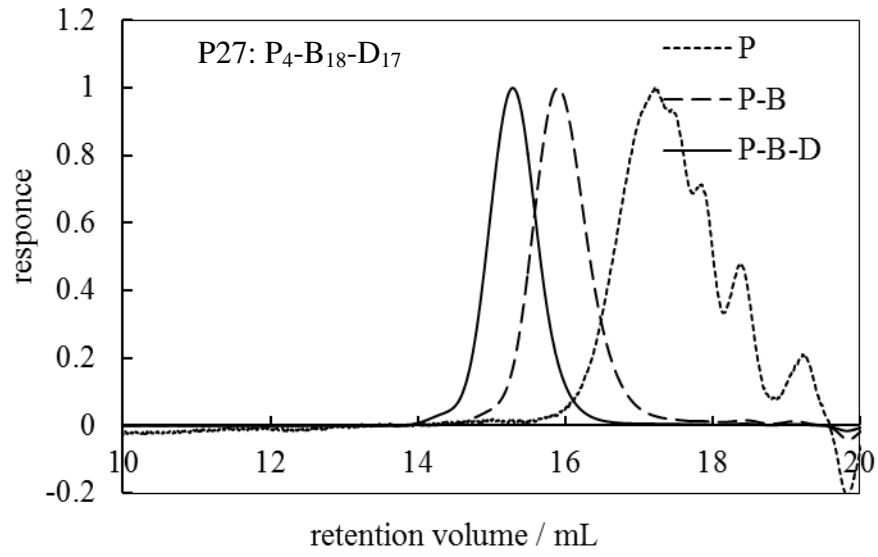


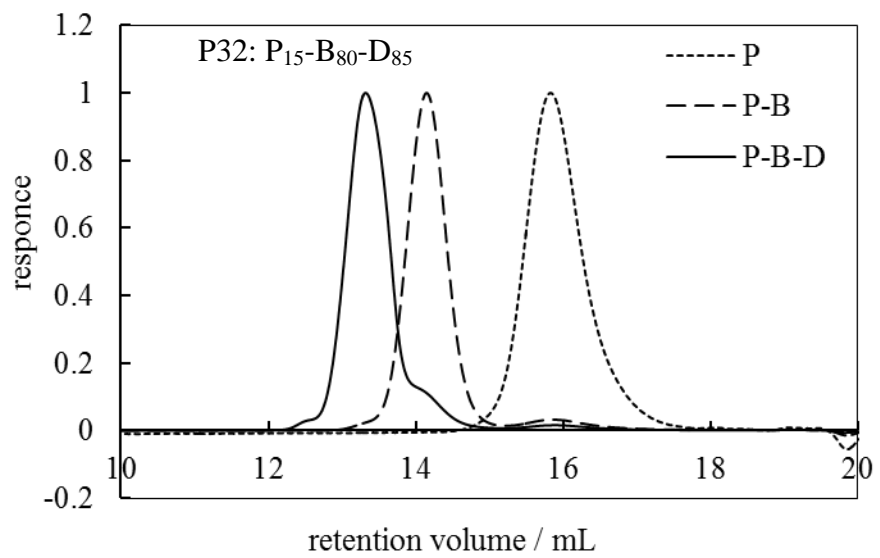
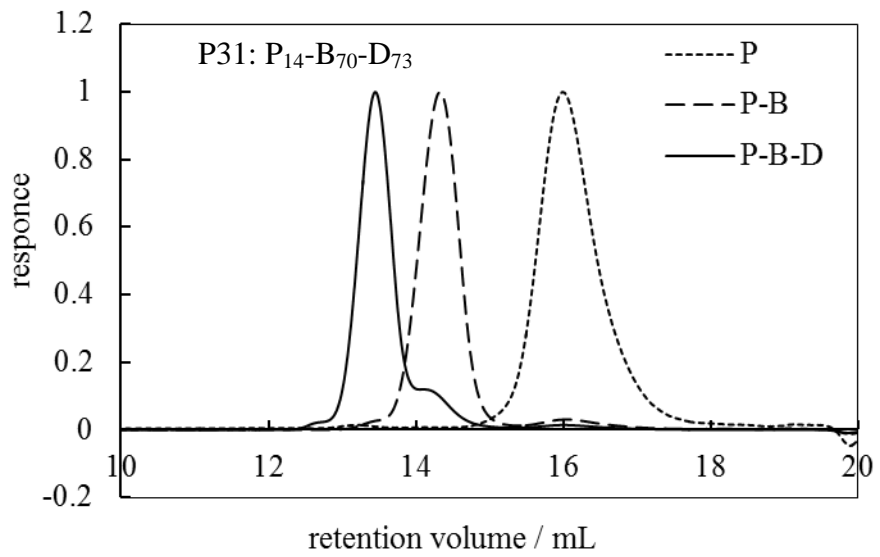
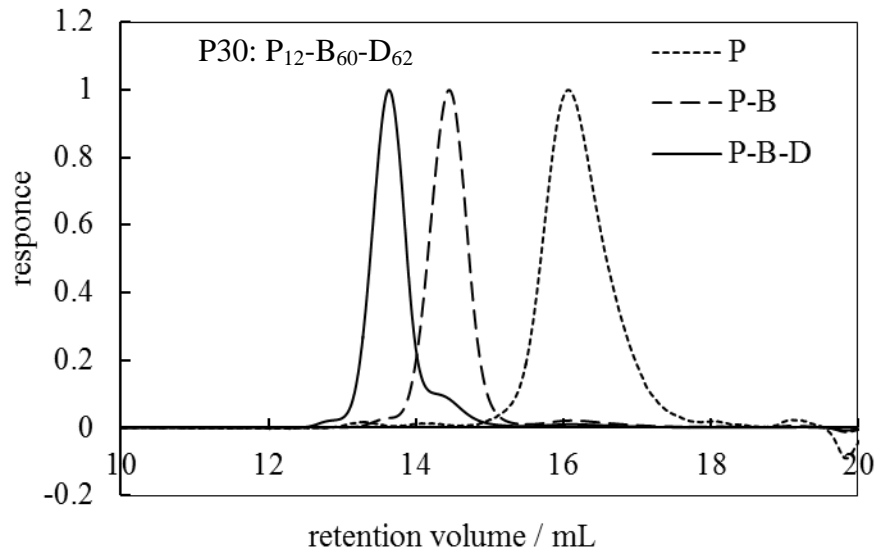


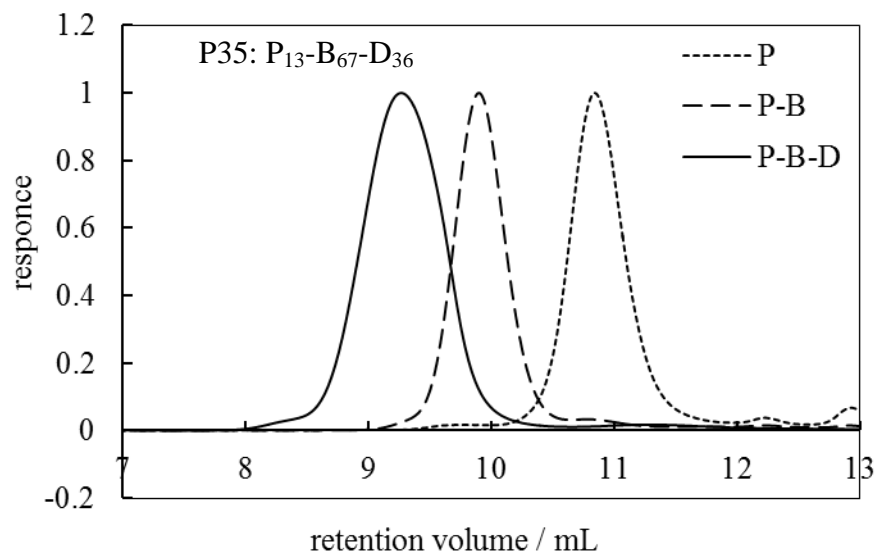
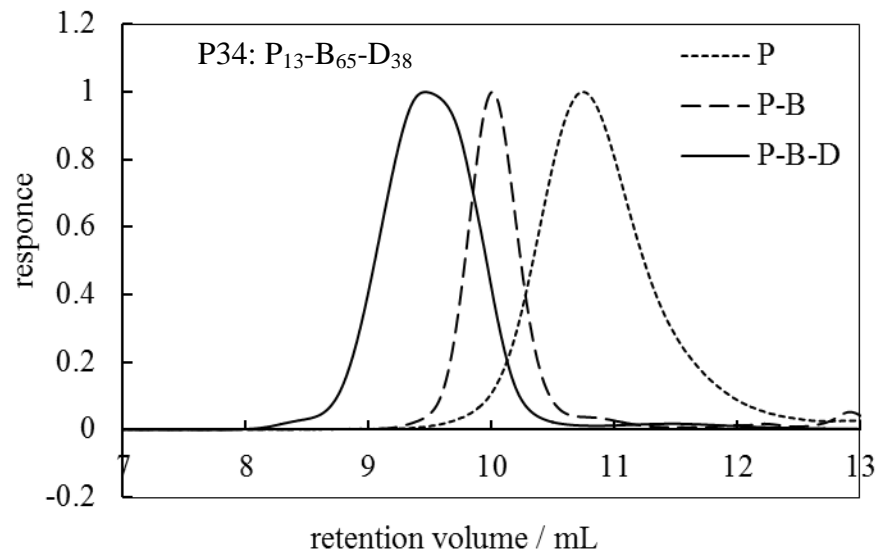
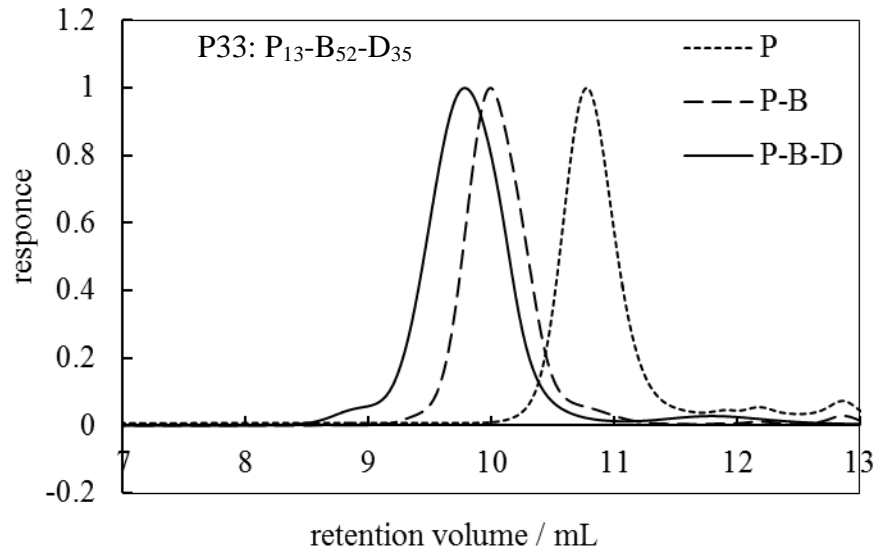


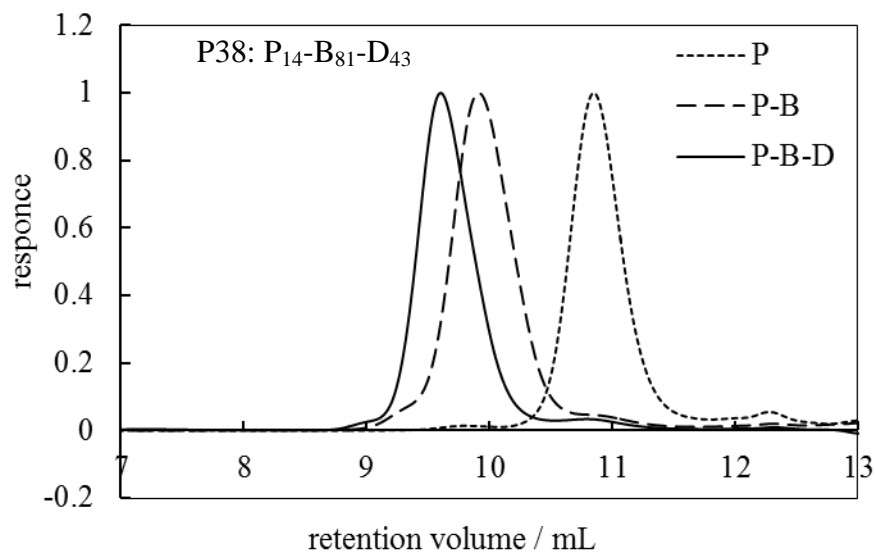
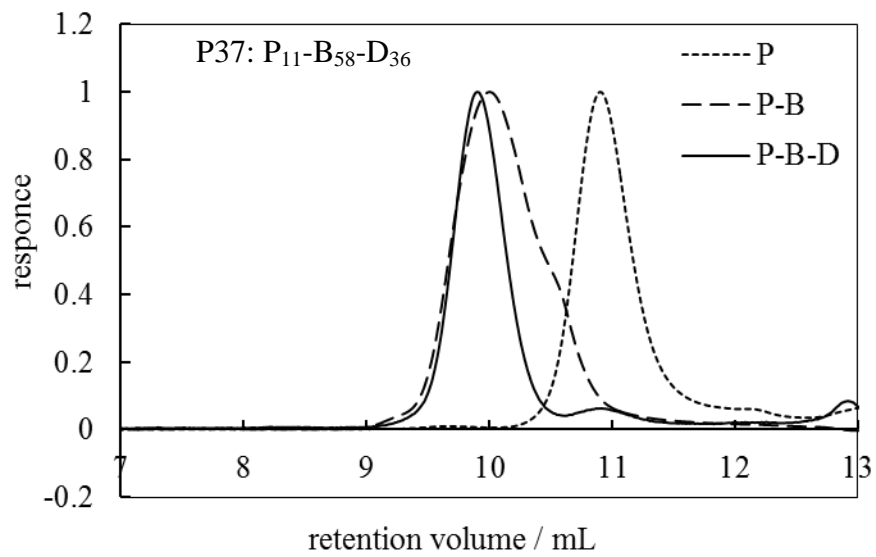
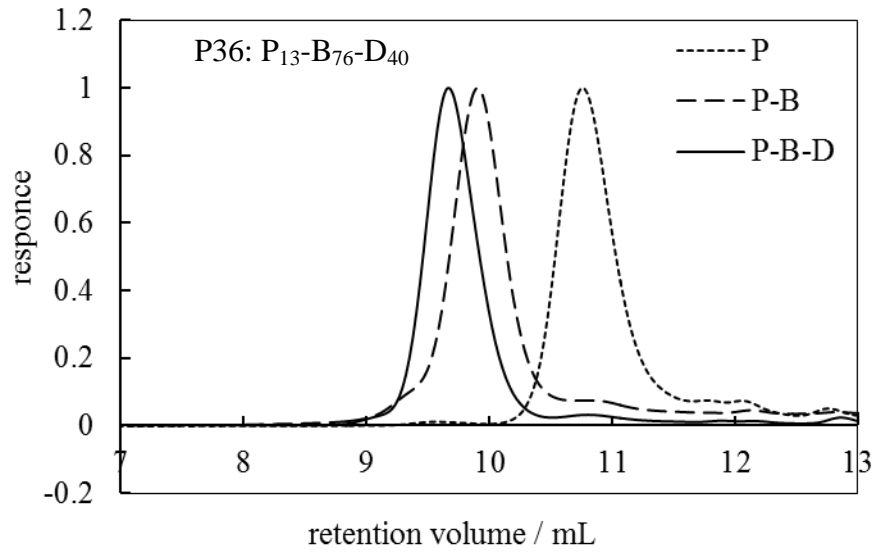






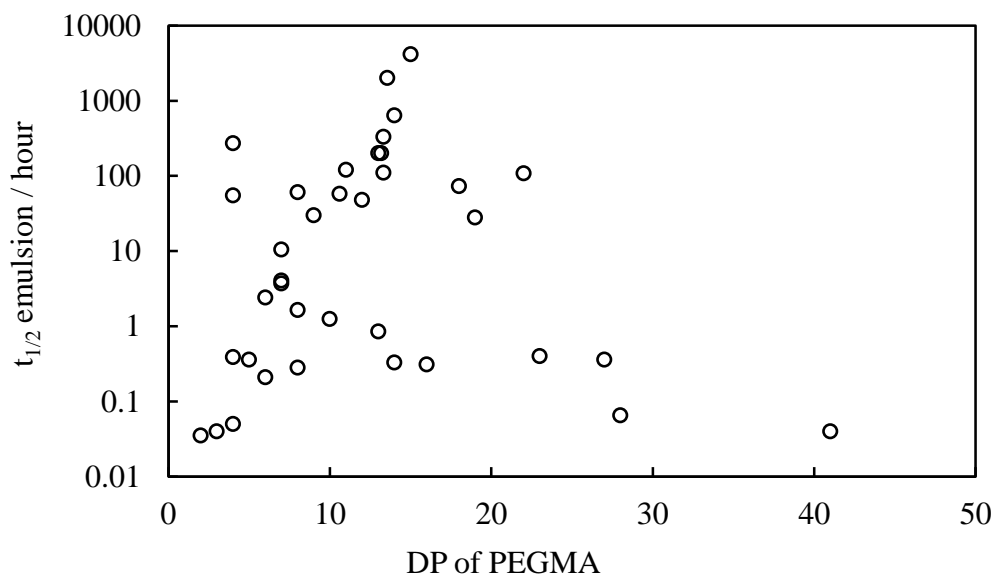
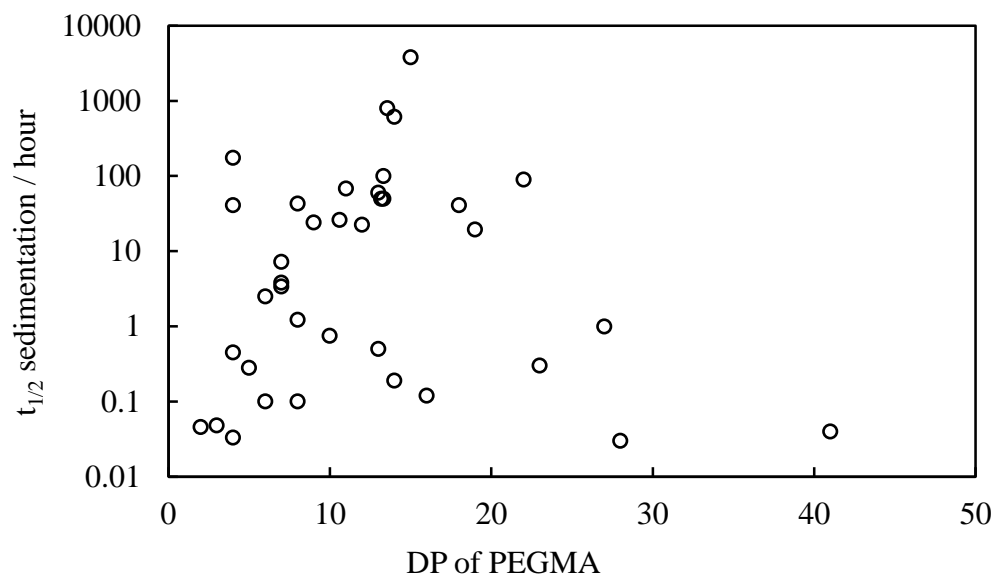




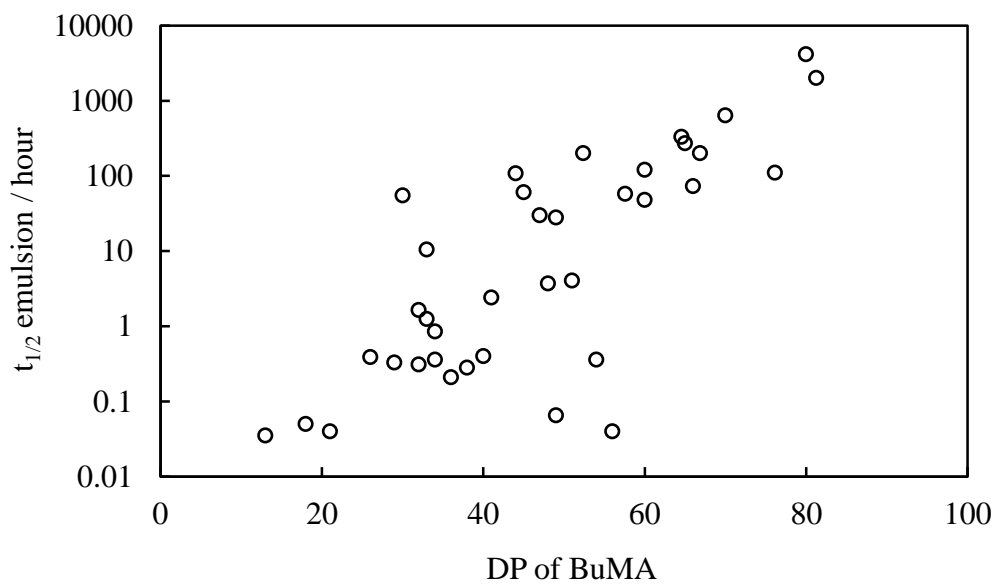
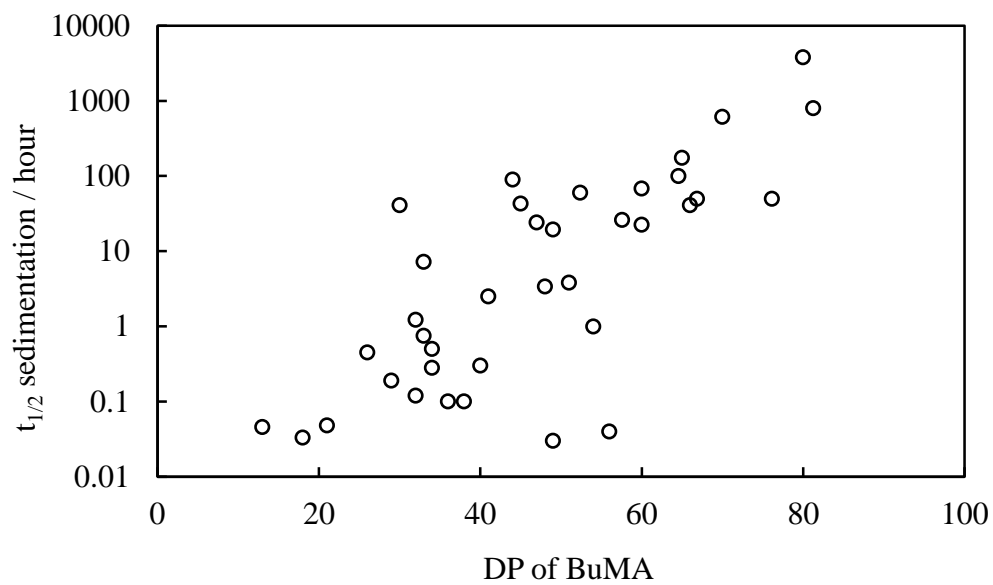




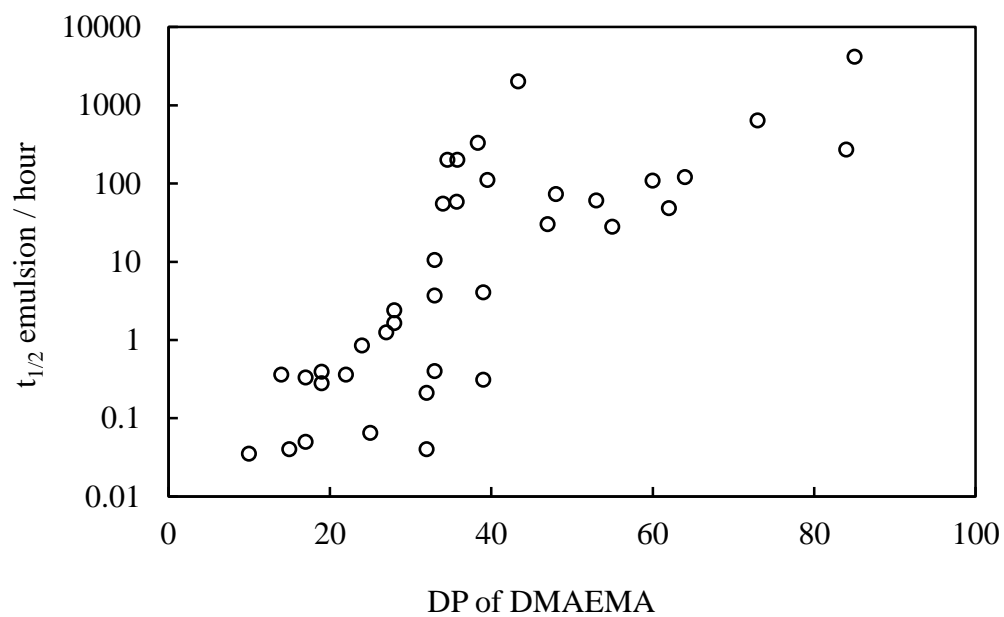
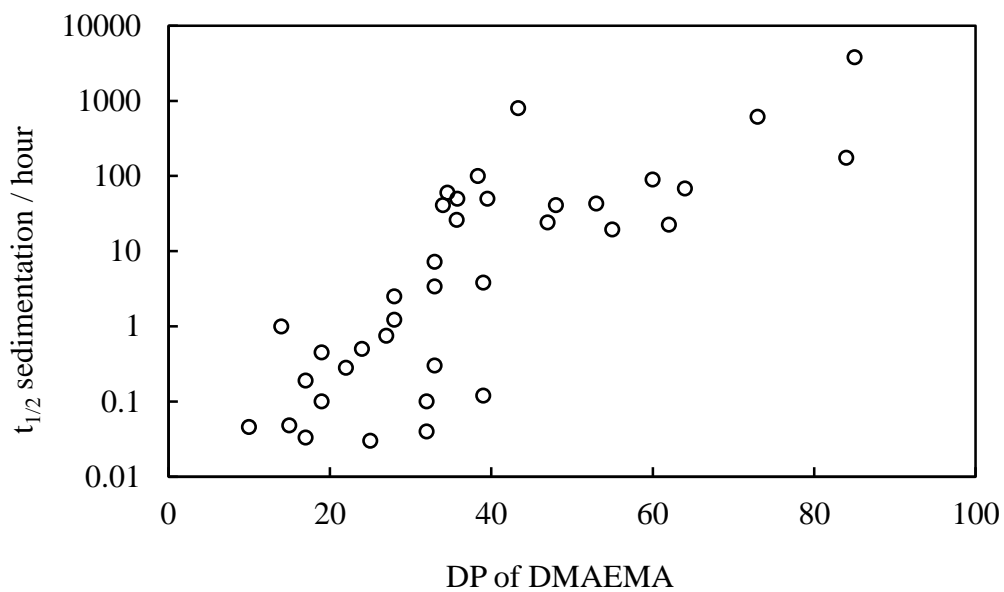
**A.2.** Variation of  $t_{1/2}$  of sedimentation and emulsion with the PEGMA block length of terpolymers at equal volume fractions of dextran-PEG phases.



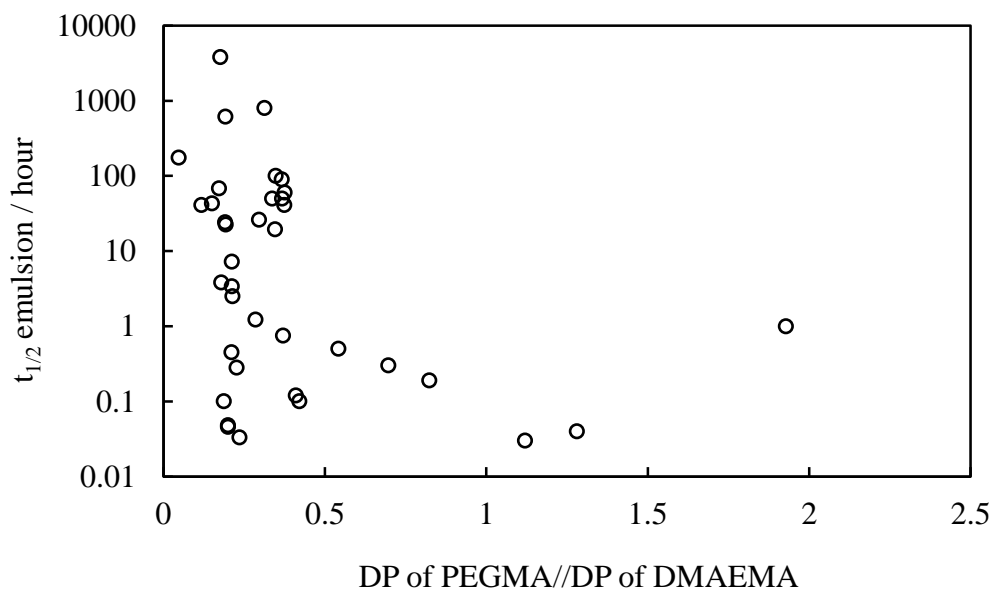
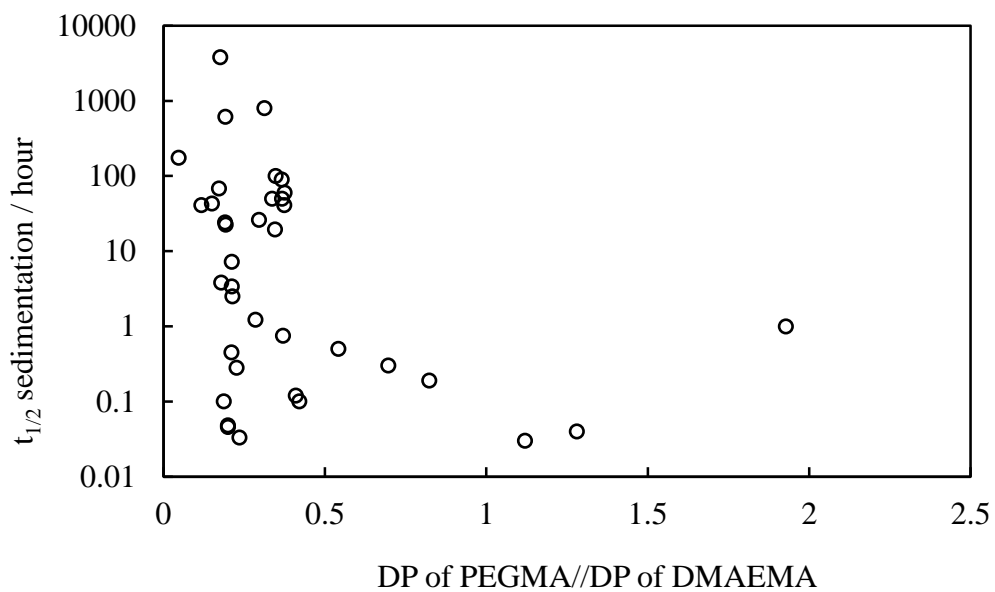
**A.3.** Variation of  $t_{1/2}$  of sedimentation and emulsion with the BuMA block length of terpolymers at equal volume fractions of dextran-PEG phases.



**A.4.** Variation of  $t_{1/2}$  of sedimentation and emulsion with the DMAEMA block length of terpolymers at equal volume fractions of dextran-PEG phases.



**A.5.** Variation of  $t_{1/2}$  of sedimentation and emulsion with the PEGMA/DMAEMA block length ratio of terpolymers at equal volume fractions of dextran-PEG phases.



**A.6.** Variation of  $t_{1/2}$  of sedimentation and emulsion with the  $M_n$  of terpolymers at equal volume fractions of dextran-PEG phases.

